Fundamentals of Human Monocular Depth Perception

The Foundational Physics and Geometry of the Monocular Depth Perception of Humans



Fundamentals of Human Monocular Depth Perception

The Foundational Physics and Geometry of the Monocular Depth Perception of Humans

> Dr. Christopher S. Baird West Texas A&M University

2025

Public Domain Open Educational Resource (OER)

All text, diagrams, figures, tables, and data in this book have been placed in the public domain by the author, Dr. Christopher S. Baird. Anyone may reproduce, print, transmit, upload, distribute, present, or change any part of this book or all of this book without attribution and without permission. All images in this book are original creations of Dr. Christopher S. Baird and have been placed in the public domain.

Contents

1	The Basics of Light, Color, and Vision	1
	1.1 Fundamentals of Light and Vision	2
	1.2 Detecting the Properties of Light	3
	1.3 Detecting Color	4
2	The Coordinate Systems of Human Monocular Vision	7
	2.1 Defining the Image Coordinates	8
	2.2 Defining the Object Coordinates: Rectangular Coor. and Cylindrical Coor. About the z Axis	8
	2.3 Defining the Object Coordinates: Spherical Coordinates	10
	2.4 Defining the Object Coordinates: Cylindrical Coordinates About the y Axis	11
3	Plotting the Observed Location as a Function of the Object's Phys. Loc.	13
	3.1 Plotting for Rectangular Coordinates and Cylindrical Coordinates About the z Axis	13
	3.2 Plotting for Spherical Coordinates	20
	3.3 Plotting for Cylindrical Coordinates About the y Axis	20
4	Observed Object Length as a Function of Position	27
	4.1 Observed Object Length in Rectangular Coordinates/Cylindrical Coordinates About the z Axis	29
	4.2 Observed Object Length in Spherical Coordinates	31
	4.3 Observed Object Length in Cylindrical Coordinates About the y Axis	31
5	Plotting Observed Length as a Function of Spherical Coordinates	35
6	Plotting Observed Length as a Function of Original Object Coordinates	41
7	Observed Sphere Diameter as a Function of Position	49
8	Observed Object Area as a Function of Position	51
	8.1 Observed Object Area in Rectangular Coordinate/Cylindrical Coordinates About the z Axis	52
	8.2 Observed Object Area in Spherical Coordinates	53
	8.3 Observed Object Area in Cylindrical Coordinates About the y Axis	53
9	Plotting the Observed Object Area as a Function of Spherical Coordinates	55

10	Plotting the Observed Object Area as a Function of Original Object Coor.	61
11	Mapping to a Flat Display Screen	67
	11.1 Rectilinear Projection	68
	11.2 Stereographic Projection	70
	11.3 Equidistant Projection	71
	11.4 Equisolid Angle Projection	72
	11.5 Orthographic Projection	73
	11.6 Slight Pincushion Projection	73
	11.7 Plotting the Flat Display Screen Projection Equations	74
	11.8 Using Rectangular Display Screen Coordinates	75
	11.9 Using Rectangular Coordinates for the Object Location	76
	11.10 Using Cylindrical Coordinates About the z Axis for the Object Location	76
	11.11 Using Spherical Coordinates for the Object Location	76
	11.12 Using Cylindrical Coordinates About y Axis for the Object Location	77
	11.13 Plotting Various Surfaces Using All Projection Methods	77
12	Human Depth Perception Cues	107
	12.1 Motion Parallax	108
	12.2 Kinetic Depth Effect	108
	12.3 Depth from Optical Expansion	108
	12.4 Familiar Shape	109
	12.5 Relative Size	110
	12.6 Familiar Size	110
	12.7 Estimated Size	112
	12.8 Uniform Size	112
	12.9 Parallel Lines	113
	12.10 Texture Gradient	118
	12.11 Horizon Effect	118
	12.12 Occlusion	120
	12.13 Surface Shading	122
	12.14 Recess Shading	125
	12.15 Shadow Shape	125
	12.16 Shadow Size, Location, and Blurriness	126
	12.17 Atmospheric Effects	127
	12.18 Accommodation and Pupil Response	129
	12.19 Depth from Defocusing	129
	12.20 Binocular Parallax	130
	12.21 Vergence	131
	12.22 Summary	131
Citations		133

Chapter 1

The Basics of Light, Color, and Vision

The human visual system uses both monocular (one-eye) and binocular (two-eye) visual cues in order to enable depth perception¹. Human vision involves light from the three-dimensional world being projected onto the two-dimensional retinas. Because of this, visual cues must be used in order to infer depth, i.e. in order to enable the visual perception of the three-dimensional nature of the external world².

It is often thought by the general public that human depth perception arises solely from the use of two eyes. However, traditional computer screens, mobile device screens, television screens, projector screens, paintings, drawings, photographs, and printed posters all present the same image to both eyes (except in the rare cases where lenticular lens, holography, "3D" glasses, or other stereoscopic systems are used). Therefore, the perception of depth that is experienced when viewing images presented through any of these methods relies solely on one-eye depth perception cues³. In other words, in almost all situations where a human is viewing a three-dimensional object that is not literally present in physical form, it is only monocular depth cues that are being used to perceive depth, and not binocular depth cues. For this reason, monocular depth perception cues are far more significant and are used far more frequently than many people realize.

Artists who draw, paint, or print on flat surfaces, as well as illustrators, graphic designers, and computer animators, all rely solely on monocular depth perception cues in most cases in order to convey a sense of depth⁴. As such, becoming an expert in any of these fields involves learning the foundational principles of human monocular depth perception.

Binocular depth perception cues exploit the use of two eyes that are laterally separated by a fixed distance⁵. Humans can only make use of binocular depth cues when directly viewing the physical three-dimensional world and when viewing images created by stereoscopic systems such as "3D" movies, holograms, stereoscopes, and lenticular lens systems. In all other cases—such as when viewing paintings, drawings, photographs, magazines, posters, television screens, movie screens, computer screens, and mobile device screens—the human visual system must rely solely on monocular depth cues.

The purpose of this book is to pursue a systematic investigation of the foundational physics and geometry of human monocular depth perception. Human monocular depth perception is broadly significant because it involves the fields of mathematics, physics, biology, psychology, art,

and engineering. Specifically, human monocular depth perception involves mathematics because it deals with geometric relationships⁶; it involves physics because it deals with the physical nature of light and motion⁷; it involves biology because it deals with the human eyes and brain⁸; it involves psychology because it deals with human perception⁹; it involves art because it is employed by artists to create a convincing sense of depth¹⁰; and it involves engineering because it enables engineers to construct and display three-dimensional models using computers, as well as build machine vision systems¹¹. Therefore, this book should be of interest to mathematicians, physicists, biologists, psychologists, photographers, illustrators, artists, engineers, graphic designers, video game developers, and computer animators. In view of this fact, the language used in this book has been deliberately designed to be accessible to a broad audience.

1.1 Fundamentals of Light and Vision

A physical three-dimensional object in the real world reflects, transmits, or emits light from the various points on its surface. Regardless of where the light originally came from (whether from reflection, transmission, or emission), each point on the object's surface acts like a source of light waves that travel radially outward from that point in all possible directions¹². These light waves then travel outward until they encounter the human eve or some other object. The light coming from the object contains information about the object's shape and its spatial distribution of color, brightness, and polarization¹³. However, as the light waves travel away from the various points on the object's surface, the light waves overlap with each other, thereby mixing up the information that is being carried by the light.

When some of the mixed-up light from the object propagates through a converging lens, the

refractive effects of the lens cause the light waves to be redirected and collected. All of the waves of light that emanated from the same point on the object's surface are redirected by the lens so that they all meet at the same point in space, called the image point. This process happens for all of the sets of light waves emanating from all of the points on the object's surface, meaning that there is a corresponding image point in physical threedimensional space for each object point. The final result is that the light is assembled into a threedimensional optical image which has the same shape, spatial distribution of color, spatial distribution of brightness, and spatial distribution of polarization as the original object. Because there is a unique one-to-one mapping from each object point to an associated image point for every point on the surface of the three-dimensional physical object, the optical image is necessarily threedimensional¹⁴.

However, capturing and effectively analyzing a three-dimensional optical image is difficult. For this reason, a two-dimensional image capture surface is typically used, whether that be a projector screen, a camera sensor, or the eye's retina. The two-dimensional image capture surface intercepts most of the light that was destined to form the three-dimensional optical image. Because of this, the three-dimensional optical image is projected and collapsed down to a two-dimensional image.

Note that the imaging surface captures most of the light associated with the three-dimensional optical image, so it would be incorrect to say that the captured two-dimensional image is a cross-section of the three-dimensional optical image. Rather, the entire three-dimensional image is condensed down to a two-dimensional image and is captured¹⁵. The ultimate result is that when a two-dimensional image capture surface is used to capture the three-dimensional optical image that was formed by a converging lens, the object's

explicit depth information is lost. This is the case with the images captured by human retinas.

However, because of the physics and geometry that constrain how real three-dimensional objects can exist and move throughout threedimensional space, depth information is still indirectly retained in the two-dimensional images that are captured by the retina. The human visual system must therefore use advanced techniques that rely on assumptions about how the physics and geometry works in order to properly extract the indirect depth information contained in the two-dimensional images, as well as fill in some of the depth information that was lost, in order to create the visual experience in the brain of seeing three-dimensional objects. These techniques are called depth perception cues. It's amazing how convincingly three-dimensional our visual perception of the outside world feels despite the fact that our retinas are actually only capturing twodimensional images.

When the light rays coming from an external object encounter the human eye, they first travel through the transparent cornea at the front, then they travel through the aqueous humor behind the cornea, and then they travel through the main lens, as shown in Fig. 1. In doing so, the rays of light are redirected and form an image on the

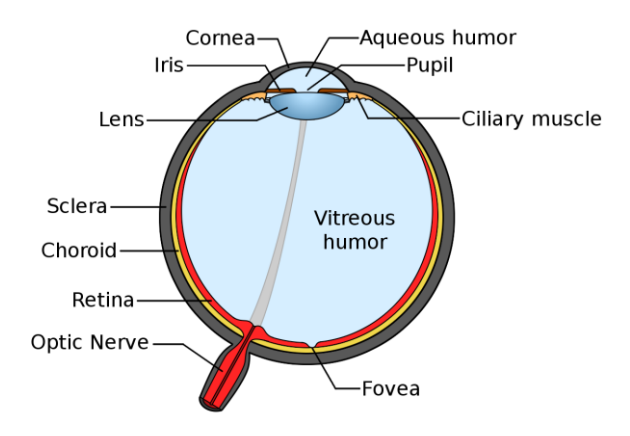


Figure 1. Anatomy of the human eye.

retina that is on the back inner surface of the eye. The cornea, aqueous humor, and the main lens collectively act like a single, effective lens. This effective lens is a converging, adaptive, gradientindex lens¹⁶.

After exiting the lens, these rays of light then travel through the transparent, gel-like vitreous humor and then strike the retina, forming a two-dimensional image that is captured. In this way, the three-dimensional optical image that would be formed by the effective lens of the eye if nothing was in the way is collapsed into a two-dimensional image on the retina.

The retina contains a dense spatial array of photoreceptor cells that are able to capture and convert bits of light to electrical signals¹⁷. After collection and pre-processing of the electrical signals in the eye, these signals are sent along the optic nerves to the brain where they are then assembled and visually experienced as a three-dimensional object.

1.2 Detecting the Properties of Light

Human vision is able to detect and capture four basic properties of light: color, brightness, spatial distribution, and temporal variation.

Brightness is detected by the retina's ability to measure the varying amounts of optical energy density striking a group of photoreceptor cells each fraction of a second and produce electric signals that encode this information¹⁸.

The spatial distribution of the light is captured by employing a spatial array of sensitive photoreceptor cells distributed across the retina.

The temporal variation of the light is captured by continuously reacquiring and stacking images at a high frequency; about 20 to 60 images per second, depending on the illumination levels and other factors¹⁹. The image acquisition frequency of the human visual system depends strongly on the overall brightness of the scene that is being

observed. In low-lighting conditions, the human brain sets the image acquisition frequency to a lower value because this allows the retinas more time to collect more light for each image, thereby boosting sensitivity²⁰. In this way, a high temporal resolution is sacrificed to enable detection of objects in low-lighting conditions.

The ability of human vision to detect the temporal variation information that is carried by a stream of light is crucial to detecting the motion of physical objects. The true motion of an object through three-dimensional space is governed by the laws of physics. Because of this, depth information can be extracted from the observed motion of the object. In this way, the human visual system's ability to detect the temporal variation of the light entering the eye helps enable depth perception. Depth cues that use motion include motion parallax, the kinetic depth effect, and optical expansion.

The high frequency of image acquisition in human vision enables motion perception at a high temporal resolution, which causes depth cues that use motion to be highly effective. For this reason, motion parallax, the kinetic depth effect, and optical expansion tend to be the most accurate and the most frequently used monocular depth perception cues.

Interestingly, because a low lighting condition leads the human visual system to use a low image acquisition frequency, a low lighting condition impairs the use of motion-related depth cues and thereby ultimately causes a decreased ability to properly perceive depth²¹.

1.3 Detecting Color

The color information carried by the light that enters the eye is detected through the utilization of three different types of cone-shaped photo-receptor cells that are sensitive to three different wavelength ranges: long-wavelength colors (L),

mid-wavelength colors (M) and short-wavelength colors (S). The L, M, and S cone cells are often also referred to as red-sensitive, green-sensitive, and blue-sensitive cone cells, respectively. The red-sensitive cone cells can detect red colors more sensitively than the other two cone types. The green-sensitive cone cells can detect green colors more sensitively than the other two types. And the blue-sensitive cone cells can detect blue colors more sensitively than the other two types.

With that said, referring to the cone cells types as red, green, and blue can be misleading because each type detects a wide range of colors rather than just a single color. The red-sensitive cone cells detect red, orange, yellow, and green colors. The green-sensitive cone cells detect red, orange, yellow, green, and blue colors. Lastly, the blue-sensitive cone cells detect green, blue, and violet colors. By comparing the relative strength of the electrical signals coming from a spatial group of L, M, and S cone cells, the human brain is able to reconstruct the original color²².

The central part of the retina called the macula has a far higher density of cone cells than anywhere else in the retina. As a result, the part of the optical image that lands on the macula can be experienced at a far higher resolution than other parts of the image. The central part of the macula, called the fovea, is the part of the macula with the highest cone cell density, reaching a peak density of nearly 200,000 cone cells per square millimeter²³.

The fovea is almost exactly lined up with the eye's optical axis, which is the line that is perpendicular to the plane of the lens and runs through the center of the lens. This arrangement has the benefit of the fovea (which sees with the highest resolution) being placed almost exactly at the location where lies the part of the image that has the highest intensity and the lowest amount of chromatic aberration, because it is lined up with

the center of the lens.

This arrangement also has the benefit of being aligned with the gaze direction, meaning that if a person wants a certain part of a distant object to have its image fall on the fovea, thus enabling the person to see that part of the distant object in the greatest detail, the person must simply gaze directly at that part of the distant object. In other words, in order for a person to see as much detail as possible for a particular part of a distant object, he must simply point the lens of each eye directly at that part of the distant object. No matter where a person looks, the fovea stays aligned with the gaze direction and therefore stays aligned with the highest-resolution part of the received image.

High-resolution color central vision in good lighting is handled by the macula, which is the larger area that contains the fovea. Central vision therefore spans the polar angles from $\theta = 0^{\circ}$ to 9° relative to the optical axis. About 90% of the visual information sent to the brain from the retina originates from the macula. Therefore, the parts of the image of the observed external world that lies at polar angles less than 9° are the most important and seen in the greatest detail. This is not as limiting as it may sound because a person can always redirect his or her gaze to directly look at whatever is interesting and thereby bring the visual perception of it into high resolution.

The visual field that exists outside of central vision, which corresponds to polar angles greater than 9°, is called peripheral vision. The outermost portion of peripheral vision is called far peripheral vision, which corresponds to the polar angles greater than 60°. The highest-resolution vision happens only in the fovea, which spans polar angles from 0° to 1°. Thus, visual activities that require the highest-resolution vision, such as reading and drawing, must happen mostly in the fovea. Because foveal vision only happens for polar angles of less than one degree, a person

must continuously shift his gaze as he reads or draws in order to process the whole page.

Note that the visual field that is experienced by a single human eye does not extend uniformly to the hemisphere's edge at $\theta = 90^{\circ}$. Rather, the portion of the visual field by the nose has its limit typically below 90° (depending on both the gaze direction and the size of the nose), while the portion of the visual field on the side opposite of the nose typically extends beyond 90°. However, for the sake of simplicity, we will assume in this book that the limit of the human monocular visual field is the circle at 90°. Considering that almost all of human vision occurs in the central region and in the near peripheral region, this simplification is not as drastic as it sounds.

In addition to the color-sensitive cone-shaped photoreceptor cells, the retina also contains an array of rod-shaped photoreceptor cells. Under normal lighting conditions, the contributions to vision from the rod cells are negligible. In contrast, under low-lighting conditions, the rod cells are the dominant photoreceptor cells enabling vision. This is because each rod cell is about a hundred to a thousand times more sensitive than a single cone cell, once fully adapted. This is also because there are about twenty times more rod cells in the retina than cones cells, because several rod cells couple to the same single output signal (via the same interneuron), and because rod cells collect light over longer periods of time for each captured image than cone cells.

The price of extremely heightened sensitivity, which is ultimately what enables vision in low-light situations, is that rod-mediated vision has a much lower spatial resolution, a much lower temporal resolution, and zero color differentiation. In everyday terms, this means that when there is very little light present in the environment, humans cannot see details well, cannot see rapid changes well, and cannot see color. However, this is still

Chapter 1. The Basics of Light, Color, and Vision

better than seeing nothing at all when in low-light situations!

In summary, under normal lighting conditions, humans can effectively see and distinguish colors, brightness levels, the spatial distribution of the light, and the temporal variation of the light. In contrast, properties of light which humans cannot see include wave polarization, wave phase, and momentum. However, using appropriately built cameras, humans can indirectly see these other properties of light.

Chapter 2

The Coordinate Systems of Human Monocular Vision

The casting of an image of the three-dimensional world onto the concave spherical retina inside the eye is equivalent to the direct projection of the three-dimensional world onto a convex spherical front surface that is concentric with the eye. The casting of the image that was formed by the eye's effective lens onto the concave retina generates an image that is inverted top-to-bottom and also inverted left-to-right, relative to the true physical reality.

However, when processing the captured optical image, the brain corrects for this inversion by reversing the image bottom-to-top and right-to-left. Thus, the final image that is experienced by the brain is equivalent to the projection of the external world onto a convex spherical mathematical surface that surrounds and is concentric with the eye. For the sake of simplicity, this book will assume that vision consists of the external world being projected directly onto a convex spherical front surface.

Also, for simplicity, let us assume that the eye is always located at the origin of our coordinate system and the eye is always looking in the same direction, which we will call the *z* direction. In this approach, which is often used in computer-aided design and animation, the real-world process of

the eye shifting its gaze in different directions is mathematically implemented by leaving the eye gazing in the z direction and rotating the entire world in corresponding ways. Similarly, the eye physically moving its location (such as when a person walks along a sidewalk) is implemented mathematically by leaving the eye at the origin and shifting the entire world appropriately.

In order to mathematically analyze human monocular depth perception, let us carefully define the most common coordinate systems.

Because the three-dimensional physical world is directly projected onto a two-dimensional convex spherical image capture surface, the location of an object in the captured image, which is what the person sees, is specified using the angular spherical coordinates. As the result of the human retina being spherical, using any other image capture surface will introduce distortions compared to what the eye actually sees. For instance, capturing an image of the real world on a flat camera sensor, which is typically what cameras use, will necessarily introduce distortion. Because such complications do not arise if a real retina is observing the real world, these complications will be avoided until the end of this book.

Let us define the "viewing axis" as the gaze

direction, i.e. the direction that extends from the center of the fovea through the center of the lens to the outside world. I will sometimes also call the viewing axis the "central axis." Because we are only dealing with monocular vision, let us define the observer as a single human eye.

2.1 Defining the Image Coordinates

The angular spherical image coordinates are depicted in Fig. 2. They are defined as follows.

The image point's polar angle θ is the angle between the viewing axis and the line that connects the image point and the observer. The angle θ is zero on the viewing axis and increases in value as it extends away from the viewing axis. This angle ends at the edge of the viewing field, which

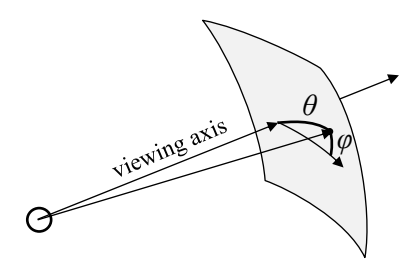


Figure 2. The image coordinate system.

is assumed to be at $\theta = 90^{\circ}$. Sometimes the word "latitude" is used to refer to this type of angle. However, latitude starts at a value of 90° on the viewing axis and decreases until it is zero on the edge of the field of view. In other words, the value for the latitude equals $(90^{\circ} - \theta)$. To avoid unnecessary confusion, latitude will not be used in this book.

The image point's azimuthal angle φ is the angle between the +x axis (which points rightwards along the image capture surface) and the line that connects the image point and the viewing axis. The angle φ is zero when the object is situated directly to the right of the viewing axis and increases in value as the object sweeps counterclockwise.

2.2 Defining the Object Coordinates: Rectangular Coordinates and Cylindrical Coordinates About the z Axis

The true location of a physical object in threedimensional space can be specified using various coordinate systems. One of the most commonly used object coordinate systems is the rectangular coordinate system. The rectangular coordinate system is especially appropriate when the physical objects are rectangular solids, as is often the case with human-made objects.

In the process of determining the manner in which the object point in rectangular coordinates physically maps to the corresponding image point in spherical coordinates, we end up establishing another coordinate system, which is cylindrical coordinates about the z axis. Thus, rectangular coordinates and cylindrical coordinates about the z axis must be handled at the same time. Note that we are using a left-handed rectangular coordinate system in this book because that is the most natural system to use from the viewpoint of the human eye.

The rectangular object coordinates and the cylindrical object coordinates about the z axis are shown in Fig. 3. They are defined as follows.

The *x* coordinate is the horizontal distance of the object from the viewing axis along the object plane. The object plane is the flat plane that contains the location of the object and is perpendicular to the viewing axis. The *x* coordinate starts at zero on the vertical axis of the object plane and increases in value as it extends rightward away from the vertical axis.

The y coordinate is the vertical distance of the object from the viewing axis along the object plane. The y coordinate starts at zero on the horizontal axis of the object plane and increases in value as it extends upward away from the horizontal axis.

The z coordinate is the distance between the

Chapter 2. The Coordinate Systems of Human Monocular Vision

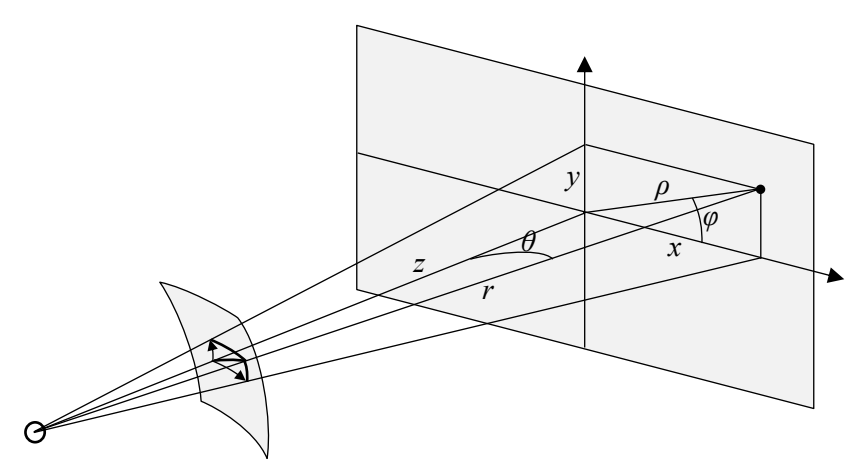


Figure 3. The object coordinate system for rectangular coordinates and cylindrical coordinates about the *z* axis.

object plane and the plane that contains the observer that is parallel to the object plane. The *z* coordinate starts at zero on the plane containing the observer and increases in value as it extends forward, away from the observer in a direction that is parallel to the viewing axis.

The cylindrical radial coordinate ρ is the distance between the object's location and the point where the viewing axis intersects the object plane. The ρ coordinate starts at zero on the viewing axis and increases in value as it extends within the object plane away from the viewing axis.

The azimuthal angle φ is the angle between the +x axis and the line within the object plane that connects the object's location and the viewing axis. The angle φ is zero when the object is sitting directly to the right of the viewing axis (i.e. on the +x axis) and increases in value as the object sweeps counterclockwise around the viewing axis while staying within the object plane.

The azimuthal angle of cylindrical coordinates about the z axis is the same as the azimuthal angle of spherical coordinates. This means that the azimuthal angle of the object's physical location has the same value as the azimuthal angle of the observed location on the image capture surface.

The radial distance r is the distance between the observer and the object. The radial distance is not actually part of the rectangular coordinate system or the cylindrical coordinate system about the z axis, but is defined here because it will be needed in the derivations. The r coordinate starts at zero at the observer's location and increases in value as the object moves radially away from the observer.

In summary, when specifying the location of the physical object in rectangular coordinates, we use the coordinates (x, y, z). When specifying the location of the physical object in cylindrical coordinates about the z axis, we use the coordinates (ρ, φ, z) . At the same time, the observed location of the object on the convex spherical image capture surface is specified by the angular spherical coordinates (θ, φ) . We can derive the relationships between these various coordinate systems.

Applying the laws of trigonometry to the right triangle formed by the x, y, and ρ axes, we find:

$$\rho^2 = x^2 + y^2 \tag{1}$$

$$\sin \varphi = \frac{y}{\rho} \tag{2}$$

$$\cos \varphi = \frac{x}{\rho} \tag{3}$$

$$\tan \varphi = \frac{y}{x} \tag{4}$$

Applying the laws of trigonometry to the right triangle formed by the z, ρ , and r axes, we find:

Chapter 2. The Coordinate Systems of Human Monocular Vision

$$r^2 = z^2 + \rho^2 \tag{5}$$

$$\sin \theta = \frac{\rho}{r} \tag{6}$$

$$\cos\theta = \frac{z}{r} \tag{7}$$

$$\tan \theta = \frac{\rho}{z} \tag{8}$$

Solving for the spherical image coordinates in terms of the rectangular object coordinates by combining Eqs. 1 and 8, and by rearranging Eq. 4, we find:

$$\theta = \tan^{-1}\left(\frac{\sqrt{x^2 + y^2}}{z}\right) \tag{9}$$

$$\varphi = \tan^{-1}\left(\frac{y}{x}\right) \tag{10}$$

Solving for the spherical imaging coordinates in terms of the cylindrical object coordinates about the *z* axis by rearranging Eq. 8, we find:

$$\theta = \tan^{-1}\left(\frac{\rho}{z}\right) \tag{11}$$

$$\varphi = \varphi \tag{12}$$

The geometry involved when projecting image locations onto a convex spherical image capture surface leads to the spherical coordinates having circular symmetry about the viewing axis. This means that an object that is held at a fixed axial distance ρ and a fixed distance z while being swept

through various azimuthal angles φ will retain a constant polar angle θ . This can be seen in Eq. 11 by the fact that the polar angle of the observed location on the image capture sphere does not depend on the azimuthal angle of the object's physical location.

2.3 Defining the Object Coordinates: Spherical Coordinates

Alternately, we can specify the physical location of the object in three-dimensional space using spherical coordinates. When using a spherical object coordinate system and a spherical image coordinate system, there is symmetry such that the polar angles for both coordinate systems are the same and also the azimuthal angles for both coordinate systems are the same. The spherical object coordinates are shown in Fig. 4. They are defined as follows.

The radial distance r is the distance between the observer and the object, which was defined previously.

The polar angle θ is the angle of the object's physical location relative to the viewing axis.

The azimuthal angle φ is the angle between the x axis and the line connecting the object location and the viewing axis.

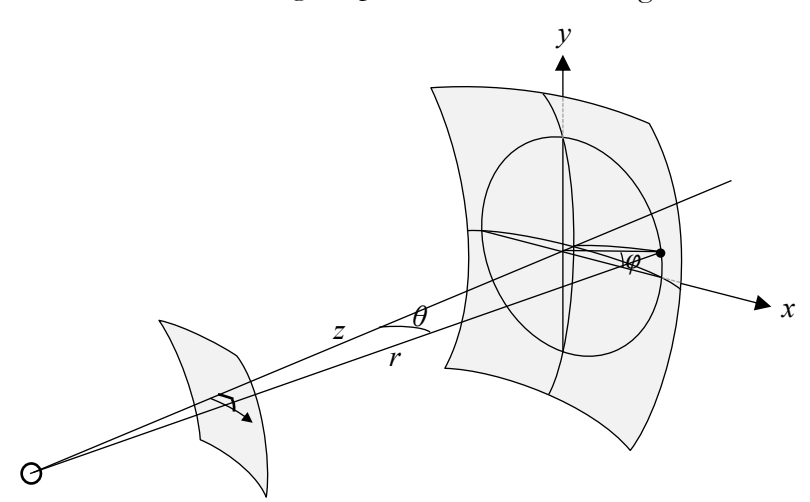


Figure 4. The object coordinate system for spherical coordinates.

For completeness, we write down in Eqs. 13 and 14 the trivial relations between the angular spherical object coordinates and the corresponding angular spherical image coordinates.

Note that the angles θ and φ must be measured in radians because they will be needed in the arc length equations. Also note that the human visual system is such that it cannot directly see the radial distance. As such, two objects that have the same polar angle and the same azimuthal angle but are at different radial distances from the observer will have the same location on the image capture surface and will therefore appear at the same location in the observed image. This can be seen by the fact that Eqs. 13 and 14 do not depend on r.

$$\theta = \theta \tag{13}$$

$$\varphi = \varphi \tag{14}$$

2.4 Defining the Object Coordinates: Cylindrical Coordinates About the *y* Axis

The last commonly used object coordinate system is cylindrical coordinates about the *y* axis. This coordinate system can be pictured as being defined by the cylindrical surface containing the object's location, that is centered on the observer, and that has its axis running parallel to the *y* axis. These object location coordinates are shown in Fig. 5. They are defined as follows.

The angle α is the horizontal angle between the viewing axis and the l line. The l line is the line connecting the observer and the point on the cylindrical surface containing the object's location that has the same x coordinate as the object's location but is parallel to the x-z plane.

The vertical *y* coordinate is the same thing as the *y* coordinate of the rectangular coordinate system, which was defined previously.

The coordinate l is the direct distance between the observer and the cylindrical coordinate object surface. In other words, l is the distance between the observer and the point (x, 0, z) if the object is located at (x, y, z). Or, equivalently, it is the distance between (0, y, 0) and the object's location at (x, y, z).

Applying the laws of trigonometry to the right triangle formed by the x, l, and z axes we find:

$$l^2 = x^2 + z^2 \tag{15}$$

$$\sin \alpha = \frac{x}{l} \tag{16}$$

$$\cos \alpha = \frac{z}{l} \tag{17}$$

$$\tan \alpha = \frac{x}{z} \tag{18}$$

Also, applying the Pythagorean theorem to the right triangle formed by the y, l, and r axes, we find:

$$r^2 = l^2 + y^2 (19)$$

To solve for the spherical image coordinates in terms of the cylindrical object coordinates about the *y* axis, we insert Eqs. 17 and 19 into Eq. 7, as well as insert Eq. 16 into Eq. 10, to find:

$$\theta = \cos^{-1}\left(\frac{l\cos\alpha}{\sqrt{l^2 + y^2}}\right) \tag{20}$$

$$\varphi = \tan^{-1} \left(\frac{y}{l \sin \alpha} \right) \tag{21}$$

Note that Fig. 5 makes clear that the angle α equals the angle θ on the x axis (when y = 0), as can be verified by inserting y = 0 into Eq. 20.

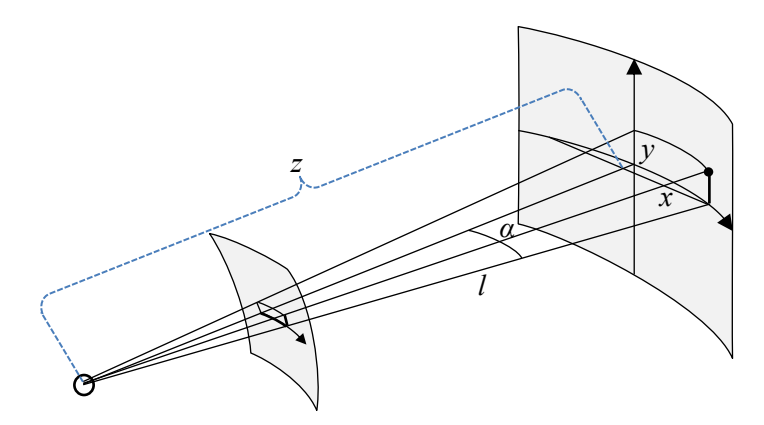


Figure 5. The object coordinate system for cylindrical coordinates about the *y* axis.

Chapter 3

Plotting the Observed Location as a Function of the Object's Physical Location

To get an intuitive sense for the meaning of the equations shown in Chapter 2, which relate the object coordinates to the image coordinates using the various image coordinate systems, and also to help us understand how depth information can be extracted from simple two-dimensional retinacaptured images, let us plot these equations. To focus on the basic aspects at work, let us plot the values of the image coordinates as the object is moved solely along one of the object coordinate directions. Note that in all of the plots below and throughout this book, all distances and lengths are presented in meters.

In addition to determining the observed location of the physical object, as observed in the

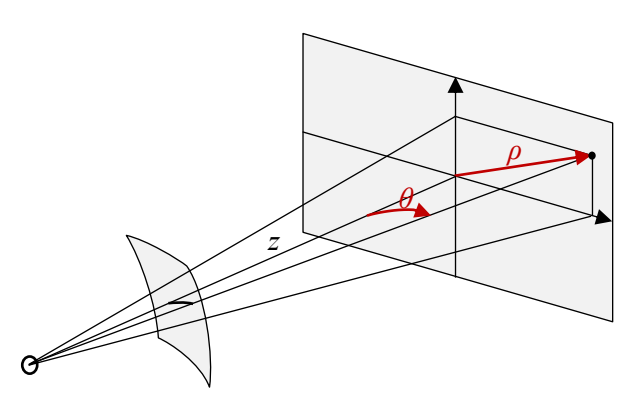


Figure 6. Plotting θ as ρ increases.

captured image, Eqs. 9-10, 11-12, 13- 14, and 20-21 also determine the observed distance between two physical objects and the observed speed of objects, because these both depend trivially on positions. By analyzing these parameters, we can show how depth perception information arises from the relations between the observed position, speed, and distances and the true position, speed, and distances.

3.1 Plotting for Rectangular Coordinates and Cylindrical Coordinates About the z Axis

Fig. 6 shows what it means to be plotting the observed polar angle θ as the object moves so that it's ρ coordinate increases steadily, with everything else held constant. This is equivalent to an object moving directly away from the viewing axis. Fig. 7 shows the resulting plot, showing θ as a function of ρ for various fixed z values, which is the plot of Eq. 11. As expected, the farther away the object gets from the viewing axis, the larger the polar angle at which it appears. However, the correspondence is clearly non-linear. Because of the non-linear relationship, an object at a fixed z that moves with increasing ρ will eventually be visually located in the far peripheral vision and will appear to be moving very slowly.

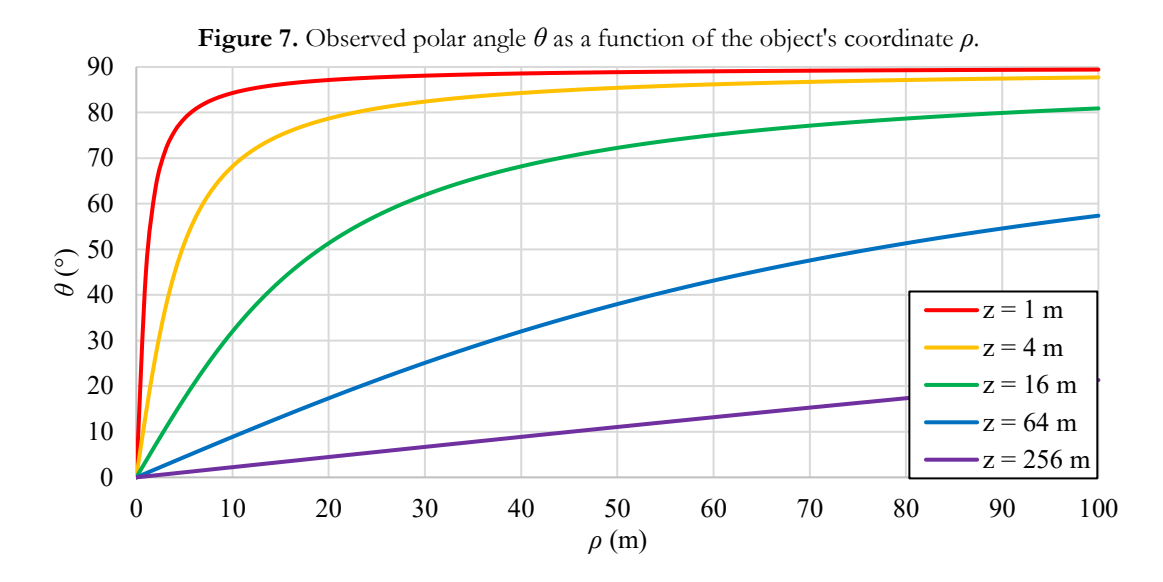
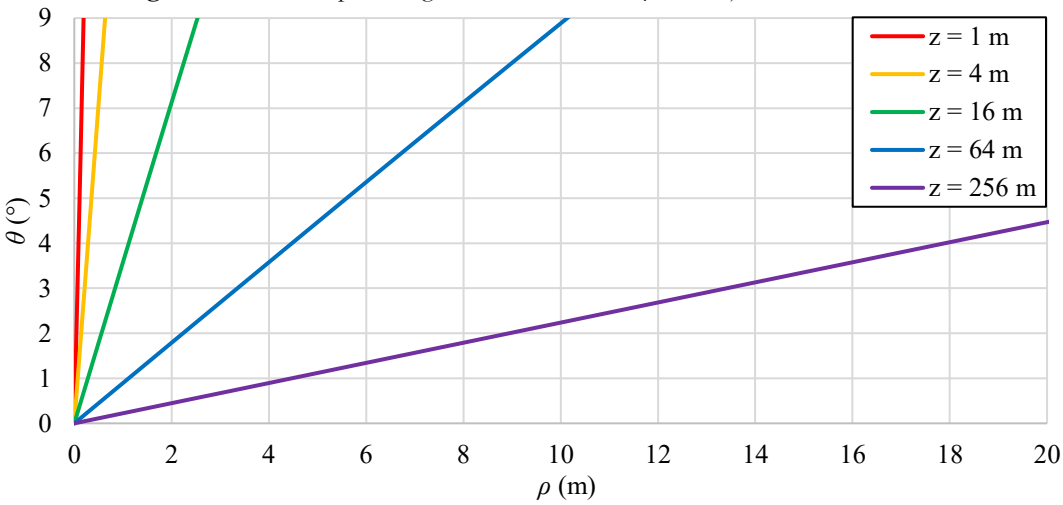


Figure 8. Observed polar angle θ as a function of ρ for objects in central vision.



This effect depends on z. For objects at very large z values, the object has to move a very large distance ρ away from the viewing axis in order to end up in the observed state of nearly motionless in the far peripheral vision. In contrast, objects with increasing distance ρ that are at extremely small z values (i.e. very close to the observer when at $\rho=0$) will almost always be in the observed state of nearly motionless in far peripheral vision. In the limit that a moving object is infinitely far away from the viewing axis $(\rho \to \infty)$ at a fixed z, the object will appear to be perfectly motionless at the polar angle of $\theta=90^\circ$. This means that a

truck that travels at a constant velocity directly eastward across your field of view as you stare continuously northward, and that barely misses you as it passes (so that it's z value is very small), will appear to be moving slowly for a long time, will then suddenly appear to be moving very quickly as it zooms past you, and then will appear to be moving slowly again for a long time.

The dependence on z shown in Fig. 7 means that for a collection of objects that are dispersed uniformly over an x-y object plane that has low z value, most of the objects will appear at large polar angles, i.e. in the peripheral vision.

For instance, for z = 1.0 m, which is about the distance between a desktop computer screen and the eye of a person who is sitting at the desk while looking at the screen, all objects on the screen that are more than $\rho = 1.7$ cm away from the viewing axis will be outside of foveal vision and all objects that are more than $\rho = 16$ cm away from the viewing axis will be outside of central vision. For this reason, a person must constantly shift his gaze to clearly see small objects or words spread out all over the computer screen.

As another example, if you are staring directly at a large fence and you are only a few meters away from the fence, then most of the fence will be in your far peripheral vision.

For object planes very far away from the observer, a wide expanse of objects in that plane will be in central vision. Using the limit for central vision as $\theta = 9.0^{\circ}$, and inverting Eq. 11 in order to apply it to this angle, we find that $\rho = 0.16z$. This means that for each additional 10 meters that the object plane becomes farther away from the observer, an additional 1.6 meters of axial distance enters central vision.

Fig. 8 shows the same information as in Fig. 7, but zoomed in so that now only the angles that correspond to central vision are presented. As this figure shows, the parts of the curves that lie within central vision are always extremely close to being linear. This means that moving objects that stay within central vision while moving in the ρ direction at a true speed that is constant will visually appear to be moving at a constant speed (assuming that the eye's gaze remains fixed). In other words, the observed speed will behave like the object's true speed.

Because humans devote so much of their attention to the central region of vision, the case of the observed motion matching the true motion could be thought of as the normal state of affairs, while the non-linearities that are observed in the

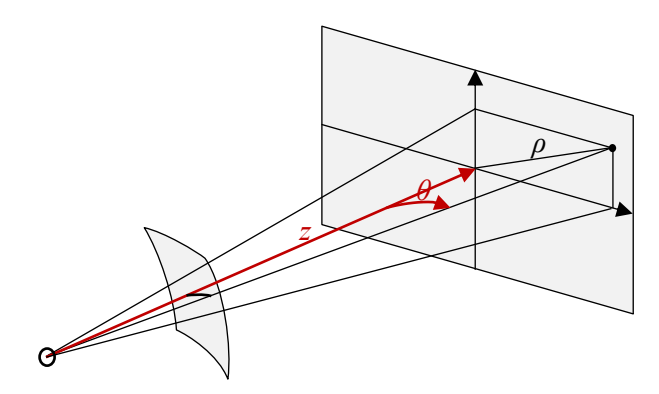


Figure 9. Plotting θ as z increases.

peripheral vision may be thought of as distortions which the brain can ignore or correct for.

Fig. 9 shows what it means to be plotting the observed polar angle θ as the object's z coordinate is increased, but everything else is held constant. This is equivalent to an object that is offset from the viewing axis moving in the z direction. Fig. 10 shows the resulting plot, showing θ as a function of z for various fixed ρ values. This figure is still plotting Eq. 11, but is varying z instead of ρ . This figure shows that the farther away that an object gets in the z direction from the observer, the closer that the object will appear to the $\theta = 0^{\circ}$ point, which we will call the central horizon point. To be clear, the central horizon point is the point where the viewing axis intercepts the spherical image capture surface and is the point where human vision sees with the highest resolution (under normal lighting conditions). In art, this point is often called the central vanishing point.

In the limit that the object is infinitely far away in the z direction, it is observed to be exactly at the central horizon point (i.e. at $\theta=0^{\circ}$) for any finite ρ value. This is called the horizon perspective effect. In everyday language, we say that as an object moves farther away from you (in the z direction), the closer that it visually *appears* to move toward the central horizon point. Note that in everyday life, the word horizon is usually meant to refer to the horizontal line formed where the

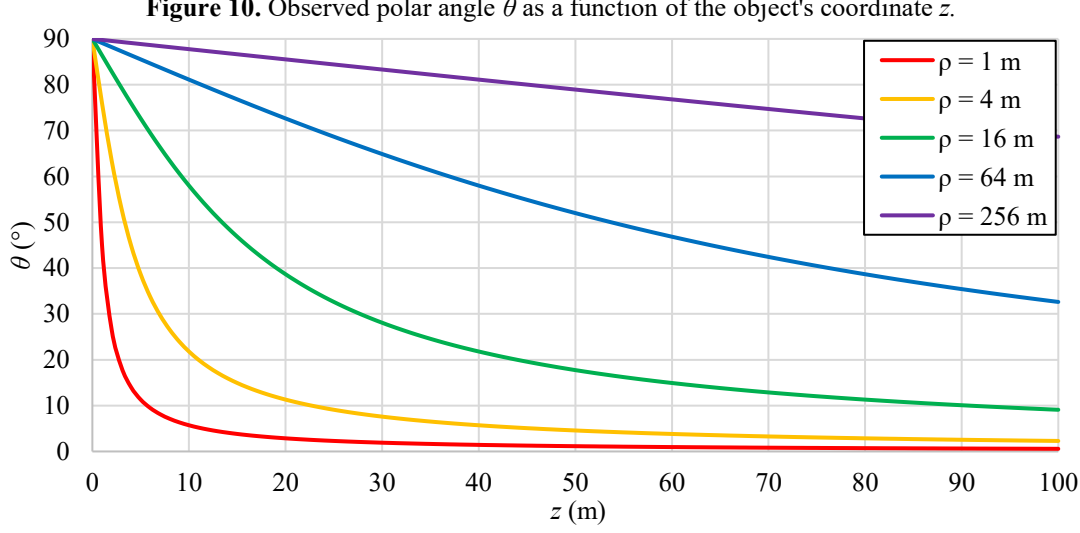


Figure 10. Observed polar angle θ as a function of the object's coordinate z.

distant sky meets the distant ground. However, this is an artifact of earthlings living on an approximately flat, infinite ground plane. In reality, the perspective horizon is the single central point at $\theta = 0^{\circ}$. This effect also leads to the fact that all parallel, straight lines that directly extend away from the observer in the z direction appear to converge at the central horizon point. That's why this point is called the central vanishing point in art and design.

Fig. 10 shows that an object at a fixed ρ value that is traveling away from the observer in the z direction at a constant true speed will appear to initially be moving quickly toward the central horizon point and then later appear to be moving more slowly toward the central horizon point.

Furthermore, Fig. 10 shows that the larger the value of ρ , the more gradual is this transition from moving quickly toward the central horizon point to then moving slowly toward the central horizon point.

Note that a plot of the polar angle θ of the observed location on the image capture sphere as a function of the azimuthal angle φ of the object's physical location is not shown because θ is constant as φ is varied. This can be seen from the fact that Eq. 11 does not depend on φ .

Also note that plots of the observed azimuthal angle φ as a function of the object's z and ρ coordinates are not shown because φ is constant as the object's z and ρ coordinates are varied. This can be seen from the fact that Eq. 12 does not depend on z or ρ . Lastly, a plot of the observed azimuthal angle φ as a function of the object location's true azimuthal angle φ is not shown because they are the same thing, as shown in Eq. 12.

Fig. 11 shows what it means to be plotting the observed polar angle θ as the object's x coordinate increases, but everything else is held constant. Fig. 12 shows what it means to be plotting the observed polar angle θ as the object's y coordinate increases, but everything else is held constant. The situation shown in Fig. 11 is equivalent to an object moving horizontally in a straight line across the observer's field of view, but typically not at the horizon level. This would be like a lowflying airplane traveling continuously eastward across your field of view while you look continuously north at the horizon.

Fig. 13 shows the resulting plot, showing θ as a function of x for various fixed y values when the object is at z = 4 m, which is plotting Eq. 9. There is symmetry such that the curve for the y = 2 m situation is the exactly the same as the curve for

Chapter 3. Plotting the Observed Location as a Function of the Object's Physical Location

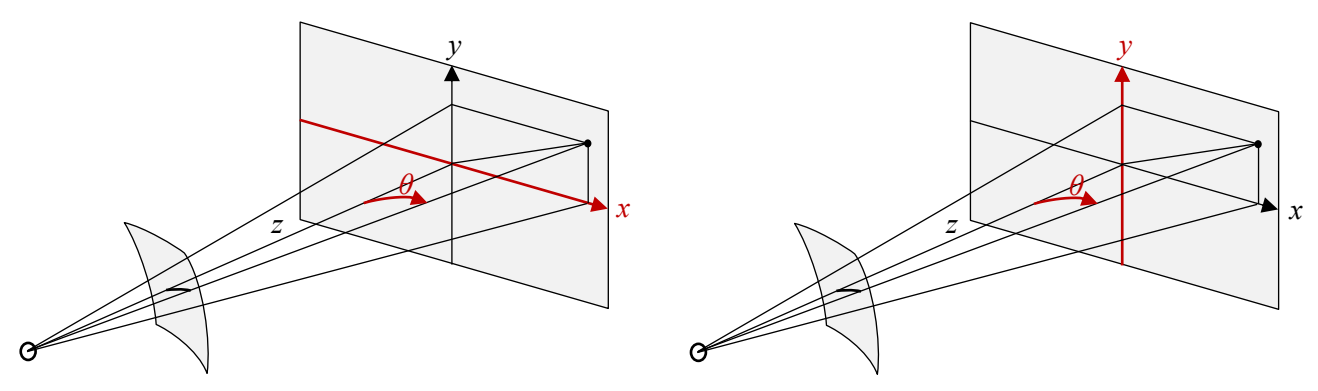
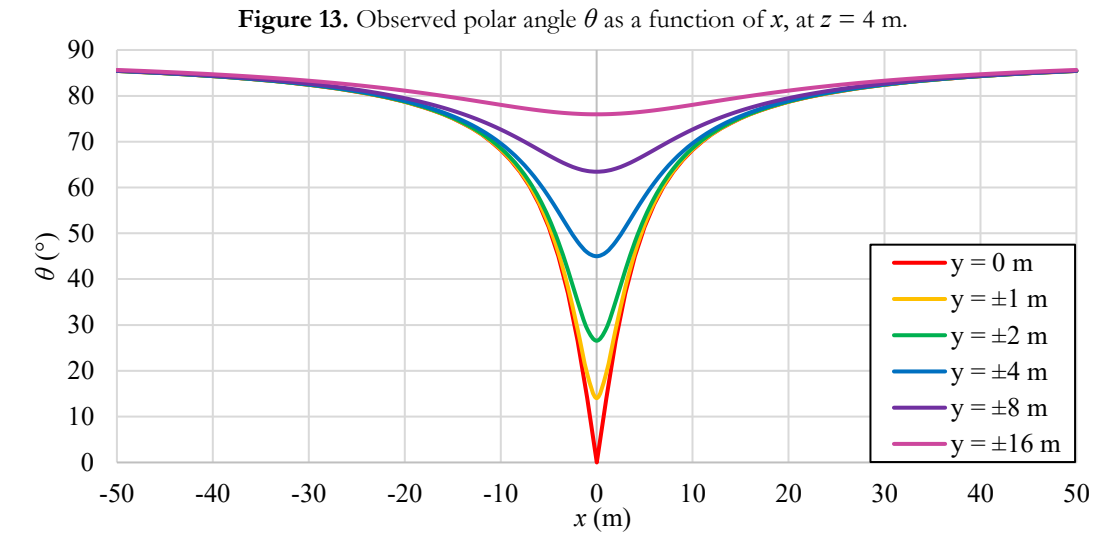


Figure 11. Plotting θ as x increases.

Figure 12. Plotting θ as y increases.



the y = -2 m situation. The same is true of all other values of y.

Fig. 13 shows that an object traveling in the *x* direction with non-zero *y* will appear to momentarily move close to the central horizon point as it passes, but never reaches the central horizon point. The higher the value of the object's *y* coordinate, the less it approaches the central horizon point as it passes by.

Figs. 14 and 15 show the same type of plot as Fig. 13, but now with z = 16 m and z = 64 m, respectively. As these figures show, increasing z causes an object traveling in the x direction at a non-zero y to spend longer at smaller polar angles and to approach closer to the central horizon point when passing.

Fig. 16 shows the exact same information as is

shown in Fig. 15, but zoomed into the region of central vision. This figure shows that for relatively large z values and very small y values, the dependence of polar angle θ on the object's physical x coordinate is approximately linear.

Instead of plotting the observed polar angle θ as a function of the object coordinate x, we can plot it as a function of the object coordinate y. However, because of the symmetry of the viewing geometry, such plots would look exactly the same as the plots in Figs. 13 to 16.

In other words, the situations shown in Figs. 11 and 12 both give rise to the exact same plots (after appropriately relabeling the axes). This is evident from the symmetry of Eq. 9. This makes sense in view of the fact that what we decide to call the *x* axis vs the *y* axis is physically arbitrary.

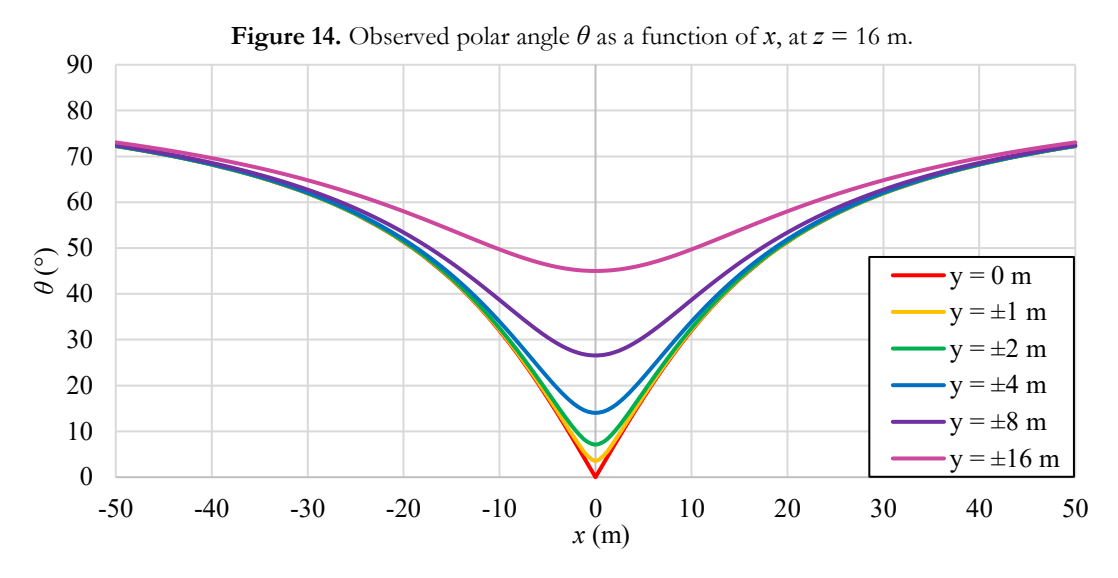


Figure 15. Observed polar angle θ as a function of x, at z = 64 m.

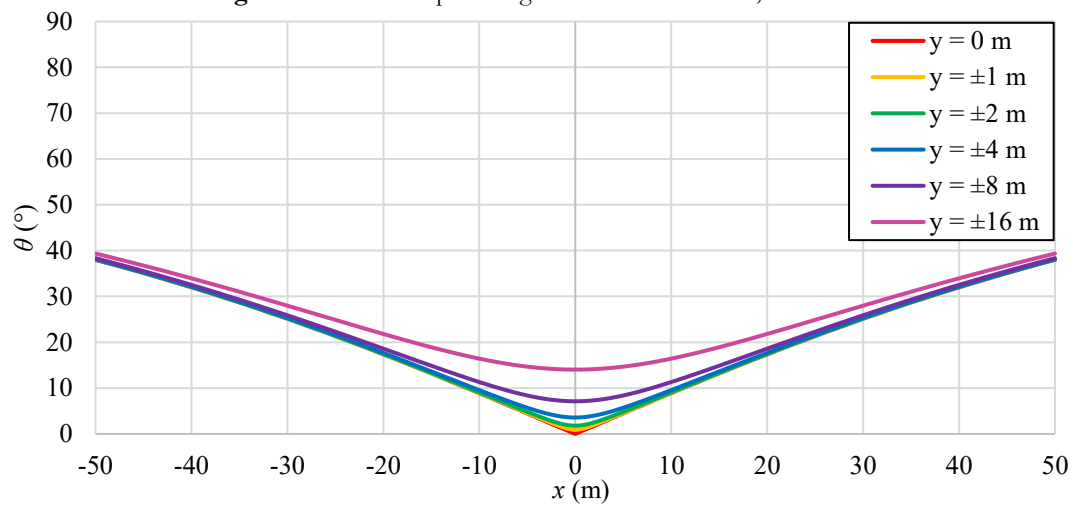
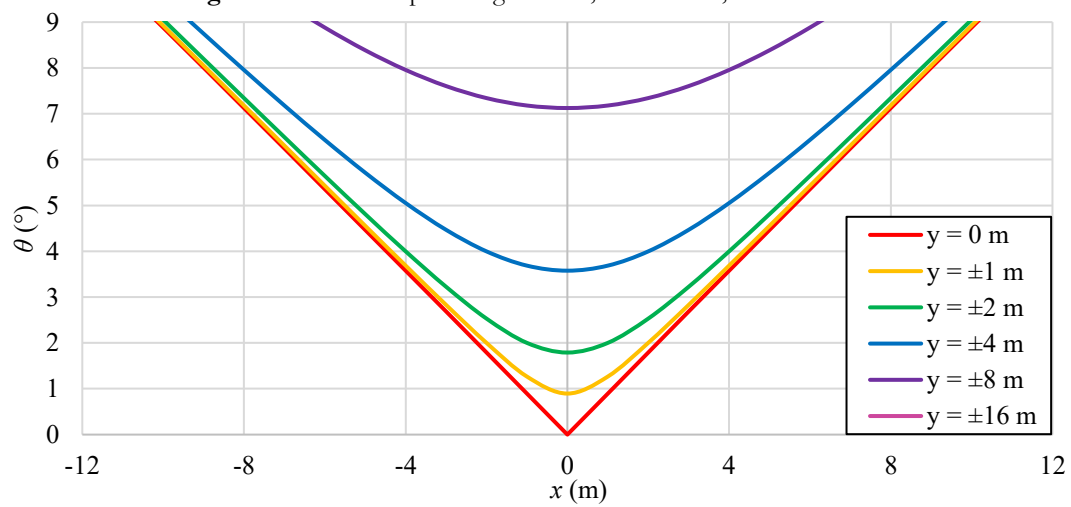


Figure 16. Observed polar angle θ vs x, at z = 64 m, for central vision.



Chapter 3. Plotting the Observed Location as a Function of the Object's Physical Location

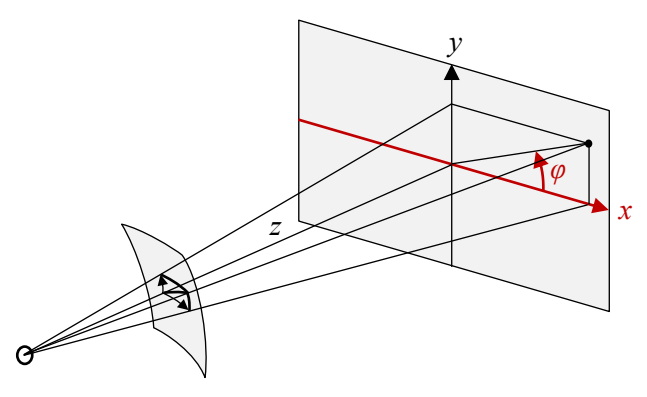


Figure 17. Plotting φ as x increases.

In fact, an object traveling along any straight line in an *x*-*y* object plane will give rise to the same types of curves as in Figs. 13 to 16 (as long as we interpret the direction that the object is traveling as the *x* direction and the direction that is perpendicular to the *x* direction and is in the object plane as the *y* direction).

So far we have only investigated the observed polar angle as a function of rectangular coordinates. Let us now investigate the observed azimuthal angle.

Fig. 17 shows what it means to be plotting the observed azimuthal angle φ as the object's x coordinate increases, but while everything else is held constant. Fig. 18 shows what it means to be plotting the observed azimuthal angle φ as the object's

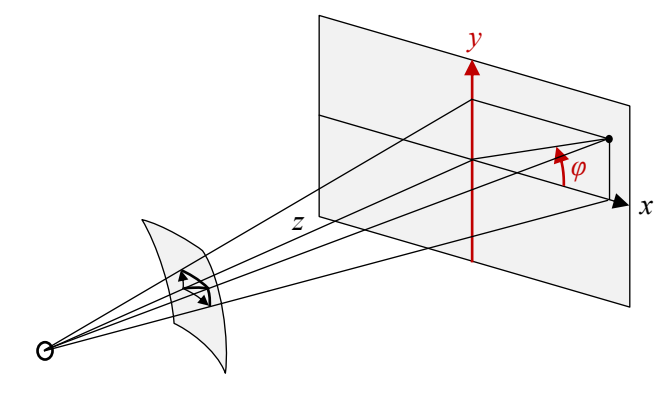
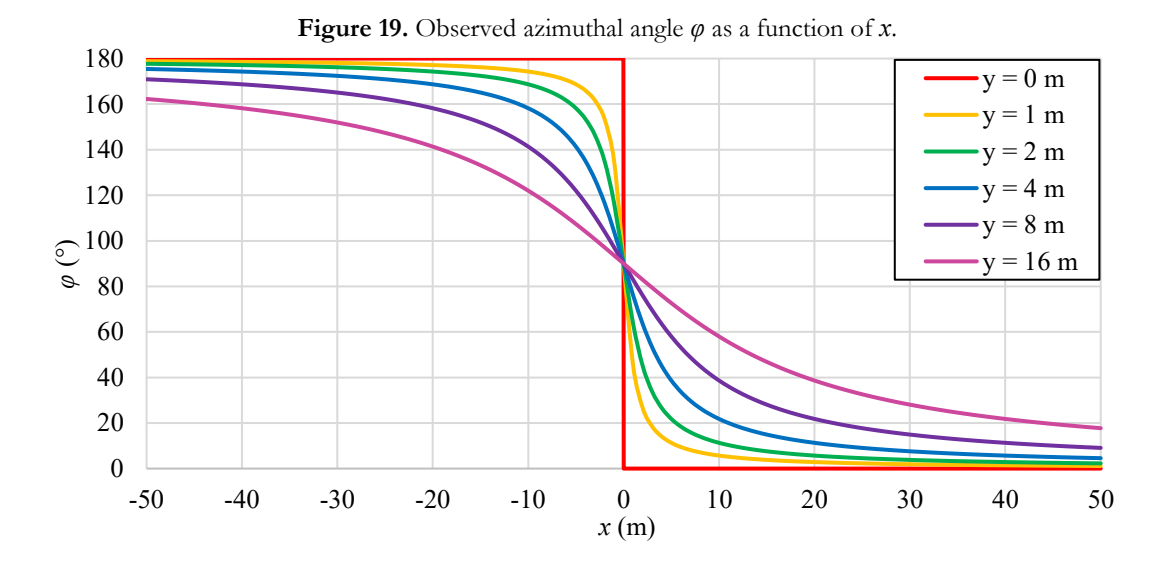


Figure 18. Plotting φ as y increases.

y coordinate increases, but while everything else is held constant. Fig. 19 shows the resulting plot of the situation in Fig. 17, which is the result of plotting Eq. 10.

Fig. 19 shows that an object traveling in the x direction with non-zero y will start at $\varphi = 180^{\circ}$ when it is infinitely far away in the -x direction, meaning that it is exactly to the left of the central horizon point. It will then sweep through the azimuthal angles from 180° to 0° as it passes the observer, and then will end up at 0° when it is infinitely far away in the +x direction, meaning that it is exactly to the right of the central horizon point. Fig. 19 also shows that the greater the value of the object coordinate y, the more gradually the object sweeps through all of these angles.



19

Note that due to symmetry, an object traveling in the y direction at a fixed x value will have the exact same plots as an object traveling in the x direction at a fixed y value (aside from an overall angle offset and vertical axis flip because of where $\varphi = 0$ is defined). In other words, the situations shown in Figs. 17 and 18 ultimately both have the same types of curves.

Fig. 19 only shows curves for positive y values. Due to symmetry, the curves for negative y values would have the same trends as in Fig. 19 but would be inverted vertically in the plot because each curve would sweep from -180° to -90° to 0° instead of sweeping from +180° to +90° to 0°.

A plot of the observed azimuthal angle φ as a function of the object coordinate z is not shown because φ is constant as the object's z coordinate changes. This is shown by the fact that Eq. 10 is independent of z. We already encountered this fact when discussing the coordinate system of cylindrical coordinates about the z axis because rectangular coordinates and cylindrical coordinates about the z axis both include the same z coordinate.

3.2 Plotting for Spherical Coordinates

The observed polar angle θ does not change as the object location's spherical coordinates r and φ are changed. Also, the observed azimuthal angle φ does not change as the object location's spherical coordinates r and θ are changed. These facts can be seen in Eqs. 13 and 14. For these reasons, none of these situations have meaningful plots and therefore none of these situations are plotted.

Furthermore, the observed polar angle θ of the object's location on the image capture sphere and the polar angle θ of the object's true location are exactly the same, as shown in Eq. 13. Similarly, the observed azimuthal angle φ and the object's true azimuthal angle φ are exactly the same, as shown in Eq. 14. Therefore, these two situations

have trivial plots and are therefore not plotted. These results arise from the fact that the object's true location coordinate system is spherical and the object's observed location coordinate system is spherical, and both systems are centered on the observer and aligned with each other.

This means that any time an object moves at a true constant speed along a curved path that is part of a sphere centered on the observer, the object will also visually appear to travel at a constant speed across the observer's field of view.

Additionally, this means that if an object is moving in the radial direction (i.e. directly toward or away from the observer in any r direction), its observed location will remain constant so that its location will visually appear to be motionless. (Its observed size, however, will change.)

3.3 Plotting for Cylindrical Coordinates About the *y* Axis

Fig. 20 shows what it means to be plotting the observed polar angle θ as the object's α coordinate increases, for various y values, while l is held fixed. This is equivalent to an object moving to the right while staying on a cylindrical surface that has its axis vertical and running through the observer's location.

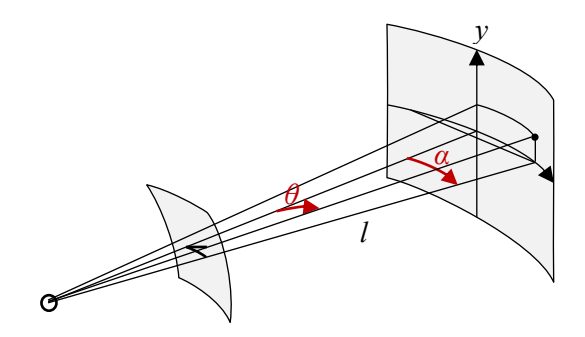


Figure 20. Plotting θ as α increases.

Fig. 21 shows the resulting plot, plotting θ as a function of α , for various y values when l is held fixed at l = 4 m, which is the plot of Eq. 20. The larger the α angle is, the more that the object ends

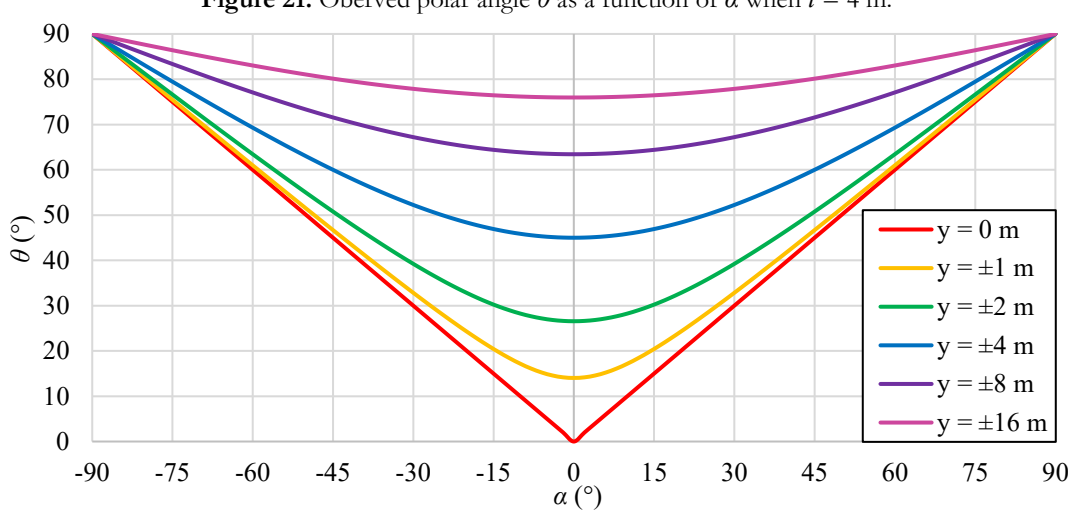
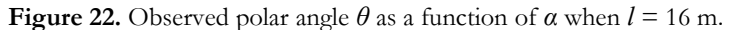
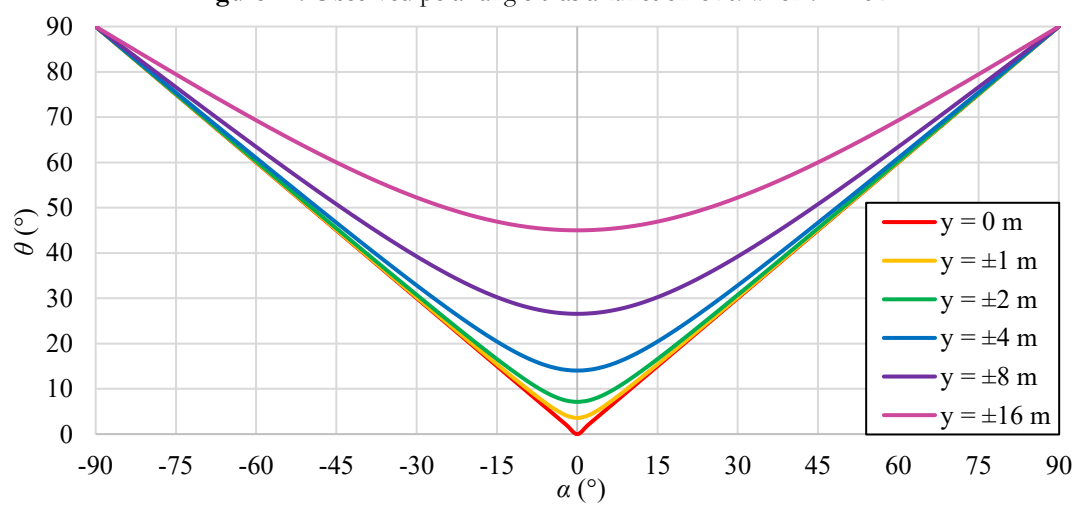
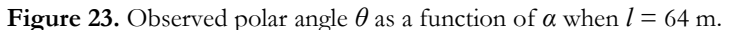
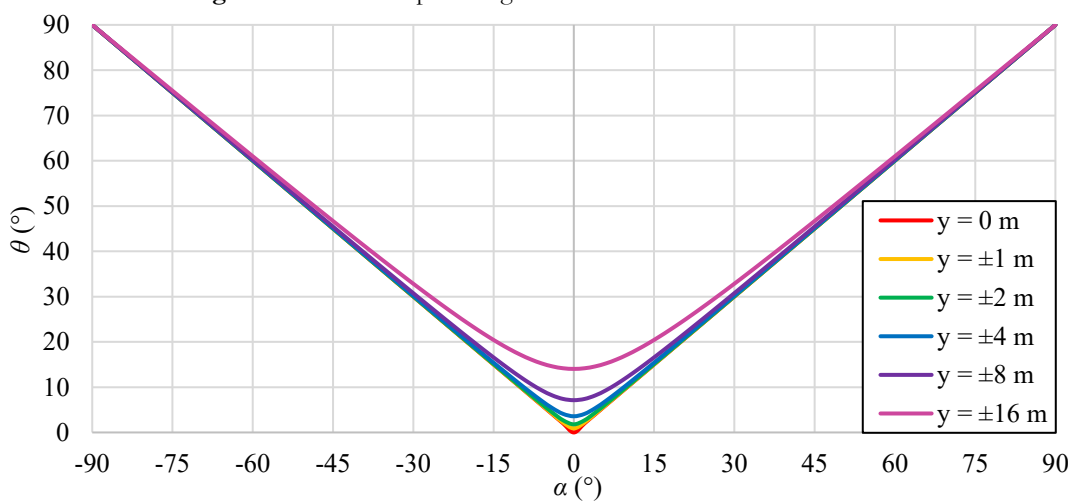


Figure 21. Oberved polar angle θ as a function of α when l=4 m.









up in the far peripheral vision. Furthermore, an object with a large y value that is traveling to the right along the cylindrical surface is farther from the central horizon point as it passes. An object moving in the α direction, starting at $\alpha = -90^{\circ}$, starts in far peripheral vision to the left of the central horizon point, moves close to the central horizon point as it zooms by, and then ends up in far peripheral vision to the right of the central horizon point. For an object location with a y value that is larger than about a quarter of its lvalue, it remains in far peripheral vision the entire time as it moves in the α direction.

Figs. 22 and 23 show the same type of plot as Fig. 21, but now with l = 16 m and l = 64 m, respectively. As these figures show, increasing l causes an object that is traveling rightwards along a cylindrical surface about the y axis to approach closer to the central horizon point. For an object with an *l* coordinate value that is much larger than its y value, and it moves rightwards across the cylinder, the curve would be approximately linear, as shown in Fig. 23. This means that such an object would visually appear to be moving at a constant speed.

Fig. 24 shows what it means to be plotting the observed polar angle θ as the object's y coordinate

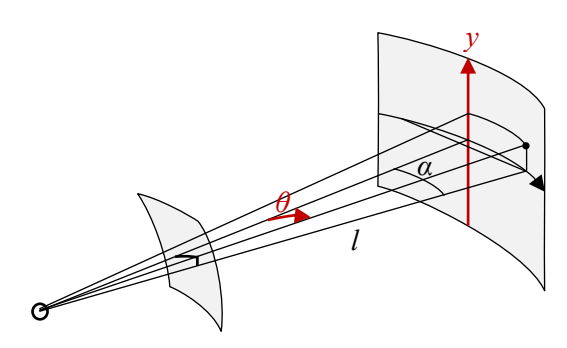


Figure 24. Plotting θ as y increases.

increases in cylindrical coordinates about the y axis, but while everything else is held constant. This is equivalent to an object that is laterally offset moving in the y direction, for various lateral offsets.

Fig. 25 shows the resulting plot, where θ is a function of y for various α values when l = 4 m, which is plotting Eq. 20. The result is similar to the result in Fig. 13, because the geometries are similar.

Figs. 26 and 27 show the same situation as in Fig. 25 but with l = 16 m and l = 64 m, respecttively. As is evident in these figures, increasing l causes the curves to flatten so that the changes in polar angle are more gradual and are overall lower, meaning that the object spends less time in far peripheral vision.

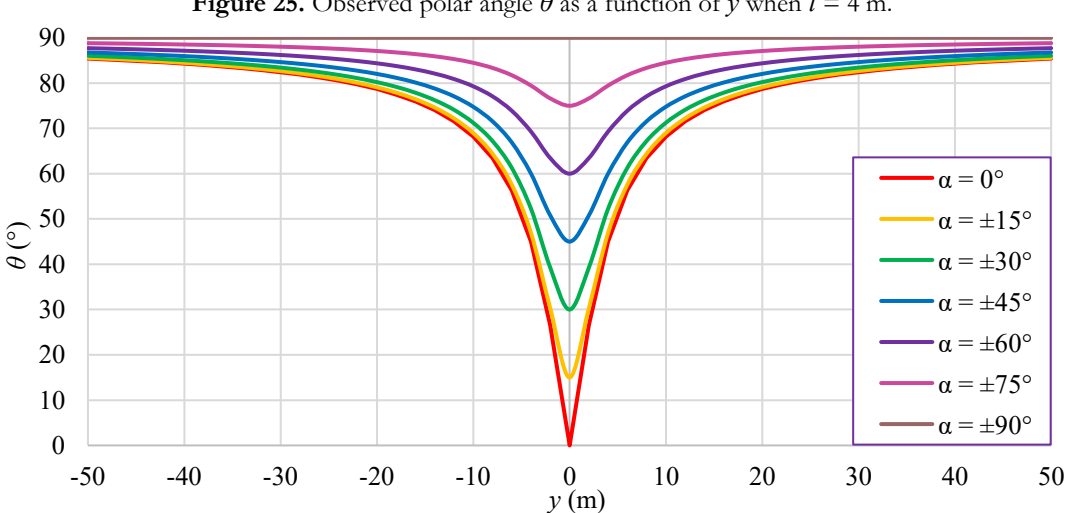


Figure 25. Observed polar angle θ as a function of y when l = 4 m.

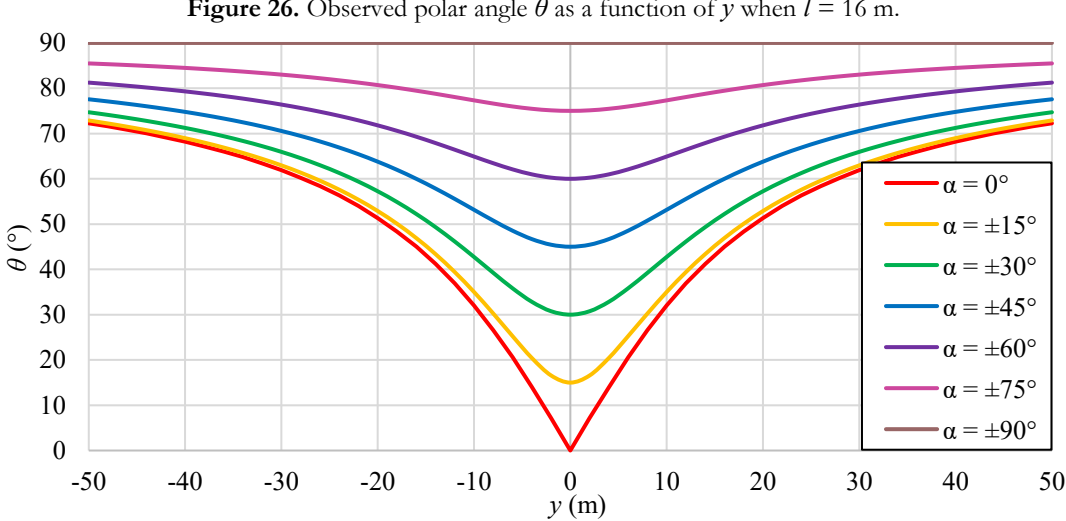
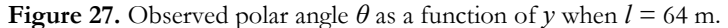


Figure 26. Observed polar angle θ as a function of y when l = 16 m.



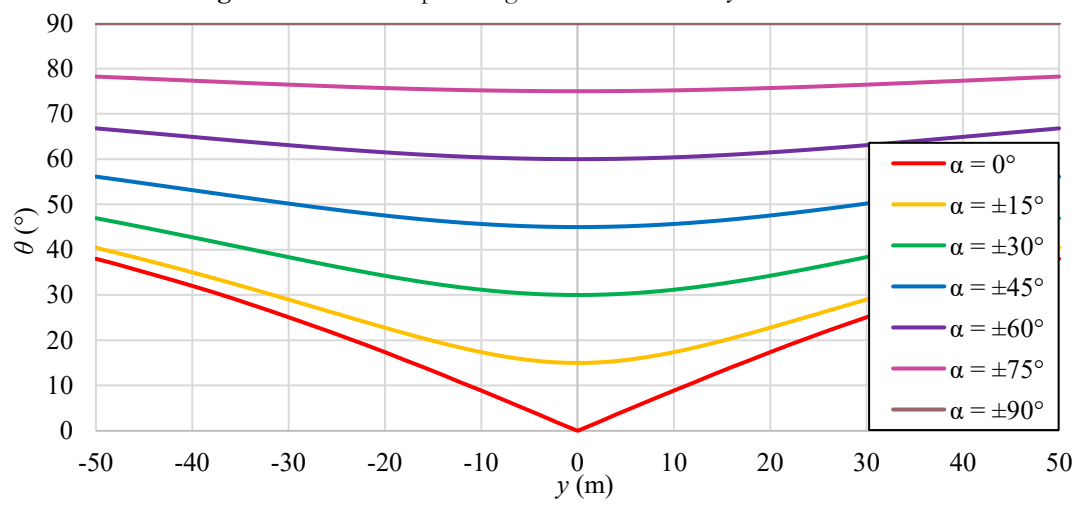


Fig. 28 shows what it means to be plotting the polar angle θ as the object's l coordinate increases, while everything else is held constant. This is equivalent to an object moving horizontally away from the observer so that l increases, but such that α and y are constant.

Fig. 30 shows the resulting plot, showing θ as a function of l for various fixed α values while yis fixed at y = 4 m, which is plotting Eq. 20. As lincreases without α increasing, the object is observed to move from far peripheral vision toward the central horizon point. This is again the perspective horizon effect.

However, the observed polar angle levels off at a non-zero value as *l* increases toward infinity and never actually reaches the central horizon point (except for the trivial case of $\alpha = 0$). This is because an object traveling in the +l direction is physically increasing its distance from the viewing axis. As l increases to large values, the object location's y value becomes negligible in comparison, so that the object is eventually effectively moving in the r direction at a fixed θ value.

Fig. 29 shows what it means to be plotting the observed azimuthal angle φ as the object's y coordinate increases, but while everything else is held

Chapter 3. Plotting the Observed Location as a Function of the Object's Physical Location

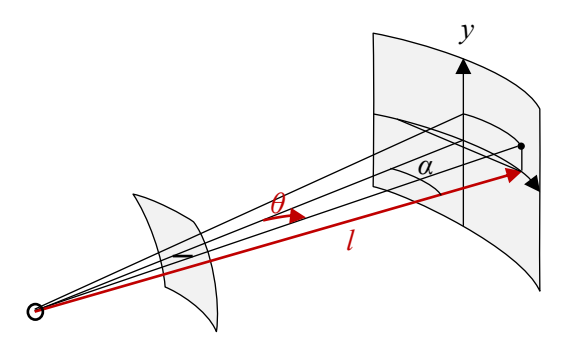


Figure 28. Plotting θ as l increases.

Figure 29. Plotting φ as y increases.

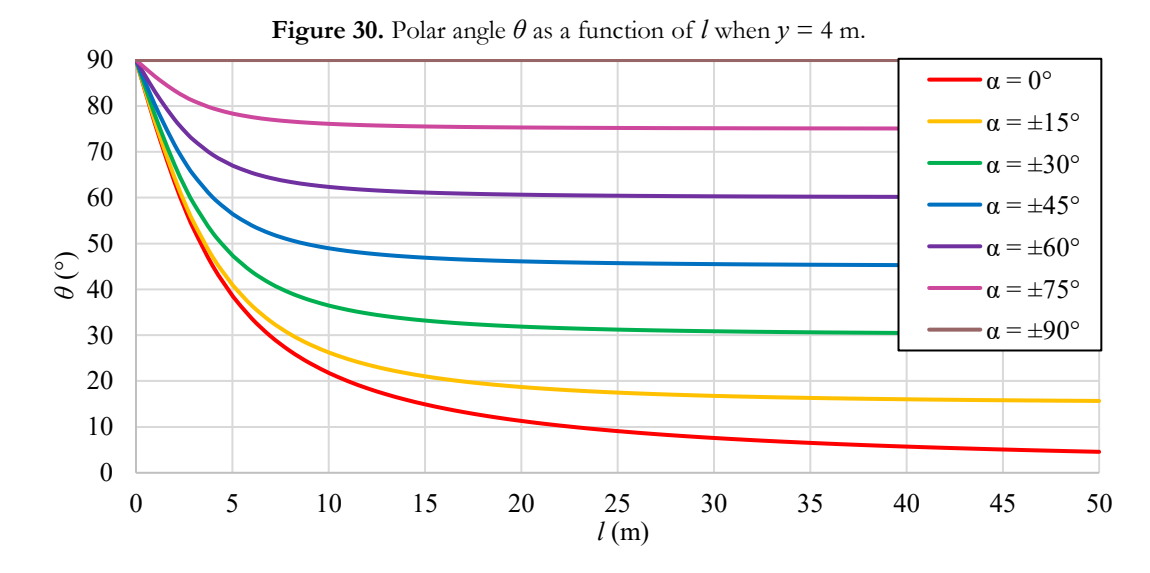
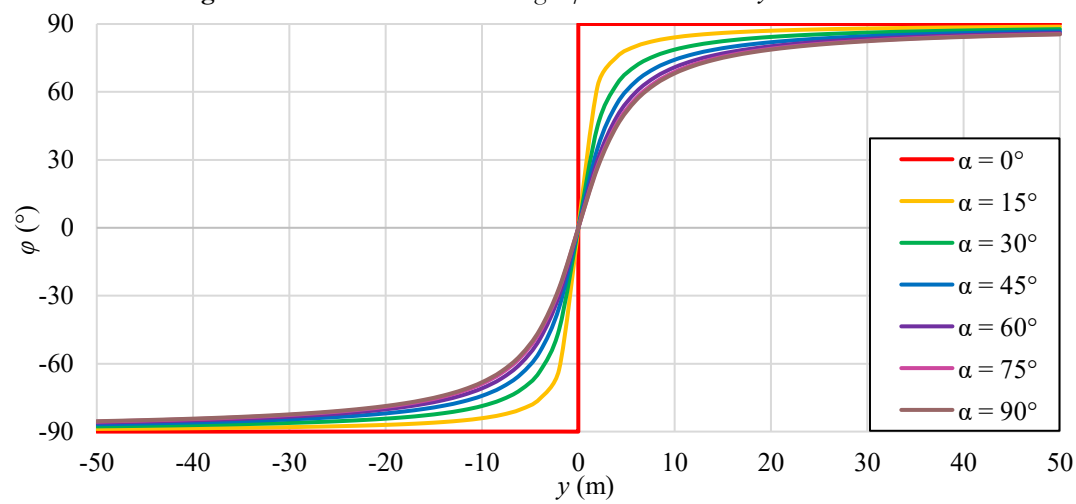


Figure 31. Observed azimuthal angle φ as a function of y when l=4 m.



constant. This is equivalent to an object that is laterally offset from the viewing axis moving in the *y* direction, for various lateral locations on the cylindrical surface. Fig. 31 shows the resulting

plot, showing φ as a function of y for various fixed α values and at l=4 m, which is plotting Eq. 21. As we can clearly see, Fig. 31 shows that an object at a positive, fixed α angle value that is

traveling in the y direction will start at $\varphi = -90^{\circ}$ when it is infinitely far away in the -y direction, meaning that it is situated downward, will then sweep through the azimuthal angles from -90° to $+90^{\circ}$ as it travels in the y direction and passes the observer, and then will end up at +90° when it is infinitely far away in the +y direction, meaning that it is situated upward. Fig. 31 also shows that the farther away that the object is from the central horizon point in the α direction, the more gradually it sweeps through all of these azimuthal angles as it travels in the y direction.

Fig. 32 shows what it means to be plotting the observed azimuthal angle φ as the object's lcoordinate increases, but while everything else is held constant. This is equivalent to an object moving horizontally away from the observer so that l increases, but such that α and y are constant.

Fig. 33 shows the resulting plot, showing φ as a function of l for various fixed α values when yis held fixed at y = 4 m, which is again plotting Eq. 21. This figure shows that as *l* increases, the fixed y value becomes increasingly negligible, so that the object appears to be approaching the +xaxis, where the azimuthal angle is zero.

If the object had a negative value for its α angle and *l* increased, then it would simply appear to be

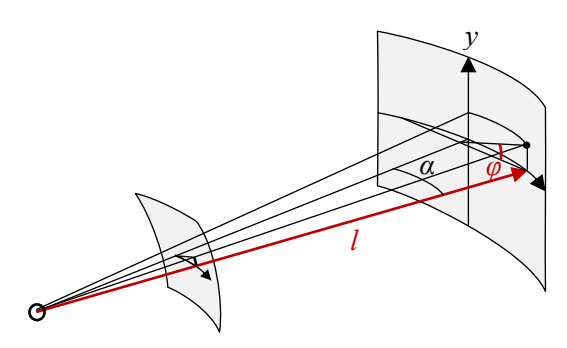


Figure 32. Plotting φ as l increases.

approaching the -x axis, where the azimuthal angle is 180° (which would correspond to a plot that would look like Fig. 33, but flipped top-tobottom and with the vertical axis of the plot labeled running from 90° to 180° instead of from 0° to 90°). This is a type of horizon perspective effect but involving the horizon line instead of the central horizon point.

For instance, an airplane that flies away from the observer in the *l* direction (so that it steadily increases its physical horizontal distance from the viewing axis) but maintains a constant altitude above the level ground will appear to be gradually moving toward the horizon line. In the limit that the airplane is very far away in the *l* direction, it will appear to be at the horizon line.

Fig. 34 shows what it means to be plotting the

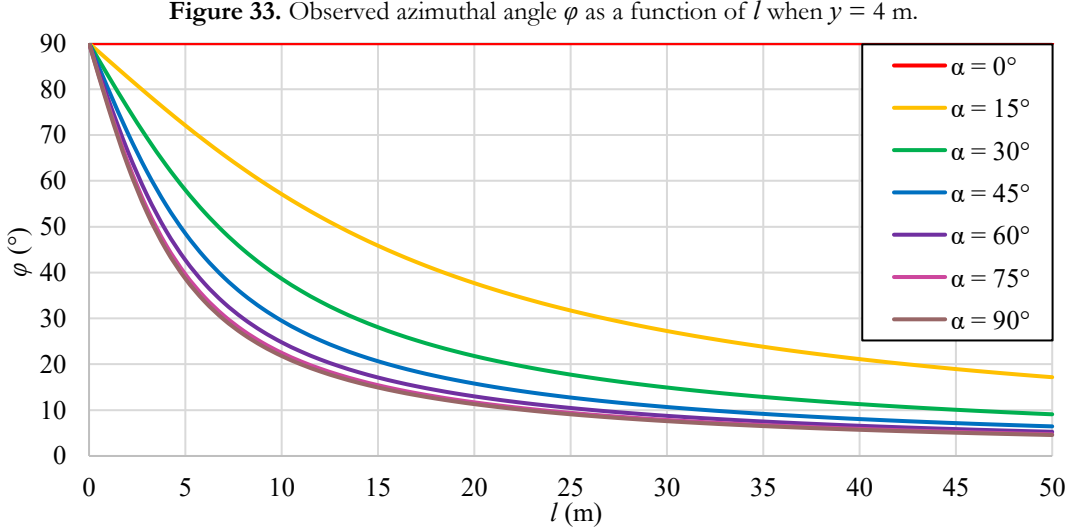


Figure 33. Observed azimuthal angle φ as a function of l when y = 4 m.

Chapter 3. Plotting the Observed Location as a Function of the Object's Physical Location

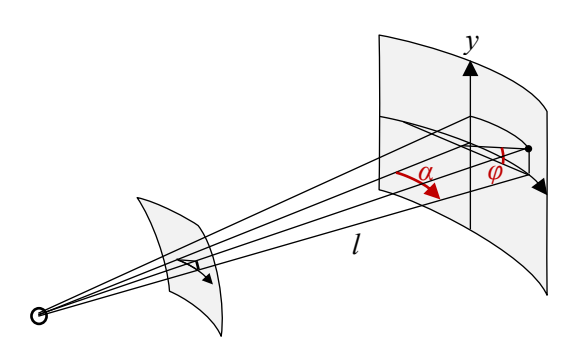


Figure 34. Plotting φ as α increases.

observed azimuthal angle φ as the object's α coordinate increases, but while everything else is still held constant. This is equivalent to an object

moving horizontally along the surface of the cylinder at a certain *y* offset.

Fig. 35 shows the resulting plot, showing φ as a function of α for various fixed y values when l is held fixed at l=16 m, which is again plotting Eq. 21. This figure shows that as α increases, the object appears to approach the +x axis, where φ is zero. However, because of the angular nature of α , the object levels off at a particular non-zero φ value by the time it ends up in far peripheral vision. Note that for negative y values, the curves would be the same as in Fig. 35, except inverted vertically because of the way that φ is defined.

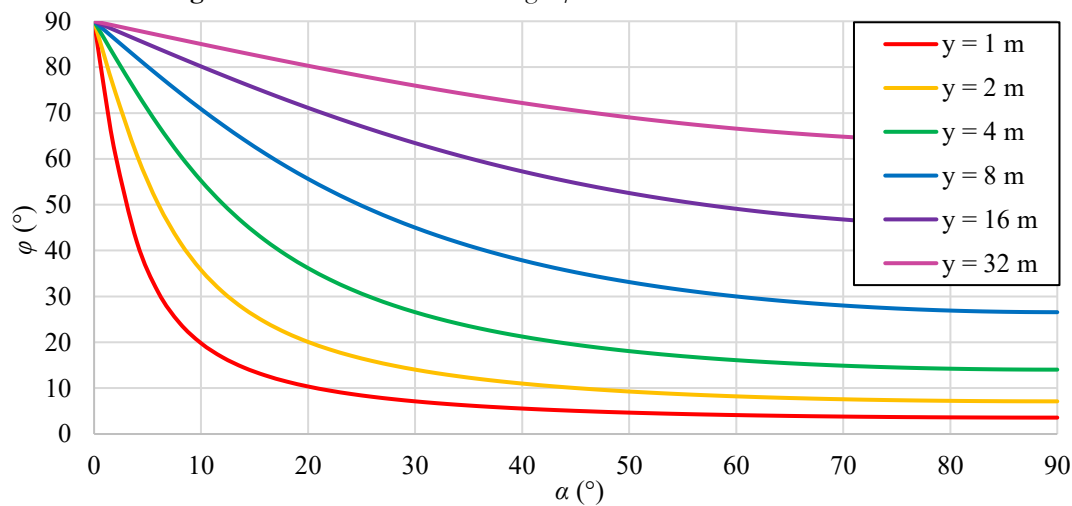


Figure 35. Observed azimuthal angle φ as a function of α when l=16 m.

Chapter 4

Observed Object Length as a Function of Position

As demonstrated in the previous chapter, the geometry of human monocular vision determines the visually perceived positions of objects. This geometry also determines the visually perceived size of objects. In this chapter, we will investigate how this geometry determines the visually perceived length of objects and then, in the next chapter, how it determines the visually perceived area of objects.

The visually perceived length of an object depends on the object's true length, which is obviously different from one object to the next. Therefore, we will not focus here on the absolute visually perceived length, but on the object's relative visually perceived length. We thus need to determine the ratio of an object's observed length to its true length, which we can call the relative observed length or the length magnification.

Because we are dealing with images formed on the human retina, without the aid of any microscopes, telescopes, mirrors, or additional lenses, the image on the retina will always be smaller than the corresponding physical object. Therefore, the magnification values will always have an absolute value that is less than one.

Also, even though the image on the retina is inverted top-to-bottom and left-to-right relative

to the physical object, and therefore the optical magnification has a negative value, the human brain reverses these inversions so that the images are experienced as non-inverted. The net effect is that the final images experienced by the brain are oriented in the same way as the physical object, so that the *overall* magnification values must be positive. Therefore, the inverted images formed on the concave spherical retina are equivalent to non-inverted direct projections of the object onto a corresponding convex spherical surface, as I have already mentioned.

A physical object that is large will have one end at a certain observed location with a certain magnification that corresponds to that location, and the other end at a different observed location with a different magnification that corresponds to that location. This means that the total observed length of a large physical object is found by calculating the integral of the magnification from one end of the object to the other.

Although evaluating such an integral can be done, it is complicated and object-dependent. However, to understand the geometrical effects themselves, we need only to analyze the infinitesimal length elements, such as dx, dy, or $d\rho$. Any real object that is sufficiently small will act to an

excellent approximation as an infinitesimal length element. With this in mind, we will investigate the point-wise length magnification, which equals the ratio of the visually perceived infinitesimal length of an object to the corresponding true infinitesimal length. The point-wise length magnification therefore takes the form of a derivative.

Due to the geometry of human monocular vision, the visually perceived length of an object, and therefore the length magnification, depends directly on the true location of the object in three-dimensional space. Each magnification parameter will therefore be a function of the object's true location coordinates.

In order to investigate the visually perceived length effects separately along each dimension, we assume that the object has length only, which extends along the one dimension of interest, and has no width or depth. (In a subsequent chapter we will consider objects that extend in more than one dimension.) For example, in order to investigate the observed length effects for an object that stretches out in the *x* direction, we use an object that is point-like in the *y* and *z* dimensions and is extended a small length *dx* in the *x* dimension.

When a length magnification parameter is the ratio of an angular observed coordinate to a distance coordinate, the units will mismatch, thereby reducing the meaning of that particular magnification parameter. To avoid this, we replace each infinitesimal angle parameter with its corresponding infinitesimal arc-length parameter. Using the standard arc-length formula from geometry, we find that these arc lengths are:

$$ds'_{\theta} = ad\theta \tag{22}$$

$$ds_{\theta} = rd\theta \tag{23}$$

$$ds_{\varphi}' = a\sin\theta \, d\varphi \tag{24}$$

$$ds_{\varphi} = r \sin\theta \, d\varphi \tag{25}$$

$$ds_{\alpha} = ld\alpha \tag{26}$$

In Eqs. 22 and 23, s_{θ} ' is the arc length that is subtending the polar angle θ and is sitting on the image capture sphere with the radius a, while s_{θ} is the arc length that is subtending the same polar angle but that is sitting on the object location sphere with the radius r. Whereas the polar angle of the object's physical location is the same as the polar angle of the object's observed location, the corresponding arc lengths are not the same. We therefore use the prime symbol to differentiate between the two.

In Eqs. 24 and 25, s_{φ}' is the arc length that is subtending the azimuthal angle φ and is sitting on the image capture sphere with the radius a, while s_{φ} is the arc length that is subtending the same azimuthal angle but that is sitting on the object location sphere with the radius r. In Eq. 26, s_{α} is the arc length that is subtending the angle α and is sitting on the object location cylinder.

We could choose to use the effective radius of the human retina as the value of the image capture sphere's radius a. However, the value for a only determines the overall scale of the observed lengths and not the parameter trends or their relationships. Thus, the actual value of a is irrelevant when analyzing the geometric effects of human monocular vision. Therefore, in order to simplify the equations, let's choose a value of a = 1 meter.

The point-wise length magnification is the ratio of the infinitesimal observed length to the corresponding infinitesimal true length, where we first assume that the true length extends in the direction of one of the basic coordinate dimensions. Each length magnification parameter $M_{a/b}$ therefore follows this pattern of notation:

$$M_{s'_{\theta}/x} = \frac{ds'_{\theta}}{dx} = \frac{ad\theta}{dx} = \frac{d\theta}{dx}$$
 when $a = 1$ (27)

Ultimately what matters is the total observed relative length, and not just one component of the observed relative length, because the eye sees the whole object. Therefore, we will need to combine the components of the observed relative length to find the total observed relative length using an equation of the form:

$$M_{\text{tot./x}} = \sqrt{M_{s'_{\theta}/x}^2 + M_{s'_{\varphi}/x}^2}$$
 (28)

In the derivations below, the resulting equations are presented both as a function of the object's original coordinates and of spherical coordinates.

4.1 Observed Object Length in Rectangular Coordinates/Cylindrical Coordinates About the z Axis

Let us start by examining objects that extend in the various dimensions of cylindrical coordinates about the z axis. To determine the observed length's s_{θ} ' component for an object extended in the ρ direction, we take the derivative of Eq. 11 with respect to ρ (remembering to set a=1 for simplicity):

$$M_{s'_{\theta}/\rho} = \frac{ds'_{\theta}}{d\rho} = \frac{d\theta}{d\rho} = \frac{d}{d\rho} \left(\tan^{-1} \left(\frac{\rho}{z} \right) \right)$$
 (29)

$$M_{s'_{\theta}/\rho} = \frac{z}{z^2 + \rho^2}$$
 or (30a)

$$M_{s_{\theta}'/\rho} = \frac{1}{r}\cos\theta \tag{30b}$$

Because Eq. 12 does not depend at all on ρ , any thin object that is extended only in the ρ direction will be observed to have zero width in the s_{φ} ' direction. In other words:

$$M_{s_{\theta}'/\rho} = 0 \tag{31}$$

The total observed relative length for an object extended in the ρ dimension is the square root of the sum of its components squared:

$$M_{\rm tot./\rho} = \sqrt{M_{s_{\theta}^{\prime}/\rho}^2 + M_{s_{\phi}^{\prime}/\rho}^2} \qquad (32)$$

$$M_{\text{tot.}/\rho} = \frac{z}{z^2 + \rho^2} \text{ or}$$
 (33a)

$$M_{\text{tot.}/\rho} = \frac{1}{r} \cos \theta \tag{33b}$$

Let us now look at an object extended in the z direction. In order to determine the observed length's s_{θ} ' component for an object extended in the z direction, we take the derivative of Eq. 11 with respect to z:

$$M_{s'_{\theta}/z} = \frac{ds'_{\theta}}{dz} = \frac{d\theta}{dz} = \frac{d}{dz} \left(\tan^{-1} \left(\frac{\rho}{z} \right) \right)$$
 (34)

$$M_{s'_{\theta}/z} = -\frac{\rho}{\rho^2 + z^2}$$
 or (35a)

$$M_{s_{\theta}'/z} = -\frac{1}{r}\sin\theta \tag{35b}$$

Note that the negative sign in Eq. 35 means that an object at a certain position offset from the viewing axis that extends in the positive z direction away from the observer will be observed to be extending in the negative s_{θ} ' direction, i.e. toward the central horizon point. This is an important part of the perspective horizon effect. For instance, if a painted stick at an arbitrary location has its red end at a certain z value and its blue end at a larger z value, then its blue end will appear to be closer to the central horizon point. The negative signs in Eq. 35 are also important in ensuring the accuracy of subsequent derivations.

Because Eq. 12 does not depend at all on z, any object that is extended only in the z direction will be observed to have zero width in the s_{φ} ' direction. In other words:

$$M_{s_{\varphi}'/z} = 0 \tag{36}$$

The total observed relative length for an object that is extended in the *z* direction is therefore:

$$M_{\text{tot./z}} = \sqrt{M_{s'_{\theta}/z}^2 + M_{s'_{\varphi}/z}^2}$$
 (37)

$$M_{\text{tot./z}} = \frac{\rho}{\rho^2 + z^2} \text{ or } (38a)$$

$$M_{\text{tot./z}} = \frac{1}{r} \sin \theta \tag{38b}$$

Let us now look at an object extended in the s_{φ} direction. Because Eq. 11 does not depend at all on φ , any object that is extended only in the s_{φ}

direction will be observed to have zero width in the $s\theta'$ direction. In other words:

$$M_{s_{\theta}'/s_{\varphi}} = 0 \tag{39}$$

In order to determine the observed length's s_{φ} ' component for an object extended in the s_{φ} direction, we take the derivative of Eq. 12 with respect to s_{φ} to find:

$$M_{s_{\varphi}'/s_{\varphi}} = \frac{ds_{\varphi}'}{ds_{\varphi}} = \frac{a\sin\theta d\varphi}{r\sin\theta d\varphi} = \frac{1}{r}$$
 (40)

$$M_{s'_{\varphi}/s_{\varphi}} = \frac{1}{\sqrt{\rho^2 + z^2}}$$
 or (41a)

$$M_{S_{\varphi}'/S_{\varphi}} = \frac{1}{r} \tag{41b}$$

The total observed relative length for an object that is extended in the s_{φ} direction is therefore:

$$M_{\text{tot./s}_{\varphi}} = \sqrt{M_{s'_{\theta}/s_{\varphi}}^2 + M_{s'_{\varphi}/s_{\varphi}}^2}$$
 (42)

$$M_{\text{tot.}/s_{\varphi}} = \frac{1}{\sqrt{\rho^2 + z^2}} \text{ or } (43a)$$

$$M_{\text{tot./}s_{\varphi}} = \frac{1}{r} \tag{43b}$$

Let us now look at the objects extended in the various dimensions of rectangular coordinates. In order to determine the relative observed length's s_{θ} ' component for an object that is extended in the x direction, as a function of position, we take the derivative with respect to x of Eq. 9 to find:

$$M_{s_{\theta}'/x} = \frac{ds_{\theta}'}{dx} = \frac{d\theta}{dx} = \frac{d}{dx} \left(\tan^{-1} \left(\frac{\sqrt{x^2 + y^2}}{z} \right) \right) (44)$$

$$M_{s'_{\theta}/x} = \frac{xz}{(x^2+y^2+z^2)\sqrt{x^2+y^2}}$$
 or (45a)

$$M_{s'_{\theta}/x} = \frac{1}{r}\cos\theta\cos\varphi$$
 (45b)

In order to find the relative observed length's s_{φ} ' component for an object that is extended in the x direction, as a function of position, we take the derivative with respect to x of Eq. 10 to find:

$$M_{s'_{\varphi}/x} = \frac{ds'_{\varphi}}{dx} = \frac{a\sin\theta d\varphi}{dx} = \sin\theta \frac{d\varphi}{dx}$$

$$M_{s_{\varphi}'/x} = \sin\theta \frac{d}{dx} \left(\tan^{-1} \left(\frac{y}{x} \right) \right)$$
 (46)

$$M_{s'_{\varphi}/x} = -\frac{y}{\sqrt{x^2 + y^2 + z^2}\sqrt{x^2 + y^2}}$$
 or (47a)

$$M_{s_{\varphi}'/x} = -\frac{1}{r}\sin\varphi \tag{47b}$$

The total observed relative length for an object that is extended in the *x* direction is therefore:

$$M_{\text{tot./x}} = \sqrt{M_{s'_{\theta}/x}^2 + M_{s'_{\varphi}/x}^2}$$
 (48)

$$M_{\text{tot./x}} = \frac{\sqrt{y^2 + z^2}}{x^2 + y^2 + z^2}$$
 or (49a)

$$M_{\text{tot./x}} = \frac{1}{r} \sqrt{1 - \cos^2 \varphi \sin^2 \theta} \quad (49b)$$

In order to find the relative observed length's s_{θ} ' component for an object that is extended in the y direction, as a function of position, we take the derivative with respect to y of Eq. 9 to find:

$$M_{s'_{\theta}/y} = \frac{ds'_{\theta}}{dy} = \frac{d\theta}{dy} = \frac{d}{dy} \left(\tan^{-1} \left(\frac{\sqrt{x^2 + y^2}}{z} \right) \right)$$
 (50)

$$M_{s'_{\theta}/y} = \frac{yz}{(x^2+y^2+z^2)\sqrt{x^2+y^2}}$$
 or (51a)

$$M_{s'_{\theta}/y} = \frac{1}{r}\cos\theta\sin\varphi$$
 (51b)

In order to find the relative observed length's s_{φ} ' component for an object that is extended in the y direction, as a function of position, we take the derivative with respect to y of Eq. 10 to find:

$$M_{s'_{\varphi}/y} = \frac{ds'_{\varphi}}{dy} = \frac{a\sin\theta d\varphi}{dy} = \sin\theta \frac{d\varphi}{dy}$$

$$M_{s_{\varphi}'/y} = \sin\theta \frac{d}{dy} \left(\tan^{-1} \left(\frac{y}{x} \right) \right)$$
 (52)

$$M_{s'_{\varphi}/y} = \frac{x}{\sqrt{x^2 + y^2 + z^2} \sqrt{x^2 + y^2}}$$
 or (53a)

$$M_{s_{\varphi}'/y} = \frac{1}{r}\cos\varphi \tag{53b}$$

The total observed relative length for an object that is extended in the *y* direction is therefore:

$$M_{\text{tot./y}} = \sqrt{M_{s'_{\theta}/y}^2 + M_{s'_{\phi}/y}^2}$$
 (54)

Chapter 4. Observed Object Length as a Function of Position

$$M_{\text{tot./y}} = \frac{\sqrt{x^2 + z^2}}{x^2 + v^2 + z^2}$$
 or (55a)

$$M_{\text{tot./y}} = \frac{1}{r} \sqrt{1 - \sin^2 \varphi \sin^2 \theta} \quad (55b)$$

Note that the z coordinate of the rectangular coordinate system is the same as the z coordinate of the cylindrical coordinate system about the z axis, and therefore the results are the same as in Eqs. 34 to 38. However, for completeness, and to present them in rectangular coordinates, we write them here:

$$M_{s'_{\theta}/z} = -\frac{\sqrt{x^2 + y^2}}{x^2 + y^2 + z^2}$$
 or (56a)

$$M_{s_{\theta}'/z} = -\frac{1}{r}\sin\theta \tag{56b}$$

$$M_{s_{\varphi}'/z} = 0 \tag{57}$$

$$M_{\text{tot./z}} = \frac{\sqrt{x^2 + y^2}}{x^2 + y^2 + z^2}$$
 or (58a)

$$M_{\text{tot.}/z} = \frac{1}{r}\sin\theta \tag{58b}$$

4.2 Observed Object Length in Spherical Coordinates

In order to find the relative observed length's s_{θ} ' component for an object that is extended in the s_{θ} direction, as a function of position, we take the derivative with respect to s_{θ} of Eq. 13 to find:

$$M_{s'_{\theta}/s_{\theta}} = \frac{ds'_{\theta}}{ds_{\theta}} = \frac{ad\theta}{rd\theta} = \frac{1}{r}\frac{d\theta}{d\theta}$$

$$M_{s'_{\theta}/s_{\theta}} = \frac{1}{r}$$
(59)

Because Eq. 14 does not depend at all on s_{θ} , any thin object that is extended only in the s_{θ} direction will be observed to have zero width in the s_{φ} ' direction. In other words:

$$M_{s_{\varphi}'/s_{\theta}} = 0 \tag{60}$$

The total observed relative length for an object that is extended in the s_{θ} direction is therefore:

$$M_{\text{tot./s}_{\theta}} = \sqrt{M_{s'_{\theta}/s_{\theta}}^2 + M_{s'_{\varphi}/s_{\theta}}^2}$$

$$M_{\text{tot./s}_{\theta}} = \frac{1}{r}$$
(61)

In order to find the relative observed length's s_{φ} ' component for an object that is extended in the s_{φ} direction, as a function of position, we take the derivative with respect to s_{φ} of Eq. 14 to find:

$$M_{s'_{\varphi}/s_{\varphi}} = \frac{ds'_{\varphi}}{ds_{\varphi}} = \frac{a\sin\theta d\varphi}{r\sin\theta d\varphi} = \frac{1}{r}\frac{d\varphi}{d\varphi}$$

$$M_{s'_{\varphi}/s_{\varphi}} = \frac{1}{r}$$
(62)

Because Eq. 13 does not depend at all on φ , any thin object that is extended only in the s_{φ} direction will be observed to have zero width in the s_{θ} ' direction. In other words:

$$M_{s_{\theta}'/s_{\varphi}} = 0 \tag{63}$$

The total observed relative length for an object that is extended in the s_{φ} direction is therefore:

$$M_{\text{tot./}s_{\varphi}} = \sqrt{M_{s'_{\theta}/s_{\varphi}}^2 + M_{s'_{\varphi}/s_{\varphi}}^2}$$

$$M_{\text{tot./}s_{\varphi}} = \frac{1}{r}$$
(64)

Because Eqs. 13 and 14 do not depend at all on r, any thin object that is extended only in the r direction will be observed to have zero width in the s_{θ}' and s_{φ}' directions. In other words:

$$M_{s_{\alpha}'/r} = 0 \tag{65}$$

$$M_{s_{\alpha}'/r} = 0 \tag{66}$$

$$M_{\text{tot./}r} = 0 \tag{67}$$

4.3 Observed Object Length in Cylindrical Coordinates About the *y* Axis

In order to find the relative observed length's s_{θ} ' component for an object that is extended in the s_{α} direction, as a function of position, we take the derivative with respect to s_{α} of Eq. 20 to find:

$$M_{s'_{\theta}/s_{\alpha}} = \frac{ds'_{\theta}}{ds_{\alpha}} = \frac{ad\theta}{ld\alpha} = \frac{1}{l}\frac{d\theta}{d\alpha}$$

$$M_{s'_{\theta}/s_{\alpha}} = \frac{1}{l} \frac{d}{d\alpha} \left(\cos^{-1} \left(\frac{l \cos \alpha}{\sqrt{l^2 + y^2}} \right) \right)$$
 (68)

$$M_{s'_{\theta}/s_{\alpha}} = \frac{\sin \alpha}{\sqrt{l^2 \sin^2 \alpha + y^2}}$$
 or (69a)

$$M_{s'_{\theta}/s_{\alpha}} = \frac{1}{r} \frac{\cos \varphi}{\sqrt{1-\sin^2 \theta \sin^2 \varphi}}$$
 (69b)

In order to find the relative observed length's s_{φ} ' component for an object that is extended in the s_{α} direction, as a function of position, we take the derivative with respect to s_{α} of Eq. 21 to find:

$$M_{s'_{\varphi}/s_{\alpha}} = \frac{ds'_{\varphi}}{ds_{\alpha}} = \frac{a\sin\theta d\varphi}{ld\alpha} = \frac{\sin\theta}{l} \frac{d\varphi}{d\alpha}$$

$$M_{s_{\varphi}'/s_{\alpha}} = \frac{\sin \theta}{l} \frac{d}{d\alpha} \left(\tan^{-1} \left(\frac{y}{l \sin \alpha} \right) \right)$$
 (70)

$$M_{s_{\varphi}'/s_{\alpha}} = -\frac{y\cos\alpha}{\sqrt{l^2+y^2}\sqrt{l^2\sin^2\alpha+y^2}}$$
 or (71a)

$$M_{s'_{\varphi}/s_{\alpha}} = -\frac{1}{r} \frac{\cos\theta\sin\varphi}{\sqrt{1-\sin^2\theta\sin^2\varphi}}$$
 (71b)

The total observed relative length for an object that is extended in the s_{α} direction is therefore:

$$M_{\text{tot./}s_{\alpha}} = \sqrt{M_{s_{\theta}'/s_{\alpha}}^2 + M_{s_{\varphi}'/s_{\alpha}}^2}$$
 (72)

$$M_{\text{tot./s}_{\alpha}} = \frac{1}{\sqrt{l^2 + \gamma^2}} \text{ or}$$
 (73a)

$$M_{\text{tot./}s_{\alpha}} = \frac{1}{r} \tag{73b}$$

In order to find the relative observed length's s_{θ} ' component for an object that is extended in the l direction, as a function of position, we take the derivative with respect to l of Eq. 20 to find:

$$M_{s'_{\theta}/l} = \frac{ds'_{\theta}}{dl} = \frac{ad\theta}{dl} = \frac{d\theta}{dl}$$

$$M_{s'_{\theta}/l} = \frac{d}{dl} \left(\cos^{-1} \left(\frac{l \cos \alpha}{\sqrt{l^2 + y^2}} \right) \right) \tag{74}$$

$$M_{s'_{\theta}/l} = -\frac{y^2 \cos \alpha}{(l^2 + y^2)\sqrt{l^2 \sin^2 \alpha + y^2}}$$
 or (75a)

$$M_{s_{\theta}'/l} = -\frac{1}{r} \frac{\cos \theta \sin \theta \sin^2 \varphi}{\sqrt{1 - \sin^2 \theta \sin^2 \varphi}}$$
 (75b)

In order to find the relative observed length's s_{φ} ' component for an object that is extended in the l direction, as a function of position, we take the derivative with respect to l of Eq. 21 to find:

$$M_{s'_{\varphi}/l} = \frac{ds'_{\varphi}}{dl} = \frac{a\sin\theta d\varphi}{dl} = \sin\theta \frac{d\varphi}{dl}$$

$$M_{s_{\varphi}'/l} = \sin\theta \frac{d}{dl} \left(\tan^{-1} \left(\frac{y}{l \sin \alpha} \right) \right)$$
 (76)

$$M_{s_{\varphi}'/l} = -\frac{y \sin \alpha}{\sqrt{l^2 + y^2} \sqrt{l^2 \sin^2 \alpha + y^2}}$$
 or (77a)

$$M_{S'_{\varphi}/l} = -\frac{1}{r} \frac{\sin \theta \cos \varphi \sin \varphi}{\sqrt{1 - \sin^2 \theta \sin^2 \varphi}}$$
 (77b)

The total observed relative length for an object that is extended in the *l* direction is therefore:

$$M_{\text{tot.}/l} = \sqrt{M_{s'_{\theta}/l}^2 + M_{s'_{\varphi}/l}^2}$$
 (78)

$$M_{\text{tot./}l} = \frac{|y|}{l^2 + v^2} \text{ or}$$
 (79a)

$$M_{\text{tot.}/l} = \frac{1}{r} \sin \theta |\sin \varphi|$$
 (79b)

In order to find the relative observed length's s_{θ} ' component for an object that is extended in the y direction, as a function of position, we take the derivative with respect to y of Eq. 20 to find:

$$M_{s'_{\theta}/y} = \frac{ds'_{\theta}}{dy} = \frac{ad\theta}{dy} = \frac{d\theta}{dy}$$

$$M_{s_{\theta}'/y} = \frac{d}{dy} \left(\cos^{-1} \left(\frac{l \cos \alpha}{\sqrt{l^2 + y^2}} \right) \right)$$
 (80)

$$M_{s'_{\theta}/y} = \frac{ly \cos \alpha}{(l^2 + v^2)\sqrt{l^2 \sin^2 \alpha + v^2}}$$
 or (81a)

$$M_{s'_{\theta}/y} = \frac{1}{r}\cos\theta\sin\varphi$$
 (81b)

In order to find the relative observed length's s_{φ} ' component for an object that is extended in the y direction, as a function of position, we take the derivative with respect to y of Eq. 21 to find:

$$M_{s'_{\varphi}/y} = \frac{ds'_{\varphi}}{dy} = \frac{a\sin\theta d\varphi}{dy} = \sin\theta \frac{d\varphi}{dy}$$

$$M_{s'_{\varphi}/y} = \sin\theta \frac{d}{dy} \left(\tan^{-1} \left(\frac{y}{l \sin \alpha} \right) \right)$$
 (82)

Chapter 4. Observed Object Length as a Function of Position

$$M_{s'_{\varphi}/y} = \frac{l \sin \alpha}{\sqrt{l^2 + y^2} \sqrt{l^2 \sin^2 \alpha + y^2}}$$
 or (83a)

$$M_{s_{\varphi}'/y} = \frac{1}{r}\cos\varphi \tag{83b}$$

The total observed relative length for an object that is extended in the *y* direction is therefore:

$$M_{\text{tot./y}} = \sqrt{M_{s'_{\theta}/y}^2 + M_{s'_{\varphi}/y}^2}$$
 (84)

$$M_{\text{tot./y}} = \frac{l}{l^2 + v^2}$$
 or (85a)

$$M_{\text{tot./y}} = \frac{1}{r} \sqrt{1 - \sin^2 \varphi \sin^2 \theta}$$
 (85b)

Note that Eq. 85 is the same as Eq. 55. This is not surprising because the *y* coordinate of the cylindrical coordinate system about the *y* axis is the same as the *y* coordinate of the rectangular coordinate system. Eq. 85 has been included here for completeness and in order to represent the result in this other coordinate system.

Plotting Observed Length as a Function of Spherical Coordinates

To acquire an intuitive sense for what the length equations mean, we can plot the total observed length relative to the true object length (i.e. the length magnification) as a function of the object's position in spherical coordinates (r, θ, φ) . In this way, these plots represent how the total observed relative length of the object changes as the object moves along one of the spherical coordinate directions. In all of the plots below, all lengths are shown in meters. Keep in mind that the observed lengths correspond to a one-meter-radius image capture sphere.

Generally, the observed length of an object being smaller than the true length arises from two main mechanisms.

First, the farther away the object is, the shorter it looks because it takes up a smaller portion of the entire view. This is a type of perspective effect which we call the distance-perspective effect.

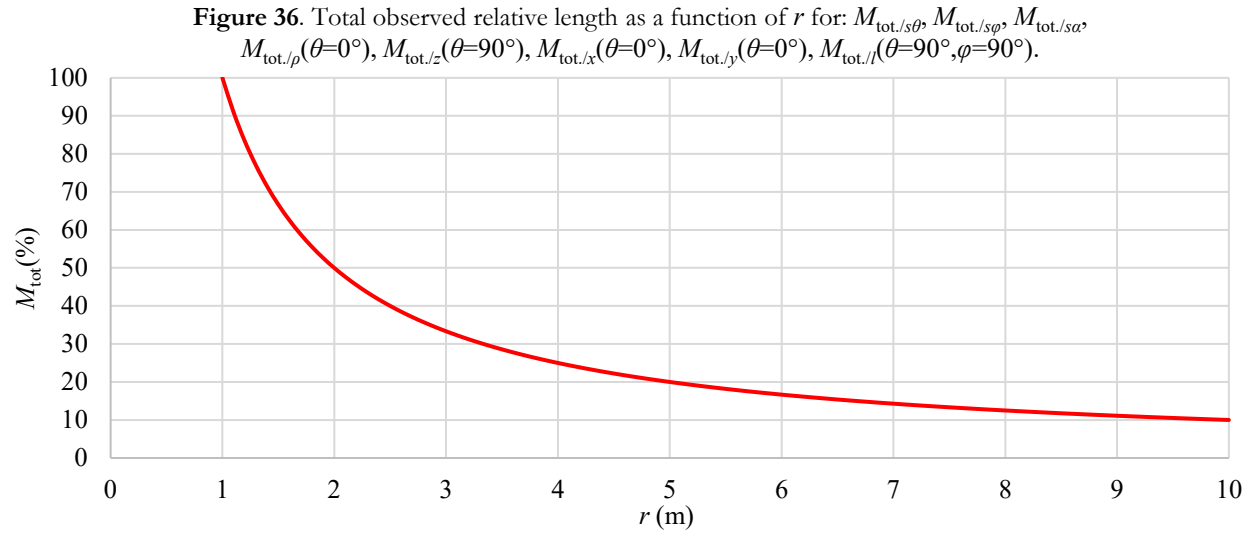
Secondly, for an object that is only extended in one direction (like a pencil), it will look shorter if it is somewhat tilted away from the observer. In art, this effect is called "foreshortening." If the object is tilted so that it extends directly away from the observer (i.e. it is extended in the *r* direction), then it will appear to have zero length. In contrast, if the object is tilted such that its

broadside is directly viewed (i.e. it's extended in a direction that is perpendicular to the *r* direction), then it will have zero shortening from this tilt effect.

In the plots below, the perceived shortening sometimes arises from the distance-perspective effect, sometimes arises from the foreshortening tilt effect, and sometimes arises from both. When the object is oriented such that its broadside is directly viewed, the total observed relative length then only depends on how far away the object is from the observer, which is the distance r.

The first thing to note is that all of the total observed length equations when expressed in spherical coordinates (i.e. Eqs. 33b, 38b, 43b, 49b, 55b, 58b, 61, 64, 73b, 79b, and 85b) depend on the r coordinate as (1/r), no matter in which direction the object is extended and no matter where the object is located. This means that no matter in which direction the object is extended and no matter where it is located, if it moves directly away from the observer, its total observed length decreases as (1/r). This function is plotted in Fig. 36.

For instance, if an object directly moves to twice the distance from the observer as originally, then it will appear one half as long as originally.



Or, if an object directly moves to three times the distance from the observer as originally, then it will appear one third as long as originally. This is true no matter how the object is oriented, so that the word length may be called height if the object is oriented vertically.

When the object is extended in the s_{θ} , s_{φ} , or s_{α} direction, it is always viewed exactly from broadside no matter where it is located. This means that in these three cases, the total observed relative length depends only on r and nothing else. Therefore, the entire equation is M = (1/r), as can be seen in Eqs. 43b, 61, 64, and 73b. This means that Fig. 36 shows the plot for Eqs. 43b, 61, 64, and 73b for all object locations.

Note that M is only 100% at r = 1 m, meaning that the observed height equals the true height. This is because we are using a one-meter-radius image capture sphere. If we instead used an image capture sphere with a different radius, it would shift the location of the M = 100% point but it would still be a (1/r) curve.

In all of the other types of situations, when the object is at special locations where it is being viewed broadside, the M equation reduces down to M = 1/r and looks exactly the same as in Fig. 36. In other words, Fig. 36 is also the exact same

resulting plot for when the object is extended in the ρ direction (Eq. 33b) at the locations where $\theta = 0^{\circ}$, for when the object is extended in the z direction (Eqs. 38b and 58b) at the locations where $\theta = 90^{\circ}$, for when the object is extended in the x direction (Eq. 49b) at the locations where $\theta = 0^{\circ}$, for when the object is extended in the y direction (Eqs. 53b and 85b) at the locations where $\theta = 0^{\circ}$, and for when the object is extended in the t direction (Eq. 79b) at the locations where t direction (Eq. 79b) at the locations where t direction (Eq. 79b) at the locations where

To be clear, even when the object is sitting at any other location besides these special locations, the object's observed length will still decrease at a rate of (1/r) if the object moves directly in the r direction, no matter the direction that the object is extended in. Although, the associated equation may be more complicated than just M = (1/r).

The (1/r) dependence means that if an object moves directly away from the observer at a constant true velocity, its visually perceived length would shorten quickly at first and then would shorten more gradually later on. In the limit that the object moves infinitely far away, its perceived length reduces to zero. For instance, the distant stars are so far away from the earth, that they appear as point particles of light with zero length.

Chapter 5. Plotting Observed Length as a Function of Spherical Coordinates

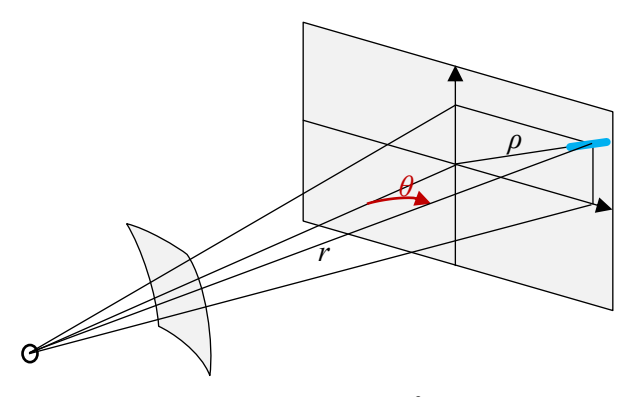
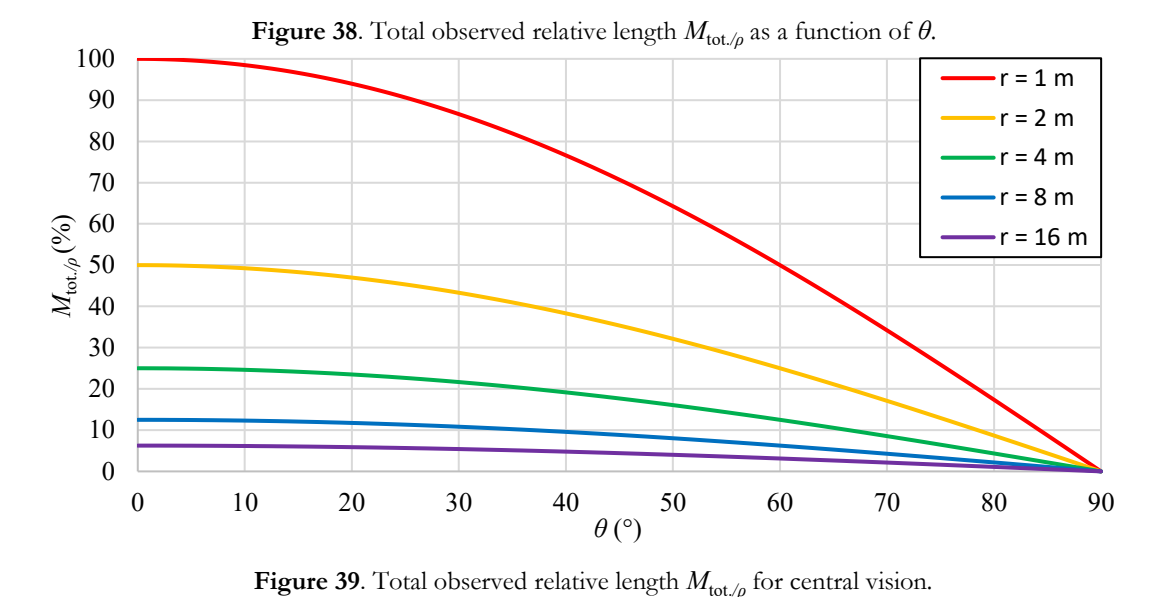


Figure 37. Plotting $M_{\text{tot./}\rho}$ as θ increases.

Fig. 37 shows what it means to be plotting the object's total observed relative length when the object is extended in the ρ direction (the object is

shown in blue), as the polar angle θ is increased, but its distance r from the observer is held constant. This is an object that is extended directly away from the viewing axis and is moving away from the viewing axis in the θ direction such that it holds a constant distance r from the observer. Fig. 38 shows the resulting plot, showing $M_{\text{tot}/\rho}$ as a function of θ for various fixed r values, which plots Eq. 33b.

The farther away that the object is from the viewing axis in the θ direction, the shorter it will appear. Note that the data points in a given line in Fig. 38 represent the different locations that all have the same r value.



100 90 80 70 W for % 60 80 40 40 r = 1 m r = 2 m30 r = 4 m20 r = 8 m10 r = 16 m0 2 3 7 8 9 1 5 6 θ (°)

Chapter 5. Plotting Observed Length as a Function of Spherical Coordinates

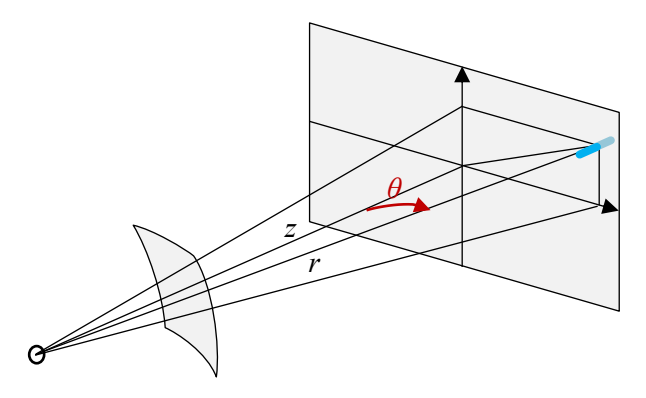


Figure 40. Plotting $M_{\text{tot./z}}$ as θ increases.

Therefore, the progressive shortening as θ increases is solely due to the object tilting away from the viewer as it maintains a ρ orientation, and not from the distance-perspective effect.

Fig. 39 shows the exact same information as in Fig. 38, but now only for the central region of vision. As Fig. 39 shows, if the object maintains a fixed overall distance r, an object that is extended in the ρ direction looks approximately the same length no matter where it is located, as long as it stays within the central region of vision. In other words, an object that continues to be extended in the ρ direction does not observably tilt as it moves around, if it stays within central vision.

Fig. 40 shows what it means to be plotting the object's total observed relative length when the

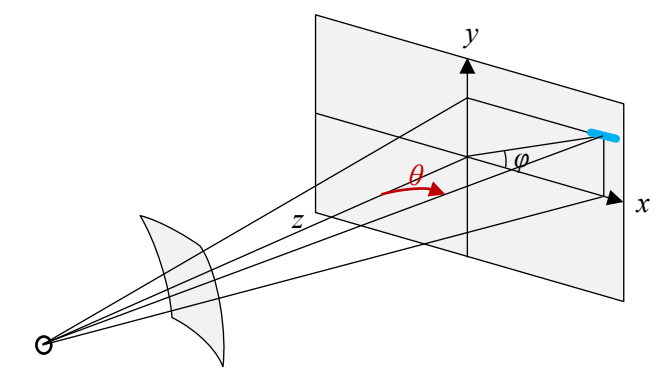
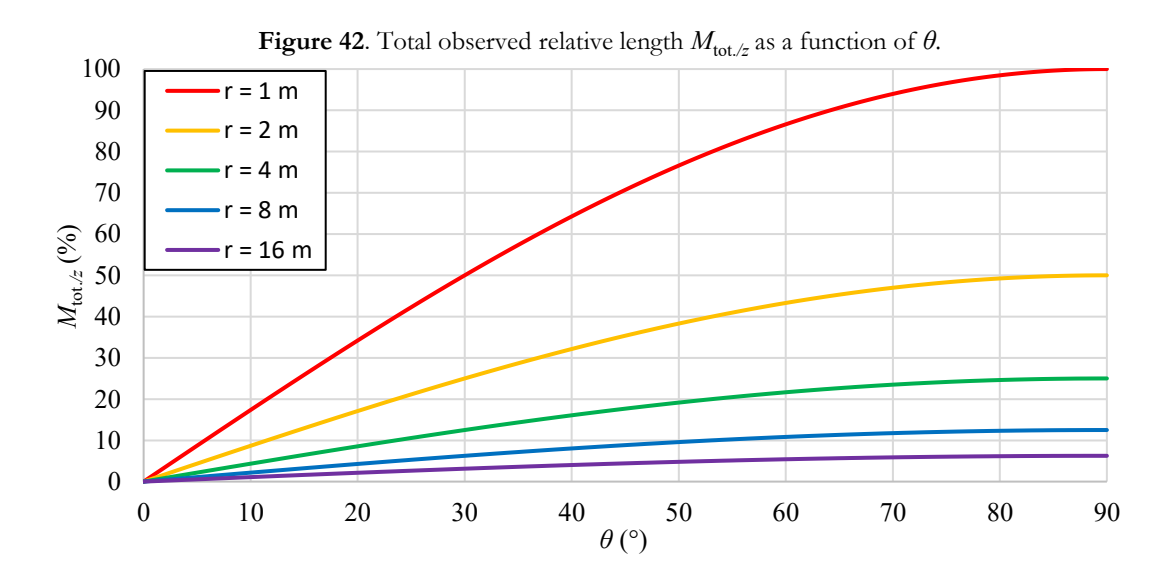
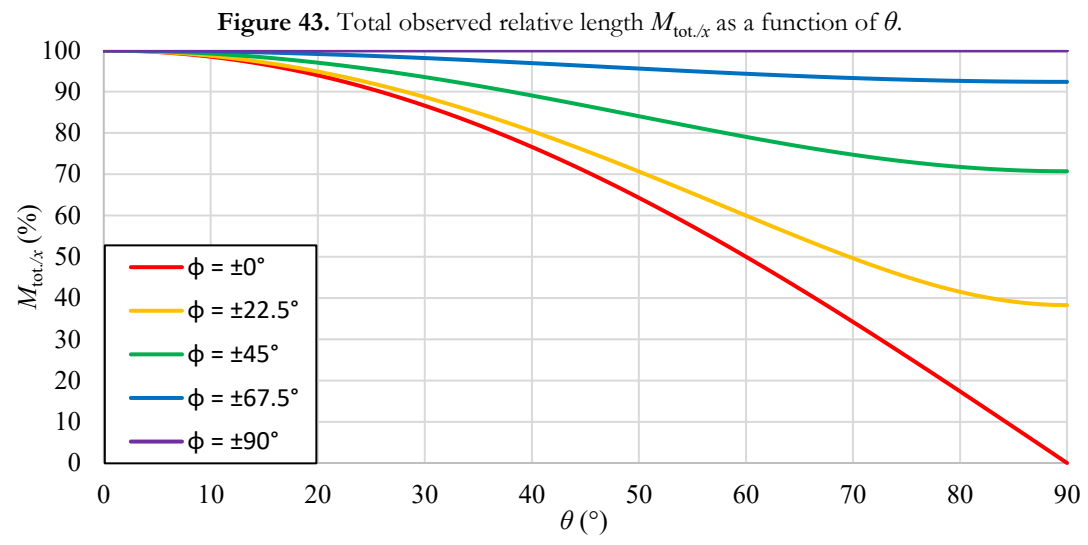


Figure 41. Plotting $M_{\text{tot./x}}$ as θ increases.

object is extended in the z direction, as the polar angle θ is increased, but its distance r from the observer is held constant. Fig. 42 then shows the resulting plot, showing $M_{\text{tot/z}}$ as a function of θ for various fixed r values, which is the plot of Eqs. 38b and 58b. On the viewing axis (at $\theta = 0^{\circ}$) the object appears to have zero length because it is oriented so that it extends directly away from the observer. As the object moves in the θ direction but remains extended in the z direction, Fig. 42 shows that the object appears to get larger. The farther away that the object is from the viewing axis in the θ direction, the longer it appears.

Note that the data points in a particular line in Fig. 42 represent the different locations that all have the same r distance. Therefore, the visually





perceived progressive lengthening that happens as θ increases is solely due to the object tilting toward broadside viewing as it remains extended in the z orientation, and not from the distance-perspective effect.

Fig. 41 shows what it means to be plotting the object's total observed relative length when the object is extended in the x direction, as the object's θ coordinate is increased.

Fig. 43 shows the resulting plot, showing $M_{\text{tot./x}}$ as a function of θ for various fixed φ values when r = 1 m, which is the plot of Eq. 49b. On the viewing axis, the object has its maximum length because it is being viewed broadside there. As the object moves in the θ direction, Fig. 43 shows that the object appears to get shorter. Because the

object maintains the same overall distance r from the observer, the change in observed length is arising purely from the tilt effect.

Fig. 44 shows what it means to be plotting the object's total observed relative length when the object is extended in the y direction, as the object's θ coordinate is increased.

Fig. 46 shows the resulting plot, showing $M_{\text{tot./y}}$ as a function of θ for various fixed φ values when r = 1 m, which is the plot of Eqs. 55b and 85b. On the viewing axis, the object has its maximum observed length because it is being viewed broadside there. As the object moves in the θ direction, Fig. 46 shows that the object appears to get shorter. Because the object maintains the same overall distance r from the observer, the

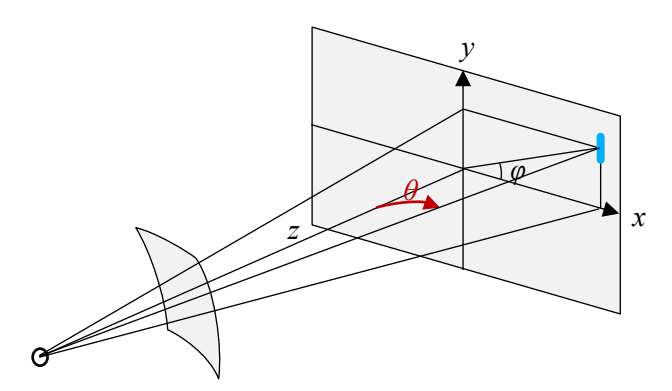


Figure 44. Plotting $M_{\text{tot./y}}$ as θ increases.

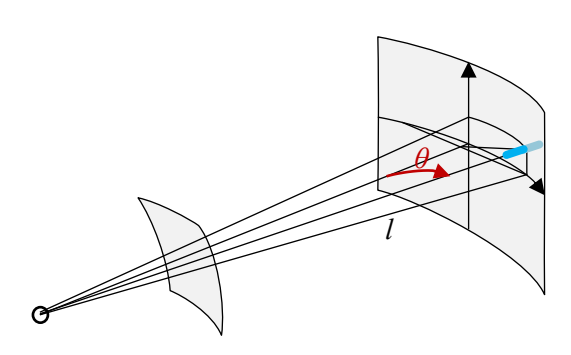


Figure 45. Plotting $M_{\text{tot./l}}$ as θ increases.

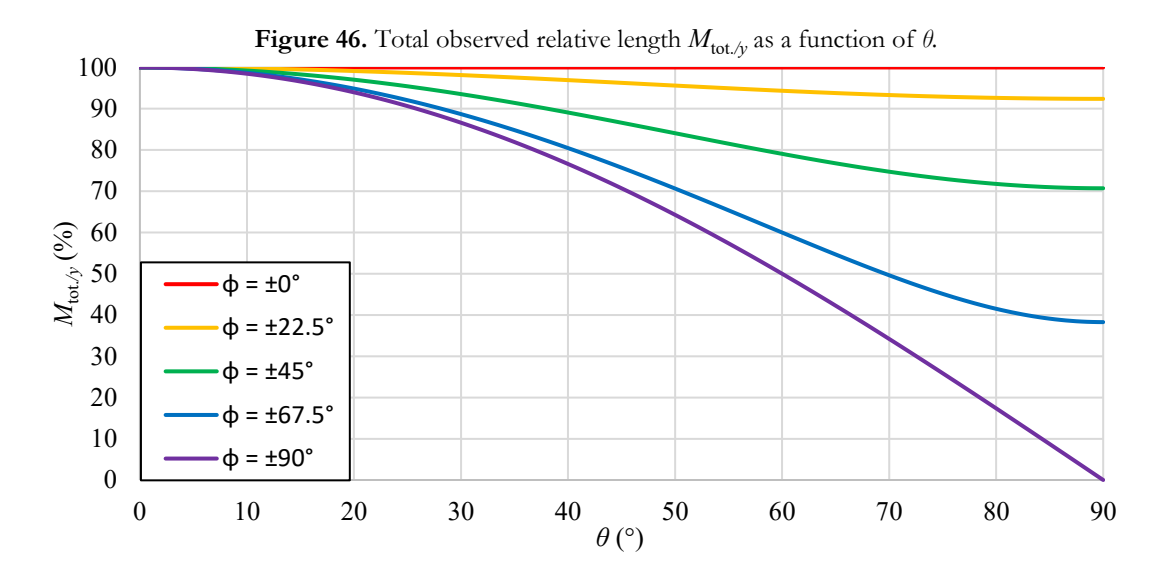
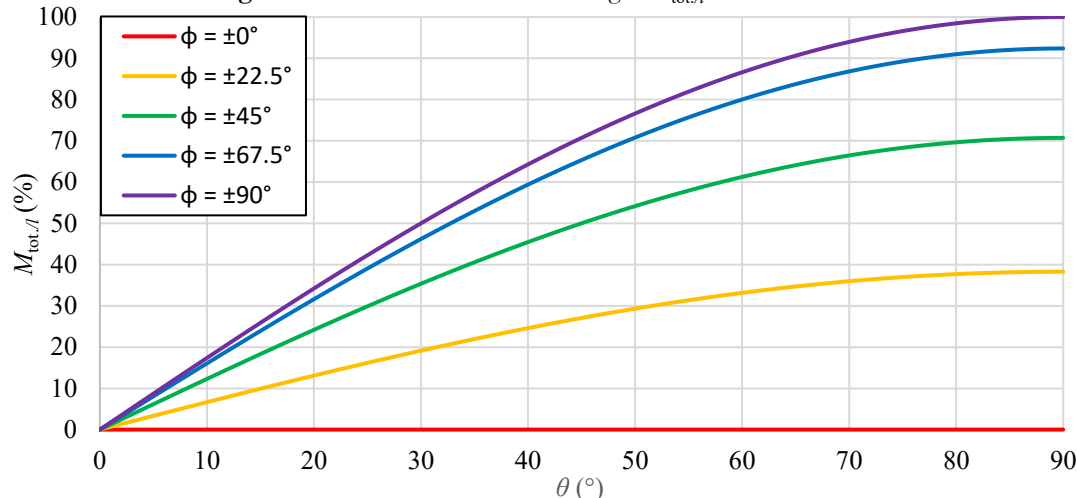


Figure 47. Total observed relative length $M_{\text{tot}/l}$ as a function of θ .



change in observed length is arising purely from the tilt effect.

Fig. 45 shows what it means to be plotting the object's total observed relative length when the object is extended in the l direction, as the object's θ coordinate is increased.

Fig. 47 shows the resulting plot, showing $M_{\text{tot.//}}$ as a function of θ for various fixed φ values when r = 1 m, which is the plot of Eq. 79b. On the

viewing axis, the object has zero observed length because it is extended directly away from the observer. As the object moves in the θ direction, Fig. 47 indicates that the object appears to get longer. Because the object maintains the same overall distance r from the observer, the change in observed length is arising purely from the tilt effect.

Plotting Observed Length as a Function of Original Object Coordinates

Instead of plotting the total observed lengths as a function of spherical coordinates, which represented an object moving in the r, θ , or φ directions, we can plot them as a function of the original object coordinates. In this way, we can see how an object extended, for instance, in the x direction changes its observed length as it travels in the y direction.

Note that plotting as a function of the object location coordinates of θ and φ is the same thing as plotting as a function of the observed spherical coordinates, and therefore leads to the same plot shown in Fig. 36. For this reason, they will not be plotted again here. This leaves us with the task of plotting the visually perceived lengths of objects that extend in rectangular coordinate directions as

they move in rectangular coordinate directions, as well as plotting the visually perceived lengths of objects that extend in the cylindrical-about-the-y-axis coordinate directions as they move in cylindrical-about-the-y-axis coordinate directions.

Fig. 48 shows what it means to be plotting the object's total observed relative length when the object is extended in the ρ direction, as the object's ρ coordinate is increased, but everything else is held constant, which is plotting Eq. 33a. Fig. 49 shows what it means to be plotting the object's total observed relative length when the object is extended in the z direction, as the object's z coordinate is increased, but everything else is held constant, which is plotting Eq. 38a.

The situation shown in Fig. 48 is equivalent to

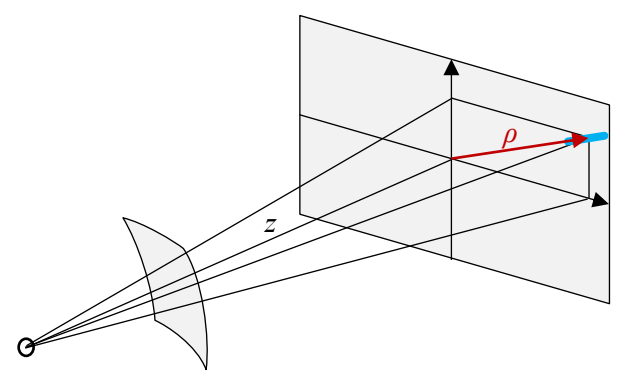


Figure 48. Plotting $M_{\text{tot./}\rho}$ as ρ increases.

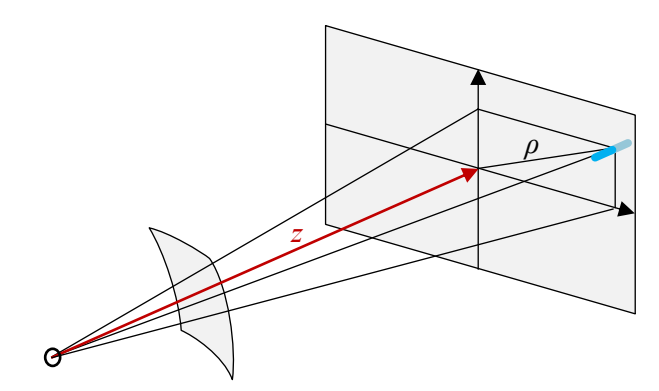
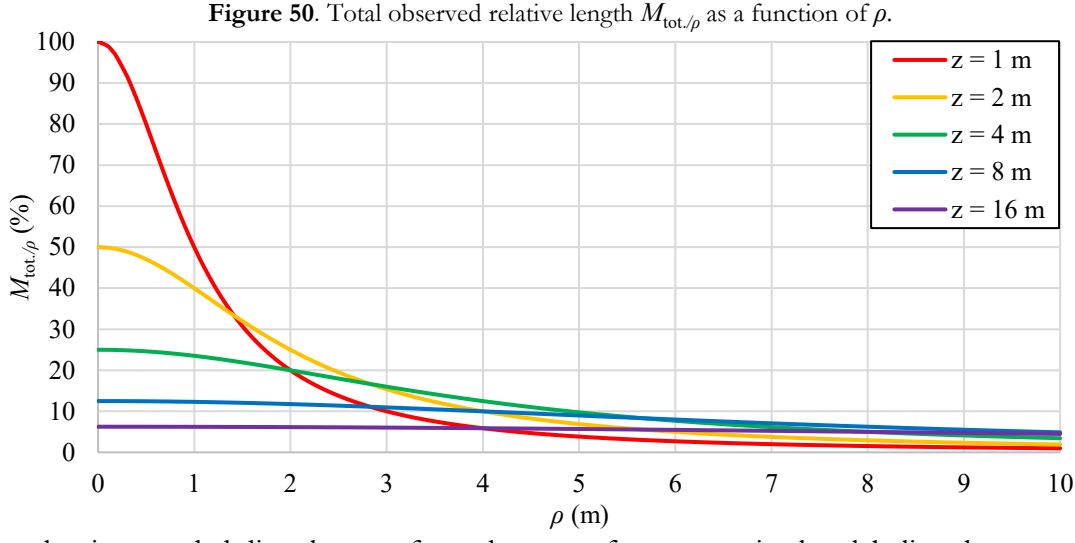


Figure 49. Plotting $M_{\text{tot./z}}$ as z increases.



an object that is extended directly away from the viewing axis and is moving away from the viewing axis. Fig. 50 shows the resulting plot, showing $M_{\text{tot}/\rho}$ as a function of ρ for various fixed z values. On the viewing axis (at $\rho = 0$) the object has its maximum observed length because it is being viewed broadside and is relatively close to the viewer. As the object moves in the ρ direction at a constant true velocity, Fig. 50 shows that the object visually appears to become shorter quickly at first and then more gradually later on. This is because, as the object moves in the ρ direction, it gets farther away from the observer and also it becomes more tilted away from the observer.

Due to mathematical symmetries, Fig. 50 also shows the plot of the situation shown in Fig. 49

after appropriately relabeling the axes.

Fig. 51 shows what it means to be plotting the object's total observed relative length when the object is extended in the ρ direction, as the object's z coordinate is increased, but everything else is held constant, which is plotting Eq. 33a. The situation in Fig. 51 is equivalent to an object that is extended directly away from the viewing axis and is moving in the z direction.

Fig. 52 shows what it means to be plotting the object's total observed relative length when the object is extended in the z direction, as the object's ρ coordinate is increased, but everything else is held constant, which is plotting Eq. 38a.

The resulting plot of the situation in Fig. 51 is shown in Fig. 53, showing $M_{\text{tot./}\rho}$ as a function of

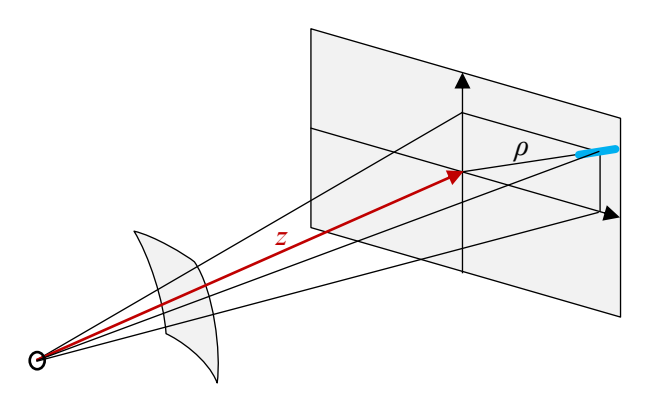


Figure 51. Plotting $M_{\text{tot./}\rho}$ as z increases.

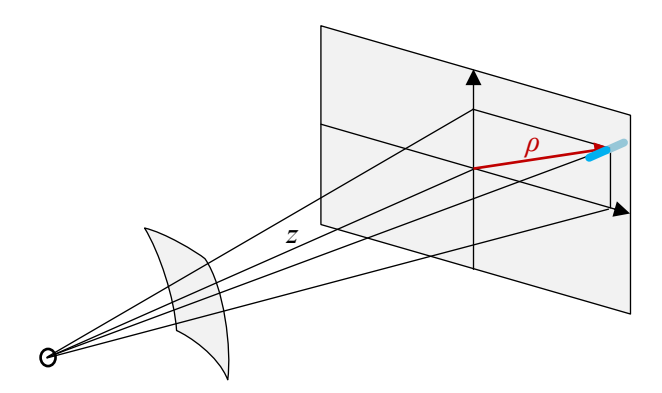
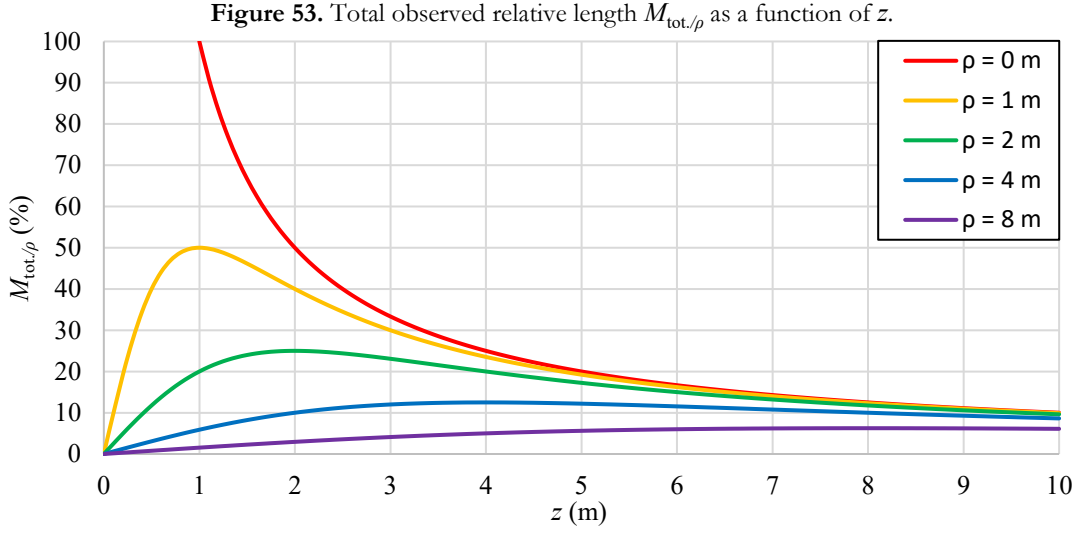


Figure 52. Plotting $M_{\text{tot./z}}$ as ρ increases.



z for various fixed ρ values. As expected, the father away that the object is from the observer in the z direction, the shorter it appears. For an object not on the viewing axis (i.e. not at $\rho = 0$), it is observed to have no length when at z = 0. This is because the object is located directly to the side of the observer (at $\theta = 90^{\circ}$) and is therefore titled directly away from the observer. Each of the curves in Fig. 53 (except the $\rho = 0$ curve) starts out very small when close to z = 0 and rapidly increases at first as z increases. This is because the object is quickly becoming tilted toward broadside-viewing as z increases. Then the observed length decreases because the object is getting far away. Note that the red ($\rho = 0$) curve is at 100% when z = 1 m. This is because we are using a one-

meter-radius image capture sphere and the object is literally on this sphere at this point and is being viewed broadside. There are no data points for the red curve for z < 1 m because that would be inside the imaging sphere.

Due to mathematical symmetries, Fig. 53 also shows the plot of the situation shown in Fig. 52 after relabeling the horizontal axis as ρ , the legend as z, and the horizontal axis as $M_{\text{tot}/z}$.

Fig. 54 shows what it means to be plotting the object's total observed relative length when the object is extended in the x direction, as the object's x coordinate is increased, which is the plot of Eq. 49a.

Fig. 55 shows what it means to be plotting the object's total observed relative length when the

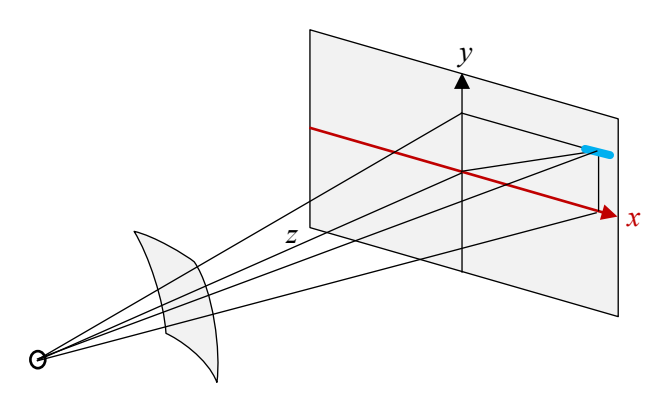


Figure 54. Plotting $M_{\text{tot./x}}$ as x increases.

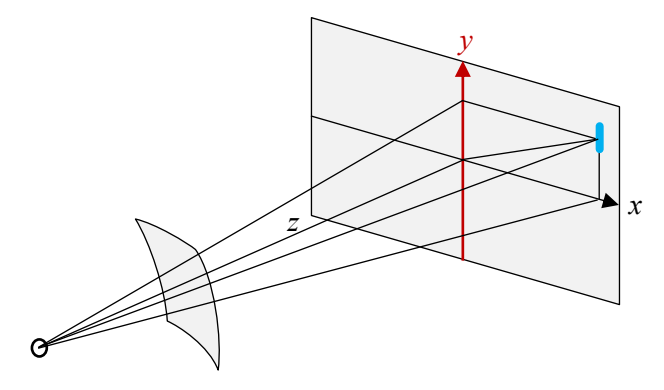


Figure 55. Plotting $M_{\text{tot./y}}$ as y increases.

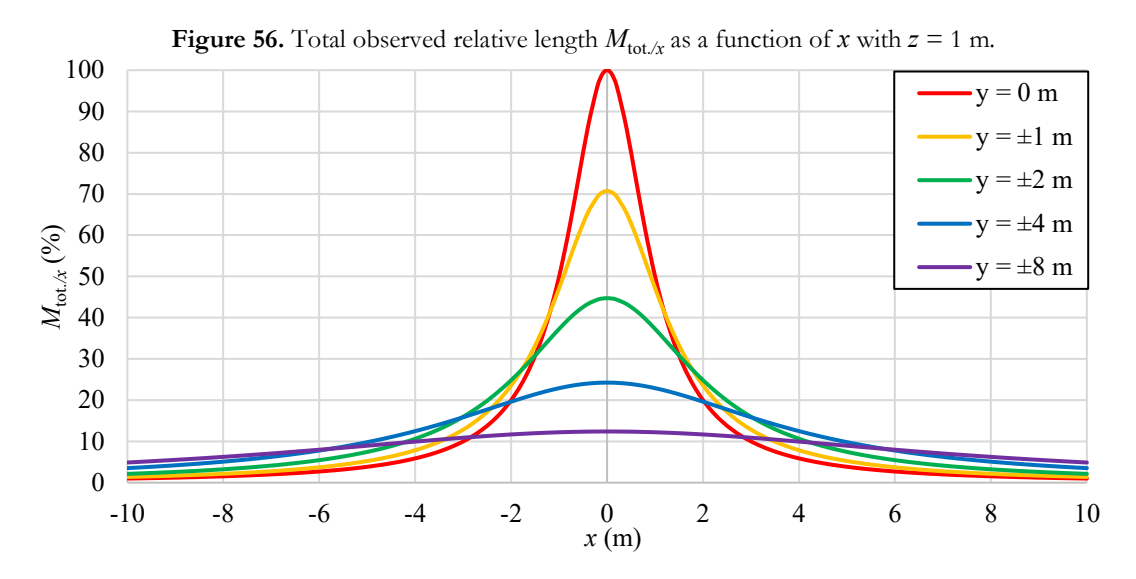
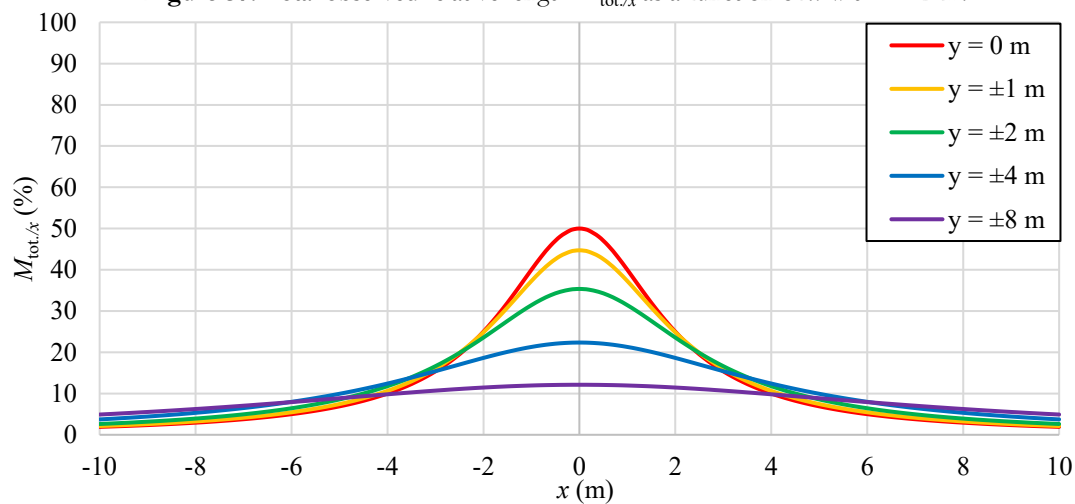


Figure 57. Total observed relative length $M_{\text{tot}/x}$ as a function of x with z = 2 m.



object is extended in the *y* direction, as the object's *y* coordinate is increased, which is the plot of Eq. 55a.

Fig. 56 shows the resulting plot for the situation shown in Fig. 54, which shows $M_{\text{tot./x}}$ as a function of x for various fixed y values. At x = 0, the object's observed length is at a maximum because it is being viewed broadside.

As the object starts far off to the left and moves in the *x* direction, Fig. 56 shows that the object appears to get larger as it approaches the viewing axis, both because it is getting closer and because it is getting tilted more toward broadside.

Fig. 57 shows the exact same information as is shown in Fig. 56, but with z = 2 m.

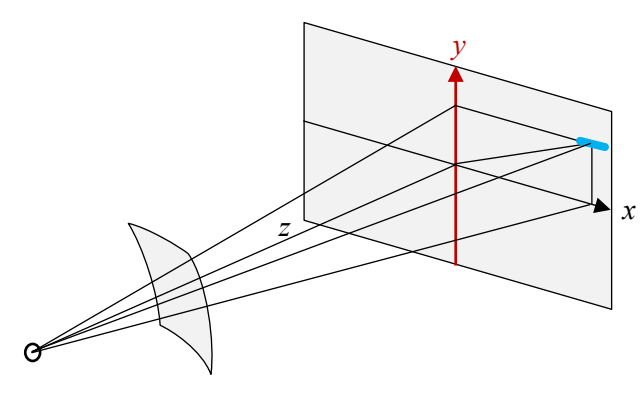
Due to mathematical symmetries, Figs. 56 and 57 also show the plots arising from the situation presented in Fig. 55. We now move on.

The situations listed in Table 1 and shown in Figs. 58 to 63 have the exact same mathematical forms and all have the same resulting plot, which is shown in Fig. 64.

Keep in mind that that the z coordinate of the rectangular coordinate system and the z coordinate of the cylindrical coordinate system about the z axis are exactly the same.

		1	0 11 1	0
Length element	As a function of	For various fixed	Equation	Figure
$M_{ m tot./x}$	у	x	Eq. 49a	Fig. 58
$M_{ m tot./x}$	z	x	Eq. 49a	Fig. 59
$M_{ m tot./y}$	x	y	Eq. 55a	Fig. 60
$M_{ m tot./y}$	z	y	Eq. 55a	Fig. 61
$M_{ m tot./z}$	x	z	Eq. 58a	Fig. 62
$M_{ m tot./z}$	у	z	Eq. 58a	Fig. 63

Table 1. These situations all have the same plot shown in Fig. 64 after appropriate relabeling of axes.



z x

Figure 58. Plotting $M_{\text{tot./x}}$ as y increases.

Figure 59. Plotting $M_{\text{tot./x}}$ as z increases.

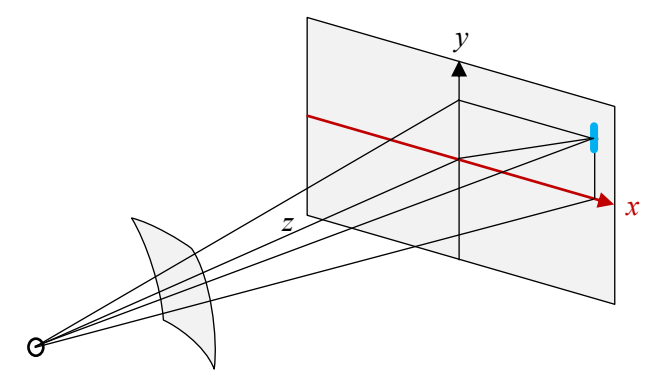


Figure 60. Plotting $M_{\text{tot./y}}$ as x increases.

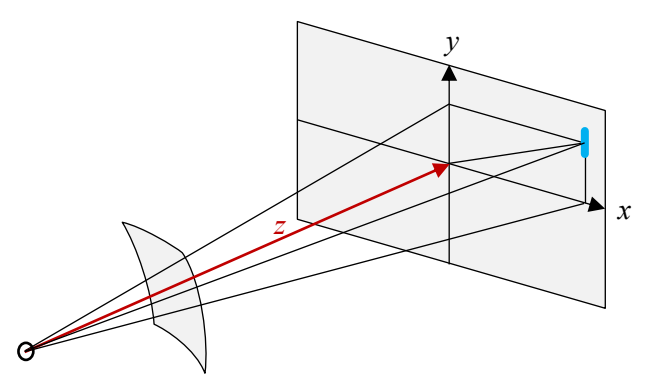


Figure 61. Plotting $M_{\text{tot./y}}$ as z increases.

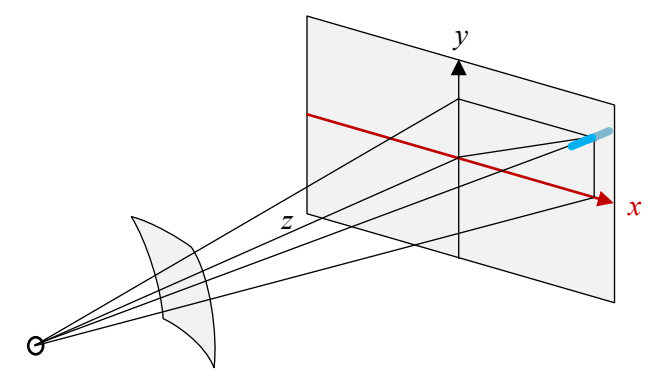


Figure 62. Plotting $M_{\text{tot./z}}$ as x increases.

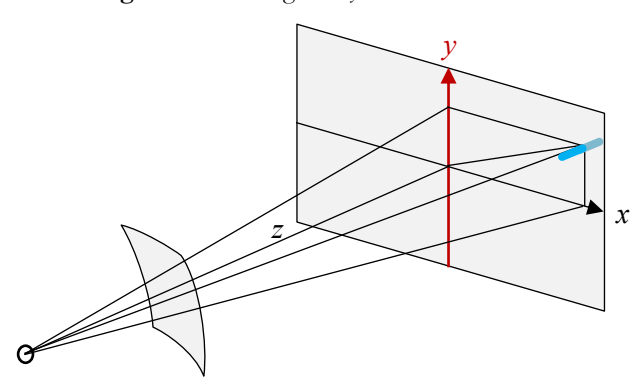


Figure 63. Plotting $M_{\text{tot}/z}$ as y increases.

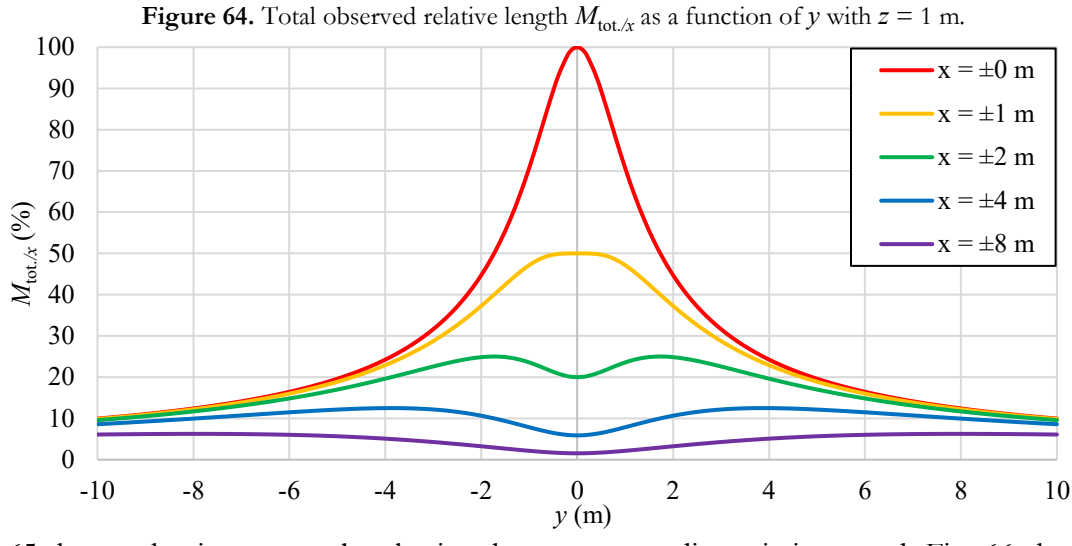


Fig. 65 shows what it means to be plotting the object's total observed relative length when the object extends in the s_{α} direction, as the object's

y coordinate is increased. Fig. 66 shows what it means to be plotting the object's total observed relative length when the object extends in the s_{α}

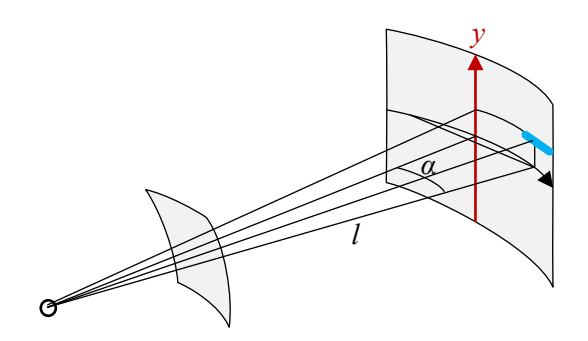


Figure 65. Plotting $M_{\text{tot./s}\alpha}$ as y increases.

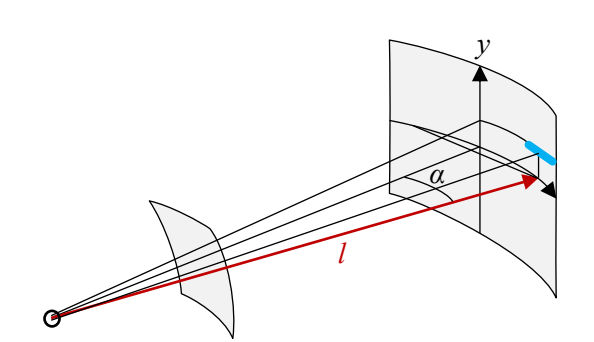
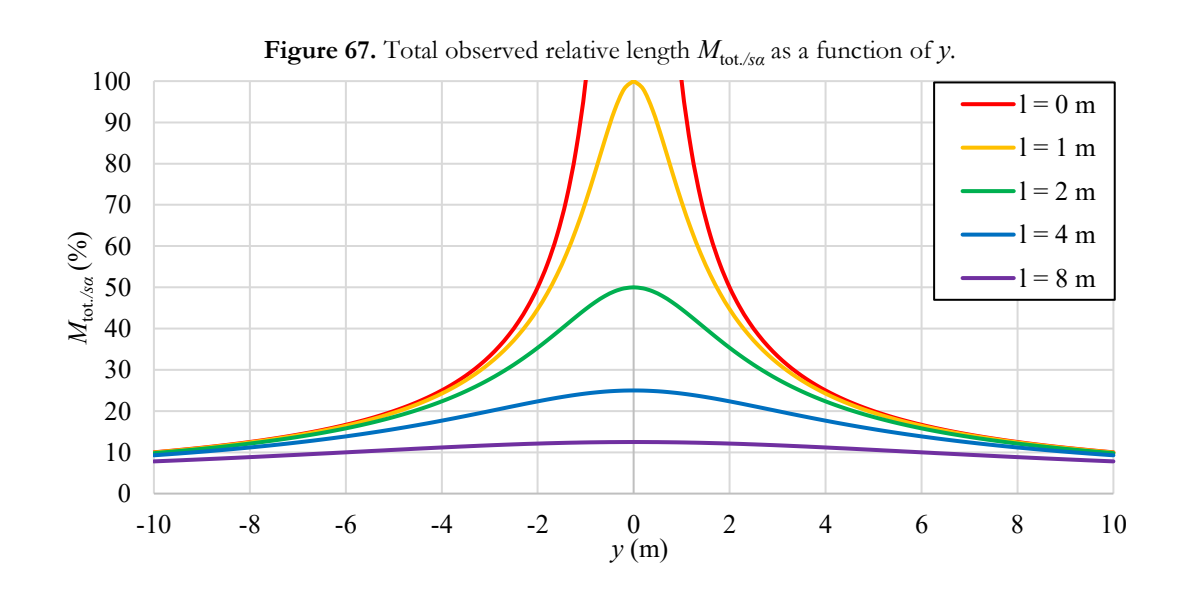


Figure 66. Plotting $M_{\text{tot./s}\alpha}$ as l increases.



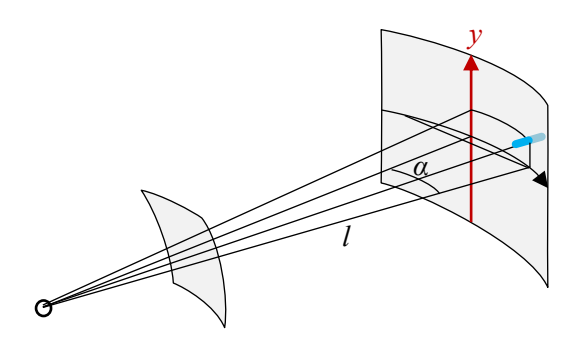


Figure 68. Plotting $M_{\text{tot.}/l}$ as y increases.

direction, as the object's l coordinate is increased. Fig. 67 shows the resulting plot for the situation in Fig. 65, showing $M_{\text{tot./sa}}$ plotted as a function of y for various l values, which is the plot of Eq. 73a as y changes.

As an object at l = 0 moves in the y direction away from y = 0, it becomes progressively shorter because it gets farther away from the observer. At the same time, the object continues being exactly broadside viewed. For the curves with higher l values, the general trend remains the same but the object becomes shorter more gradually because it is already farther away.

Because of mathematical symmetry, the plot for the situation in Fig. 66, which is the plot of Eq. 73a as a function of *l*, looks exactly like the plot in Fig. 67 (after appropriately relabeling the

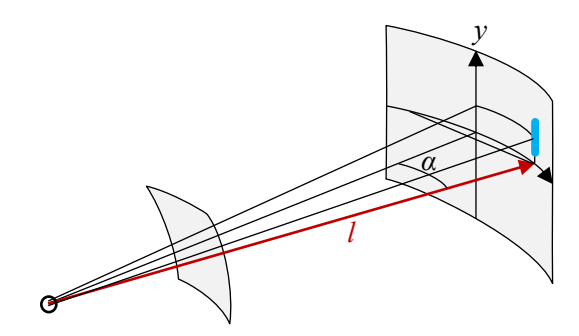
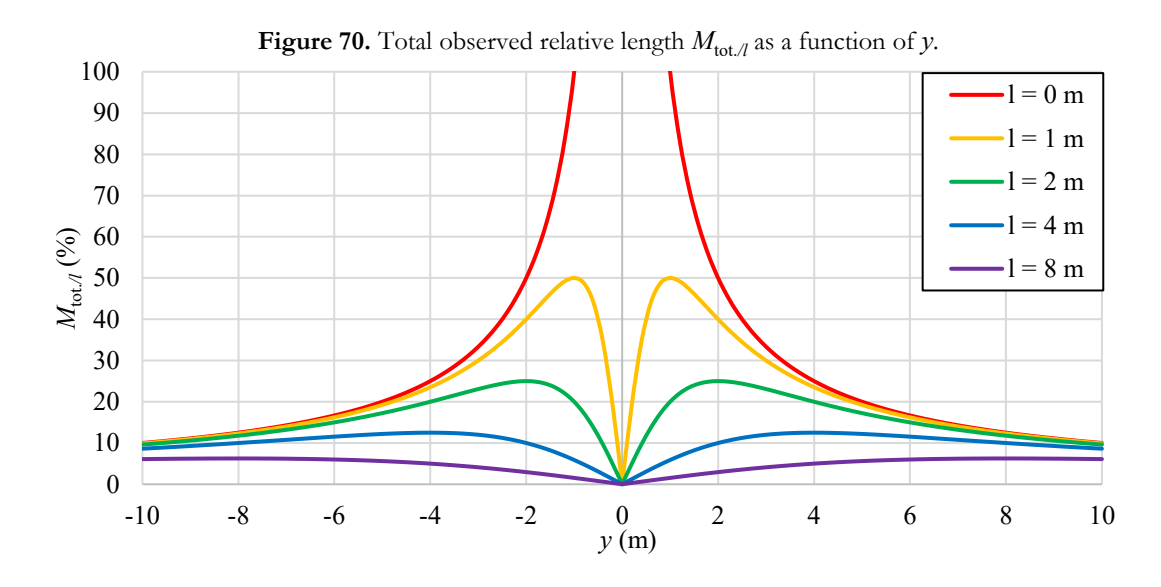


Figure 69. Plotting $M_{\text{tot./y}}$ as l increases.

axes and realizing that l is always positive).

Fig. 68 shows what it means to be plotting the object's total observed relative length when the object is extended in the l direction, as the object's y coordinate is increased. Fig. 69 shows what it means to be plotting the object's total observed relative length when the object is extended in the y direction, as the object's l coordinate is increased. Fig. 70 shows the resulting plot for the situation in Fig. 68, showing $M_{tot,l}$ plotted as a function of y for various l values, which is the plot of Eq. 79a.

For an object with $l \ge 1$, it is observed to have no length when at y = 0. This is because the object is extended directly away from the observer at y = 0. For objects with l < 1, there are no data points at or near y = 0 because that would



47

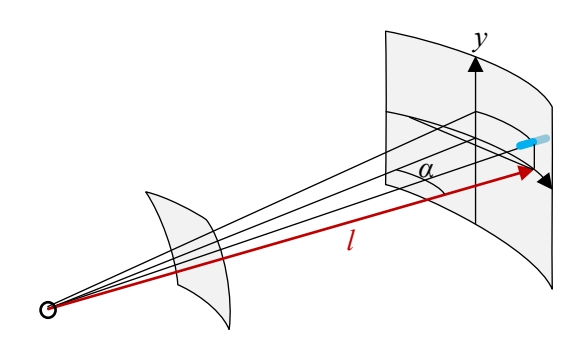


Figure 71. Plotting $M_{\text{tot},l}$ as l increases.

correspond to being inside the imaging sphere.

Each of the curves (except the l=0 curve) in Fig. 70 starts out very small when close to y=0 and rapidly increases at first as y increases. This is because the object is quickly becoming tilted more toward broadside-viewing as y increases. Then later the observed length decreases because the object is getting farther away. Because of mathematical symmetry, the plot for the situation in Fig. 69, which is the plot of Eq. 86 as a function of l, looks exactly like the plot in Fig. 70 (after appropriately relabeling the axes and realizing that l is always positive). The observed relative lengths change for the same reasons.

Fig. 71 shows what it means to be plotting the object's total observed relative length when the object is extended directly in the *l* direction, as the

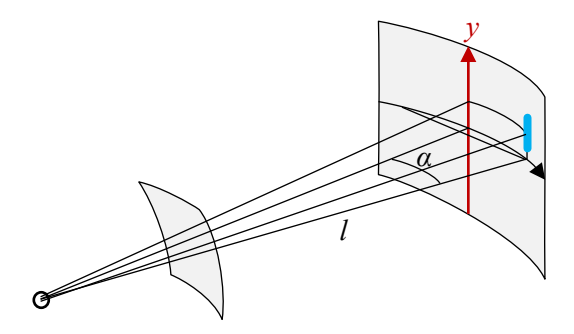
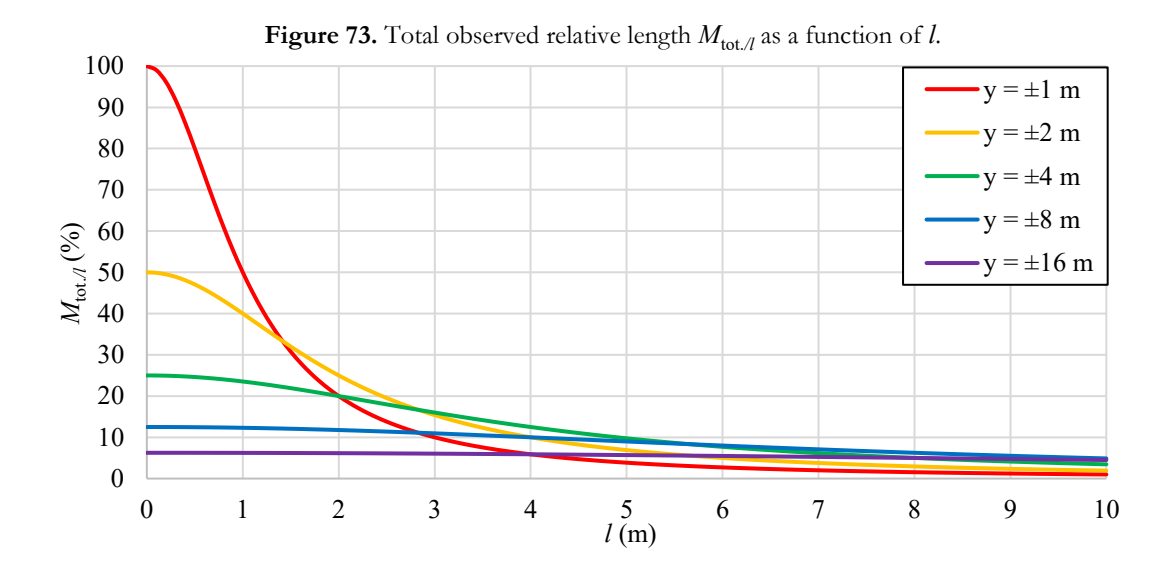


Figure 72. Plotting $M_{\text{tot./y}}$ as y increases.

object's l coordinate is increased. Fig. 72 shows what it means to be plotting the object's total observed relative length when the object is extended in the y direction, as the object's y coordinate is increased. Fig. 73 shows the resulting plot for the situation in Fig. 71, showing $M_{\text{tot}/l}$ plotted as a function of l for various y values, which is the plot of Eq. 79a.

Fig. 73 shows that the object has a peak observed length at l=0 (i.e. when the object is directly overhead or underfoot of the viewer). This is because the object is being viewed exactly broadside at these locations. The object shortens as it moves in the l direction because it is getting farther away and because it's tilting away. Because of symmetry, the plot for Fig. 72, which is the plot of Eq. 85a, looks exactly like the plot in Fig. 73.



48

Observed Sphere Diameter as a Function of Position

If an object has a shape that is extended in more than one direction, then the length equations will not be enough. Instead, several length equations should be applied together in order to find areas, as will be one in Chapter 8. However, for the case of a spherical object, the situation is especially simple. Such an object has the special property that the object as a whole never tilts away from the viewer. In other words, a sphere that is held at a fixed distance always looks exactly the same size no matter how the sphere is oriented.

A sphere is visually equivalent to a flat circle of the same radius being oriented so that it is always being viewed exactly broadside. In terms of the coordinate systems used above, this is equivalent to an object always being extended along spherical coordinate directions. Therefore, the observed relative diameter equation for a sphere is the same as Eq. 61. Specifically, a small sphere with a true diameter *d* will be observed as a circle with an observed relative diameter of:

$$M_{\text{tot./d}} = \frac{1}{r} \text{ or} \tag{86}$$

$$M_{\text{tot.}/d} = \frac{1}{\sqrt{x^2 + y^2 + z^2}}$$
 or (87)

$$M_{\text{tot.}/d} = \frac{1}{\sqrt{\rho^2 + z^2}} \text{ or }$$
 (88)

$$M_{\text{tot.}/d} = \frac{1}{\sqrt{l^2 + y^2}}$$
 (89)

Eqs. 86 to 89 all mean the same thing but are expressed in the various coordinate systems. Because a sphere does not involve the tilt effect, its observed size depends only on its overall distance r from the observer (as usual, we are assuming that the object is small enough that the equations above can be used directly without integration). The plot of Eq. 86 is the same as shown in Fig. 36.

Fig. 74 shows what it means to be plotting the object's total observed relative diameter when the object is a sphere, as the object's *x* coordinate is

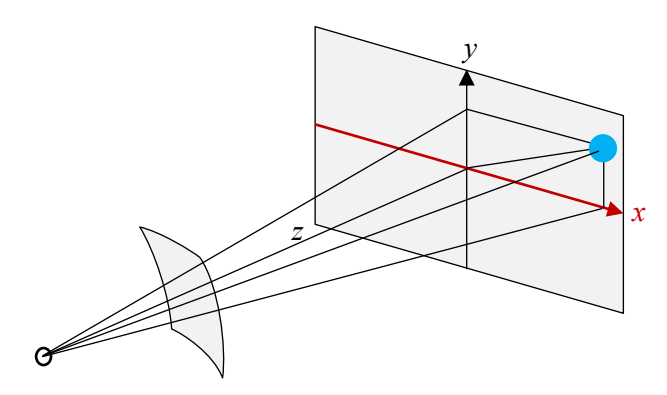
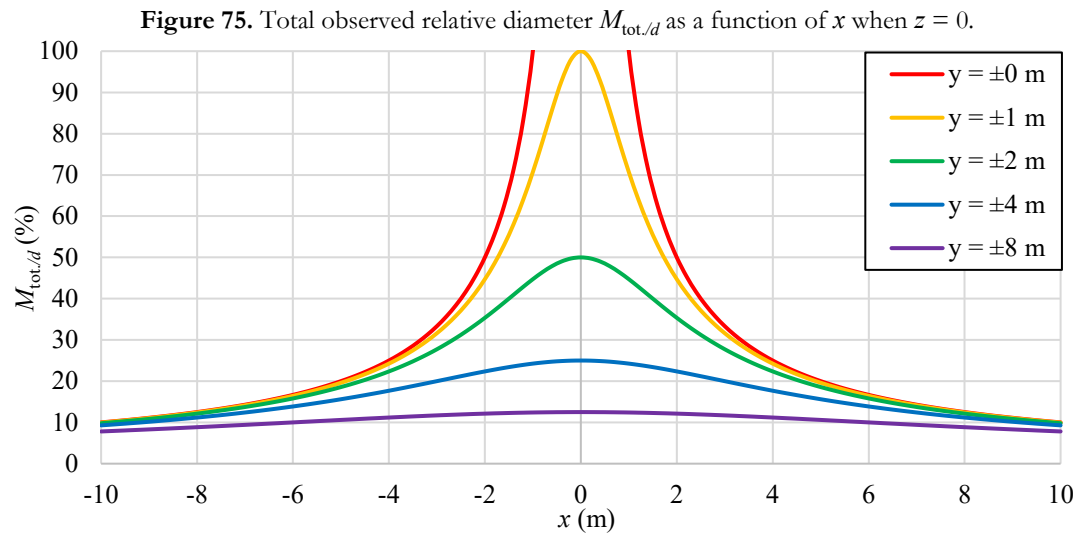


Figure 74. Plotting $M_{\text{tot.}/d}$ as x increases.

Chapter 7. Observed Sphere Diameter as a Function of Position



increased. The resulting plot is shown in Fig. 75, showing $M_{\text{tot}/d}$ plotted as a function of x for various y values when z = 0, which is the plot of Eq. 87. Because of mathematical symmetry, the plot in Fig. 75 is exactly what you get when you

plot Eq. 87 as a function of y, Eq. 87 as a function of z, Eq. 88 as a function of ρ , Eq. 88 as a function of z, Eq. 89 as a function y, and Eq. 89 as a function of l (with the appropriate relabeling of the axes and range limitations).

Observed Object Area as a Function of Position

We next investigate how the geometry of human monocular vision determines the observed area of objects. As was the case with observed length, the observed area depends on the true object area, which is different from one object to the next. Therefore, of importance here is not the absolute observed area, but the relative observed area, which is calculated relative to the true area of the object. We therefore need to analyze the ratio of the observed area to the actual area, which we will call the relative observed area or the area magnification.

As with length magnification, area magnification values will also be less than one because we are dealing with the naked eye when no mirrors, lenses, telescopes, or microscopes are involved.

Just as was the case with lengths, when the relative observed area relates an angle parameter to a meter parameters, the units mismatch, giving the associated magnification a confusing and less useful meaning. To avoid this, we again transform each angle-length parameter to a meters-length parameter, just like we did before, and assume an imaging sphere with a radius of one meter.

A large object will have one of its parts seen at one location with a certain magnification and other parts at other locations seen with different magnifications. Calculating the total area would therefore require evaluating integrals over many locations in an object-specific way. However, to make more general statements, we therefore again focus on small objects that can be approximated as existing at a single location, meaning that we use derivatives. The point-wise area magnification is the ratio of the observed small-object area to the true small-object area.

For small two-dimensional patches that are extended in coordinate directions of smoothly-varying coordinate systems, the patch is approximately flat and thus the patch can be assumed to be a flat rectangle with an area equal to its width times its height. For instance, the true area of a small patch extended in a plane parallel to the x-y plane is $dA_{x,y} = dx dy$. When a rectangular patch is projected onto the image capture sphere, which is also locally flat on small scales, we end up with a parallelogram-shaped patch.

One pair of sides of the parallelogram extends in the l_1 direction and has the length dl_1 and the other pair of sides extends in the l_2 direction and has the length dl_2 . In other words, dl_1 is the observed line on the image capture sphere that corresponds to two edges of the true rectangular patch and dl_2 is the line on the imaging sphere that

corresponds to the other two edges of the true rectangle.

In general, the line segments dl_1 and dl_2 are not necessarily perpendicular (i.e. the parallelogram is not necessarily a rectangle), and thus we must calculate the area of a parallelogram that is not necessarily a rectangle. Also, dl_1 does not typically extend in just the s_{θ} ' direction or just the s_{φ} ' direction, but extends in an odd direction, with an s_{θ} ' component and an s_{φ} ' component. Similarly, dl_2 extends in an odd direction.

The best method of calculating the area of a parallelogram with sides extending in odd directions is using the magnitude of the cross product:

$$dA_{\text{observed}} = \left| d\vec{\mathbf{l}}_1 \times d\vec{\mathbf{l}}_2 \right|$$

Because we are dealing with a very small patch of area, the spherical image capture surface is locally flat and we can compute the cross product of the vectors with the r, s_{θ} ', and s_{φ} ' components, as if it were a rectilinear coordinate system:

$$\begin{split} dA_{\mathrm{observed}} &= |\left(dl_{1,s'_{\theta}}dl_{2,s'_{\phi}} - dl_{1,s'_{\phi}}dl_{2,s'_{\theta}}\right)\vec{\mathbf{r}} \\ &+ \left(dl_{1,s'_{\phi}}dl_{2,r} - dl_{1,r}dl_{2,s'_{\phi}}\right)\vec{\mathbf{\theta}} \\ &+ \left(dl_{1,r}dl_{2,s'_{\theta}} - dl_{1,s'_{\theta}}dl_{2,r}\right)\vec{\mathbf{\phi}}| \end{split}$$

The observed patch of area always lies on the image capture sphere and never extends in the r direction, meaning that the r components are all zero: $d_{1,r} = 0$ and $d_{2,r} = 0$, leading to:

$$dA_{\text{observed}} = \left| dl_{1,s'_{\theta}} dl_{2,s'_{\theta}} - dl_{1,s'_{\theta}} dl_{2,s'_{\theta}} \right|$$

We can expand each length element, keeping in mind that the edges of the true patch are extended in coordinate directions.

$$dA_{\text{observed}} =$$

$$\left| \frac{dl_{1,s'_{\theta}}}{dx} dx \frac{dl_{2,s'_{\theta}}}{dy} dy - \frac{dl_{1,s'_{\theta}}}{dx} dx \frac{dl_{2,s'_{\theta}}}{dy} dy \right|$$

$$= \left| \frac{dl_{1,s'_{\theta}}}{dx} \frac{dl_{2,s'_{\theta}}}{dy} - \frac{dl_{1,s'_{\theta}}}{dx} \frac{dl_{2,s'_{\theta}}}{dy} \right| dxdy$$

$$=\left|\frac{dl_{1,s'_{\boldsymbol{\theta}}}}{dx}\frac{dl_{2,s'_{\boldsymbol{\phi}}}}{dy}-\frac{dl_{1,s'_{\boldsymbol{\phi}}}}{dx}\frac{dl_{2,s'_{\boldsymbol{\theta}}}}{dy}\right|dA_{x,y}$$

We can now write down the relative observed area, which is the observed area divided by the true area.

$$\frac{dA_{\text{observed}}}{dA_{x,y}} = \left| \frac{dl_{1,s'_{\theta}}}{dx} \frac{dl_{2,s'_{\phi}}}{dy} - \frac{dl_{1,s'_{\phi}}}{dx} \frac{dl_{2,s'_{\theta}}}{dy} \right|$$

$$\frac{dA_{\text{observed}}}{dA_{x,y}} = \left| M_{s'_{\theta}/x} M_{s'_{\phi}/y} - M_{s'_{\phi}/x} M_{s'_{\theta}/y} \right|$$

To be consistent with our other notation, we can label the observed relative area, which is also called the area magnification, using the notation:

$$M_{\text{obs./}x,y} = \frac{dA_{\text{observed}}}{dA_{x,y}}$$

so that we finally have:

$$M_{\text{obs.}/x,y} = \left| M_{s'_{\theta}/x} M_{s'_{\theta}/y} - M_{s'_{\theta}/x} M_{s'_{\theta}/y} \right|$$
 (90)

All other types of object area patches will follow the same formulation.

8.1 Observed Object Area in Rectangular Coordinate/Cylindrical Coordinates About the z Axis

Inserting the appropriate observed relative length equations from Eqs. 29 to 57 into the appropriate area magnification definitions such as Eq. 90, we find the equations below. Mathematically working out the extensive details is left to the reader.

For a small patch of area that lies in a plane that is parallel to the *x-y* plane, it has the area magnification:

$$M_{\text{obs./x,y}} = \frac{z}{(x^2 + y^2 + z^2)^{3/2}}$$
 or (91)

$$M_{\text{obs./x,y}} = \frac{1}{r^2} \cos \theta \tag{92}$$

For a small patch of area that lies in a plane that is parallel to the *x-z* plane, the patch has the area magnification:

$$M_{\text{obs.}/x,z} = \frac{|y|}{(x^2 + y^2 + z^2)^{3/2}} \text{ or } (93)$$

$$M_{\text{obs.}/x,z} = \frac{1}{r^2} \sin \theta |\sin \varphi| \tag{94}$$

For a small patch of area that lies in a plane that is parallel to the *y-z* plane, the patch has the area magnification:

$$M_{\text{obs./y,z}} = \frac{|x|}{(x^2 + y^2 + z^2)^{3/2}} \text{ or }$$
 (95)

$$M_{\text{obs./y,z}} = \frac{1}{r^2} \sin \theta |\cos \varphi|$$
 (96)

For a small patch of area that extends in the ρ and z directions, the patch has the area magnification:

$$M_{\text{obs.}/\rho,z} = 0 \tag{97}$$

For a small patch of area that extends in the ρ and s_{φ} directions, the patch has the area magnification:

$$M_{\text{obs.}/\rho, s_{\varphi}} = \frac{z}{(z^2 + \rho^2)^{3/2}} \text{ or } (98)$$

$$M_{\text{obs.}/\rho,s_{\varphi}} = \frac{1}{r^2} \cos \theta \tag{99}$$

Note that Eqs. 92 and Eq. 99 are the same equation because both represent a patch of area in a plane parallel to the *x-y* plane.

For a small patch of area that extends in the s_{φ} and z directions, it has the area magnification:

$$M_{\text{obs./}s_{\varphi},z} = \frac{\rho}{(z^2 + \rho^2)^{3/2}} \text{ or } (100)$$

$$M_{\text{obs./s}_{\varphi},z} = \frac{1}{r^2} \sin \theta \tag{101}$$

8.2 Observed Object Area in Spherical Coordinates

Inserting the appropriate observed relative length equations from Eqs. 59 to 66 into the appropriate area magnification definitions, we find the equations below.

For a small patch of area that lies on the object coordinate sphere, i.e. is extending in the s_{θ} and

 s_{φ} directions, it has the area magnification:

$$M_{\text{obs./}s_{\theta},s_{\varphi}} = \frac{1}{r^2} \tag{102}$$

Because the object location surface is a sphere and the image capture surface is a sphere, the only object area patch that can be observed as a non-zero image area patch is the one represented in Eq. 102. All other possibilities are expected to be zero, as can be verified by doing the calculation:

$$M_{\text{obs./}r,s_{\theta}} = M_{\text{obs./}r,s_{\theta}} = 0 \qquad (103)$$

8.3 Observed Object Area in Cylindrical Coordinates About the *y* Axis

Inserting the appropriate observed relative length equations from Eqs. 68 to 83 into the appropriate area magnification definitions, we find the equations below.

For a small patch of area that extends in the s_{α} and l directions, it has the area magnification:

$$M_{\text{obs.}/s_{\alpha},l} = \frac{|y|}{(l^2 + v^2)^{3/2}} \text{ or } (104)$$

$$M_{\text{obs./s}_{\alpha},l} = \frac{1}{r^2} \sin \theta |\sin \varphi|$$
 (105)

Note that Eqs. 104 and 105 are the exact same as Eqs. 93 and 94 because they both involve area patches in the same plane.

For a small patch of area that extends in the s_{α} and y directions, it has the area magnification:

$$M_{\text{obs./}s_{\alpha},y} = \frac{l}{(l^2 + v^2)^{3/2}} \text{ or } (106)$$

$$M_{\text{obs./s}_{\alpha,\mathcal{Y}}} = \frac{1}{r^2} \sqrt{1 - \sin^2 \theta \sin^2 \varphi}$$
 (107)

For a small patch of area that extends in the *l* and *y* directions, it has the area magnification:

$$M_{\text{obs./l,y}} = 0 \tag{108}$$

Plotting the Observed Object Area as a Function of Spherical Coordinates

To get an intuitive sense of what the area equations mean, we can plot the observed relative area as a function of the object's position in spherical coordinates (r, θ, φ) . In this way, these plots represent how the observed relative area of the object changes as the object moves along one of the spherical coordinate directions. In all of the plots below, all areas are shown in square meters. Keep in mind that the observed areas correspond to a one-meter-radius image capture sphere.

Generally, the observed area appearing smaller than the true area arises from two mechanisms. First, the farther away the object, the smaller it looks because it takes up a smaller portion of the entire view. As mentioned previously, this is the distance-perspective effect. Secondly, an object that is only extended in two directions (like a credit card), will look smaller if it is somewhat tilted away from the observer. If the object is tilted so that it lies in a plane that extends directly away from the observer (i.e. it extends in the rdirection), then it will appear to have zero area. In contrast, if the object is tilted so that its broadside is directly viewed (i.e. it lies in a plane that is perpendicular to the r direction), then it will have zero shrinking from this tilt effect.

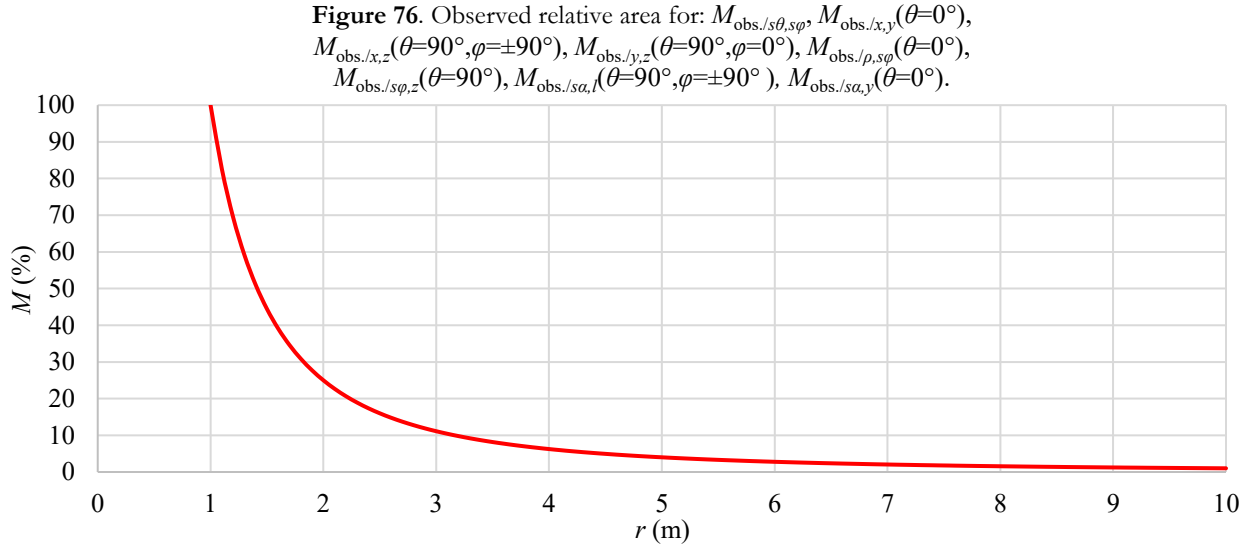
In the plots below, the perceived diminished

size sometimes arises from the distance-perspective effect, sometimes from the tilt effect, and sometimes from both effects. When the object is oriented so that its broadside is directly viewed, the total observed relative area then only depends on how far away the object is from the observer, which is the distance r.

The first thing to notice is that all of the observed area equations in spherical coordinates (Eqs. 92, 94, 96, 99, 101, 102, 105, and 107) depend on r as $(1/r^2)$, even if they depend on other coordinates, no matter in which direction the object is extended and no matter where the object is located. This means that no matter in which direction the object is extended and no matter where it is located, if it moves directly away from the observer, its total observed area will decrease as $(1/r^2)$.

For instance, if a patch of area moves directly to twice the distance from the observer as it was originally, then it will appear to have an area that is one fourth as large as originally. Or, if a patch of area moves to three times the distance from the observer as it was originally, then it will appear to have an area that is one ninth as large as originally. This is true no matter how the object is oriented. It should make sense that the observed

Chapter 9. Plotting the Observed Object Area as a Function of Spherical Coordinates



area depends on r as $(1/r^2)$ when we remember that the observed length of a line depended on r as (1/r). Any patch of area that is small enough acts like a square patch, and the area of a square is width squared, so that the r-functionality part of all area equations should be $(1/r)(1/r) = (1/r^2)$, as they are.

This dependence is plotted in Fig. 76. Note that the observed relative area is 100% at r = 1 because we are using a one-meter-radius image capture sphere. For r < 1, the object is inside the image capture sphere and there is no image.

When the patch of area is extended in the s_{θ} and s_{φ} directions, it is always viewed exactly from broadside no matter where it is located. This means that in this case, the observed relative area depends only on r and nothing else. Therefore, the entire area equation is $M = (1/r^2)$, as can be seen in Eq. 102. This means that Fig. 76 shows the observed area for this case for all locations of the object.

In all the other cases, when the object is at special locations where it is being viewed broadside, the corresponding area M equation reduces down to $M = (1/r^2)$ and the plot looks the same as in Fig. 76. In other words, Fig. 76 is also the exact same plot that results for when the object is

extended in the following ways: in the x and y directions at the locations where $\theta = 0^{\circ}$ (Eq. 92), when it's extended in the x and z directions at the locations where $\theta = 90^{\circ}$ and $\varphi = \pm 90^{\circ}$ (Eq. 94), when it's extended in the y and z directions at the locations where $\theta = 90^{\circ}$ and $\varphi = 0^{\circ}$ (Eq. 96), when it's extended in the ρ and s_{φ} directions at the locations where $\theta = 0^{\circ}$ (Eq. 99), when it's extended in the s_{φ} and z directions at the locations where $\theta = 90^{\circ}$ (Eq. 101), when it's extended in the s_{α} and z directions at the locations where z_{α} and z directions at the locations where z z directi

Note that for situations where the object is extended in the ρ and z directions (Eq. 97), in the r and s_{θ} directions (Eq. 103), or in the r and s_{θ} directions (Eq. 103), the object has zero observed area because it is tilted so that it extends directly away from the observer.

Fig. 77 shows what it means to be plotting the object's observed relative area when the object is extended in the x and y directions (the object is shown in blue), as the object's θ coordinate is increased, but its distance r from the observer is held constant. Fig. 78 shows what it means to be plotting the object's observed relative area when

Chapter 9. Plotting the Observed Object Area as a Function of Spherical Coordinates

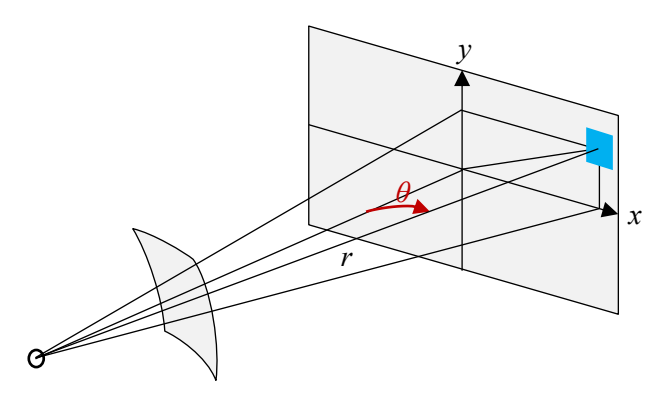


Figure 77. Plotting $M_{\text{obs./x,y}}$ as θ increases.

the object is extended in the ρ and s_{φ} directions, as the object's θ coordinate is increased, but its distance r from the observer is held constant. Fig. 79 shows the resulting plot of $M_{\text{obs./x,y}}$ as a function of θ for various fixed r values, which is the plot of Eq. 92 and the situation shown in Fig. 77.

Because the overall distance from the observer r is being held constant for each curve, the change in observed area along a curve is purely a result of the tilt effect. Fig. 79 is also the exact same plot that results when plotting $M_{\text{obs},/\rho,s\varphi}$ as a function of θ for various fixed r values, which is the plot of Eq. 99 and the situation shown in Fig. 78.

Fig. 80 shows what it means to be plotting the object's observed relative area when the object is extended in the *x* and *z* directions, as the object's

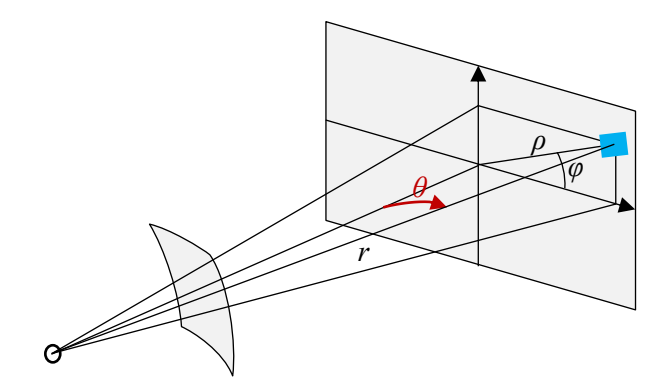
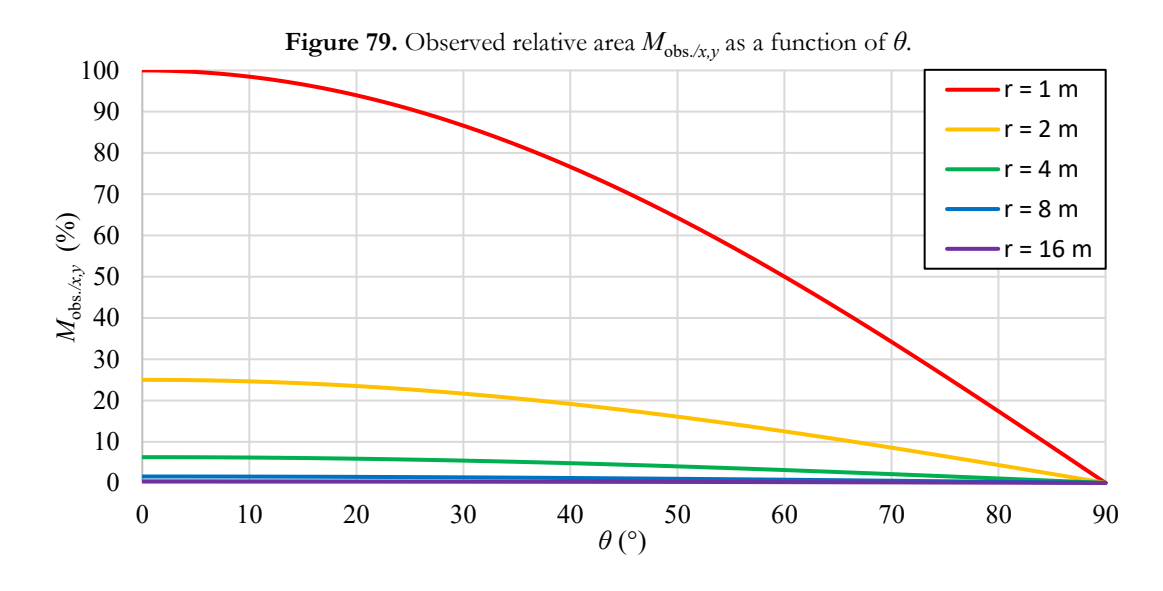


Figure 78. Plotting $M_{\text{obs.}/\rho,s\varphi}$ as θ increases.

 θ coordinate is increased for various fixed φ values for r = 1. Fig. 81 shows what it means to be plotting the object's observed relative area when the object is extended in the s_{α} and l directions, as the object's θ coordinate is increased for various fixed φ values for r = 1.

Fig. 82 shows the resulting plot of $M_{\text{obs./x,z}}$ as a function of θ for various fixed φ values, which is the plot of Eq. 94 and is the situation shown in Fig. 80. Because the overall distance from the observer r is being held constant for each curve, the change in observed area along a curve is purely a result of the tilt effect. Fig. 82 is also the exact same plot that results when plotting $M_{\text{obs./sa,I}}$ as a function of θ for various fixed φ values, which is shown in Fig. 81 and is the plot of Eq. 105.



Chapter 9. Plotting the Observed Object Area as a Function of Spherical Coordinates

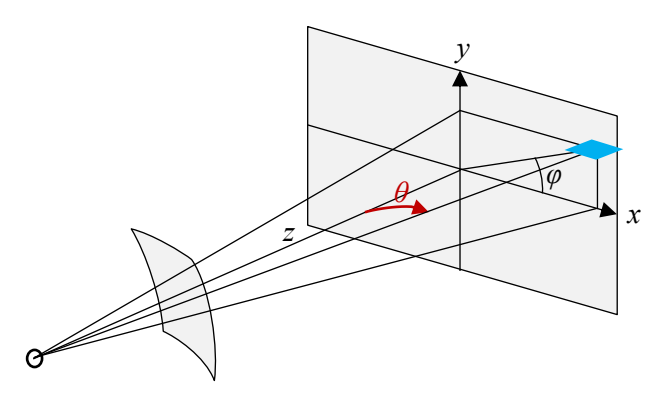


Figure 80. Plotting $M_{\text{obs./x,}z}$ as θ increases.

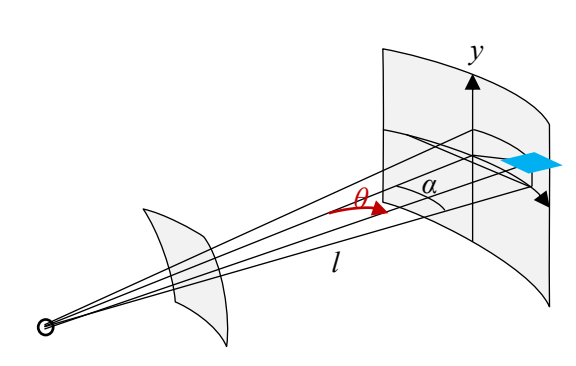


Figure 81. Plotting $M_{\text{obs./sa,l}}$ as θ increases.

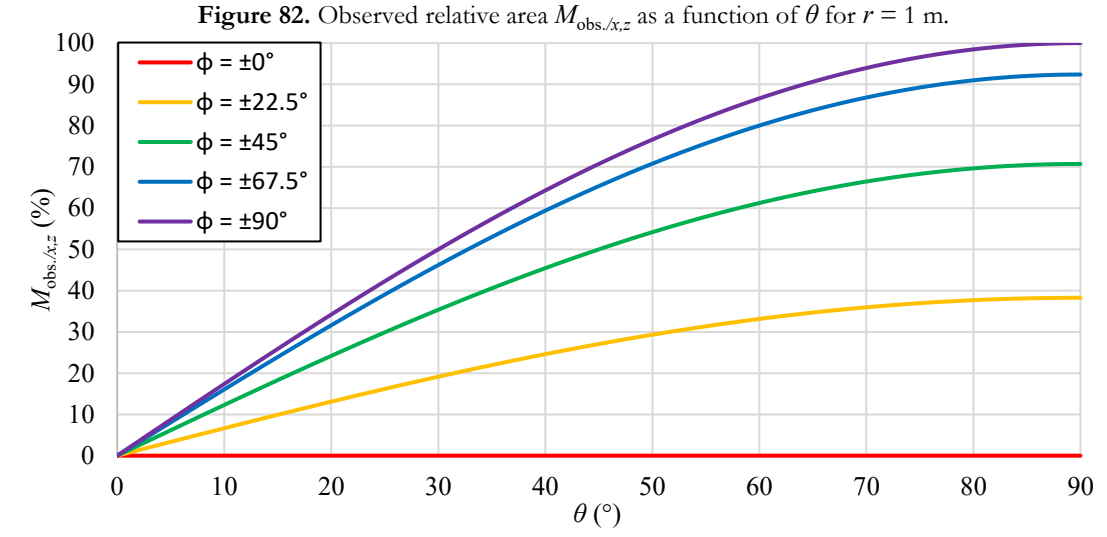


Fig. 83 shows what it means to be plotting the object's observed relative area when the object is extended in the y and z directions, as the object's θ coordinate is increased for various fixed φ values for r=1. Fig. 85 shows the resulting plot,

showing $M_{\text{obs./y,z}}$ as a function of θ for various fixed φ values, which is the plot of Eq. 98.

Because the overall distance from the observer r is being held constant for each curve, the change in observed area along a curve is a result of tilt.

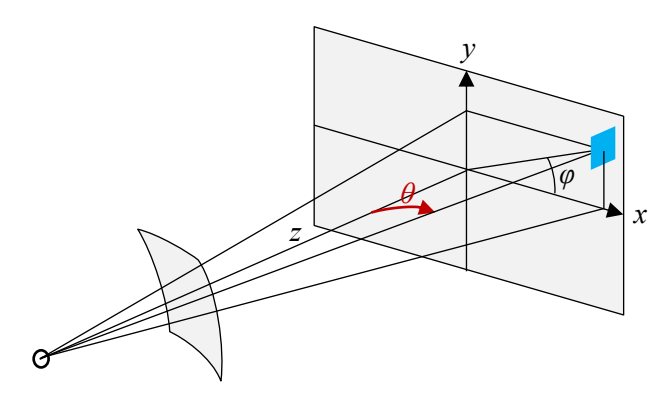


Figure 83. Plotting $M_{\text{obs./y,}z}$ as θ increases.

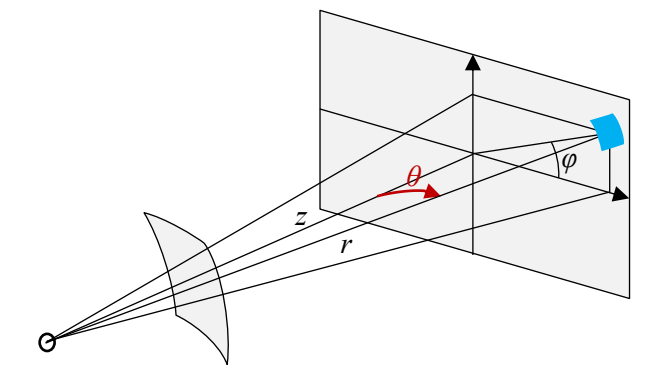


Figure 84. Plotting $M_{\text{obs./s}\varphi,z}$ as θ increases.

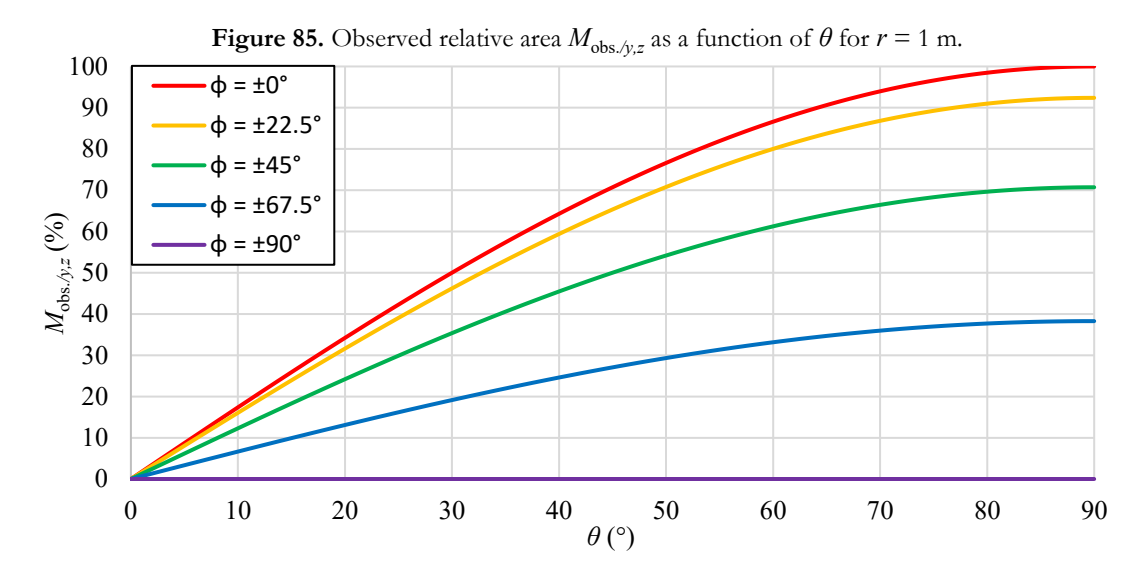


Figure 86. Observed relative area $M_{{\rm obs./s}\varphi,z}$ as a function of θ .

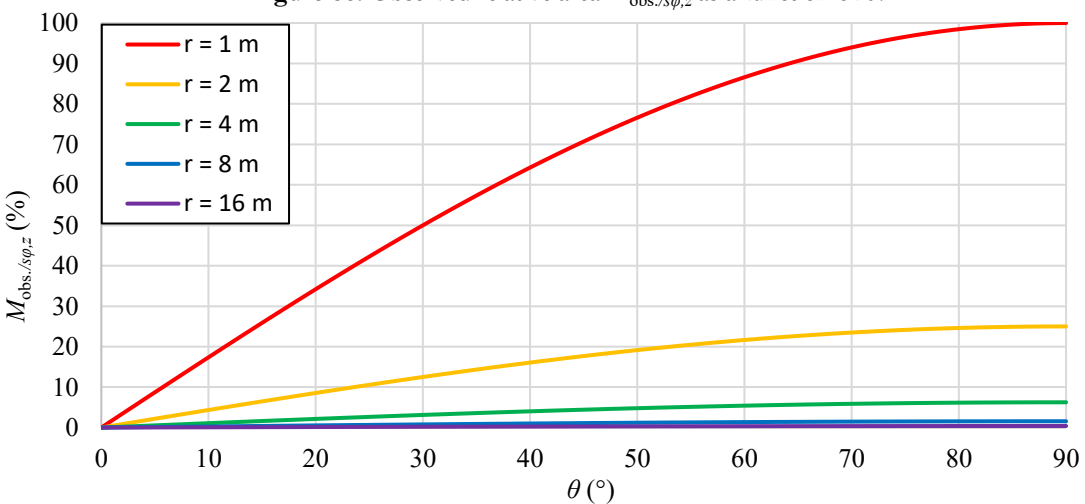
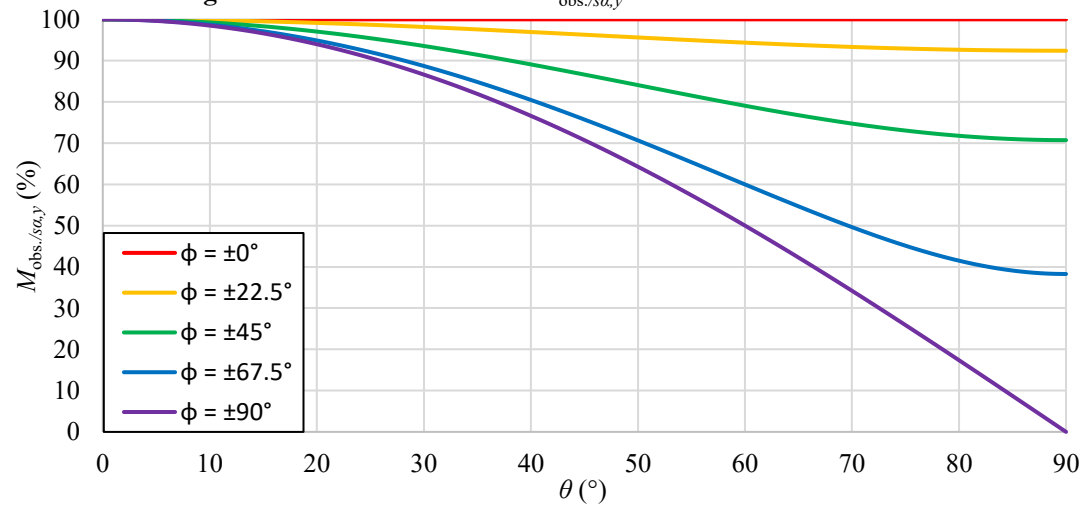


Figure 87. Observed relative area $M_{\text{obs./sa,y}}$ as a function of θ for r = 1 m.



Chapter 9. Plotting the Observed Object Area as a Function of Spherical Coordinates

Fig. 84 shows what it means to be plotting the object's observed relative area when the object is extended in the s_{φ} and z directions, as the object's θ coordinate is increased for various fixed r values. Fig. 86 shows the resulting plot, showing $M_{\text{obs./s}\varphi,z}$ as a function of θ for various fixed r values, which is the plot of Eq. 101. Because the overall distance from the observer r is being held constant for each curve, the change in observed area along a curve is purely a result of the tilt effect.

Fig. 88 shows what it means to be plotting the object's observed relative area when the object is extended in the s_{α} and y directions, as the object's θ coordinate is increased for various fixed φ values when r = 1. Fig. 87 shows the resulting

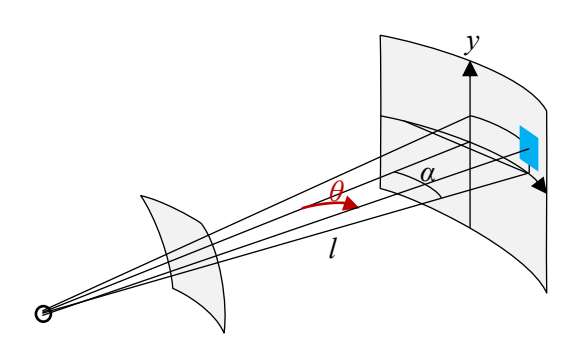


Figure 88. Plotting $M_{\text{obs./sa,y}}$ as θ increases.

plot, showing $M_{\text{obs./sa,y}}$ as a function of θ for various fixed φ values when r = 1, which is the plot of Eq. 107. Because the overall distance from the observer r is being held constant for each curve, the change in observed area along a curve is purely a result of the tilt effect.

Plotting the Observed Object Area as a Function of Original Object Coordinates

We can now plot the area equations as a function of the object's position in rectangular coordinates, cylindrical coordinates about the *z* axis, and cylindrical coordinates about the *y* axis. The situations listed in Table 2 and shown in Figs. 89 to 95 all have the exact same mathematical form. Thus, all of these situations have the same resulting plot,

which is shown in Fig. 96. Note that the situations shown in Figs. 89, 90, and 91 only exactly match the plot in Fig. 96 when the third coordinate is zero. However, when the third coordinate is not zero in these cases, the resulting plot still has the same trends as in Fig. 96 but is simply scaled uniformly smaller.

Table 2. The situations that all have the same plot, shown in Fig. 96, after appropriate relabeling of axes.

Area patch	As a function of	For various fixed	Equation	Figure
$M_{ m obs./x,y}$	z	x or y	Eq. 91	Fig. 89
$M_{ m obs./x,z}$	y	x or z	Eq. 93	Fig. 90
$M_{ m obs./\it y,\it z}$	x	y or z	Eq. 95	Fig. 91
$M_{ ext{obs.}/ ho,sarphi}$	z	ρ	Eq. 98	Fig. 92
$M_{ ext{obs./}sarphi,z}$	ρ	z	Eq. 100	Fig. 93
$M_{ m obs./s}$ α,l	у	l	Eq. 104	Fig. 94
$M_{ ext{obs./sa,y}}$	1	y	Eq. 106	Fig. 95

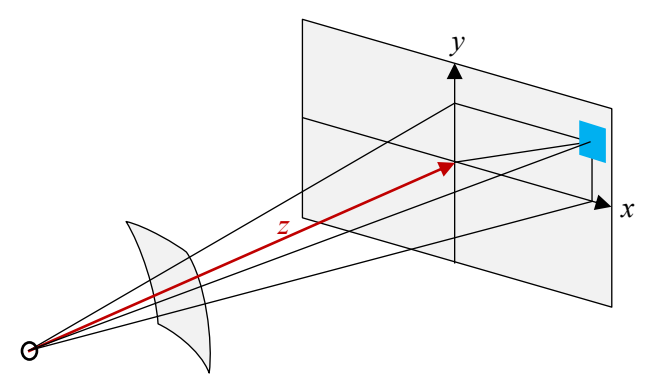


Figure 89. Plotting $M_{\text{obs./x},y}$ as z increases.

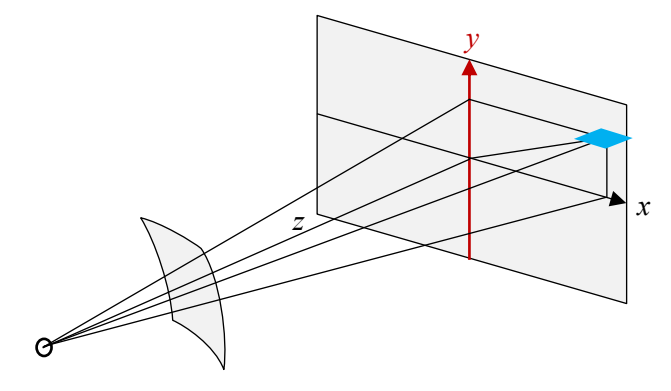


Figure 90. Plotting $M_{\text{obs./x,z}}$ as y increases.

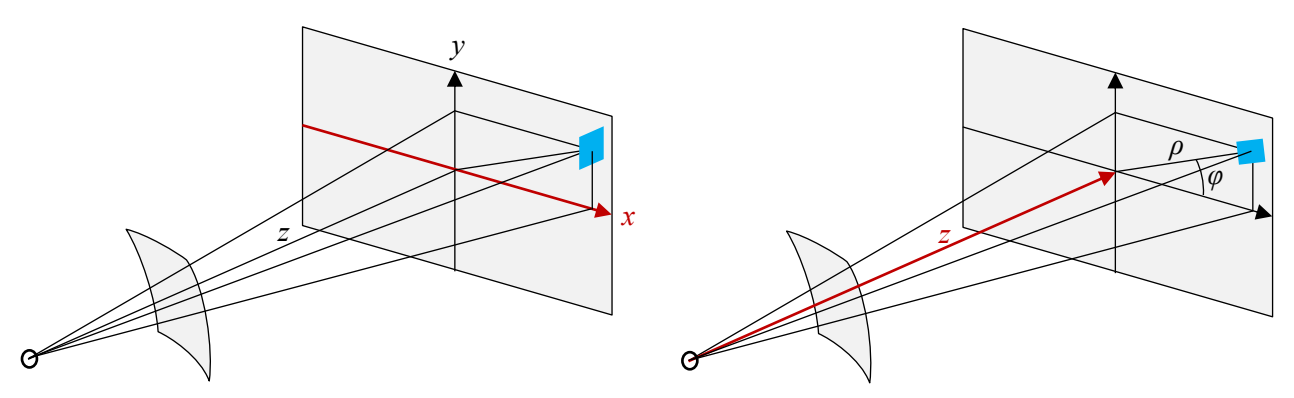


Figure 91. Plotting $M_{\text{obs./y,z}}$ as x increases.

Figure 92. Plotting $M_{\text{obs./}\rho,s\varphi}$ as z increases.

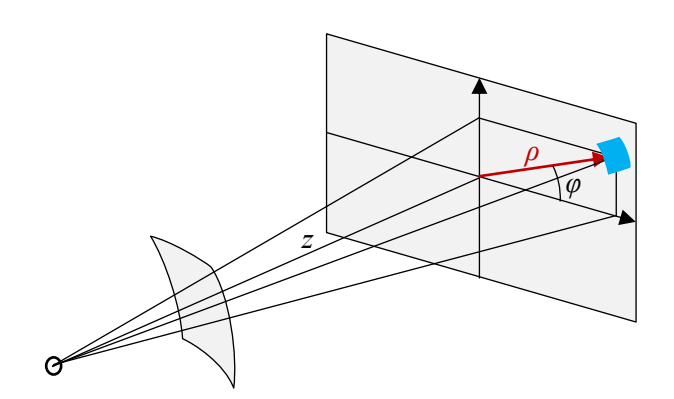


Figure 93. Plotting $M_{{
m obs./s}\varphi,z}$ as ho increases.

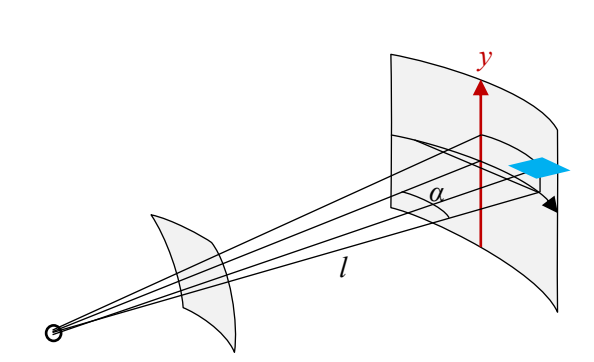


Figure 94. Plotting $M_{\text{obs./sa,l}}$ as y increases.

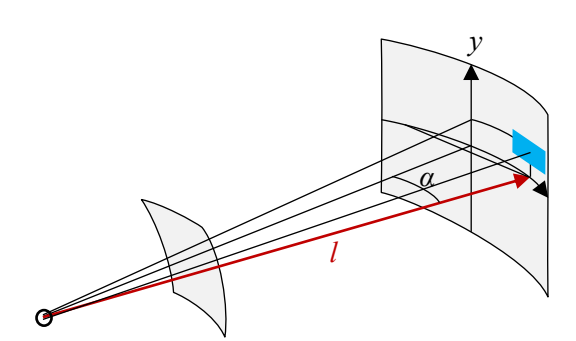
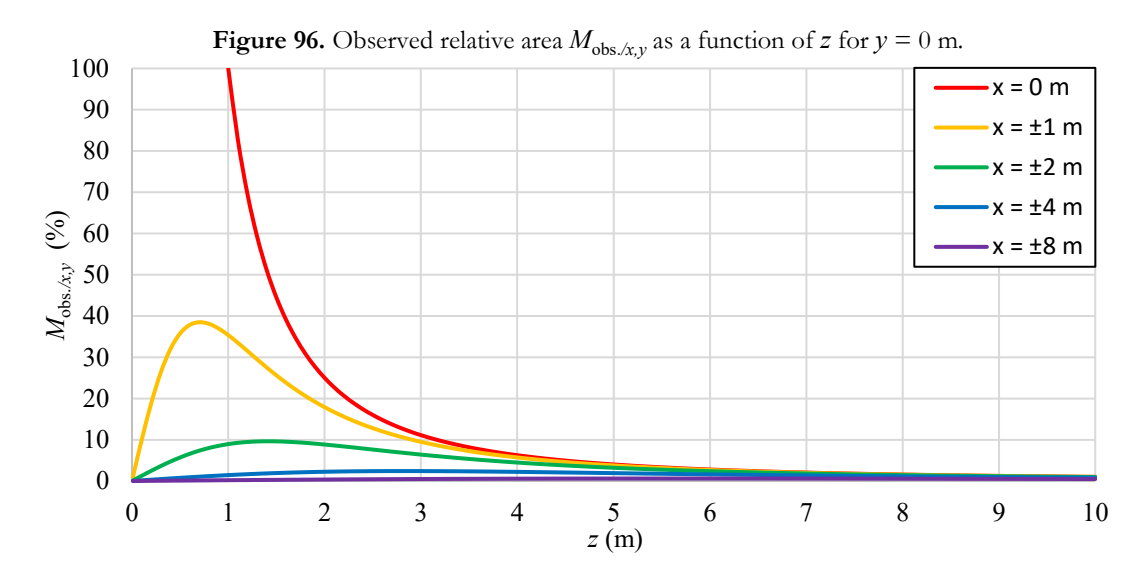


Figure 95. Plotting $M_{\text{obs./sa,y}}$ as l increases.

Chapter 10. Plotting the Observed Object Area as a Function of Original Object Coordinates



The situations listed in Table 3 and shown in Figs. 97 to 106 all have the exact same mathematical forms. Therefore, all of these situations have the exact same resulting plot, which is shown in Fig. 107, after appropriate relabeling of the axes. Note that the situations shown in Figs. 97 to 102 only exactly match the plot in Fig. 107 when the third coordinate is zero. However, when the third coordinate is not zero in these cases, the resulting plot still has the same trends as in Fig. 107 but is

simply scaled uniformly smaller.

In all of the situations listed in Table 3, the decreasing observed size is a result of the distance-perspective effect and the tilt effect. In each of these situations, as the object moves away from the viewing axis or away from the observer, as the case may be, it is observed to tilt at the same rate as the other situations and to increase in distance from the observer at the same rate as the other situations.

Table 3. The situations that all have the same plot, shown in Fig. 107, after appropriate relabeling of axes.

Area patch	As a function of	For various fixed	Equation	Figure
$M_{ m obs./x,y}$	x	z	Eq. 91	Fig. 97
$M_{ m obs./x,y}$	y	Z	Eq. 91	Fig. 98
$M_{ m obs./x,z}$	x	y	Eq. 93	Fig. 99
$M_{ m obs./x,z}$	Z	y	Eq. 93	Fig. 100
$M_{ m obs./\it y,\it z}$	y	x	Eq. 95	Fig. 101
$M_{ m obs./\it y,\it z}$	Z	x	Eq. 95	Fig. 102
$M_{ ext{obs.}/ ho,s\phi}$	ρ	z	Eq. 98	Fig. 103
$M_{ ext{obs./}sarphi,z}$	Z	ρ	Eq. 100	Fig. 104
$M_{ m obs./s}$ α,l	l	у	Eq. 104	Fig. 105
$M_{ ext{obs./s}lpha,y}$	у	1	Eq. 106	Fig. 106

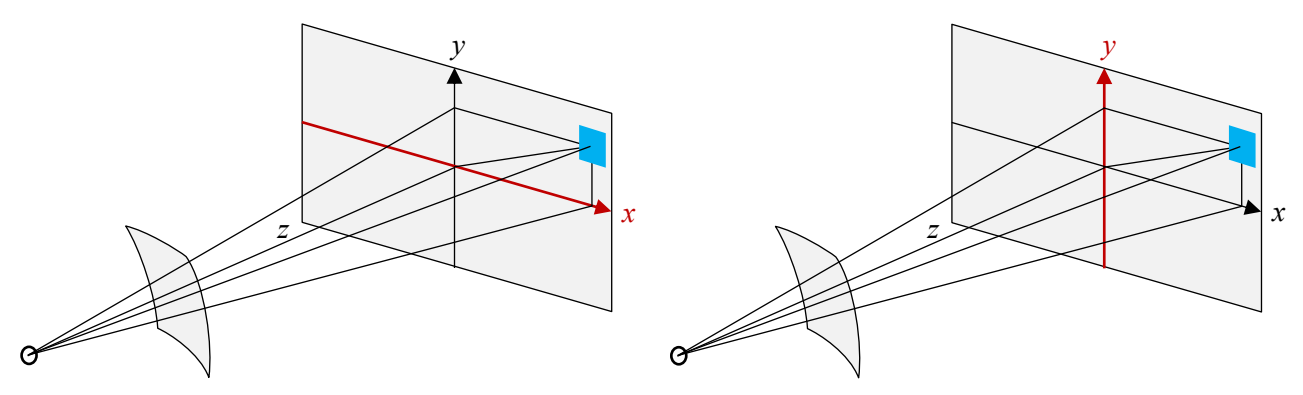


Figure 97. Plotting $M_{\text{obs./x,y}}$ as x increases.

Figure 98. Plotting $M_{\text{obs./x},y}$ as y increases.

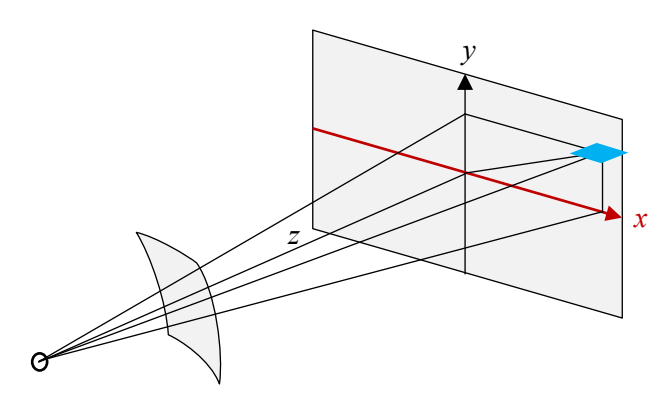


Figure 99. Plotting $M_{\text{obs./x,z}}$ as x increases.

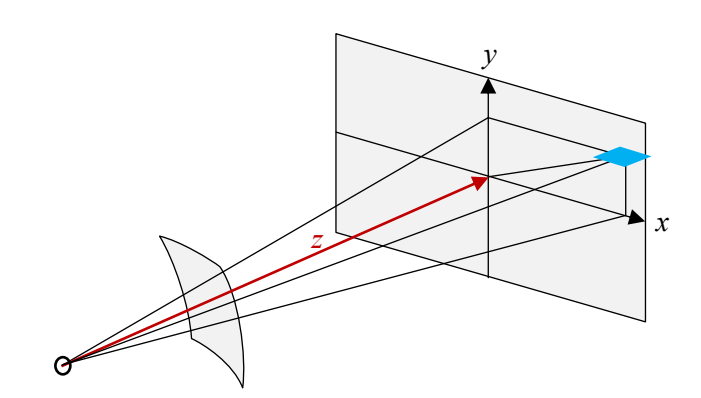


Figure 100. Plotting $M_{\text{obs./x,z}}$ as z increases.

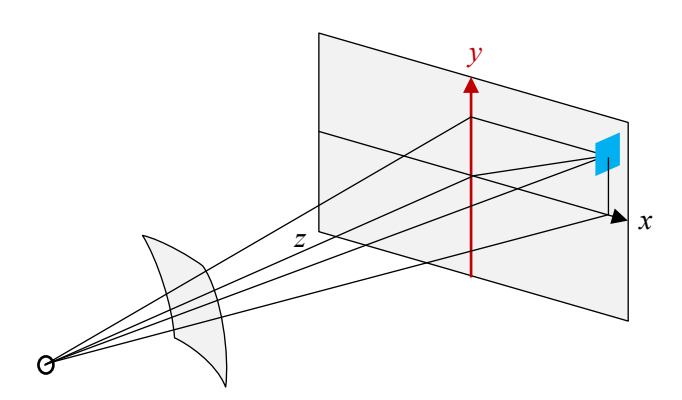


Figure 101. Plotting $M_{\text{obs./y,z}}$ as y increases.

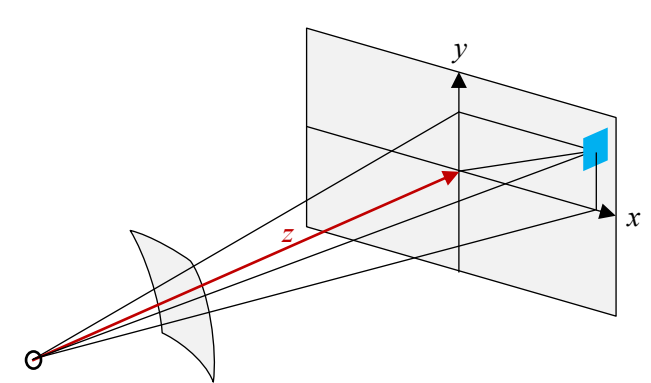


Figure 102. Plotting $M_{\text{obs./y,}z}$ as z increases.

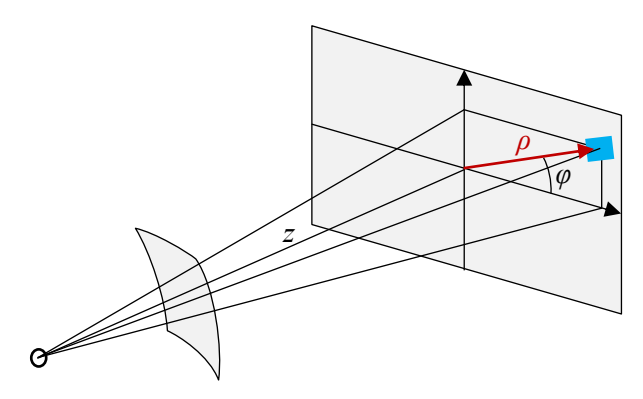


Figure 103. Plotting $M_{\text{obs./}\rho,s\varphi}$ as ρ increases.

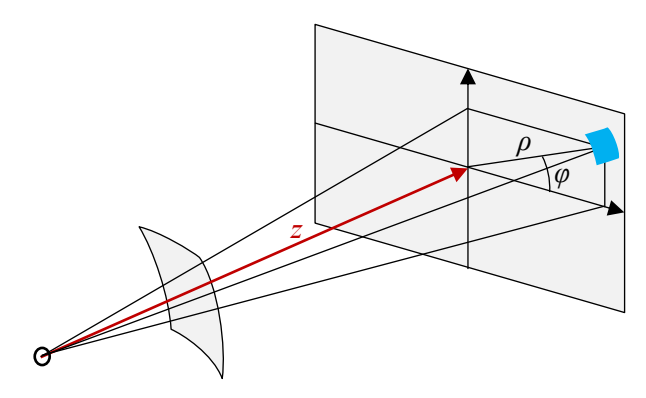


Figure 104. Plotting $M_{\text{obs./s}\varphi,z}$ as z increases.

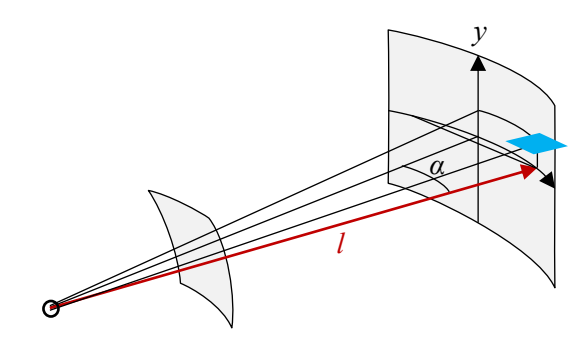


Figure 105. Plotting $M_{\text{obs./sa},l}$ as l increases.

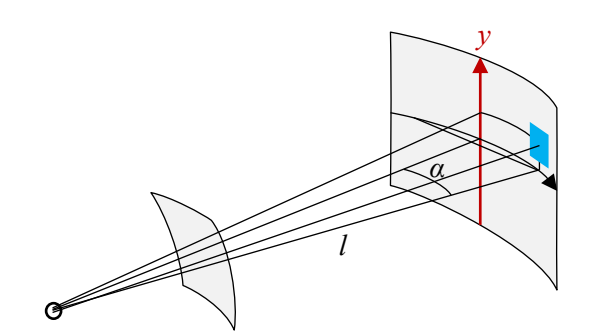
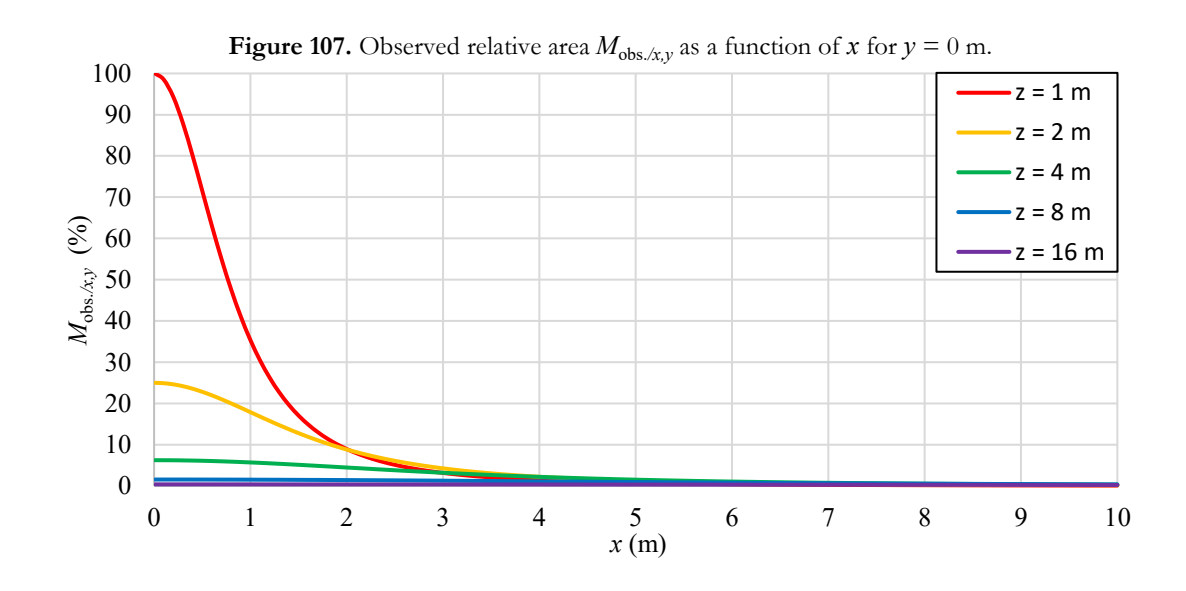


Figure 106. Plotting $M_{\text{obs./sa,y}}$ as y increases.



Chapter 11

Mapping to a Flat Display Screen

Traditional computer screens, television screens, movie projector screens, mobile device display screens, paintings, drawings, photographic prints, and printed posters all involve presenting a two-dimensional image on a *flat* display surface that is supposed to give the same visual experience as looking at a physically present three-dimensional object or scene. However, the human retina is a spherical imaging surface. Also, the eye is a small, point-like observer that sees in terms of spherical coordinate angles. Therefore, what is seen on the spherical image capture surface must be somehow mapped to a flat display screen.

There are several approaches for doing this mapping. None of these approaches are exactly correct because there is simply no way to map a spherical image capture surface to a flat display screen without distortions. This means that threedimensional objects displayed on a flat screen will never exactly match what is seen by the human eye when looking at the same objects in the real world. To be clear, this fact has nothing to do with humans using two eyes in unison for vision. Even when just using one eye, three-dimensional objects that are displayed on a flat screen will never exactly match what the human eye sees when viewing the same objects in the physically real world. (Note that the use of a standard flat display screen also has the problem of presenting the same image to both eyes, thereby failing to reproduce the parallax effect; but that is a different defect from what we are discussing here.)

For there to be no distortions, the computer display screen or projector screen would have to be spherical, with the observer's eye located at the exact center of this spherical screen, and with objects in the scene shown at the correct spherical coordinates.

Most computer screens and projector screens are flat due to price and complexity issues. However, the screens in Omni Theaters, IMAX Dome theaters, MSG Spheres, planetariums, and dome flight simulators use spherically shaped projector screens in order to more accurately and immersively present the three-dimensional world.

Even though displaying the three-dimensional physical world on a flat screen introduces distortions and field-of-view limitations, when done cleverly, the distortions can be minimized enough that images can be convincingly experienced as three-dimensional.

When analyzing the mathematics of mapping an image from a spherical image capture surface to a flat display screen, this mapping process is called projection. However, this word is used in a general sense and does not necessarily imply a rectilinear projection or an isometric projection.

A spherical surface centered on the observer

and a flat surface situated in front of the observer and perpendicular to the viewing direction both have azimuthal symmetry and therefore have the same azimuthal angle φ . This means that all that needs to be mapped is the polar angle θ to a radial distance d of a point on the flat display screen from the center of the display screen.

In practice, a flat display screen cannot be infinitely large. This means that objects located near $\theta=90^{\circ}$ must either be mapped to a small enough radius that they fit on the display screen or be left outside the field of view. In the latter case, this means that objects in the real world which humans can see in their peripheral vision are not displayed at all on the display screen.

Projecting all of the hemispherical image capture surface onto a finite-sized, flat display screen preserves all of the information, but it also introduces the most distortion, so that the image may feel less real.

In practice, after each projection operation, a scale factor is applied to the resulting flat image in order to display it on a particular screen at a particular size according to the wishes of the user. This is commonly called the image zoom level. This scaling does not change the appearance of the image on the flat display screen other than its overall size. The application of a scaling factor will therefore be ignored here.

To simplify the equations, we will continue to assume that the image capture sphere has a radius of one meter: a = 1.

11.1 Rectilinear Projection

The rectilinear projection, which is also called the "central perspective projection" or the "standard projection," introduces the least amount of distortion. This means that the objects and scenes that are displayed on the flat display screen feel the most real when this projection is used. For this reason, the rectilinear projection is the most

common projection used in movies, television, photography, drawing, and painting. The rectilinear projection is so commonly used that some professionals working in these fields do not even know that other projections exist.

Even though using the rectilinear projection produces the least distortion, the tradeoff is that a large portion of the hemispherical, real-world field of view ends up off the screen. In other words, only a small central section of the image capture hemisphere fits on the display screen. As a result, visual information is lost and the peripheral portions of human vision are completely excluded, making the vision experience feel less immersive.

The larger the display screen, the smaller the amount of peripheral vision that is excluded, and the more immersive the experience feels. This is one of the reasons that movie theaters use large screens and that homeowners tend to buy the biggest television screen that they can afford. As mentioned previously, the only way to display the entire image capture hemisphere without distortion is by using a spherical display screen such as found in dome theaters.

The loss of the peripheral image information when using a rectilinear projection is not as significant as it sounds. Keep in mind that the great majority of photoreceptive cone cells in humans are situated in the central region of vision.

With that said, sometimes retaining peripheral visual information is more important than lack of distortion. In such cases, some other projection must be used. For instance, the rectilinear projection is typically not used for panoramic photography or for all-sky scientific photography.

Also, the rectilinear projection fails to properly include lateral perspective effects. In other words, any object that moves directly away from the viewing axis (i.e. in the ρ direction) should appear to get smaller as it moves, because it is moving

farther away from the observer. However, in the rectilinear projection, an object that is moving directly away from the viewing axis does not change size at all, in terms of its actual size on the display screen, no matter how far it goes. This drawback is not as bad as it sounds because the object typically moves off the screen, and thus out of view, before it travels enough distance that the lack of lateral perspective becomes obvious.

The rectilinear projection consists of extending the radial line that goes from the observer through the object on the image capture sphere until it meets the flat display screen, as is shown in Fig. 108.

In Figs. 108-113, the solid black circle or semicircle represents the hemispherical image capture surface, the solid black horizontal line represents the flat display screen, the image shown in the long grey box represents what you would actually see on the display screen, the solid grey arrows show the projection directions, and the dashed lines are drawn to represent various polar angles.

As shown in Fig. 108, we end up with a right triangle with a as the adjacent side and d as the opposite side. Applying trigonometry, we find: $d/a = \tan \theta$. Setting a = 1, as we have done previously, this becomes:

$$d = \tan \theta \tag{109}$$

Fig. 108 makes it clear that the entire image capture hemisphere cannot fit on a finite flat display screen when the rectilinear projection is used. An infinitely large display screen would be needed to contain the entire image capture hemisphere.

Because of the ability to scale a flat image (i.e. zoom in and out), one can choose to use a very large mathematical flat display screen to capture a large amount of the hemispherical image capture surface and then scale the result down in order to fit it onto the physical display screen. However, the drawback of this approach is that the objects in the scene become very small in the image.

By combining Eq. 109 with Eqs. 9, 11, and 20, we can derive the equations that can tell us how to take the object's physical location (x, y, z) or $(\rho,$ φ , z) or (α, y, l) and compute the object's location (d, φ) on the flat display screen, leading to Eqs. 110-112 (remembering that the φ coordinate of the flat display screen image is the same as the φ coordinate of the spherical image capture surface and therefore no additional equations are needed for φ):

$$d = \frac{\sqrt{x^2 + y^2}}{z} \tag{110}$$

$$d = \frac{\rho}{z} \tag{111}$$

$$d = \frac{\sqrt{x^2 + y^2}}{z}$$

$$d = \frac{\rho}{z}$$

$$d = \frac{\sqrt{l^2 \sin^2 \alpha + y^2}}{l \cos \alpha}$$
(110)
$$(111)$$

As Eq. 111 shows, this projection leads to the fact that the object's radial distance d from the central horizon point on the flat display screen, and the object's radial distance ρ from the viewing axis in

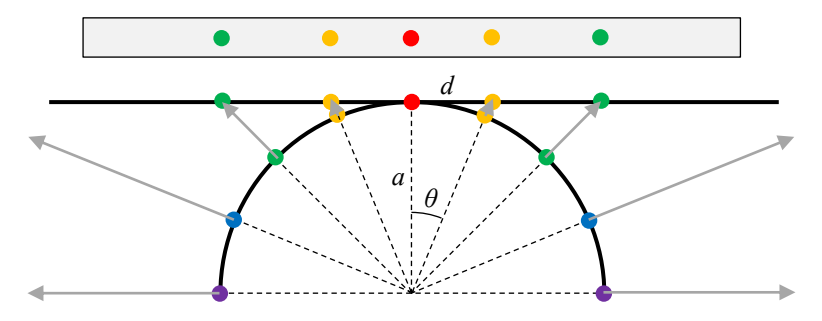


Figure 108. Rectilinear projection.

the original physical reality are linearly proportional to each other with the coefficient of proportionality being (1/z). This means that lines that were straight in the physical reality will end up straight on the flat display screen.

For all objects in the original physical reality that were in the same x-y plane (i.e. at the same zvalue), they were projected onto the spherical image capture surface because of the nature of human vision and then projected back to a flat display screen along the same rays when using the rectilinear projection. This means that if the flat display screen were infinitely large, if the image scale factor was chosen so that the physical size of objects on the display screen exactly equaled the physical size of the objects in the original physical reality, if the image perfectly recreated the correct colors and brightness, and if the person viewing the display screen were standing at the exact location relative to the scene where the camera had been, then there would be zero distortion. This means that the image on the flat display screen would look just like the original physical reality (if viewing the image with only one eye and if ignoring depth from defocusing and if the person continuously gazed directly at

the central horizon point on the screen).

But in most real-world situations, flat display screens are nowhere near infinitely large (they can range in size from a few centimeters on a handheld mobile device to a few dozen meters in movie theatres), the viewer does not typically gaze continuously at exactly the center of the display screen, the viewer is typically much closer than the camera had been, and the image scale factor is rarely chosen to make the physical size of the objects on the display screen equal the size of the same objects in the original physical reality. For these reasons, in addition to the lack of peripheral vision information, using the rectilinear projecttion in practice always involves some amount of distortion. Despite this fact, the human brain is tremendously forgiving so that even when the presented image has large amounts of distortion, the brain can still visually experience depth. As a result, rectilinear-projected images on a flat movie theatre screen can feel incredibly real.

11.2 Stereographic Projection

Although the rectilinear projection typically produces the least distortion, it suffers from the flaw of excluding peripheral-vision information. We

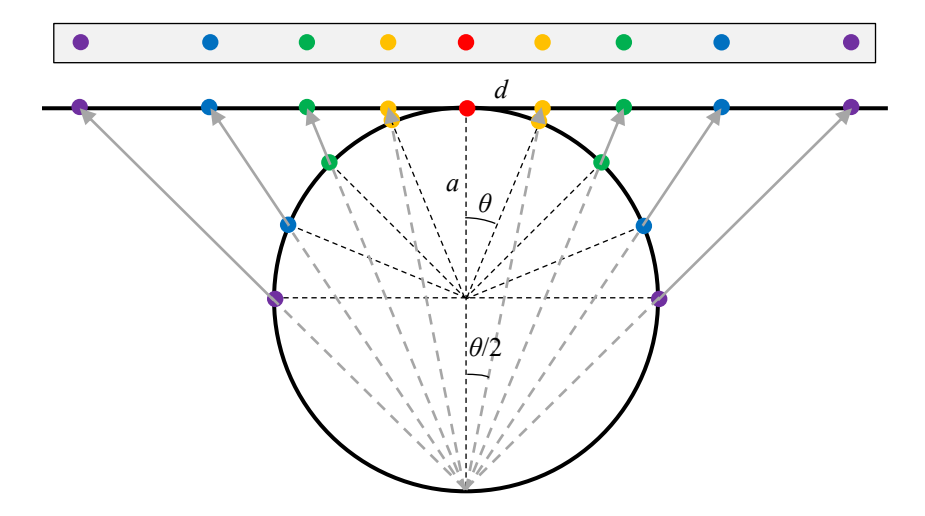


Figure 109. Stereographic projection.

can instead use a projection method that is nearly identical to the rectilinear projection but manages to fit the entire image capture hemisphere on the finite flat display screen. One common way of doing this is by taking Eq. 109 and replacing θ with $\theta/2$, leading to Eq. 113 (note that an overall factor of two is also included in order to give Eq. 113 the same sense of scale as Eq. 109).

This approach is called the stereographic projection. This approach graphically means that we are still projecting a point on the imaging sphere outward along a straight ray, but the ray now originates from the bottom of the image capture sphere instead of from its center where the observer sits, as shown in Fig. 109.

The stereographic projection preserves angles. This means that a particular angle between two physical lines in the real world, when seen on the flat display screen, will be the same angle no matter where it is located on the display screen (assuming that the distance of this angular object from the observer is constant and it is always viewed broadside).

Looking at Fig. 109, we see that a right triangle is formed with d as its opposite side, 2a as its adjacent side, and $\theta/2$ as its angle. This angle can be proven to have a value of $\theta/2$ by recognizing that this right triangle contains the smaller right triangle with the angle θ and an isosceles triangle, so that the two acute angles of the isosceles triangle must be equal to each other and also must

add up to θ , which is only possible if each is $\theta/2$. Applying trigonometry to the right triangle that has the angle $\theta/2$ in Fig. 109, we end up with the equation $\tan(\theta/2) = d/(2a)$. Setting a = 1, we finally find what we already expected:

$$d = 2 \tan \frac{\theta}{2} \tag{113}$$

By combining Eq. 113 with Eqs. 9, 11, and 20, and using various trigonometric identities, we can derive the equations that can tell us how to take the object's physical location (x, y, z) or (ρ, φ, z) or (α, y, l) and compute the object's location (d, φ) on the flat display screen, leading to:

$$d = 2\frac{\sqrt{x^2 + y^2 + z^2} - z}{\sqrt{x^2 + y^2}} \tag{114}$$

$$d = 2\frac{\sqrt{\rho^2 + z^2} - z}{\rho} \tag{115}$$

$$d = 2\frac{\sqrt{l^2 + y^2} - l\cos\alpha}{\sqrt{y^2 + l^2\sin^2\alpha}}$$
 (116)

11.3 Equidistant Projection

The equidistant projection simply maps the polar angle to the radial location on the display screen by setting them equal to each other:

$$d = \theta \tag{117}$$

This is a simple linear relationship. As shown in Fig. 110, this means that a series of objects that are arranged on the image capture sphere with equal spacing will appear on the flat display screen

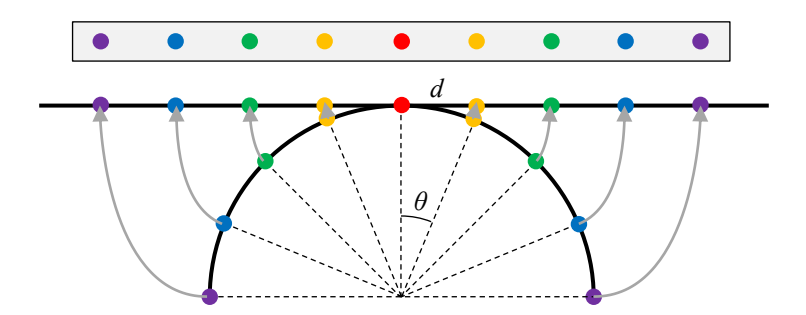


Figure 110. Equidistant projection.

to still have equal spacing. This can be thought of as taking the semicircle and unrolling it until it becomes a flat line.

As usual, the thick black semicircle in Fig. 110 represents the hemispherical image capture surface, the thick black horizontal line represents the flat display screen and the grey box represents what would actually appear on the display screen.

We will again assume that the chosen image scaling factor is such that the entire image capture hemisphere ends up on the display screen.

This equidistant projection preserves angular distance ($\Delta\theta$) relationships. This means that no matter where an object is located in the real field of view and in the corresponding image on the flat display screen, the object will always extend across the same angular distance $\Delta\theta$, (if the object holds its distance r constant and continues to be viewed from broadside), and therefore it will always have the same observed length on the flat display screen if the equidistant projection is used.

Or, in other words, if the distance between two points in physical reality is held constant and the two points are the same distance r from the observer, and both points have the same azimuthal angle, then their observed separation distance on the flat display screen will be the same no matter where they are located, if the equidistant projection is used.

By combining Eq. 117 with Eqs. 9, 11, and 20, we can derive the equations that can tell us how

to take the object's true physical location (x, y, z) or (ρ, φ, z) or (α, y, l) and compute the object's location (d, φ) on the flat display screen:

$$d = \tan^{-1} \left(\frac{\sqrt{x^2 + y^2}}{z} \right) \tag{118}$$

$$d = \tan^{-1}\left(\frac{\rho}{z}\right) \tag{119}$$

$$d = \cos^{-1}\left(\frac{l\cos\alpha}{\sqrt{l^2 + y^2}}\right) \tag{120}$$

11.4 Equisolid Angle Projection

The equisolid angle projection preserves object area relations. This means that a patch of area in physical reality can be moved anywhere (as long as it maintains a constant distance from the observer and is always viewed broadside) and it will always have the same area on the display screen when this projection is used. This means that we set d equal to the straight-line distance between the object's location on the hemispherical image capture surface and the $\theta = 0$ point on the hemispherical image capture surface, as is shown in Fig. 111.

An isosceles triangle is formed by the line connecting the object's location on the hemispherical image capture surface and the $\theta = 0$ point, and the two sides each with length a. If you cut this isosceles triangle in half along its line of symmetry, you end up with a right triangle with a hypotenuse of length a, an opposite side of length a/2, and an angle of a/2. Applying trigonometry

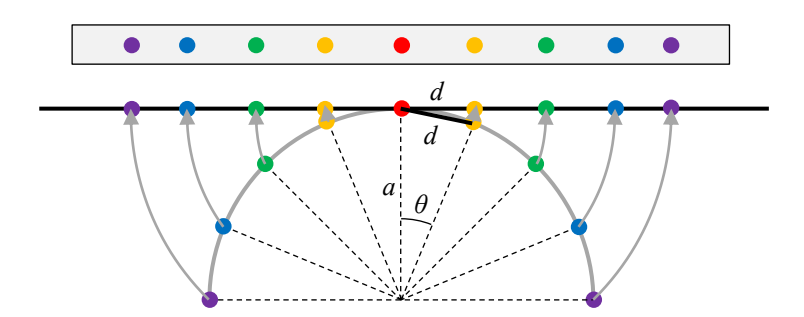


Figure 111. Equisolid angle projection.

to this right triangle, we end up with $sin(\theta/2) = (d/2)/a$. Setting a = 1, we end up with:

$$d = 2\sin\frac{\theta}{2} \tag{121}$$

Combining Eq. 121 with Eqs. 9, 11, and 20, we can derive the equations that tell us how to take the object's physical location (x, y, z) or (ρ, φ, z) or (α, y, l) and compute the object's location (d, φ) on the flat display screen:

$$d = \sqrt{2} \sqrt{1 - \frac{z}{\sqrt{x^2 + y^2 + z^2}}}$$
 (122)

$$d = \sqrt{2} \sqrt{1 - \frac{z}{\sqrt{\rho^2 + z^2}}} \tag{123}$$

$$d = \sqrt{2} \sqrt{1 - \frac{l \cos \alpha}{\sqrt{l^2 + y^2}}} \tag{124}$$

11.5 Orthographic Projection

The orthographic projection involves projecting every object on the hemispherical image capture surface directly in the *z* direction until ends up on the flat display screen, as is shown in Fig. 112.

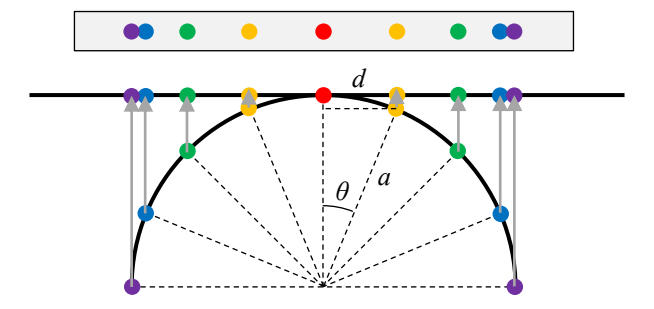


Figure 112. Orthographic projection.

The orthographic projection is similar to the stereographic projection that is shown in Fig. 109, except that instead of the projection rays emanating from the bottom of the spherical image capture surface, they effectively emanate from the point $(x, y, z) = (0, 0, -\infty)$. Looking at Fig. 112 and applying trigonometry, we find: $d/a = \sin \theta$. Setting a = 1 in this equation, it becomes:

$$d = \sin \theta \tag{125}$$

The orthographic projection leads to significant distortion at the higher polar angles (i.e. at the edge of the image on the display screen).

By combining Eq. 125 with Eqs. 9, 11, and 20, and using various trigonometry identities, we can derive the equations that can tell us how to take the object's physical location (x, y, z) or (ρ, φ, z) or (α, y, l) and compute the object's location (d, φ) on the flat display screen:

$$d = \frac{\sqrt{x^2 + y^2}}{\sqrt{x^2 + y^2 + z^2}} \tag{126}$$

$$d = \frac{\rho}{\sqrt{z^2 + \rho^2}} \tag{127}$$

$$d = \frac{\sqrt{l^2 \sin^2 \alpha + y^2}}{\sqrt{l^2 + y^2}}$$
 (128)

11.6 Slight Pincushion Projection

For the purpose of illustrating the effects that are present, I introduce here an additional projection method which is not standard and is almost never used, shown in Fig. 113.

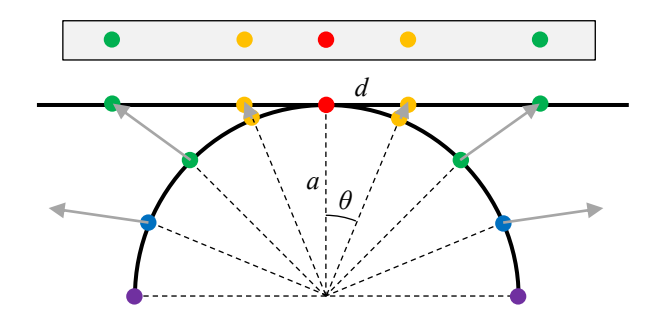


Figure 113. Slight pincushion projection.

This projection will demonstrate the effects of pincushion distortion. In terms of the language used by photographers, the rectilinear projection causes almost no distortion, whereas the stereographic projection, the equidistant projection, the equisolid angle projection, and the orthographic projection cause barrel distortion (meaning that the center of the image bulges out like a barrel), and this projection causes pincushion distortion.

Because none of the other projections cause pincushion distortion, this final projection is introduced to illustrate the associated effects. The slight pincushion projection is defined by Eq. 129. Note that this definition does not correspond to any particular geometric principle.

$$d = \frac{1}{1.2} \tan(1.2\theta)$$
 (129)

By combining Eq. 129 with Eqs. 9, 11, and 20, and by using various trigonometry identities, we derive the equations that can tell us how to take the object's physical location (x, y, z) or (ρ, φ, z) or (α, y, l) and compute the object's location (d, φ)

display screen:

$$d = \frac{1}{1.2} \tan \left(1.2 \tan^{-1} \left(\frac{\sqrt{x^2 + y^2}}{z} \right) \right)$$
 (130)

$$d = \frac{1}{1.2} \tan\left(1.2 \tan^{-1}\left(\frac{\rho}{z}\right)\right) \tag{131}$$

$$d = \frac{1}{1.2} \tan \left(1.2 \cos^{-1} \left(\frac{l \cos \alpha}{\sqrt{l^2 + y^2}} \right) \right) \quad (132)$$

11.7 Plotting the Flat Display Screen Projection Equations

To get any idea for what the projection equations mean, we can plot d as a function of θ for the various projection methods, as shown in Fig. 114.

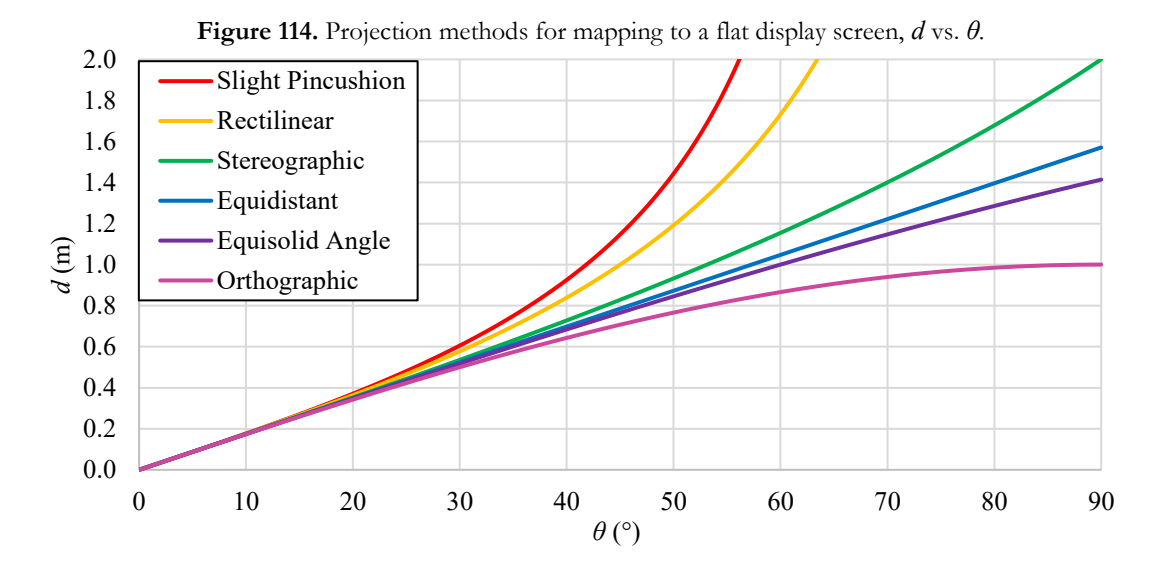


Figure 115. Projection methods for mapping to a flat display screen, d vs. tan θ . 2.0 Slight Pincushion 1.8 Rectilinear 1.6 Stereographic 1.4 Equidistant 1.2 Equisolid Angle 1.0 g Orthographic 0.8 0.6 0.4 0.2 0.0 0.0 0.2 0.4 0.6 0.8 1.0 1.2 1.4 1.6 1.8 2.0 $tan(\theta)$

Specifically, Fig. 114 shows the plots of Eqs. 109, 113, 117, 121, 125, and 129. Note that Fig. 114 shows that all of the projection methods give nearly identical results for polar angles that are less than about 15°. This means that in the central region of vision and in the near peripheral region of vision, the image shown on the flat display screen looks approximately the same no matter which of these projection methods is used.

Considering that the rectilinear projection is the projection with the least distortion and is the method that is most commonly used, let us, for comparison purposes, plot *d* instead as a function

11.8 Using Rectangular Display Screen Coordinates

Instead of using the polar display screen coordinates (d, φ) , we can use rectangular display screen coordinates $(x_{\text{screen}}, y_{\text{screen}})$, as is usually done in practice. The equations linking these coordinates are the usual polar coordinate equations which can be found using trigonometry:

$$x_{\text{screen}} = d\cos\varphi$$
 and $y_{\text{screen}} = d\sin\varphi$

Applying these two equations to the projection equations for rectilinear projection (Eqs. 110 to 112), stereographic projection (Eqs. 114 to 116),

Table 4. Equations specifying the value of c for the different projection methods, as a function of the object's real-world coordinates (x, y, z). The equations in this table are labeled: (133), (134), (135), (136), (137), (138).

Rectilinear	$\frac{1}{z}$
Stereographic	$2\frac{\sqrt{x^2+y^2+z^2}-z}{x^2+y^2}$
Equidistant	$\frac{1}{\sqrt{x^2+y^2}} \tan^{-1} \left(\frac{\sqrt{x^2+y^2}}{z} \right)$
Equisolid Angle	$\sqrt{\frac{2}{x^2 + y^2} \left(1 - \frac{z}{\sqrt{x^2 + y^2 + z^2}} \right)}$
Orthographic	$\frac{1}{\sqrt{x^2+y^2+z^2}}$
Slight Pincushion	$\frac{1}{1.2\sqrt{x^2+y^2}}\tan\left(1.2\tan^{-1}\left(\frac{\sqrt{x^2+y^2}}{z}\right)\right)$

of $\tan \theta$ for the various projection methods. The results are shown in Fig. 115.

When plotted in this way, Fig. 115 makes it clear that the pincushion projection, the rectilinear projection, and the set of all other projections are in three distinct categories. For these reasons, the rectilinear projection is considered the standard projection.

equidistant projection (Eqs. 118 to 129), equisolid angle projection (Eqs. 122 to 124), orthographic projection (Eqs. 126 to 128), and slight pincushion projection (Eqs. 130 to 132); along with the original equations for φ ; we can find the equations that determine the screen location (x_{screen} , y_{screen}) for a particular object location in the physical world in terms of the various object coordinate

Table 5. Equations specifying the value of c for the different projection methods, as a function of the object's real-world coordinates (ρ, φ, z) . The equations in this table are labeled: (139), (140), (141), (142), (143), (144).

Rectilinear	$\frac{ ho}{z}$
Stereographic	$2\frac{\sqrt{\rho^2+z^2}-z}{\rho}$
Equidistant	$\tan^{-1}\left(\frac{\rho}{z}\right)$
Equisolid Angle	$\sqrt{2}\sqrt{1-\frac{z}{\sqrt{\rho^2+z^2}}}$
Orthographic	$\frac{\rho}{\sqrt{z^2 + \rho^2}}$
Slight Pincushion	$\frac{1}{1.2} \tan \left(1.2 \tan^{-1} \left(\frac{\rho}{z} \right) \right)$

systems. When presented in condensed form by applying various trigonometric identities, we find the results that are as described in the following sections.

11.9 Using Rectangular Coordinates for the Object Location

For an object whose physical location in the real world is given in regular rectangular coordinates as (x, y, z), its location on the display screen is given by Eq. 151, where the overall multiplicative coefficient c depends on the projection method and is given in Table 4.

$$(x_{\text{screen}}, y_{\text{screen}}) = (cx, cy)$$
 (151)

11.10 Using Cylindrical Coordinates About the z Axis for the Object Location

For an object whose physical location in the real world is given in cylindrical coordinates about the z axis as (ρ, φ, z) , its location on the display screen is given by Eq. 152, where the overall multiplicative coefficient c depends on the projection

Table 6. Equations specifying the value of c for the different projection methods, as a function of the object's real-world coordinates (r, θ, φ) . The equations in this table are labeled: (145), (146), (147), (148), (149), (150).

Rectilinear	an heta
Stereographic	$2 \tan \frac{\theta}{2}$
Equidistant	θ
Equisolid Angle	$2\sin\frac{\theta}{2}$
Orthographic	$\sin heta$
Slight Pincushion	$\frac{1}{1.2}\tan(1.2\theta)$

method and is given in Table 5. Note that the equations for c in Table 5 are the same equations as in Table 6, but expressed as a function of ρ/z . Because $\rho/z = \tan \theta$, this means that plotting the equations in Table 5 as a function of ρ/z is equivalent to plotting the equations in Table 6 as a function of $\tan \theta$, which has already been done. Specifically, Fig. 115 shows the results when you plot the equations in Table 5 as a function of ρ when z = 1.

$$(x_{\text{screen}}, y_{\text{screen}}) = (c \cos \varphi, c \sin \varphi)$$
 (152)

11.11 Using Spherical Coordinates for the Object Location

For an object whose physical location in the real world is given in spherical coordinates as (r, θ, φ) , its location on the display screen is given by Eq. 159, where the overall multiplicative coefficient c depends on the projection method and is given in Table 6. Note that the equations for c in this case are the projection equations in standard form (Eqs. 109, 113, 117, 121, 125, & 129). This means

Table 7. Equations specifying the value of c for the different projection methods, as a function of the object's real-world coordinates (α, y, l) . These equations are labeled: (153), (154), (155), (156), (157), (158).

Rectilinear	$\frac{1}{l\cos\alpha}$
Stereographic	$2\frac{\sqrt{l^2+y^2}-l\cos\alpha}{y^2+l^2\sin^2\alpha}$
Equidistant	$\frac{1}{\sqrt{y^2 + l^2 \sin^2 \alpha}} \tan^{-1} \left(\frac{\sqrt{y^2 + l^2 \sin^2 \alpha}}{l \cos \alpha} \right)$
Equisolid Angle	$\sqrt{\frac{2}{y^2 + l^2 \sin^2 \alpha} \left(1 - \frac{l \cos \alpha}{\sqrt{l^2 + y^2}}\right)}$
Orthographic	$\frac{1}{\sqrt{l^2+y^2}}$
Slight Pincushion	$\frac{1}{1.2\sqrt{y^2 + l^2\sin^2\alpha}}\tan\left(1.2\tan^{-1}\left(\frac{\sqrt{y^2 + l^2\sin^2\alpha}}{l\cos\alpha}\right)\right)$

that the plot of the equations in Table 6 is already shown in Fig. 114.

$$(x_{\text{screen}}, y_{\text{screen}}) = (c \cos \varphi, c \sin \varphi)$$
 (159)

11.12 Using Cylindrical Coordinates About *y* Axis for the Object Location

For an object whose physical location in the real world is given in cylindrical coordinates about the y axis as (α, y, l) , its location on the display screen is given by Eq. 160, where the overall multiplicative coefficient c depends on the projection method and is given in Table 7.

$$(x_{\text{screen}}, y_{\text{screen}}) = (cl \sin \alpha, cy)$$
 (160)

11.13 Plotting Various Surfaces Using All Projection Methods

To illustrate the meaning of the projection equations applied to the human monocular geometry (Eqs. 133-160), we can plot various physical surfaces that exist in three-dimensional space and are extended in two of the coordinate dimensions. All of the remaining plots in this chapter were generated using only Eqs. 133-160 without the

use of any 3D display software packages or prebuilt rendering engines. This means that the plots below are mathematically accurate and contain no approximations, simplifications, models, or hardware-specific rendering parameters.

In each of the plots below, all of the coordinates are given in meters. Furthermore, neighboring grid lines running in the same direction are exactly one meter apart in the original, physical, three-dimensional space (except where noted). Therefore, the intersection of any two sets of neighboring grid lines defines a square that has an area of exactly one square meter.

All of the projection plots were created using the same screen scale. This means that, in the central region of vision (where all of the projection methods produce approximately the same screen image), every projection method produces the same size squares. In other words, because all of the plots use the same screen scale, if you cropped every image down to a few dozen pixels in the middle of the image, every image would contain the same sized squares, regardless of the projection method.

The side effect of using a constant screen scale is that, aside from the rectilinear and slight pincushion projections, each projection method has produced a differently sized overall image. To make clear that the pixels that are outside of the outermost circle are not actually part of the image, I have made these pixels grey.

Fig. 116 shows a flat x-y plane that is sitting at z = 2 m, as observed by the human monocular vision system and then projected to a flat display screen using the various projection methods. In this figure, the grid lines are running in the x and y directions and are all spaced one meter apart.

This plane physically represents an infinitely large, flat wall that the observer is staring directly at. Fig. 117 shows the same wall, but now at a distant of z = 5 m. Fig. 118 shows the same wall, but now at z = 10 m. These figures are plotting Eqs. 133-138 and Eq. 151 for the collection of (x, y, z) points that make up the grid lines.

Figs. 116-118 make clear that the rectilinear projection does not properly preserve lateral size perspective effects. The squares near the edge of each image are farther away from the observer than the squares in central vision and therefore should appear smaller, and yet they appear the same size in the rectilinear projection. However, Figs. 116-118 show that the rectilinear projection does indeed preserve straight lines whereas the other projections do not. For this reason, these other projections are often called curvilinear projections.

Because Figs. 116-118 show the same physical plane, but observed at different z distances from the observer, these figures taken together show the forward distance perspective effect, where the 1-square-meter grid squares appear smaller the farther away they are from the observer. Specifically, close inspection of Fig. 118 compared to Fig. 117 reveals that each grid square appears one fourth as large in area at z = 10 m as at z = 5 m.

This demonstrates the area perspective effect in the forward direction, where the observed area diminishes with the distance according to $(1/z^2)$, which is a special case of $(1/r^2)$ when x = y = 0. Note that all of the projections preserve this area perspective effect in the forward direction.

Fig. 119 shows a flat x-z plane sitting at y = -2 m, as observed by the human monocular vision system and projected onto a flat display screen using the various projection methods. In this figure, the grid lines are running in the x and z directions and are all spaced one meter apart. This plane physically represents an infinitely large, flat ground plane. Fig. 120 shows the same ground plane, but now at y = -5 m. These figures are plotting Eqs. 133-138 and Eq. 151 for the collection of (x, y, z) points that make up the grid lines.

Figs. 119 and 120 demonstrate the horizon perspective effect. All of the grid lines running in the z direction are parallel to each other, but because they extend away from the observer in the z direction, they appear to all be converging at the central horizon point at $\theta = 0$. Also, this effect makes the overall ground plane appear to end at the horizon line (i.e. where the sky meets the ground). Note that all of the projections preserve the horizon perspective effect. As before, Figs. 119 and 120 demonstrate that the rectilinear projection preserves straight lines.

Fig. 121 shows a flat x-z plane that is sitting at y = -5 m, the same as in Fig. 120, but now the grid lines are running in directions that are rotated 45° relative to the x and z directions. Because none of the grid lines in Fig. 121 are running in the z direction, none of the lines converge at the central horizon point at θ = 0. However, because each set of gridlines consists of lines that are parallel in the real world, each set converges at a perspective point on the horizon line that is not at the center. Because there are two different sets of parallel lines, there are two different horizon points.

Artists call this arrangement "two-point perspective." In practice, two-point perspective is useful in drawing city scenes because buildings in real life tend to be laid out along, and aligned with, a rectangular ground plane grid that is usually rotated relative to the observer.

Fig. 122 shows two y-z planes, one at x = -2 m and the other at x = 2 m, as observed by the human monocular vision system and projected onto a flat display screen using the various projection methods. In this figure, the grid lines are running in the y and z directions and are all spaced one meter apart. These planes physically represent two parallel, infinitely large walls. Fig. 123 shows the same setup but now with the planes at x = -5 m and x = 5 m. These figures are plotting Eqs. 133-138 and Eq. 151 for the collection of (x, y, z) points that make up the grid lines. These figures demonstrate that the central horizon point as a vanishing point applies to all sets of parallel lines extending in the z direction, and not just to such lines in a ground plane.

Fig. 124 shows a flat ρ - s_{φ} plane at z=5 m, as observed by the human monocular vision system and projected onto a flat display screen using the various projection methods. In this figure, the grid lines are running in the ρ and s_{φ} directions. The grid lines running in the s_{φ} direction are all one meter apart. The grid lines running in the ρ direction are all 15° apart. This plane physically represents an infinitely large dart board. Note that a ρ - s_{φ} plane is identical to an x-y plane except for the direction of the grid lines. Fig. 125 shows the same ρ - s_{φ} plane, but now at a distance of z=10 m. These figures are plotting Eqs. 139-144 and Eq. 152. for the collection of (ρ, φ, z) points that make up the grid lines.

Fig. 126 shows the cylindrical s_{φ} -z surface at $\rho = 5$ m, as observed by the human monocular vision system and projected onto a flat display screen using the various projection methods. In

this figure, the grid lines are running in the s_{φ} and z directions. All of the grid lines are one meter apart. This surface physically represents an infinitely long circular tunnel extending away from the viewer in the z direction. This figure is plotting Eqs. 139-144 and Eq. 152 for the collection of (ρ, φ, z) points that make up the grid lines.

Fig. 127 shows the spherical s_{θ} - s_{φ} surface sitting at $r=18/\pi=5.7297795$ m, as observed by the human monocular vision system and projected onto a flat display screen using the various projection methods. The observer is at the center of this sphere. In this figure, the grid lines are running in the s_{θ} and s_{φ} directions. All of the grid lines running in the s_{θ} direction are spaced 15° apart. All of the grid lines running in the s_{φ} direction are spaced one meter apart. The radius of this sphere was chosen to ensure this. This surface physically represents a spherical room. This figure is plotting Eqs. 145-150 and Eq. 159 for the collection of (r, θ, φ) points that make up the grid lines.

Fig. 128 shows the cylindrical s_{α} -y surface at l=5 m, as observed by the human monocular vision system and projected onto a flat display screen using the various projection methods. In this figure, the grid lines are running in the s_{α} and y directions. All of the grid lines are one meter apart. This surface physically represents standing on a platform in the middle of an infinitely tall grain silo. This figure is plotting Eqs. 153-158 and Eq. 160 for the collection of (α, y, l) points that make up the grid lines.

Fig. 129 shows the flat s_{α} -l plane at y = -5 m, as observed by the human monocular vision system and projected onto a flat display screen using the various projection methods. In this figure, the grid lines are running in the s_{α} and l directions. The grid lines running in the s_{α} direction are spaced one meter apart. The grid lines running in the l direction are spaced 15° apart. This surface

physically represents a flat ground plane that has been marked up like a dart board. This figure is plotting Eqs. 153-158 and Eq. 160 for the collection of (α, y, l) points that make up the grid lines.

Figs. 130-138 show more complex structures that were created by combining several of the surfaces already mentioned. Fig. 130 shows a canyon formed by the flat y-z planes at x = -5 m and at x = 5 m, and the flat x-z plane at y = -5 m, with grid lines running in the x, y, and z directions, as appropriate, and spaced one meter apart.

Fig. 131 shows a square tunnel formed by the flat x-z planes at y = -2 m and y = 2 m and the flat y-z planes at x = -2 m and x = 2 m, with grid lines spaced one meter apart.

Fig. 132 shows a larger square tunnel formed by the flat x-z planes at y = -5 m and y = 5 m and the flat y-z planes at x = -5 m and x = 5 m.

Fig. 133 shows an arched tunnel formed by the x-z plane at y = -5 m, the y-z planes at x = -5 m and x = 5 m, and the s_{φ} -z surface at $\rho = 5$ m.

Fig. 134 shows a cube-shaped room formed by the x-z planes at y = -5 m and y = 5 m, the y-z planes at x = -5 m and x = 5 m, and the x-y planes at z = 10 m and z = 0 m. Note that this room is a 10 m \times 10 m \times 10 m room with the observer located on the back wall at the middle of the wall.

Fig. 135 shows the same room shown in Fig. 134 but with markings added to aid in visually locating the parts of the walls. The floor and ceiling have been colored green with a concentric square pattern and the walls have been colored blue with the same type of pattern. Fig. 135 makes clear that the slight pincushion projection and the rectilinear projection are not able to show the

whole room, while the other projections are. In the rectilinear projection version of the image, the back two meters of the walls, floor, and ceiling are not visible. In the slight pincushion projection version of the image, the back three meters of the walls, floor, and ceiling are not visible.

Fig. 136 shows an arched room formed by the surfaces at y = -5 m, y = 5 m, x = -5 m, x = 5 m, $\rho = 5$ m, and z = 10 m. This arched room is the same as the room shown in Fig. 134, but with an arch shape added to the upper half of the room.

Fig. 137 shows a cylindrical room formed by the *x-z* planes at y = -2 m and y = 2 m, and the s_{α} -y surface at l = 5 m.

Fig. 138 shows a sealed tunnel formed by the s_{φ} -z surface at ρ = 5 m and the ρ - s_{φ} surface at z = 10 m.

In each of these figures (Figs. 116-138), the image that was generated by the rectilinear projection seems to feel the most real and natural. However, this arises partly from the fact that the images generated by the curvilinear projections (except the slight pincushion projection) end up contained within a circular image boundary, but we are used to viewing images in everyday life that are contained within rectangular boundaries.

To make the images generated by the curvilinear projections feel more real and natural, we can crop these images down to square images, at the cost of throwing away part of the image information. To demonstrate this, most of the images already shown have been cropped down to the same size. The results are shown in Figs 139-141 (to conserve space, only the rectilinear and stereographic projections are shown).

Chapter 11. Mapping to a Flat Display Screen

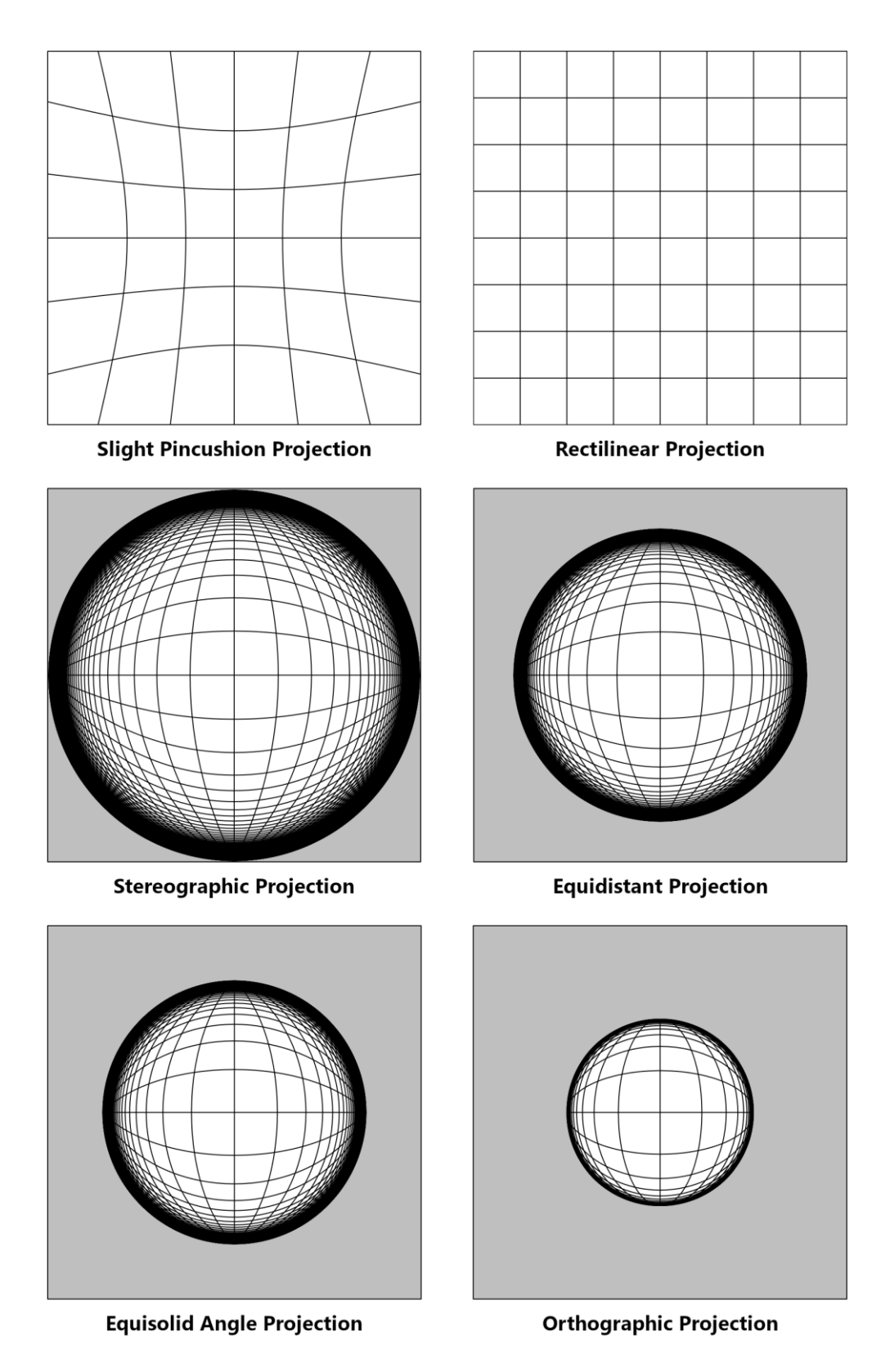


Figure 116. A flat x-y plane at z = 2 m, with grid lines running in the x and y directions, spaced one meter apart.

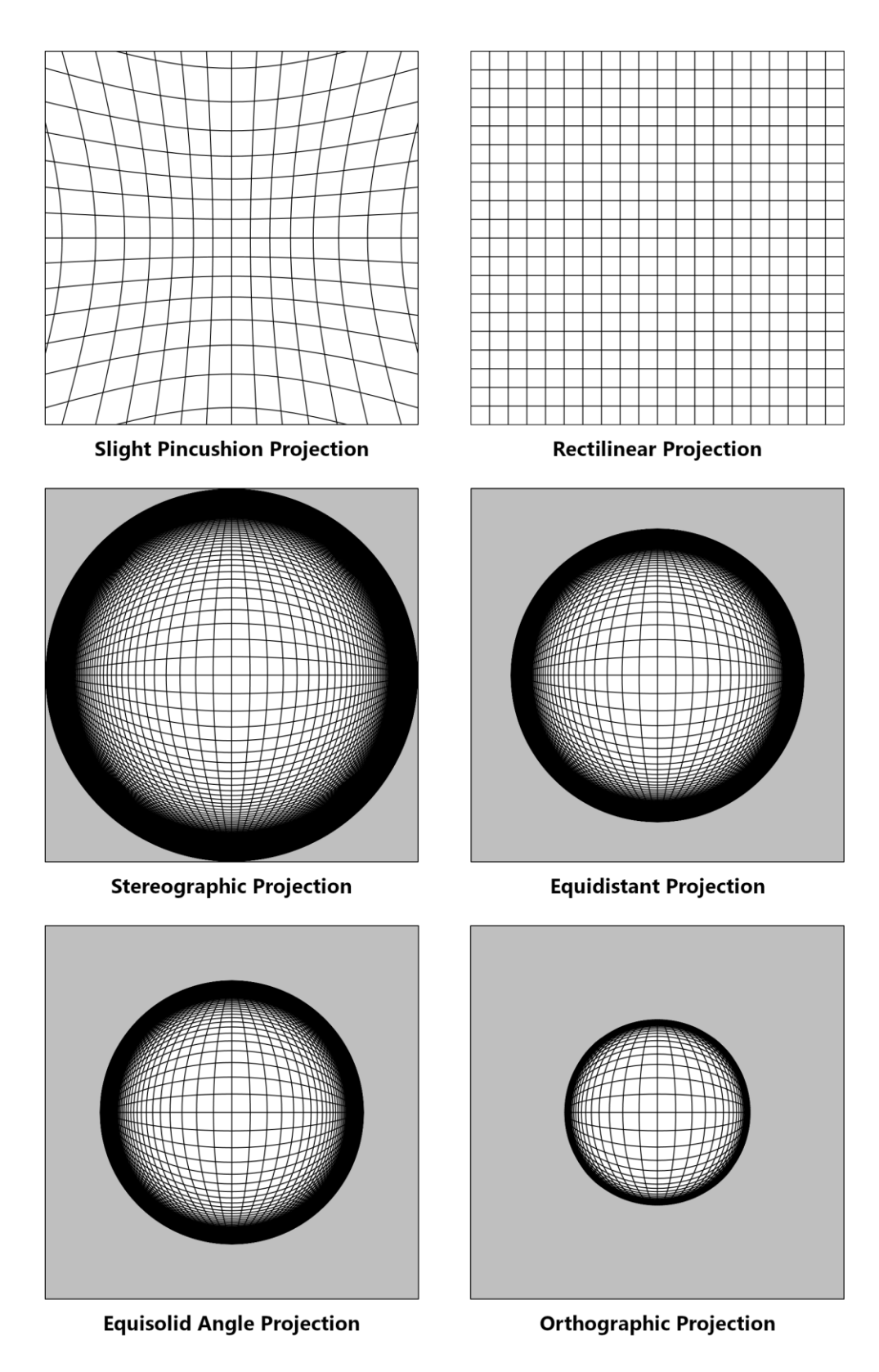


Figure 117. A flat x-y plane at z = 5 m, with grid lines running in the x and y directions, spaced one meter apart.

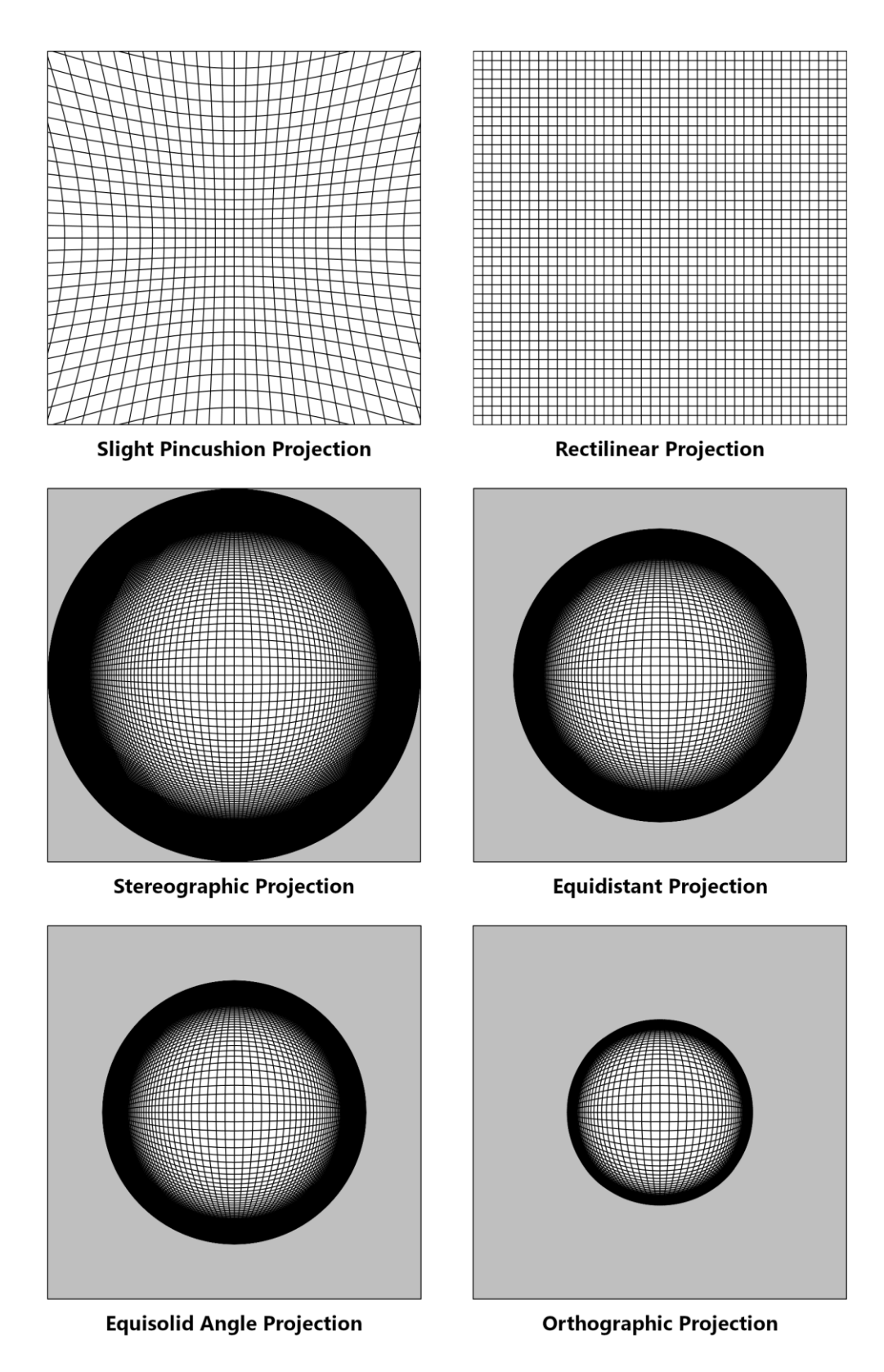


Figure 118. A flat x-y plane at z = 10 m, with grid lines running in the x and y directions, spaced one meter apart.

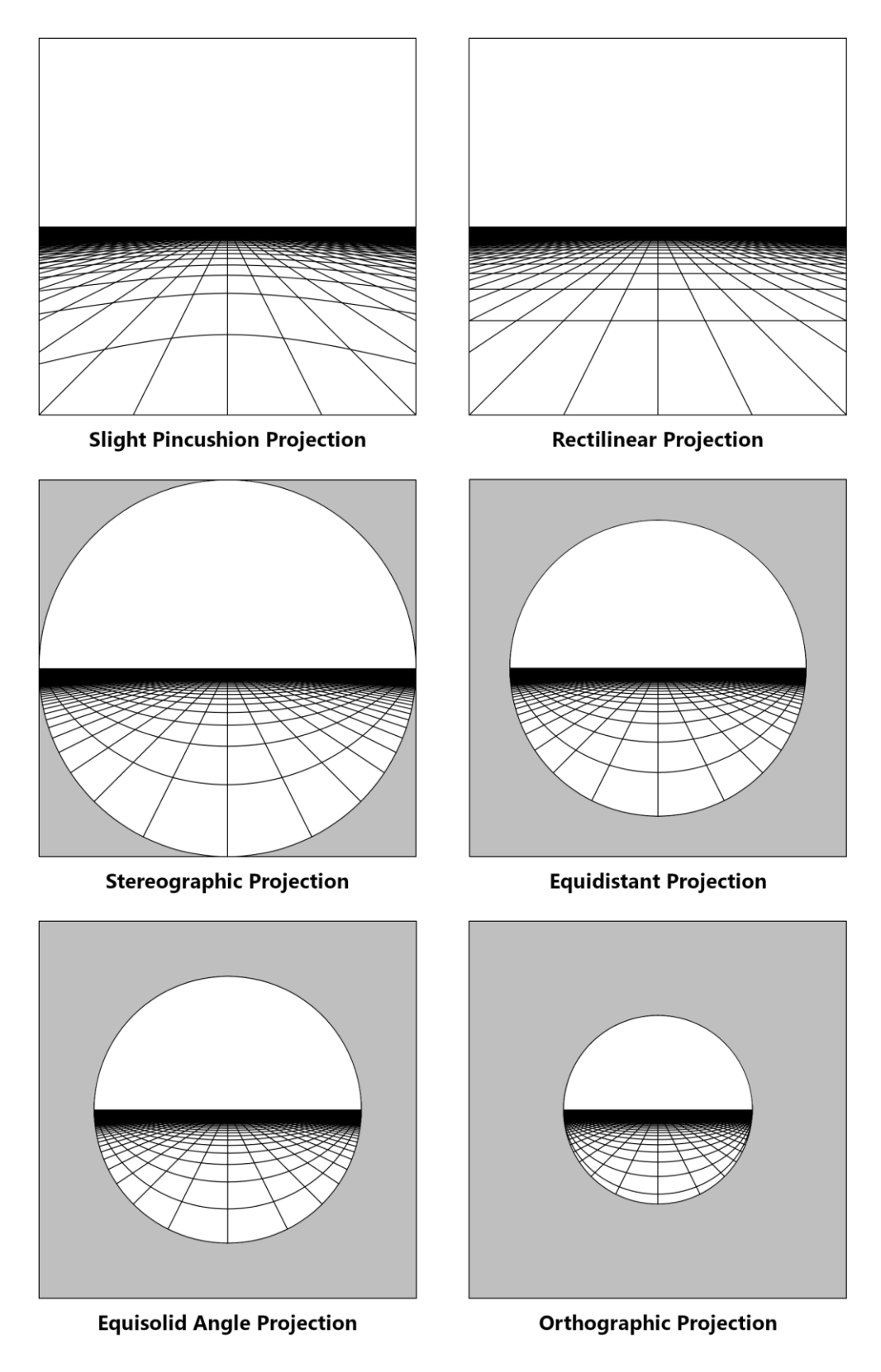


Figure 119. A flat x-z plane at y = -2 m, with grid lines running in the x and z directions, spaced one meter apart.

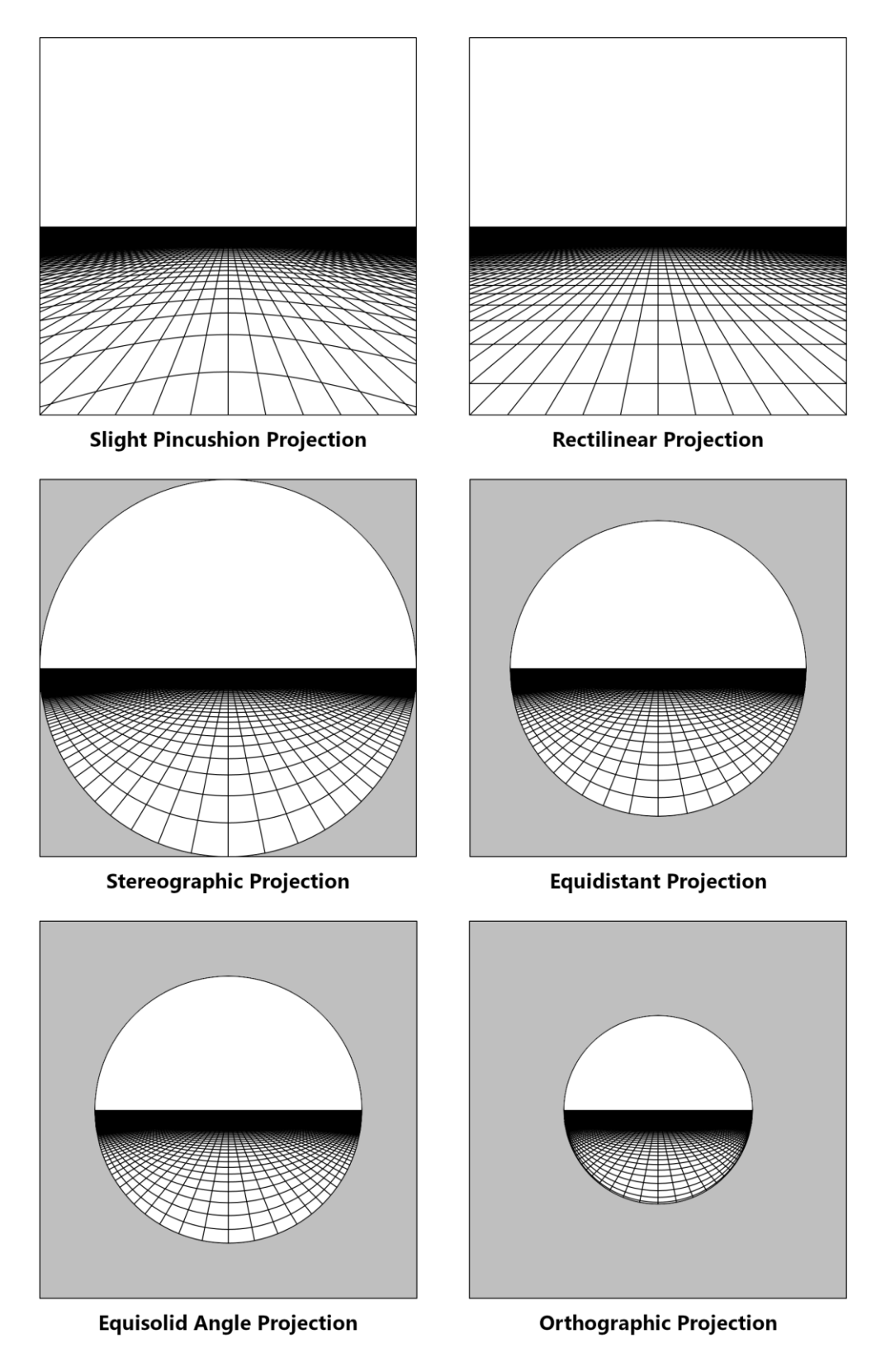


Figure 120. A flat x-z plane at y = -5 m, with grid lines running in the x and z directions, spaced one meter apart.

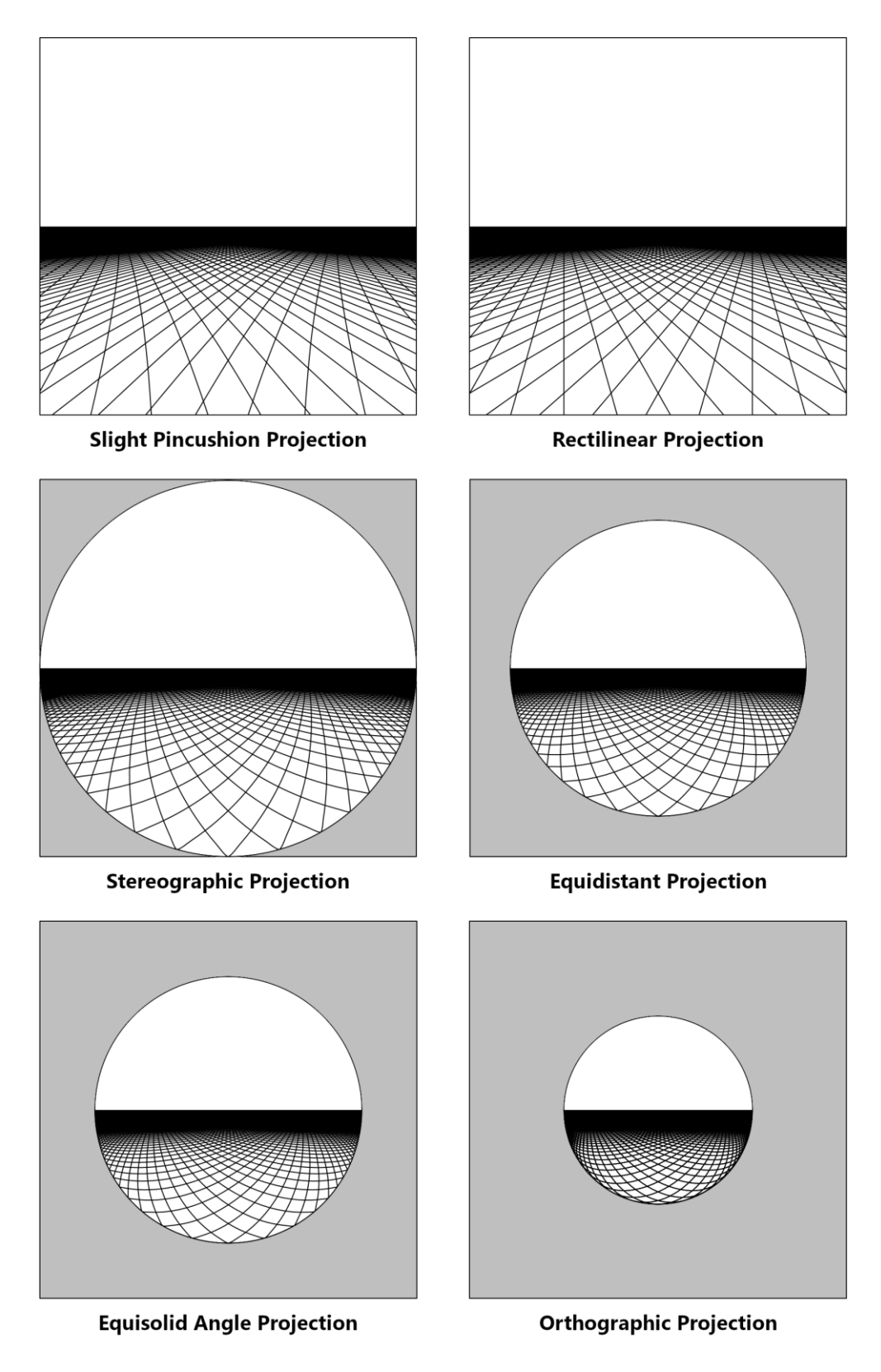


Figure 121. A flat x-z plane at y = -5 m, with grid lines running 45° relative to the x and z axes, spaced one meter apart.

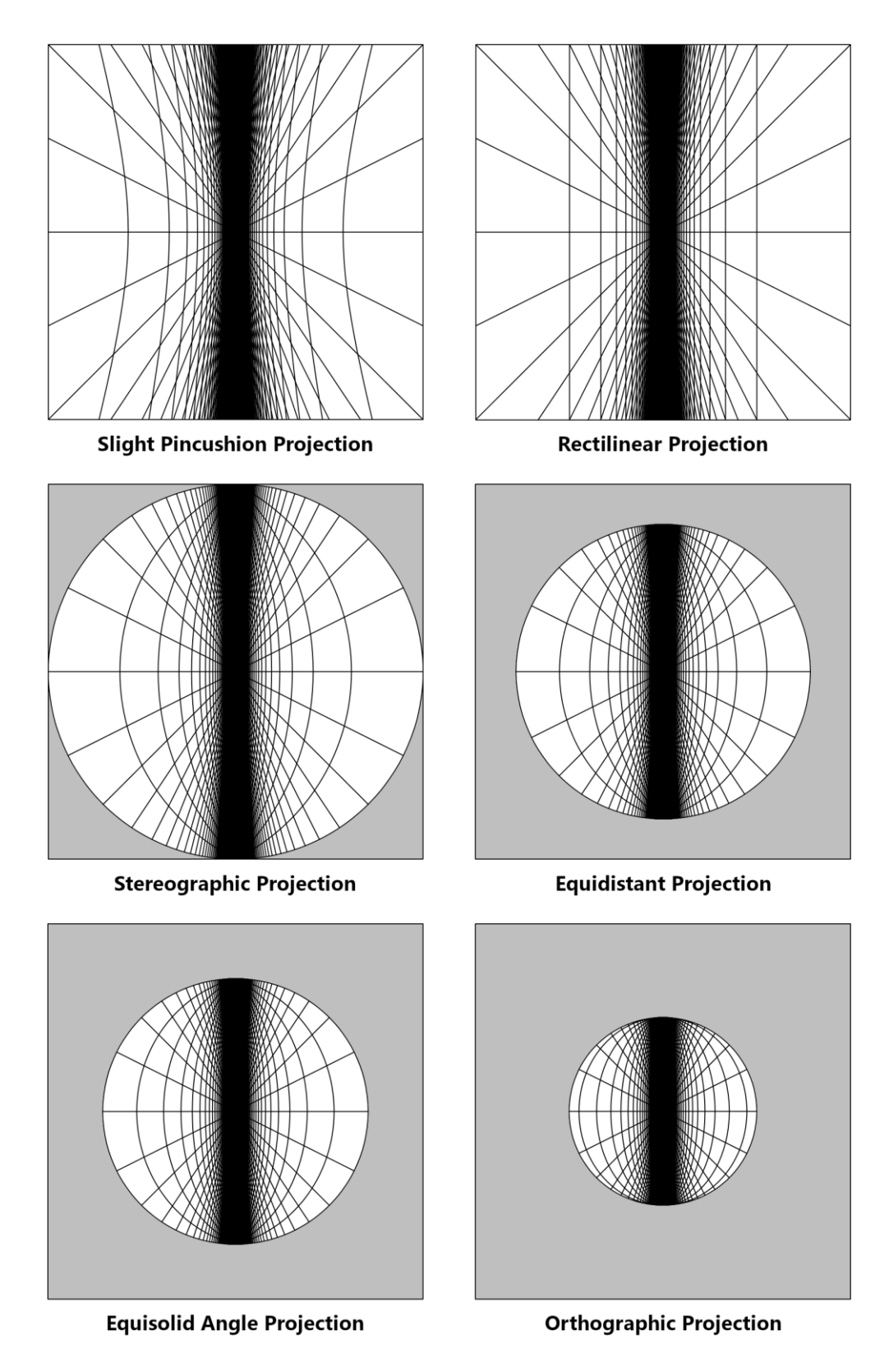


Figure 122. The y-z planes at x = -2 m and x = 2 m, with grid lines running in the y and z directions, spaced a meter apart.

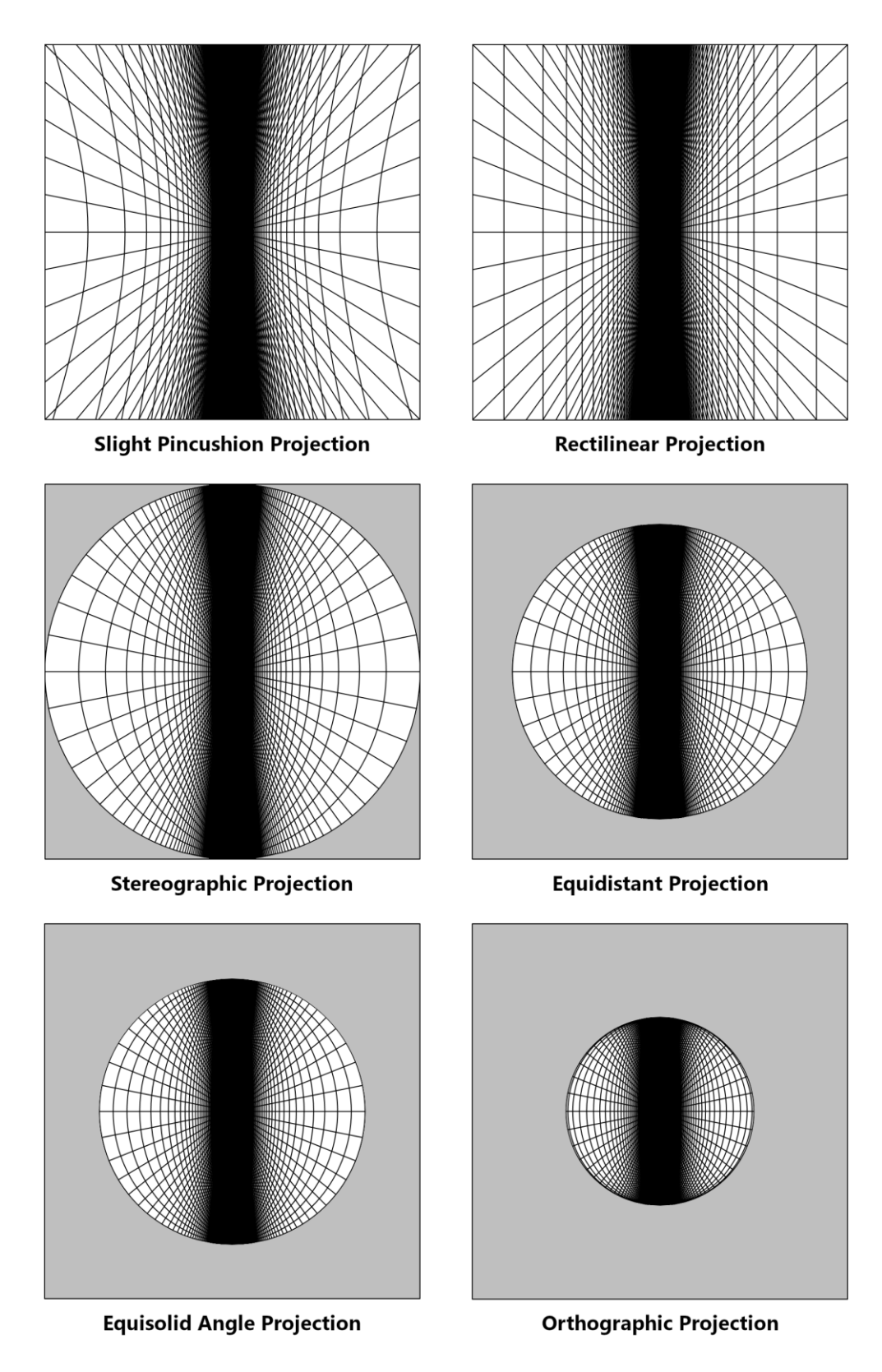


Figure 123. The y-z planes at x = -5 m and x = 5 m, with grid lines running in the y and z directions, spaced a meter apart.

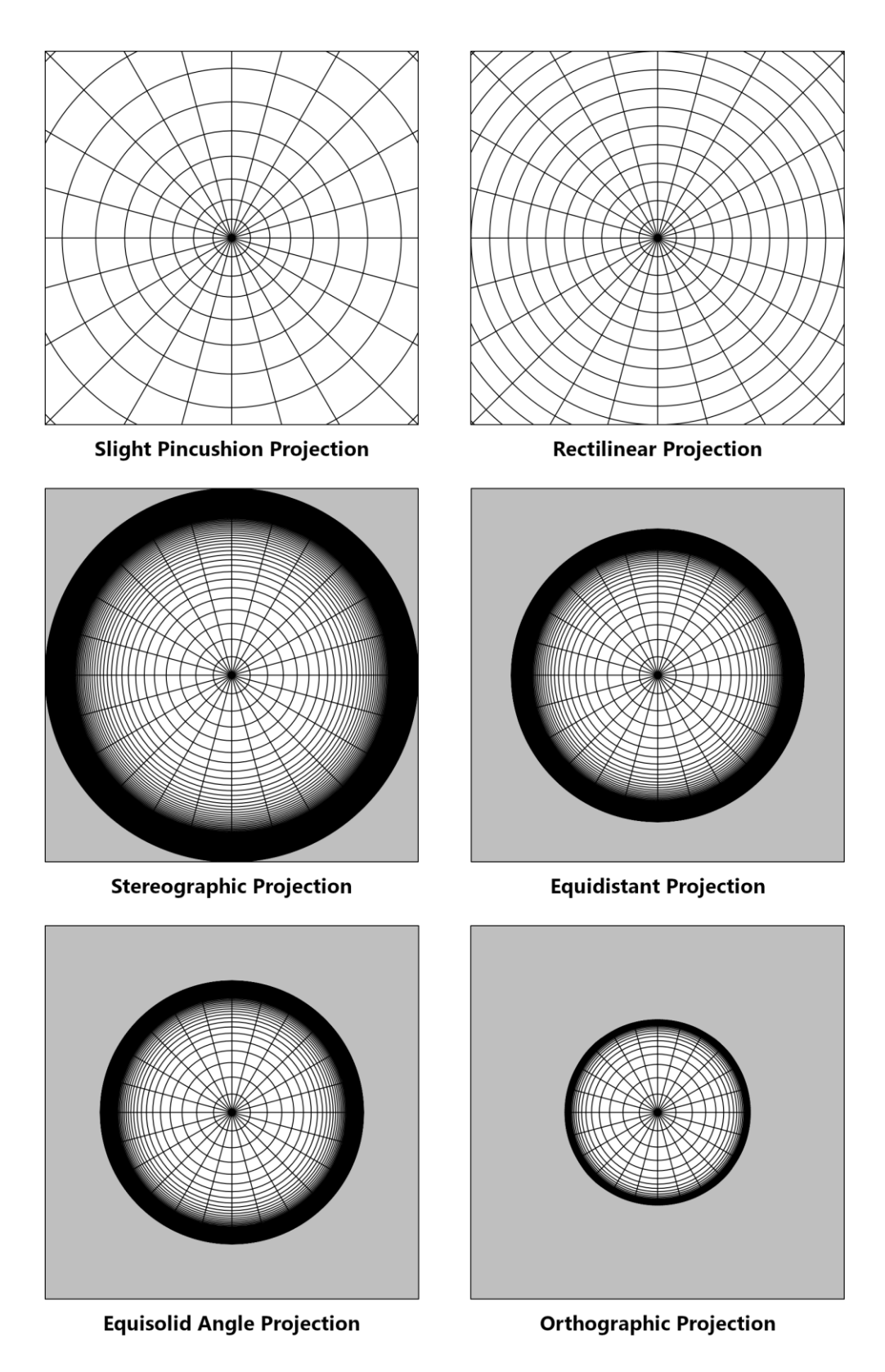


Figure 124. A flat ρ - s_{φ} plane at z=5 m, with grid lines running in the ρ and s_{φ} directions, s_{φ} lines spaced one meter apart.

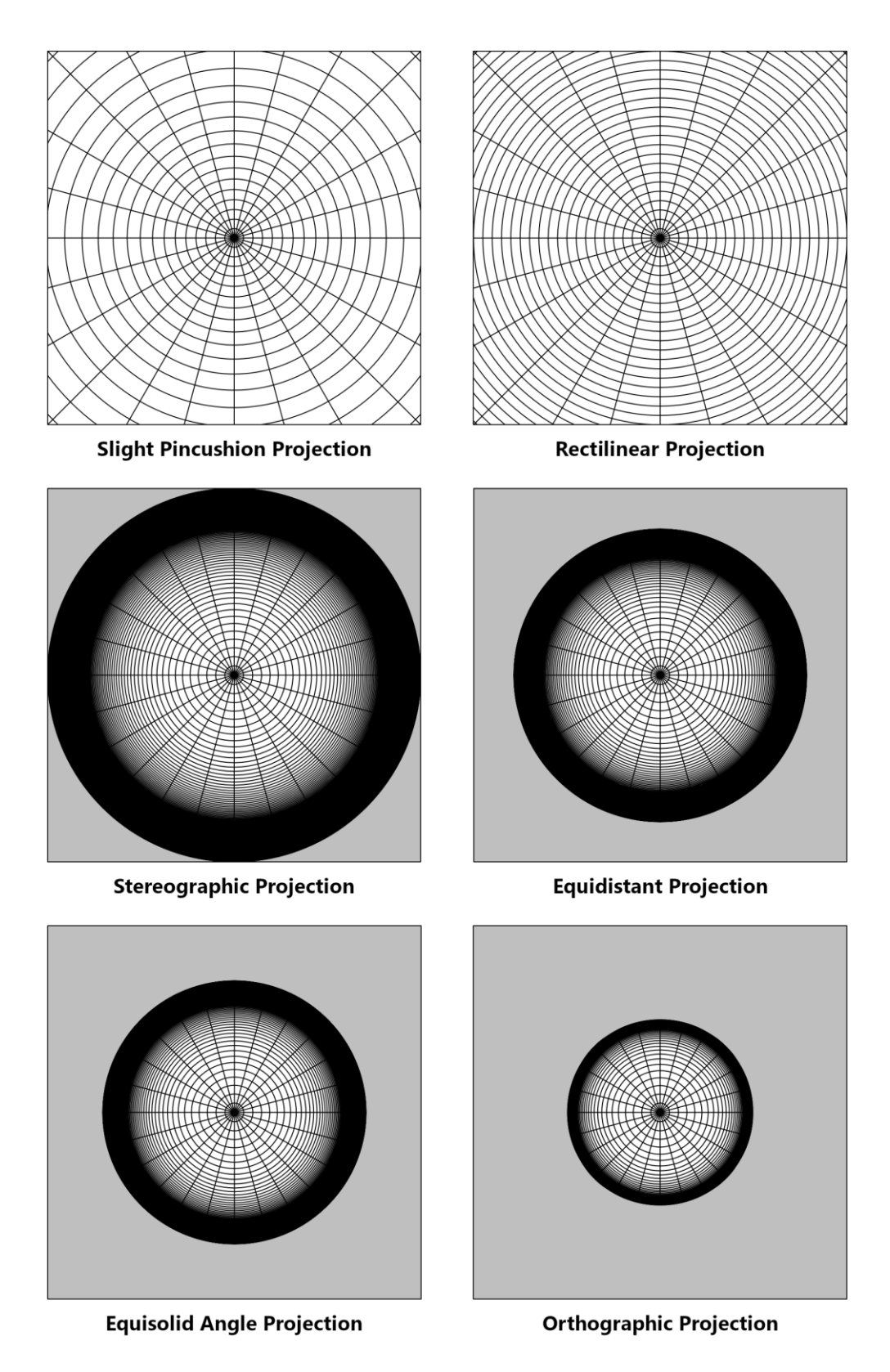


Figure 125. A flat ρ - s_{φ} plane at z=10 m, with grid lines running in the ρ and s_{φ} directions, s_{φ} lines spaced one meter apart.

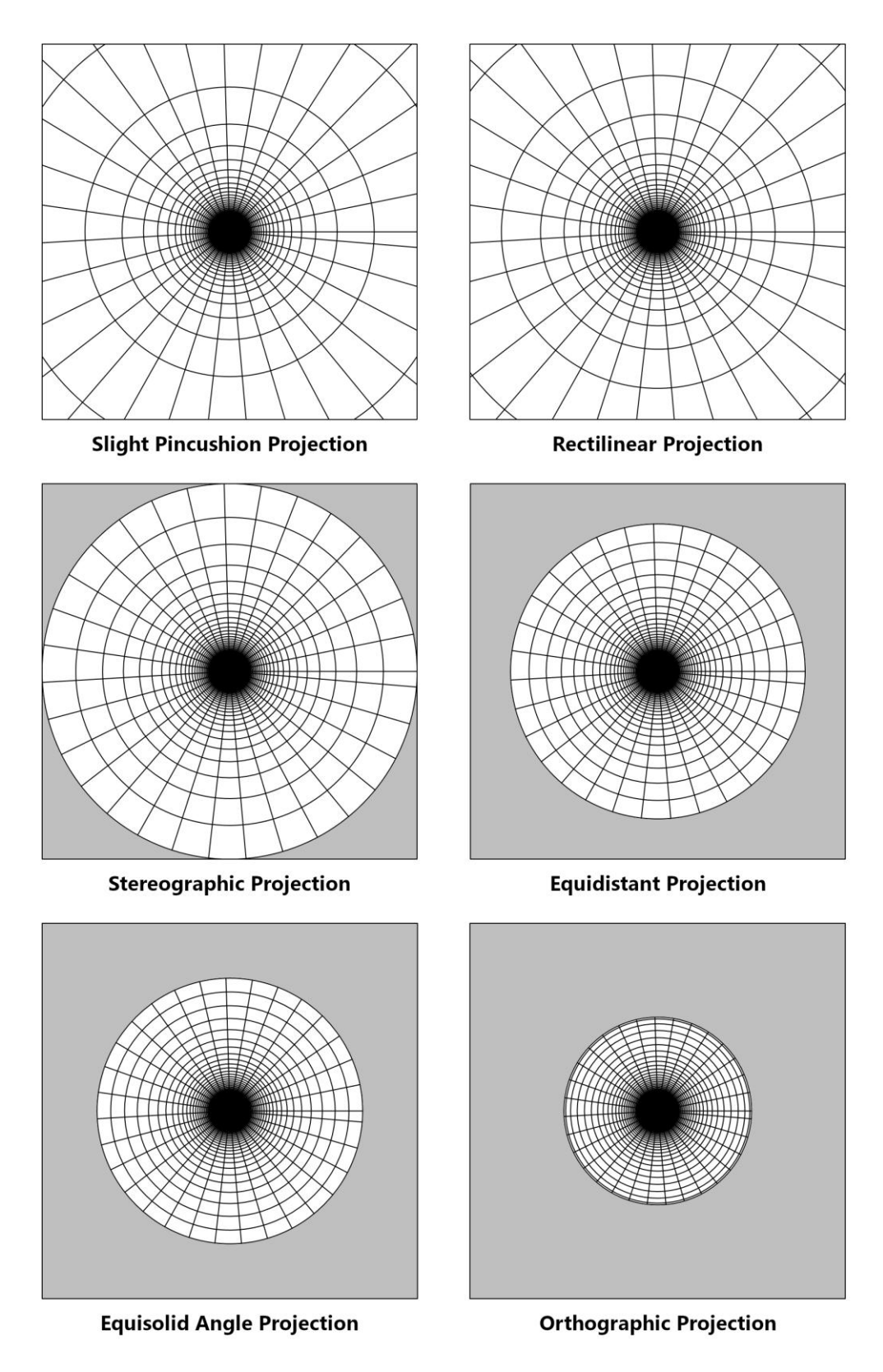


Figure 126. An s_{φ} -z tunnel surface at $\rho = 5$ m, with grid lines running in the s_{φ} and z directions, spaced one meter apart.

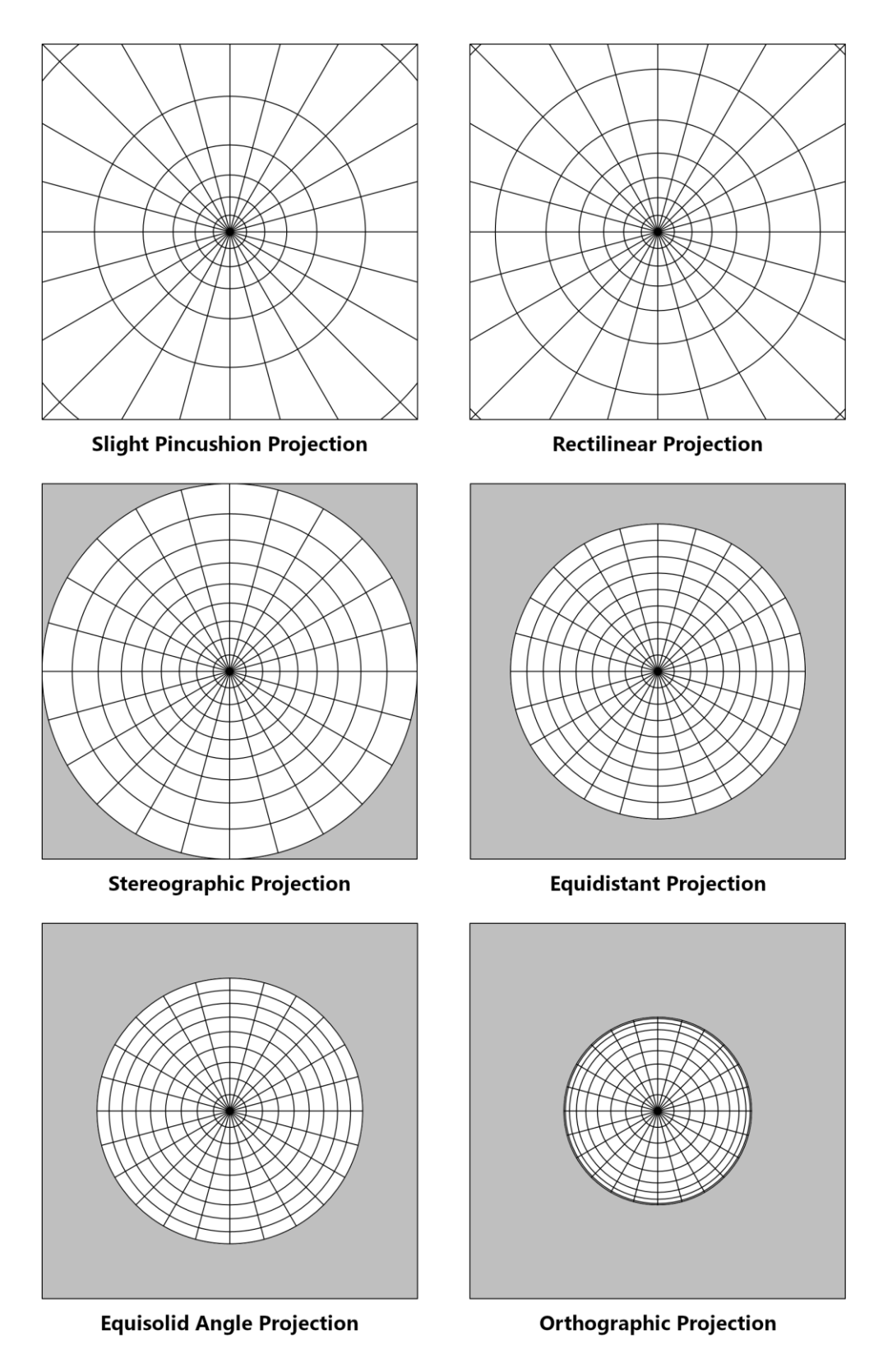


Figure 127. A spherical s_{θ} - s_{φ} surface with grid lines running in the s_{θ} and s_{φ} directions, s_{φ} lines spaced one meter apart.

Chapter 11. Mapping to a Flat Display Screen

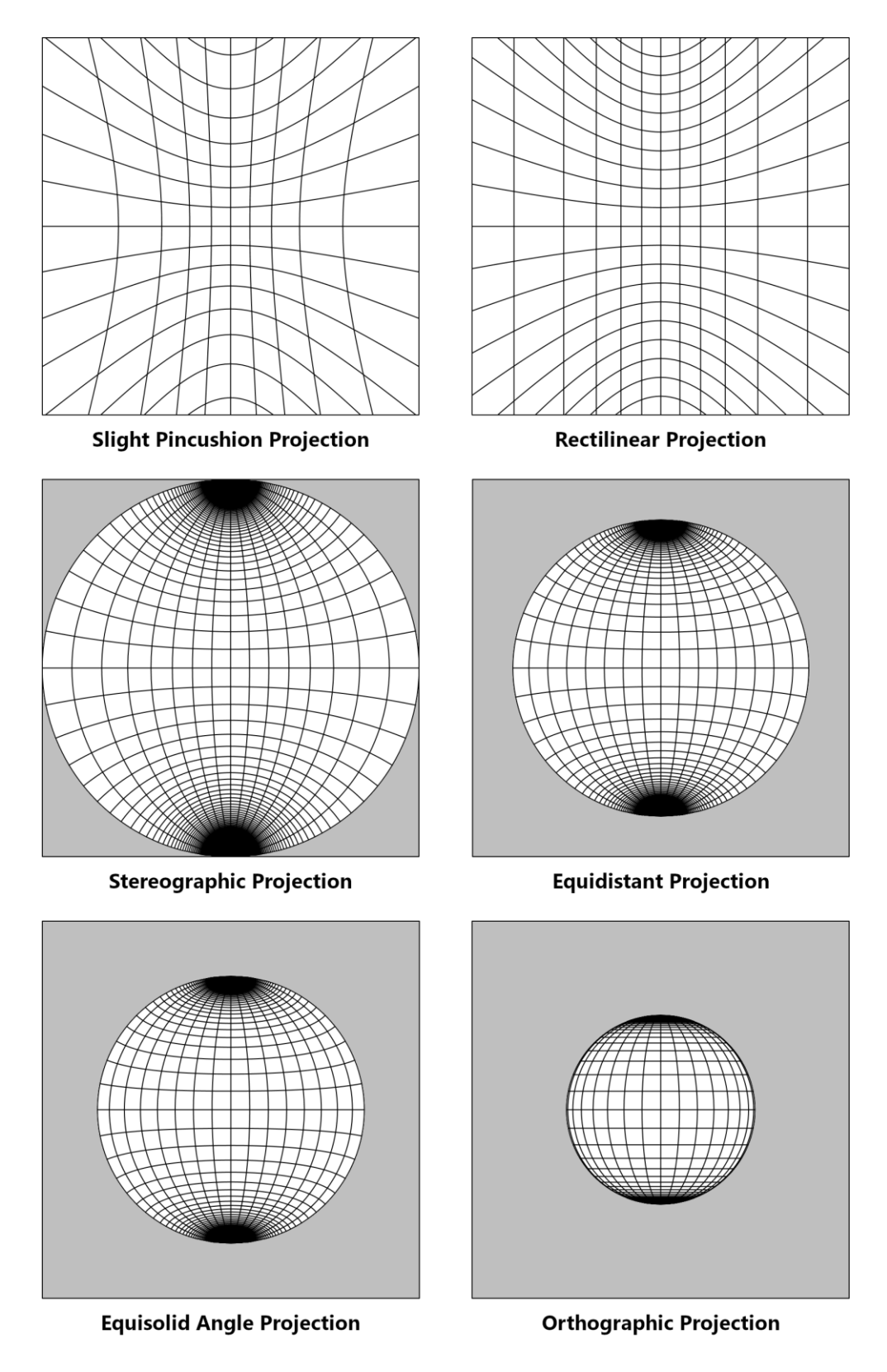


Figure 128. A cylindrical s_{α} -y surface at l = 5 m, with grid lines running in the s_{α} and y directions, spaced one meter apart.

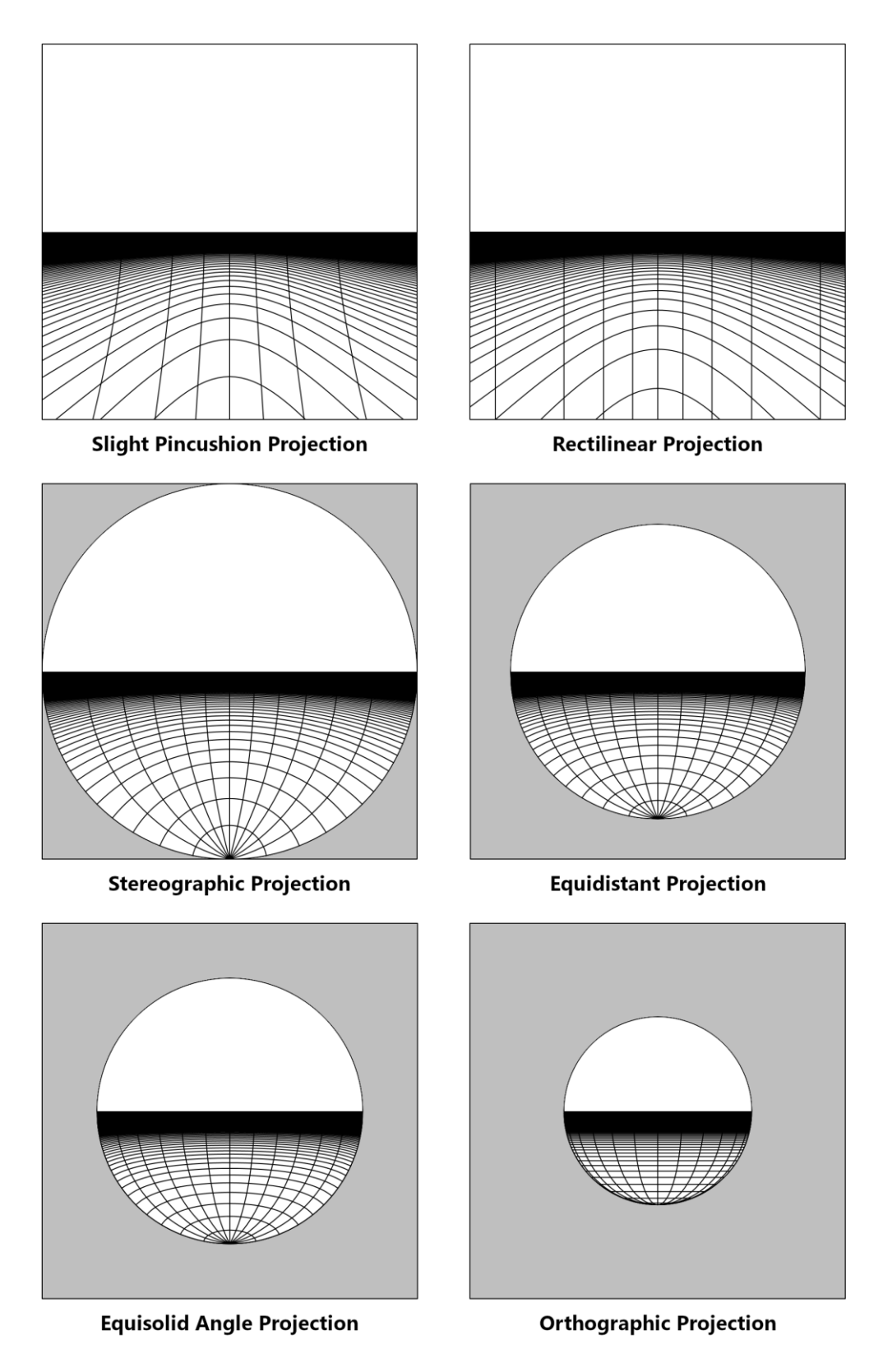


Figure 129. A flat s_{α} -l plane at y = -5 m, with grid lines running in the s_{α} and l directions, s_{α} lines spaced one meter apart.

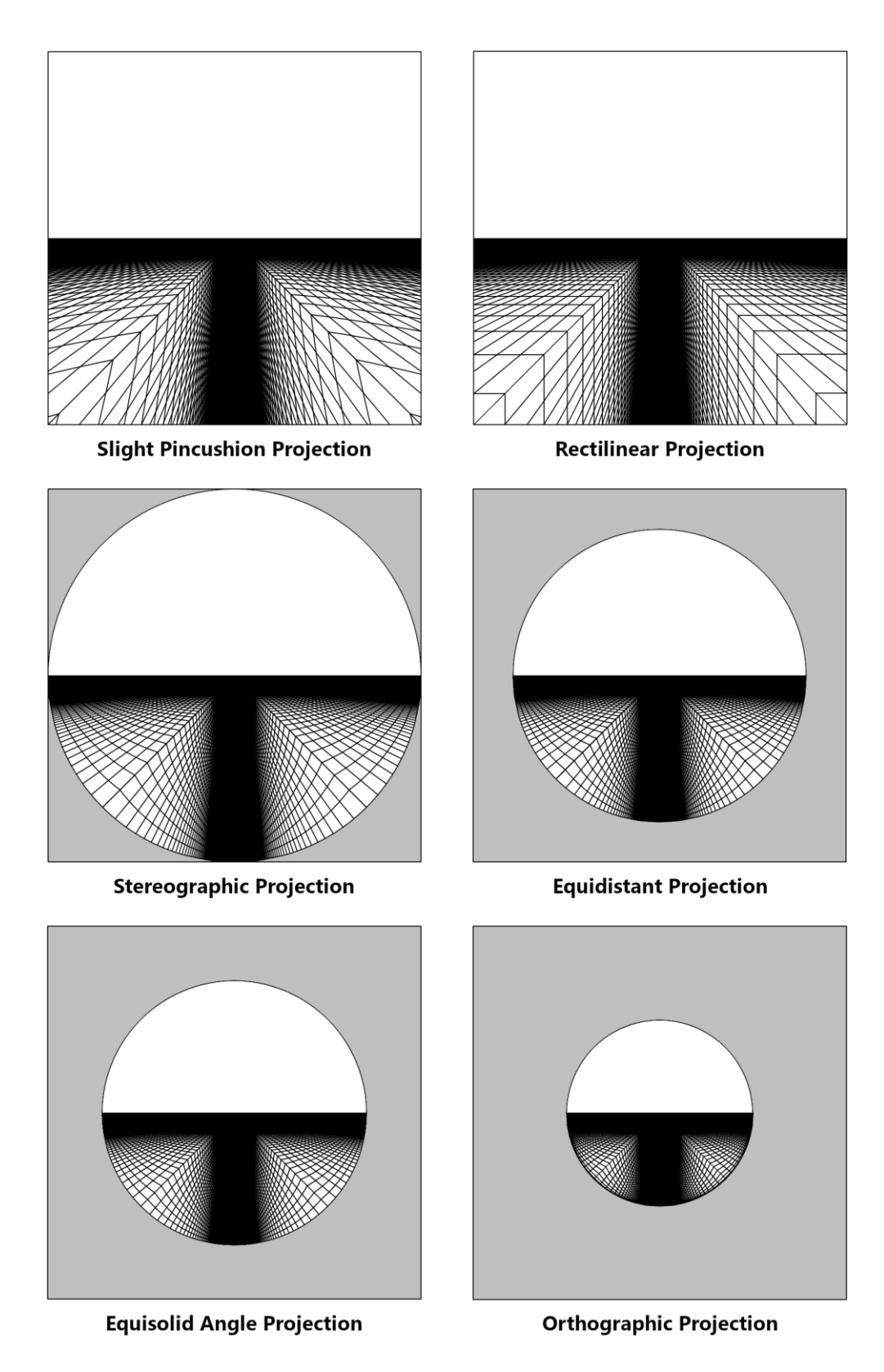


Figure 130. A canyon formed by the flat y-z planes at x = -5 m and x = 5 m, and the flat x-z plane at y = -5 m.

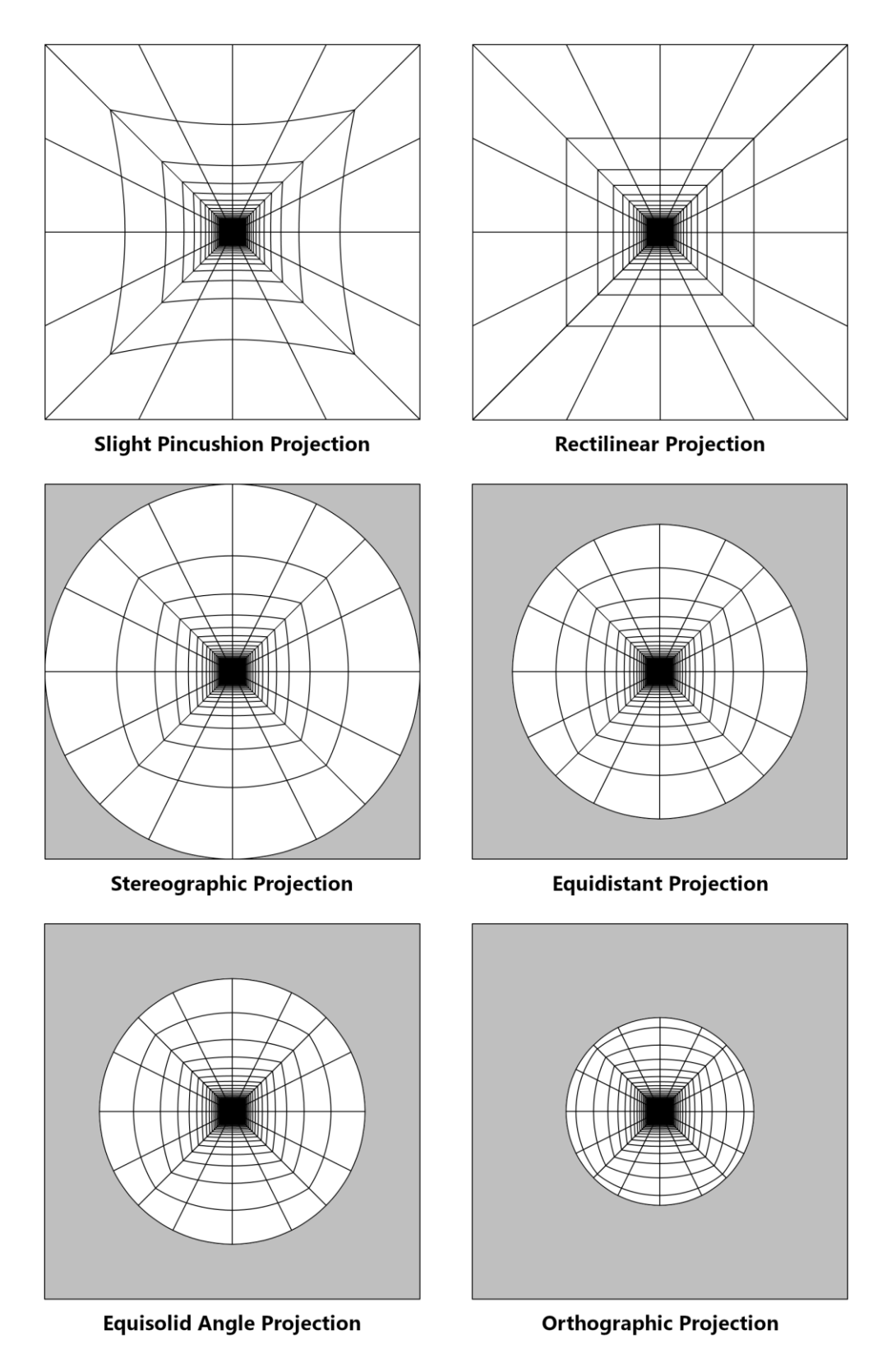


Figure 131. A square tunnel formed by the flat x-z planes at y = -2 m and y = 2 and the flat y-z planes at x = -2 and x = 2.

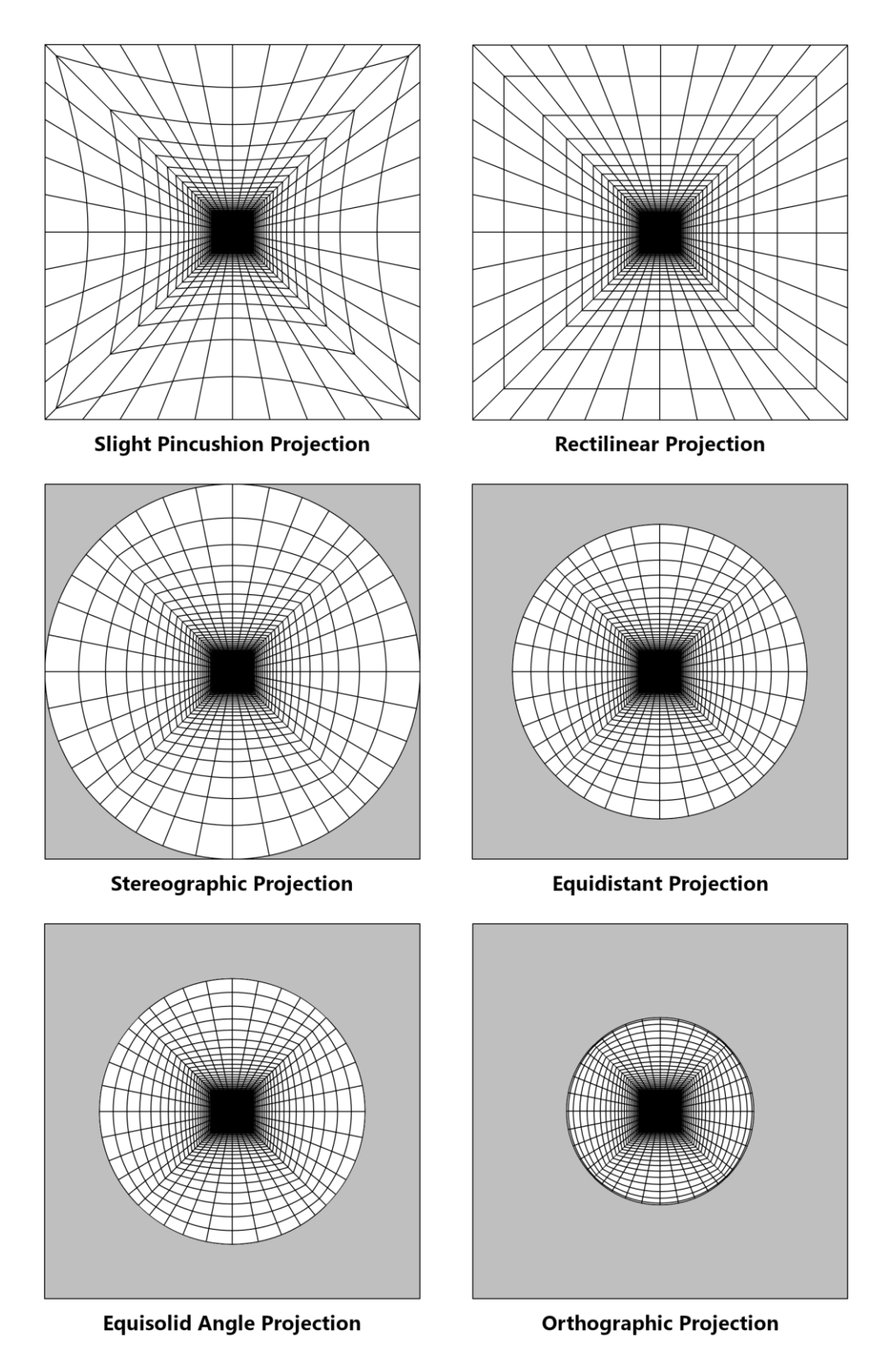


Figure 132. A square tunnel formed by the x-z planes at y = -5 m and y = 5 m and the y-z planes at x = -5 m and x = 5 m.

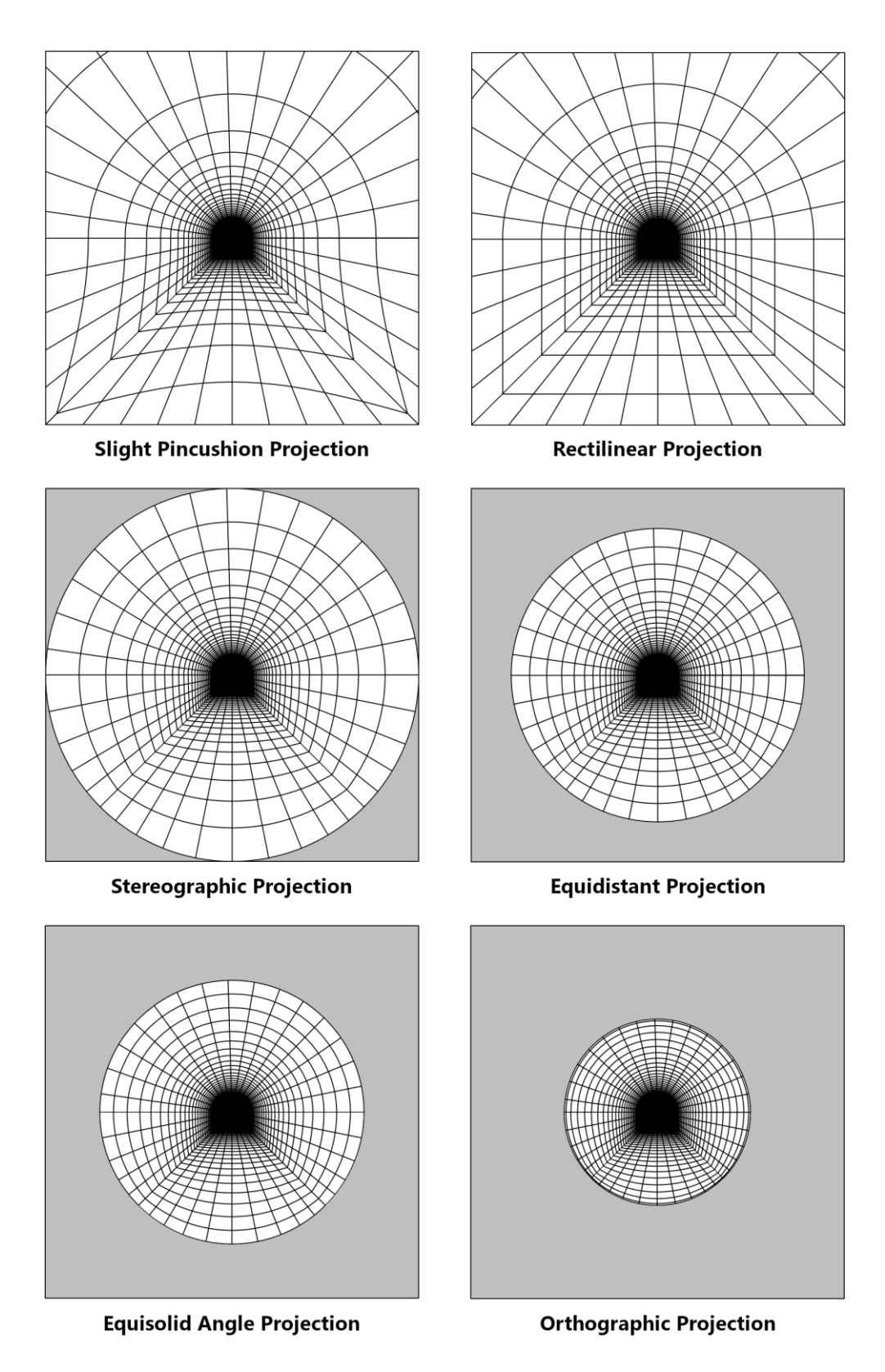


Figure 133. An arched tunnel formed by the planes at y = -5 m, x = -5 m, and x = 5 m, and the surface at $\rho = 5$ m.

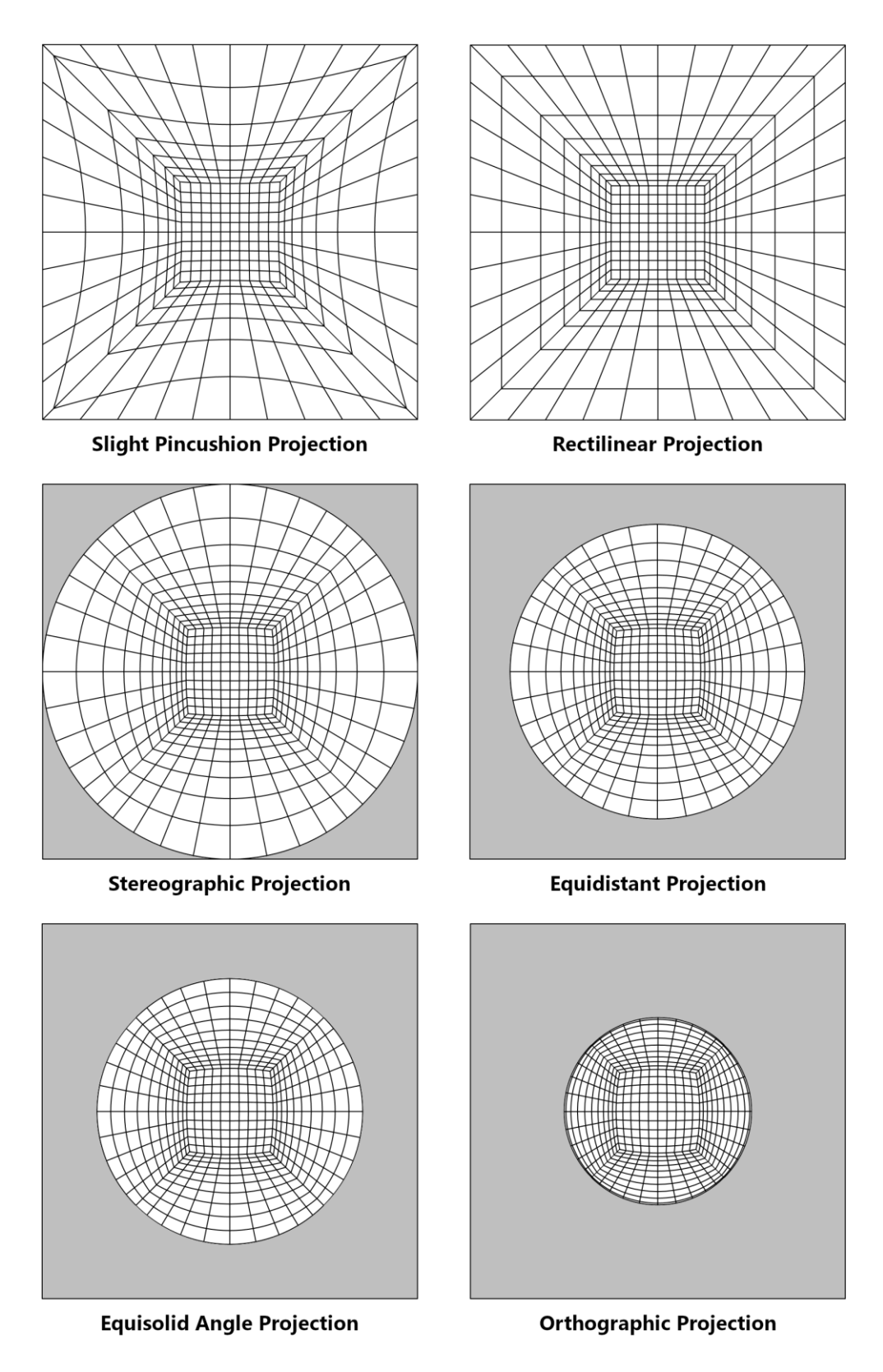


Figure 134. A room formed by the planes at y = -5 m, y = 5 m, x = -5 m, x = 5 m, and z = 10 m.

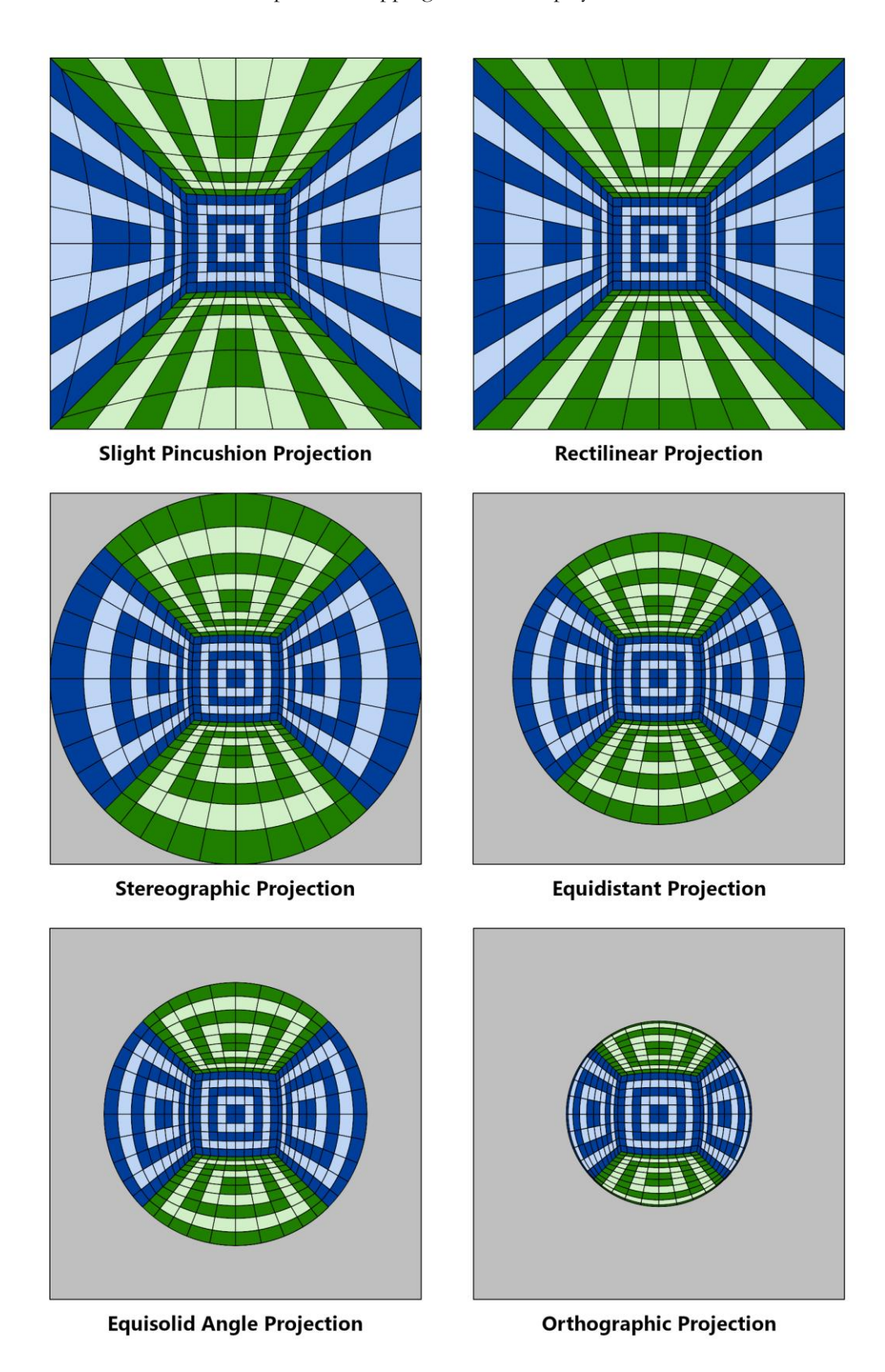


Figure 135. The room shown in Fig. 132 with markings added to aid in visually locating the parts of the walls.

Chapter 11. Mapping to a Flat Display Screen

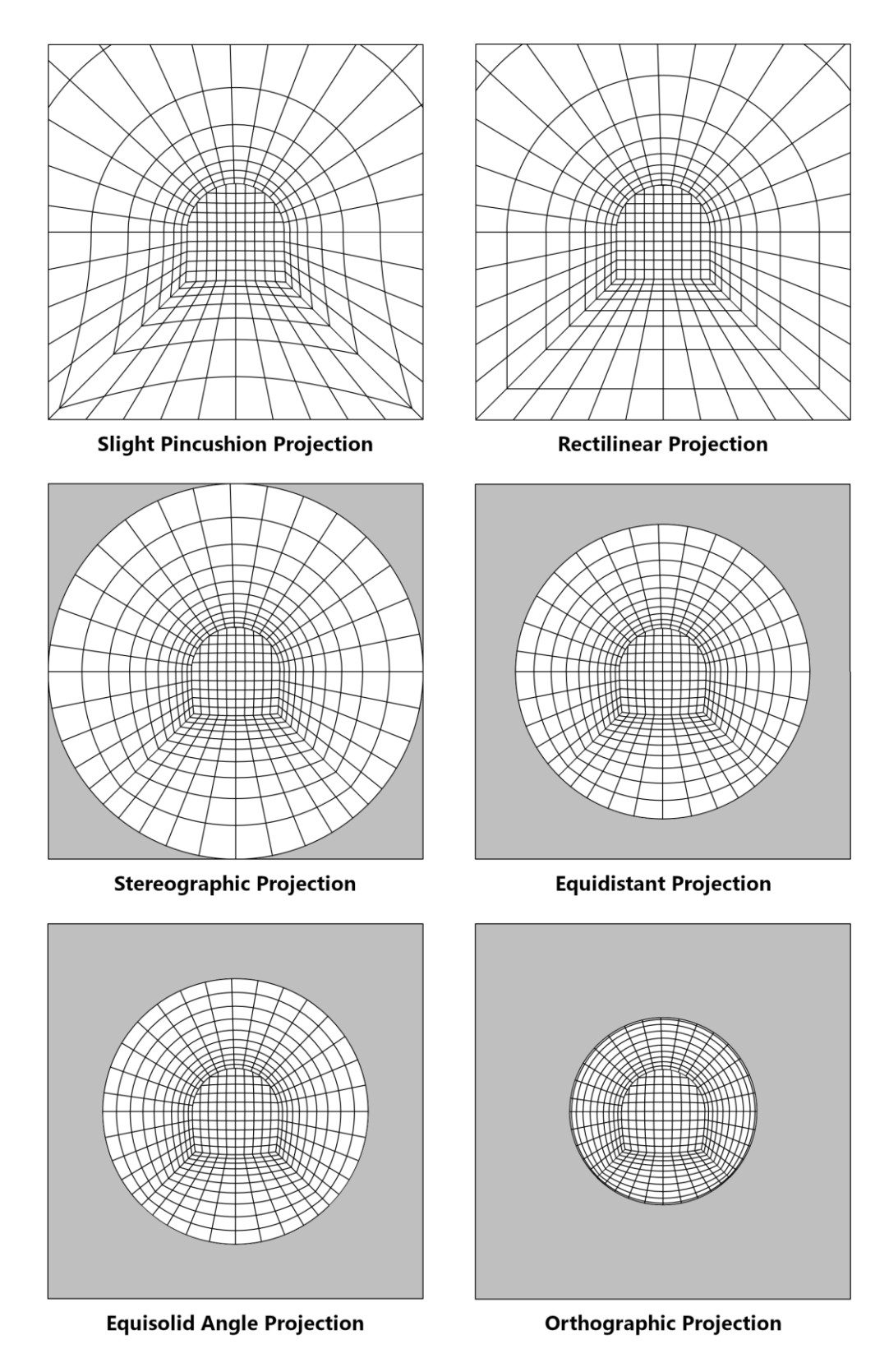


Figure 136. An arched room formed by the surfaces at y = -5 m, y = 5 m, x = -5 m, x = 5 m, x = 5 m, and z = 10 m.

Chapter 11. Mapping to a Flat Display Screen

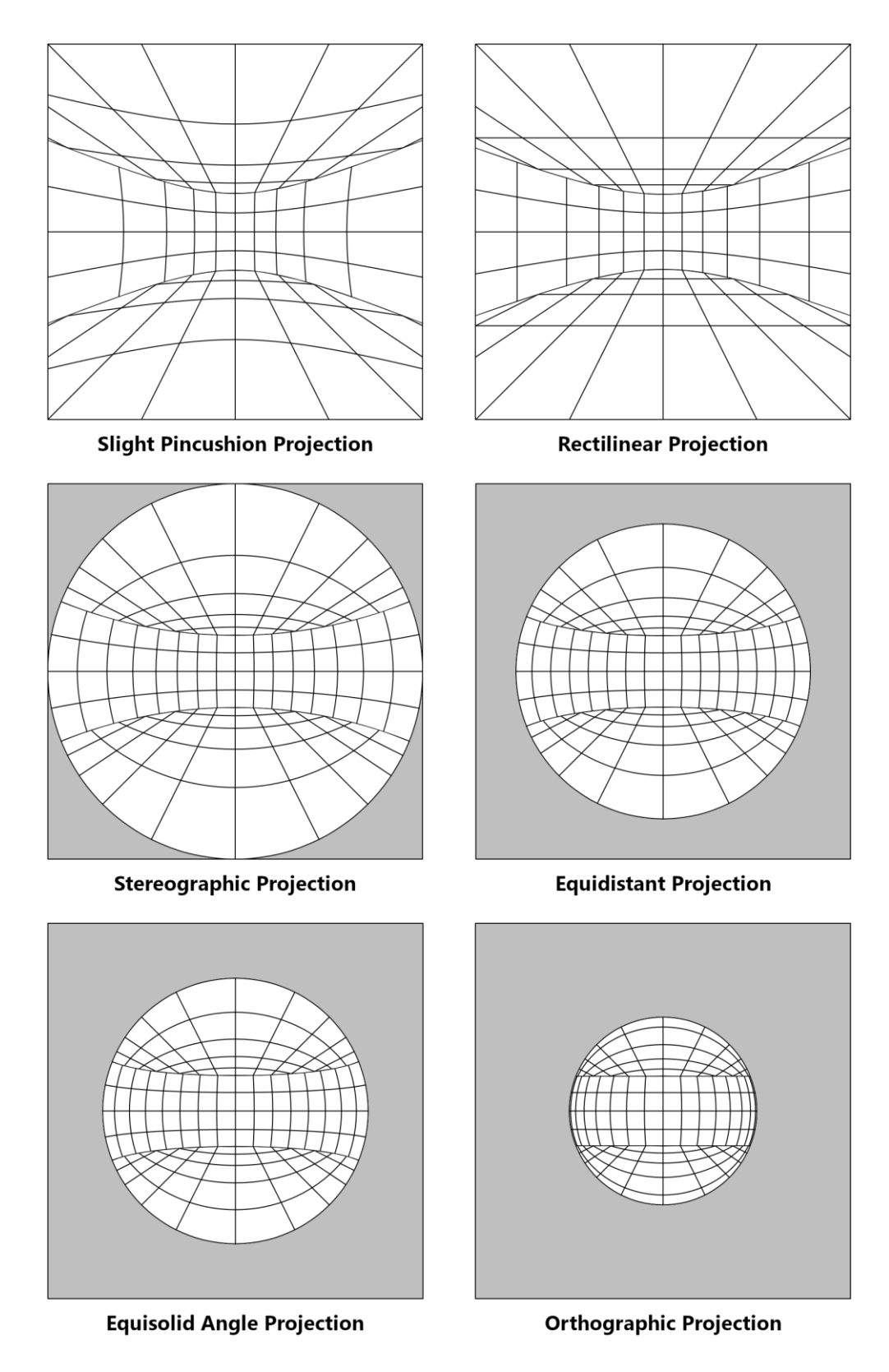


Figure 137. A cylindrical room formed by the x-z planes at y = -2 m and y = 2 m, and the s_{α} -y surface at l = 5 m.

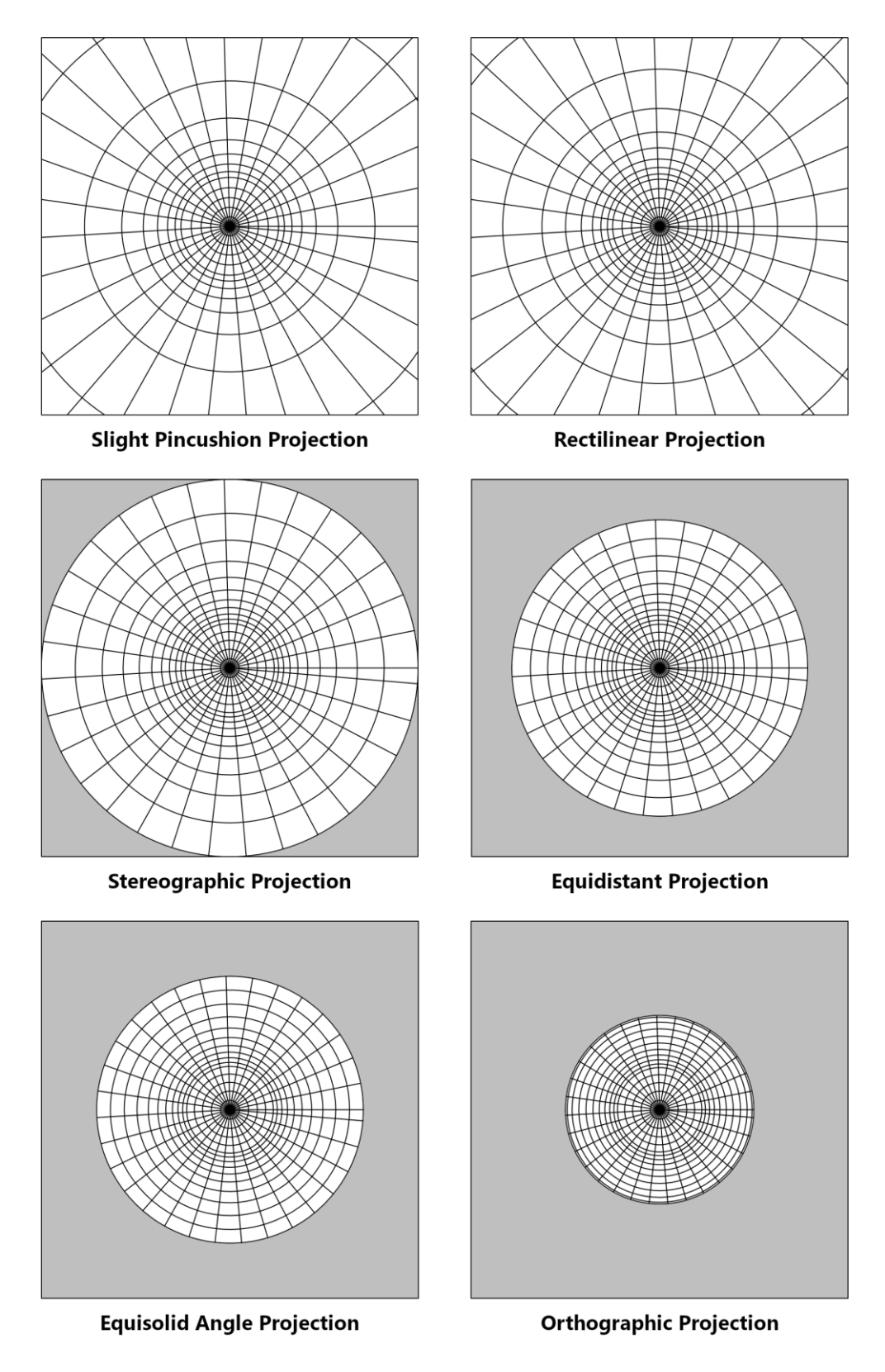


Figure 138. A sealed tunnel formed by the s_{φ} -z surface at $\rho = 5$ m and the ρ - s_{φ} surface at z = 10 m.

Chapter 11. Mapping to a Flat Display Screen

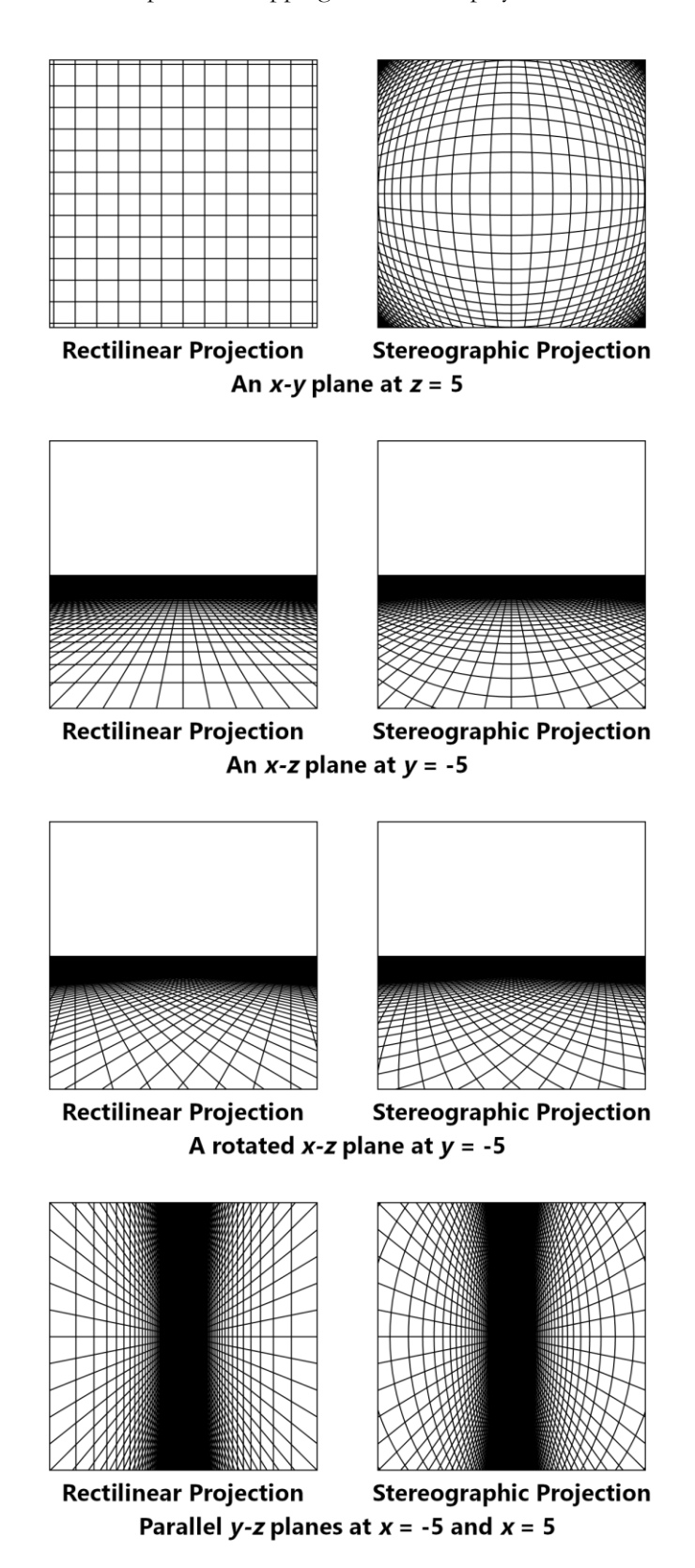


Figure 139. Cropped images for the various scenarios.

Chapter 11. Mapping to a Flat Display Screen

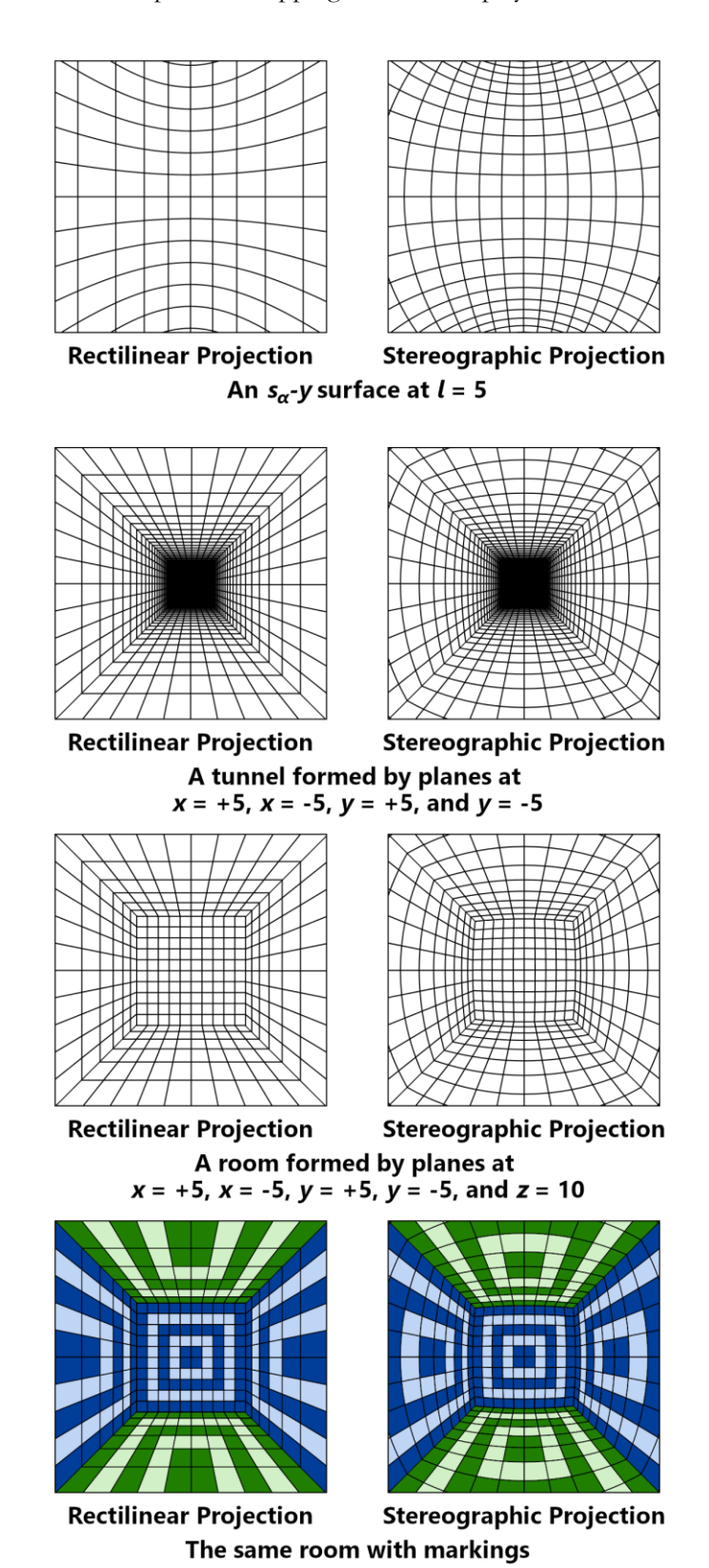


Figure 140. Additional cropped images.

Chapter 11. Mapping to a Flat Display Screen

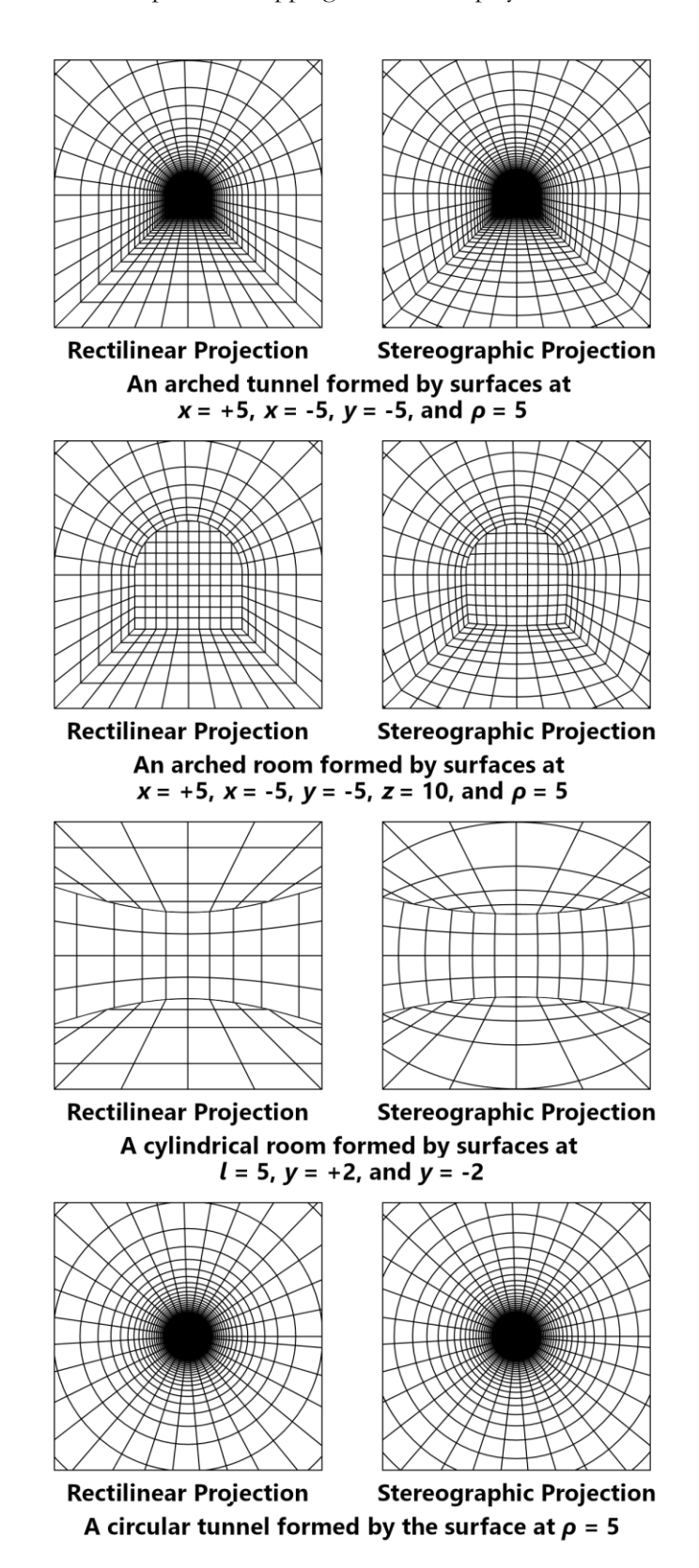


Figure 141. The last set of cropped images.

Chapter 12

Human Depth Perception Cues

As established and demonstrated in the previous chapters, depth information from three-dimensional scenes and objects is partially embedded in the two-dimensional images that humans visually experience. This is why humans can experience the external world as three-dimensional despite the fact that the human retinas only capture two-dimensional images. In summary, we have now established that depth information is preserved through the following effects:

- 1. As an object moves away from the observer in the r direction, its observed length diminishes according to the equation (1/r).
- 2. As an object moves away from the observer in the r direction, its observed area diminishes according to the equation $(1/r^2)$. This effect and the previous effect involve situations when the object moves forward, away from the observer, which are the forward size perspective effects.
- 3. As an object in front of the observer moves laterally away from the viewing axis, its observed size and area diminish in complicated ways, which are the lateral size perspective effects. An object moving in an odd direction experiences a combination of the forward size perspective effects and the lateral size perspective effects.
- 4. As an object moves away from the observer in the *z* direction, it appears to be moving toward the central horizon point.

- 5. Parallel lines that extend away from the observer in the *z* direction appear to all converge at the central horizon point.
- 6. An object that moves away from the observer not in the *z* direction, but rather in some direction in the *x-z* ground plane, appears to be moving toward some point on the horizon line that is not the central horizon point.
- 7. Parallel lines that extend away from the observer not in the *z* direction, but in some direction in an *x-z* ground plane, appear to converge at some point on the horizon line that is not the central horizon point.
- 8. As a flat object tilts away from broadside viewing without changing its distance r from the observer, its length and area appear to diminish.
- 9. An object that is moving at a constant speed will appear to move quickly when it is closer to the observer and more slowly when it is farther away from the observer. Similarly, when several objects are moving at the same physical speed in the same direction, the closer objects will appear to be moving at a faster speed.
- 10. For everyday speeds, a moving object that is very far away will appear to be motionless.

The human vision system uses these effects in various ways, along with other effects, in order to experience depth. The different ways that the human eyes and brain use these effects are called visual depth perception cues. The human monocular depth perception cues are described in the following sections. Note that some people use the term "perspective" narrowly so that only some of the effects below are types of perspective effects, while others use this term broadly to include all of the effects below. To avoid confusion, I will avoid using this term, with the understanding that all of the effects below are either perspective effects or are related or work in conjunction with perspective effects.

12.1 Motion Parallax

If you are moving smoothly as you look out at the stationary external world, it is equivalent to you staying motionless while the entire world moves in a corresponding way. As the whole world appears to move, objects that are closer to you will appear to move at a faster speed because of parallax. Your brain understands that all of the moving objects in your view have the same true speed (because it's really just one object—you that is moving through space). Therefore, your brain can determine how far away an object is from you by how fast it appears to be moving as the observer moves. Geometrically, this arises from the same parallax effect that binocular depth perception uses, but now the different images are arising from you moving your eyes to different viewing locations and not from you using two eyes. This is called motion parallax.

As an example, imagine you are on a moving train. As you look out the window, closer objects such as telephone poles appear to move quickly across your field of view, while distant objects such as mountains appear to move slowly.

12.2 Kinetic Depth Effect

Physical objects tend to move in common ways which your brain understands and can thus use to extract depth information. For instance, consider a rigid object that is rotating in place. In the physical reality, all parts of the object travel along circular paths around the same rotational axis. When viewed by a human, all parts appear to be traveling along elliptical paths around the same rotational axis (assuming that you are not staring directly done the rotational axis). This is the kinetic depth effect.

Furthermore, the apparent width of a part's elliptical path depends on how far away that part is from the rotational axis. Your brain can detect all this and extract depth information. Your brain can also do this type of thing with other common types of motion, such as projectile motion, wave motion, and walking motion.

The kinetic depth effect is different from motion parallax. While motion parallax involves a steadily moving observer looking at a motionless world (and therefore always results in the whole world seeming to move in the same direction), the kinetic depth effect instead involves a motionless observer looking at moving objects. If all visible objects are moving past a fixed observer in the same direction at the same true speed, then the kinetic depth effect ends up equivalent to motion parallax. But for all other types of object motion, they are not equivalent. There is no way in which an observer can travel though space while viewing a motionless scene that will produce a result that is equivalent to the kinetic depth effect of waving motion, walking motion, explosive motion, and so forth.

12.3 Depth from Optical Expansion

When an object is moving steadily toward you, its apparent size increases in a specific way. The *rate* at which it appears to get bigger depends on how far away it is and how fast it is moving toward you. When the object is far away, it will appear to get bigger very slowly. When the object is very close, it will appear to get bigger quickly. This

effect is called optical expansion. Your brain can deduce not only that the object is moving but also the object's distance. Note that the reverse is also true: an object moving steadily away from you appears to get smaller at a rate that is proportional to its distance.

When a baseball is thrown toward you, your brain uses optical expansion to keep track of its distance. This helps you properly catch the ball at the right time. The optical expansion depth cue is similar to the kinetic depth effect cue, except that for the kinetic depth effect cue, your brain is analyzing the apparent speed at which the object changes location in space. In contrast, for the optical expansion cue, your brain is analyzing the rate at which the perceived size of the object changes. A train that is traveling directly toward you would exhibit zero kinetic depth effect but would exhibit significant optical expansion.

To be completely clear, optical expansion does not just involve an object appearing to get bigger as it moves toward you in a vague way. Rather, it involves an object getting bigger at a specific rate that corresponds to its distance from the observer. Your brain subconsciously understands and has experience with this physics and can therefore extract depth information.

12.4 Familiar Shape

If an object has a familiar shape that you have experience with in the real world, your brain can recall from memory the true three-dimensional shape of that object and relate it to what you are seeing, thereby enabling depth perception. In this way, the three-dimensional shape of the object can be perceived without needing any other depth cues. Fig. 142 demonstrates the familiar shape depth cue.

The image on the right in Fig. 142 contains in reality a collection of straight black lines and gray areas on a flat white screen or piece of paper. However, the lines are arranged in the familiar shape of what you see when you look at a real table. You therefore perceive depth. The image

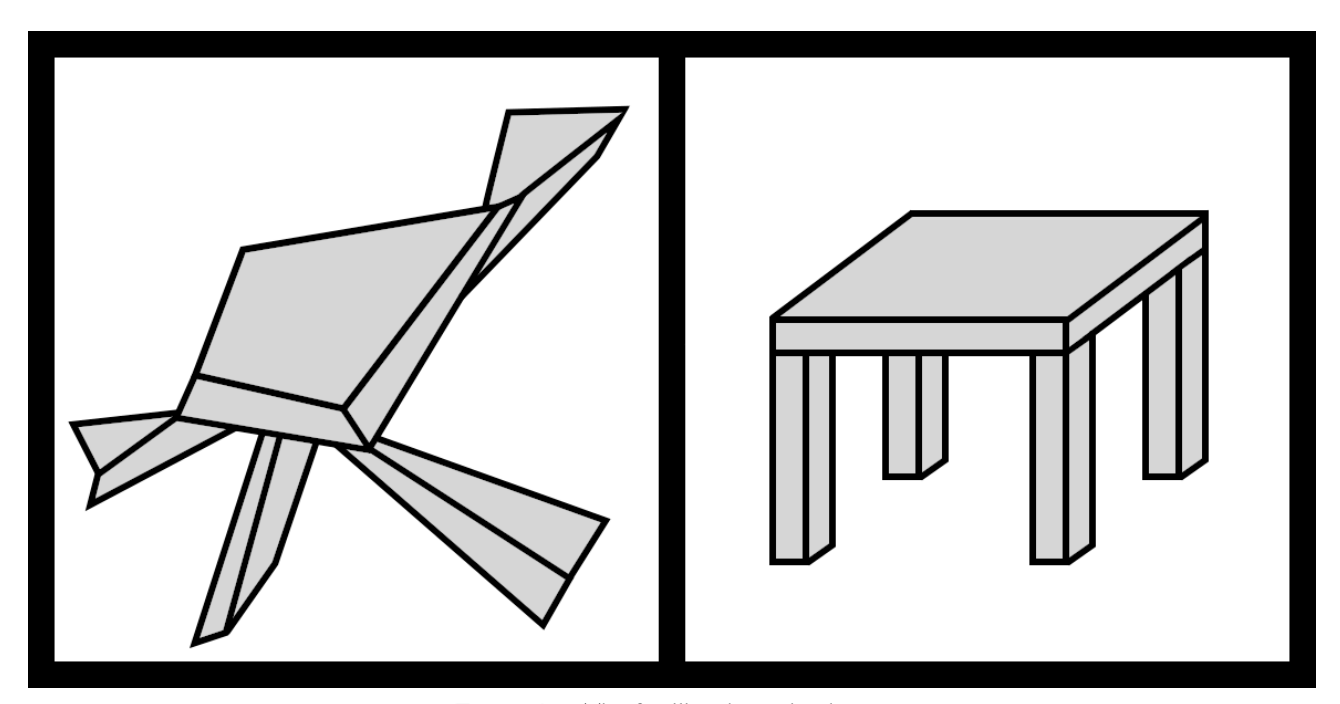


Figure 142. The familiar shape depth cue.

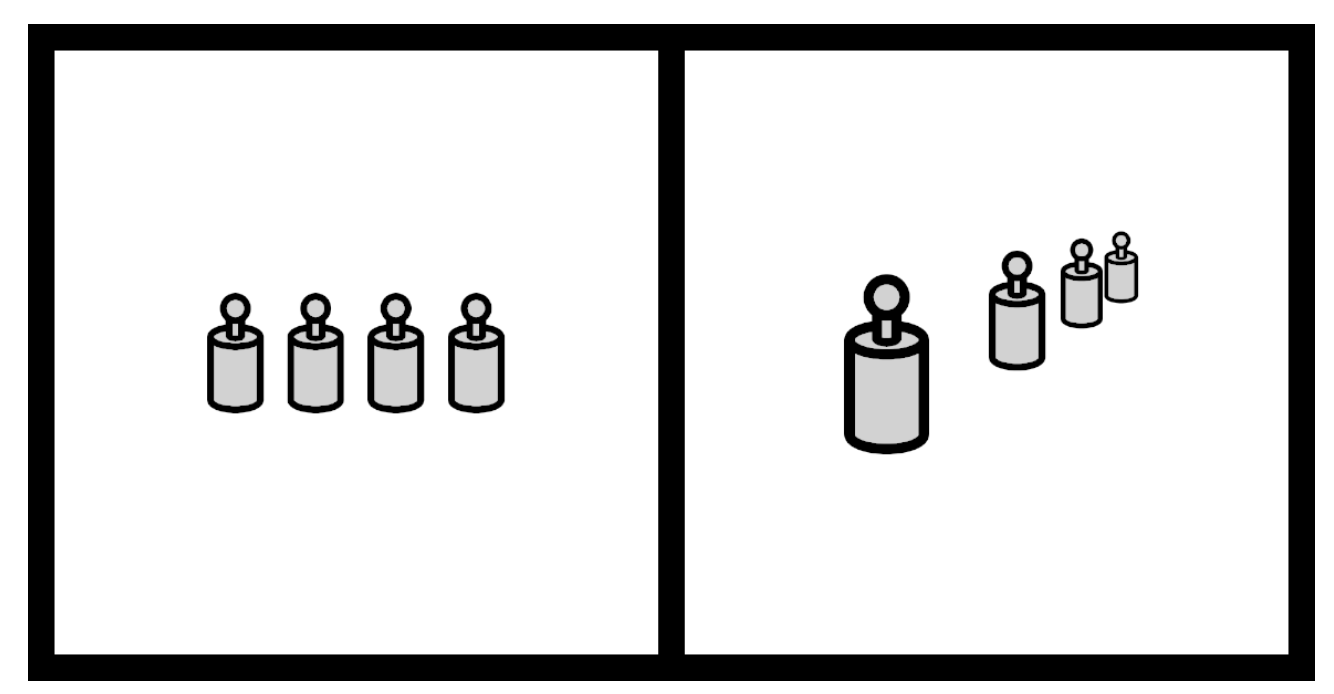


Figure 143. The relative size depth cue.

on the left shows the exact same number of lines attached to each other at the same places as the right image, but it does not seem to have depth because the angles of the lines don't match what you see when you visually observe a real table. In other words, the object on the left does not have the correct familiar shape that will occur when viewing a real table. Note that for the image on the right, I have intentionally drawn the table without perspective effects so that the only depth cue is the familiar shape cue.

12.5 Relative Size

If two objects in your field of view are the same type of object, then your brain assumes that their true physical sizes must be the same. Therefore, your brain assumes that the difference in their visually perceived sizes must be solely caused by distance perspective effects. Your brain can thus extract depth information based on how much the perceived sizes of the two objects differ. For instance, if two telephone poles are in view, then the pole that appears to be three times taller than

the other pole must be three times closer to you.

Fig. 143 demonstrates the relative size depth cue. For the image on the right, your brain notices that each of the four objects has the same shape and therefore assumes that they all have the same true size. Therefore, your brain perceives that the smaller objects must be farther away from you. In contrast, the objects in the left image in Fig. 143 all have the same size and therefore appear to be at the same distance. I have intentionally chosen an object with an unfamiliar size and shape so that the only depth cue present is the relative size depth cue (and the horizon line effect).

12.6 Familiar Size

If a certain object has a known true size, then its perceived size corresponds to how far away it is, even if there are no other objects in the field of view to compare it to. Your brain can therefore extract depth information from the perceived size of the object relative to its known true size. For instance, an apple is usually a few inches tall. An apple that appears to be much smaller than this

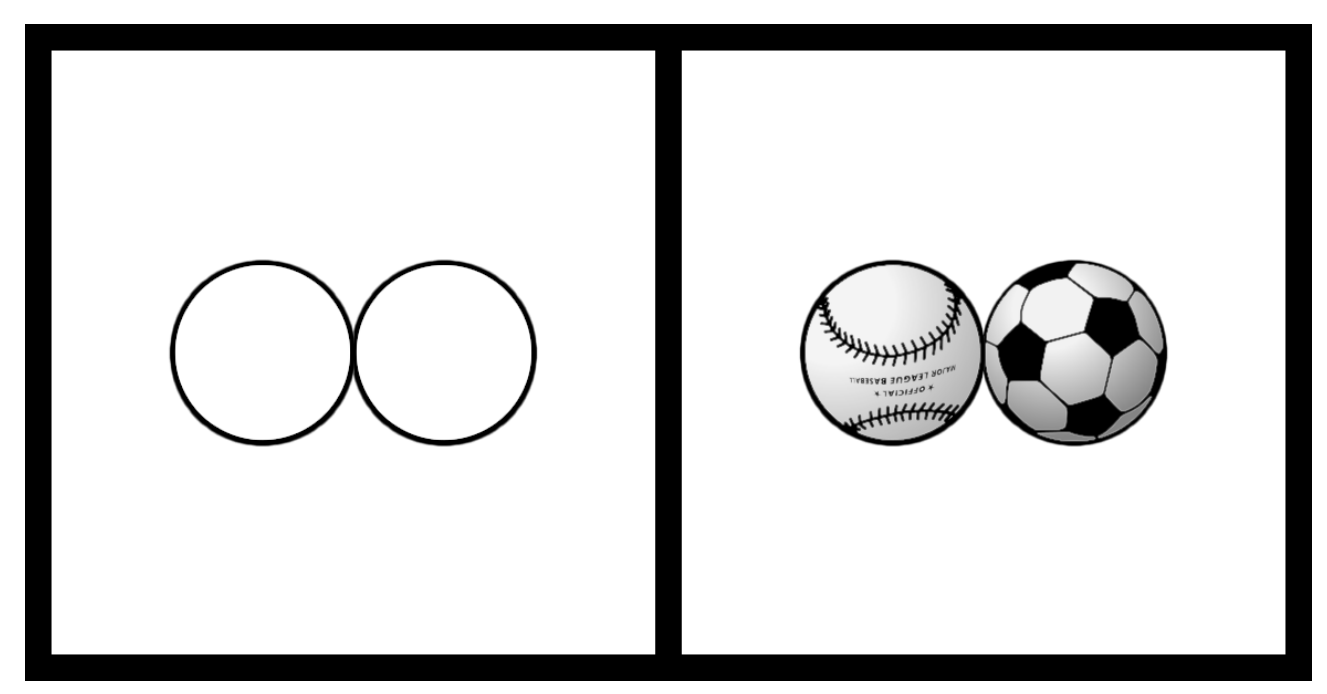


Figure 144. The familiar size depth cue.

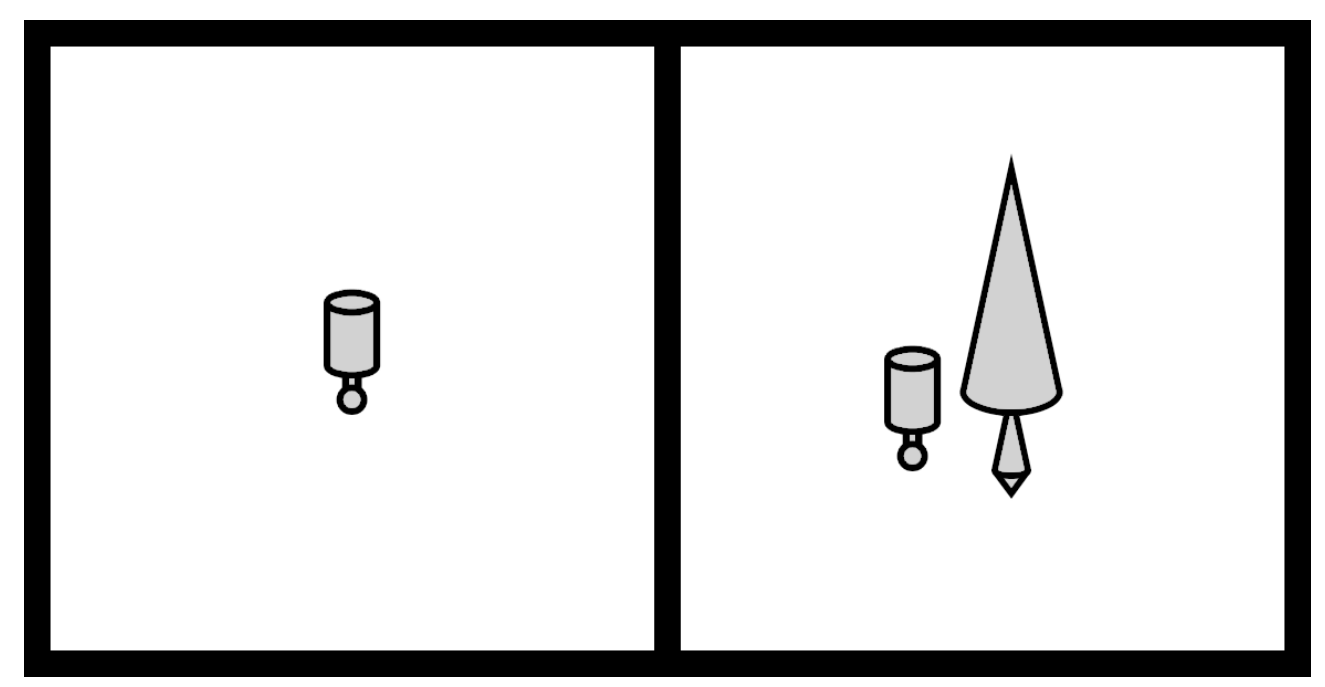


Figure 145. The estimated size depth cue.

must therefore be far away. Fig. 144 demonstrates the familiar size depth cue. The image on the left in Fig. 144 includes two non-specific, unfamiliar circular objects so that no depth cues are present.

As a result, the two objects in the left image appear to be the same distance away. In contrast, the image on the right in Fig. 144 includes two familiar objects. Because you are familiar with

baseballs and soccer balls, and you know that the true size of a baseball is smaller than the true size of a soccer ball, your brain perceives that the soccer ball must be farther away. In order to get this effect to work well while looking at Fig. 144, close one eye and try to visualize the balls as real objects in a real scene that you are trying to reach out and grab. Which ball would you reach first?

12.7 Estimated Size

Amazingly, even if you see an object by itself, with nothing of the same shape to compare it to, and the object has an unfamiliar shape and size, your brain can still extract some depth information from its perceived size by estimating its true size. In other words, your brain estimates the most probable true size of the object and then uses this as if it were a familiar size depth cue.

The estimated size depth cue is not particularly effective because the estimated size will typically not be very accurate. Fig. 145 demonstrates the estimated size depth cue.

Although the objects in the image on the right in Fig. 145 are unfamiliar and unlike each other, your brain may assume that cylindrical objects in everyday life (like soup cans) tend to have a small true size while conical objects in everyday life (like Christmas trees) tend to have a large true size. Thus, your brain may assume that the conical object in the right image is much bigger in true size and therefore must be farther away from you than the cylindrical object because it does not look that much bigger. If you are having a hard time visually perceiving the cylinder-like object in Fig. 145 as closer to you than the cone-like object, don't worry because this depth cue is not very effective.

12.8 Uniform Size

For a single, extended object that is known to be roughly constant in size along its length, the parts of the object that visually appear to be smaller must be farther away from you because of the perspective effects. For instance, a baseball bat is

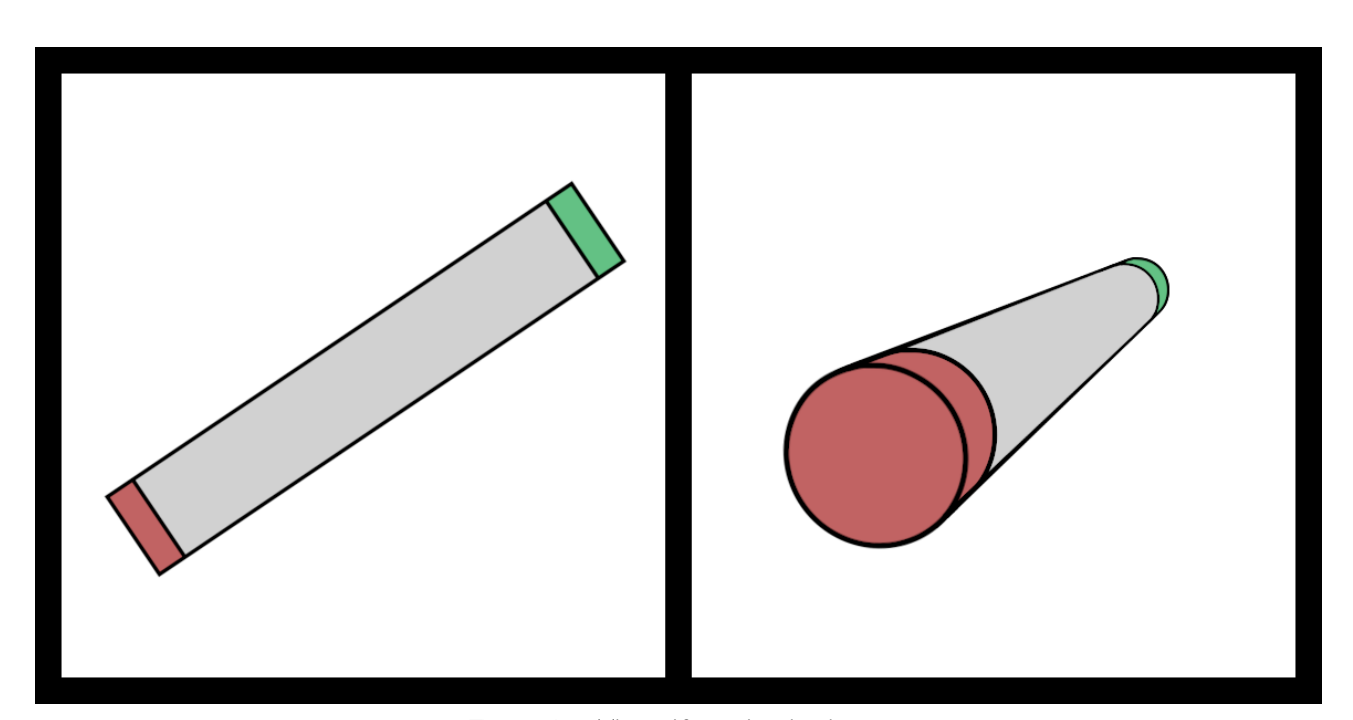


Figure 146. The uniform size depth cue.

roughly constant in cross-sectional area along its length. Therefore, the end of the baseball bat that appears to be much smaller than the other end must be farther away from you.

Fig. 146 demonstrates the uniform size depth cue. A cylindrical rod in the real world has a uniform size along its length. Therefore, when one end of the rod appears larger than the other end, your brain correctly sees the larger end—the red end in this case—as the closer end. When looking at the image on the right in Fig. 146, notice how the red end of the rod seems to be sticking out of the screen. In contrast, the image on the left shows the same rod but without this depth cue present.

12.9 Parallel Lines

This cue can be thought of as a general case of the uniform size depth cue. This is because when two lines are parallel to each other in the real world, this is equivalent to a single object having a uniform size along its length. For instance, a straight road extending away from you has a uniform width along its length but can be thought of as two parallel lines (i.e. the two sides of the road).

Two lines that are parallel to each other in the real world will be perceived as converging toward each other as they stretch farther away from you. If your brain knows that the two lines are parallel in the real world, it can extract depth information based on how close the lines appear to be. The places where the lines appear closer to each other must be farther away from you.

Fig. 147 demonstrates the parallel lines depth cue. The image on the right in Fig. 147 shows a scene involving two roads on a flat ground plane with this depth cue at work. Therefore, these roads appear to be stretching away from you into the distance. In contrast, the image on the left shows the same scene but without this depth cue present, leading it to look flat.

For a set of parallel lines that all extend exactly away from you, they will all appear to meet at the

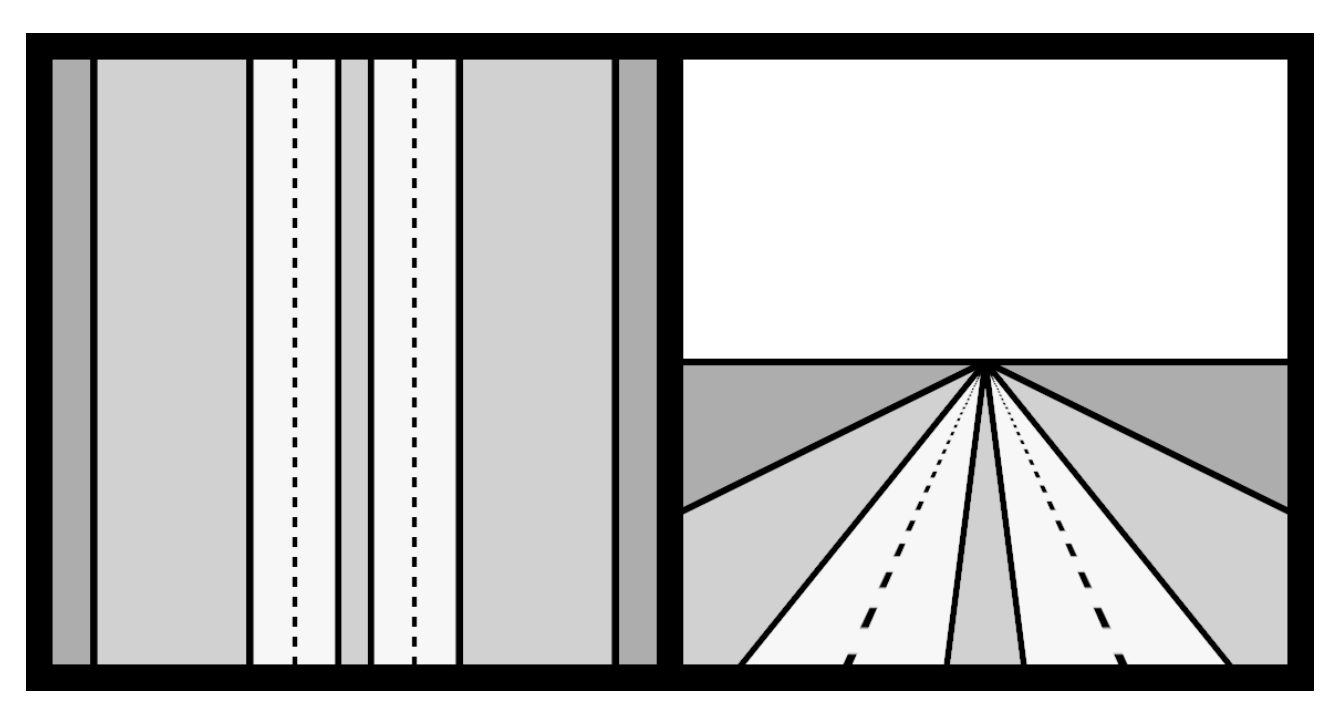


Figure 147. The parallel lines depth cue.

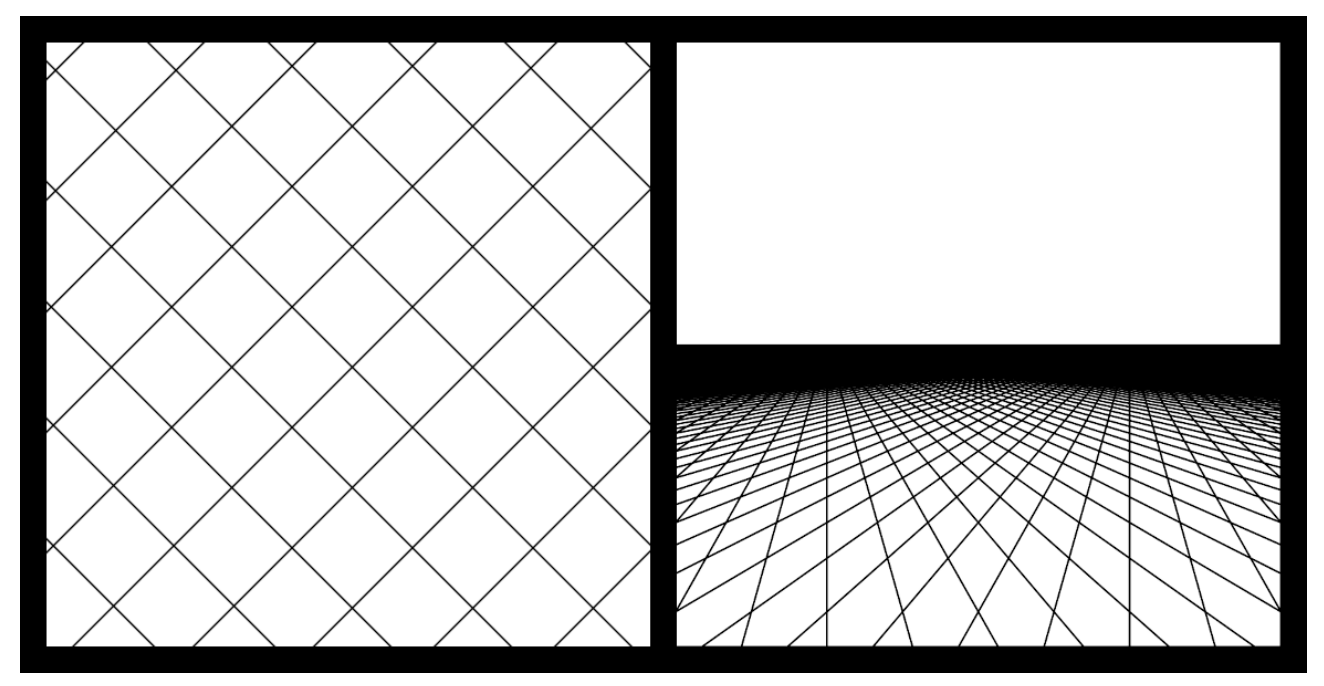


Figure 148. The parallel lines depth cue.

central horizon point (i.e. at the central vanishing point), as shown in Fig. 147. In contrast, if a set of parallel lines extends away from you at an oblique angle, then these lines will all appear to meet at one vanishing point that is not at the central horizon point. Such a situation is shown in Fig. 148.

The image on the right of Fig. 148 shows two sets of parallel lines on the ground that each has its own non-central vanishing point. The image on the left shows the same scene but without any depth cues present.

In general, every set of parallel lines has its own vanishing point. Therefore, there could be thousands of different vanishing points in a single image (or an infinite number, really). Interestingly, if all the sets of parallel lines in a scene are all parallel to the ground plane, then all of their vanishing points will lie directly on the horizon line (which is where the sky appears to meet the ground). This may seem like a rare situation, but humans love to build things with surfaces parallel to the ground, so it is quite common. It is so

common, in fact, that some people mistakenly think that vanishing points must always lie on the horizon line.

In everyday life, humans tend to build objects that have a box shape or consist of a collection of box shapes, such as buildings, desks, cabinets, shelves, books, tables, and beds. The edges of a rectangular box form three sets of parallel lines. Therefore, a collection of boxy objects that all have their faces aligned with each other will only have three vanishing points. First instance, a row of houses has most of its edges appear as lines converging at one of the three vanishing points. For such cases, artists speak of drawing in three-point perspective.

Sometimes in art, the vertical vanishing point is ignored (so that all lines that are vertical in real life are drawn as vertical on the paper). For a collection of aligned boxy objects, this reduces the situation down to two vanishing points, which artists call two-point perspective. If there is a collection of aligned boxy objects and two of the dimensions are drawn without perspective, then

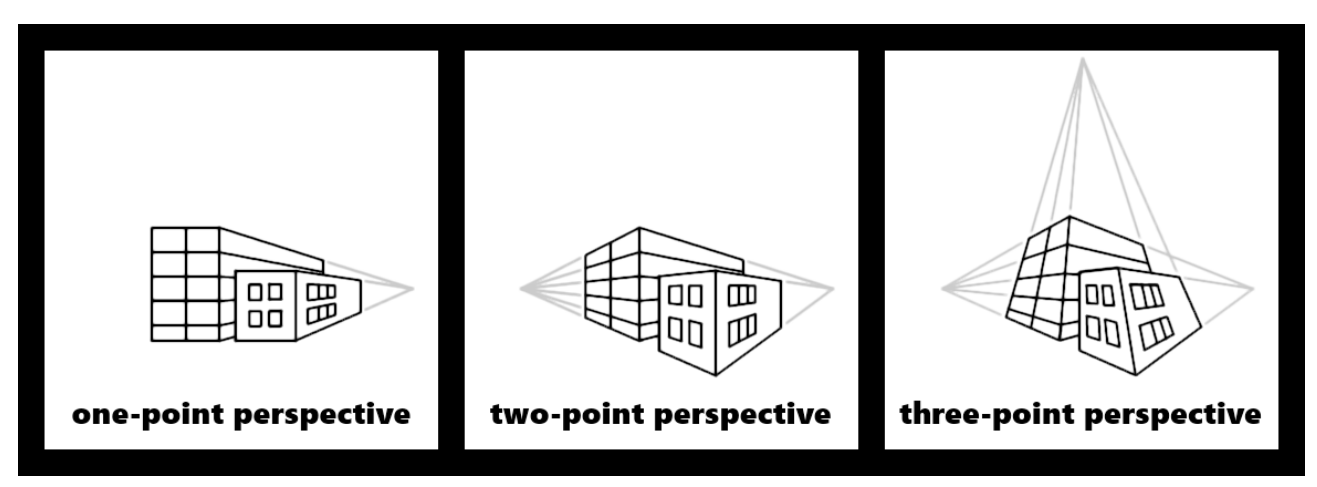


Figure 149. Different artistic point perspective approaches.

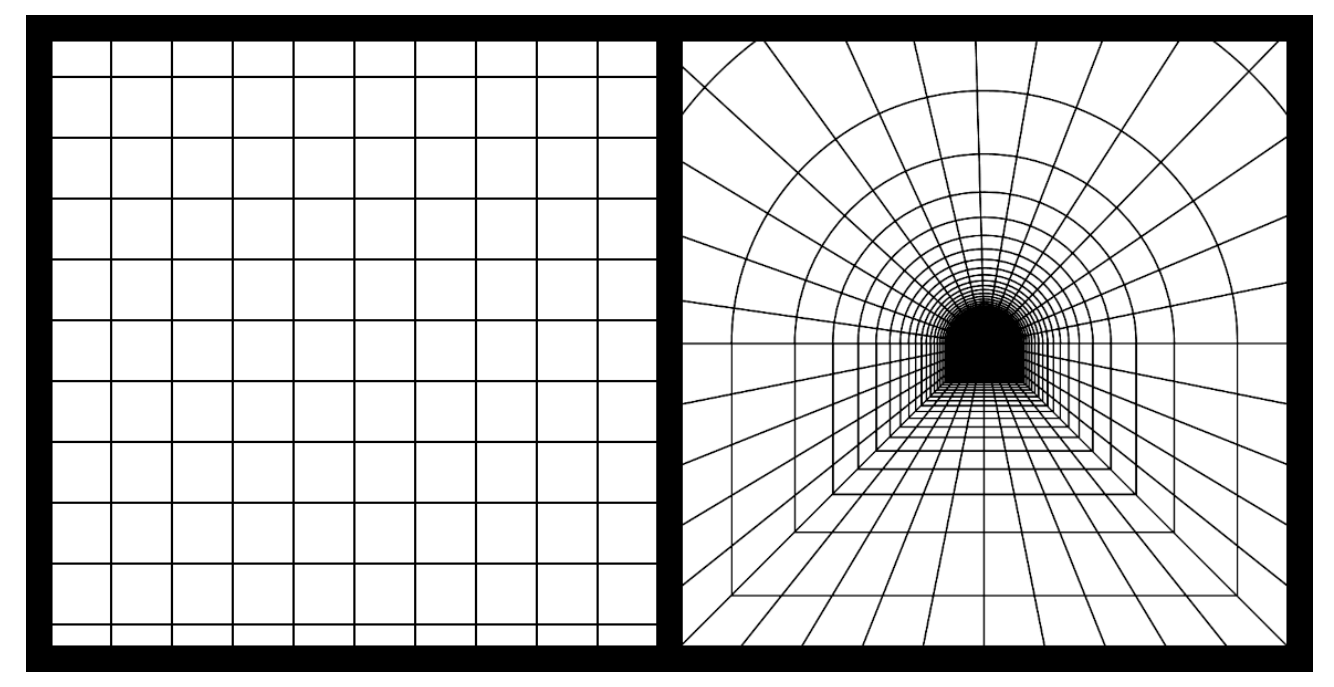


Figure 150. The parallel lines depth cue.

there is only one vanishing point, which artists call one-point perspective. These concepts are shown in Fig. 149.

Note that the parallel lines depth cue is not a special case of the horizon effect depth cue. The perception of depth established by parallel lines arises from the lines converging at a vanishing point and not from objects being close to the horizon line. In fact, the parallel lines depth cue

works even if there is no horizon line at all. The right image of Fig. 150 shows a situation where there is no horizon line but there is a collection of parallel lines converging at the central horizon point.

In the image on the right of Fig. 150, all of the lines that are running along the length of the tunnel meet at the central vanishing point. In contrast, the left image displays the same tunnel,

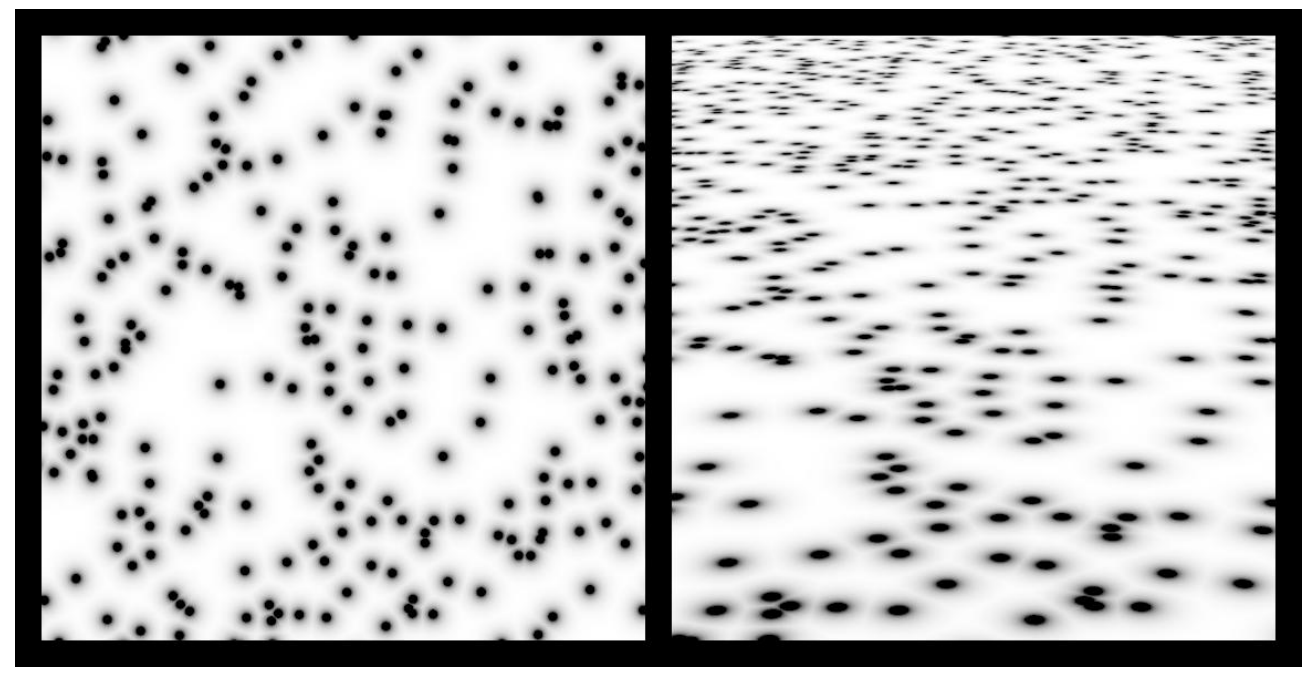


Figure 151. The texture gradient depth cue.

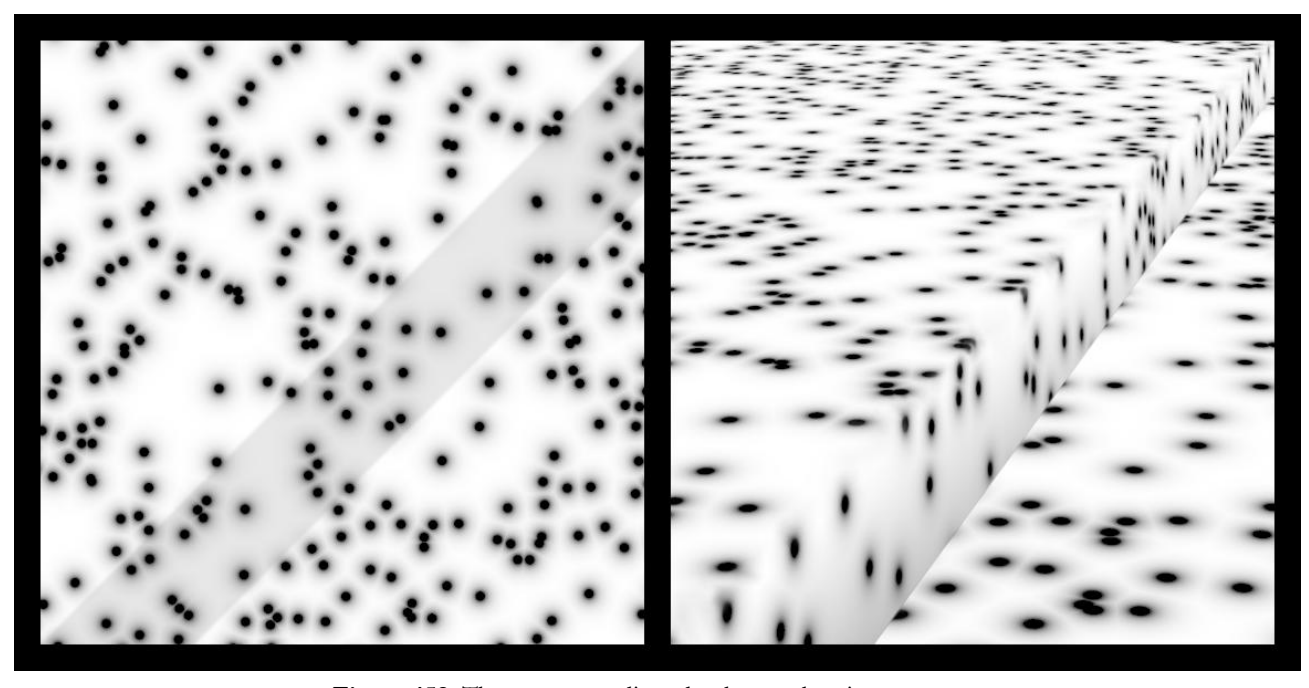


Figure 152. The texture gradient depth cue, showing a canyon.

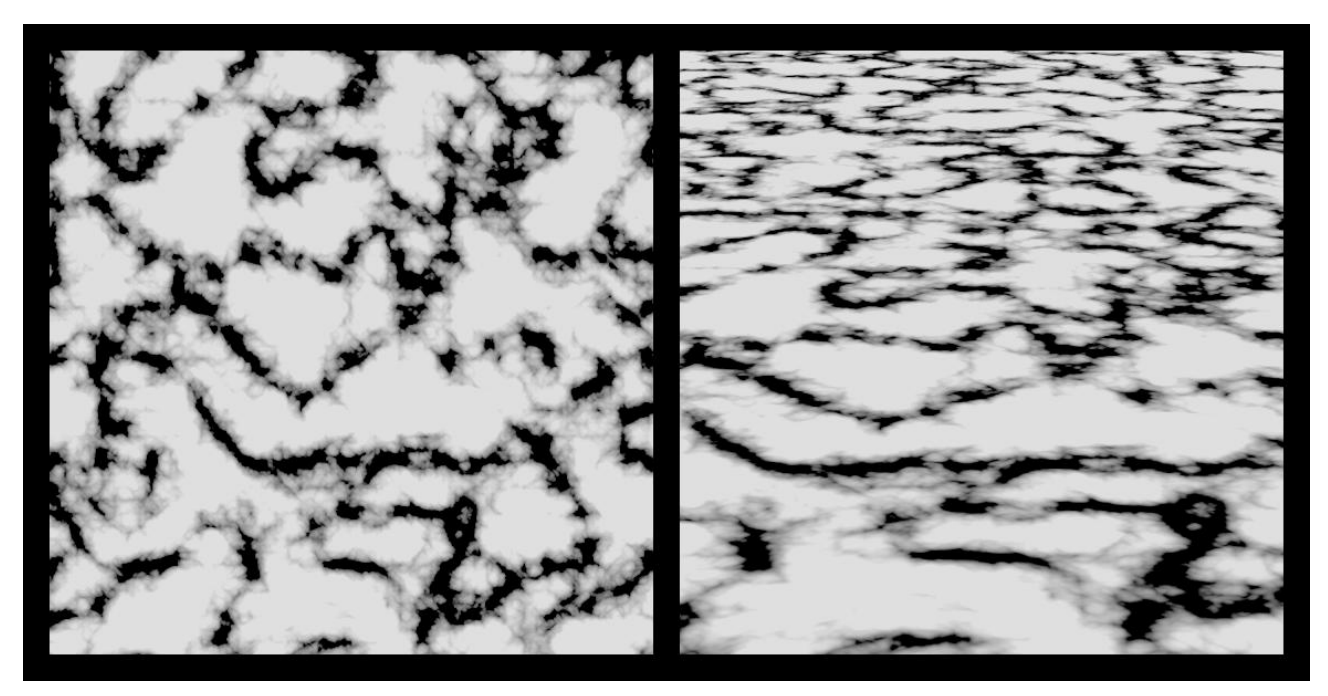


Figure 153. The texture gradient depth cue.

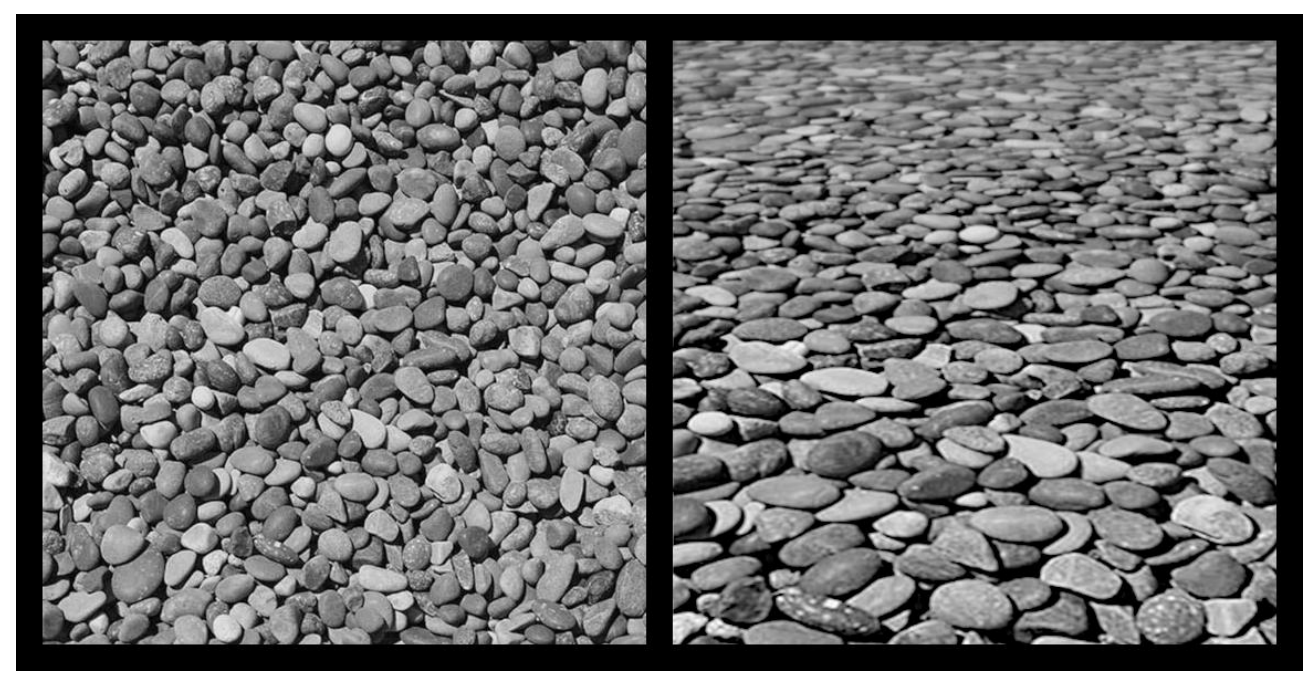


Figure 154. The texture gradient depth cue arising from a collection of small objects..

but without the parallel lines depth cue present, insofar as that is possible. Note that if there is not a horizon line but there are vanishing points, the horizon effect still occurs in the sense that the closer an object appears to be to a vanishing point, the farther away it seems to be. However, the vanishing point horizon effect still is not the parallel lines depth cue. You can have a central horizon point giving rise to a horizon effect in a scene even if no parallel lines are present.

12.10 Texture Gradient

Similar to how objects that are closer to you appear larger, parts of the pattern in a texture that are closer to you will appear larger. Your brain can therefore extract depth information from how the different parts of a texture compare to each other in perceived size. Also, the texture of a surface can indicate the tilt of the surface, which can help portray the three-dimensional shape of objects. Fig. 151 shows the texture gradient depth cue. In the image on the left in Fig. 151, all of the spots of the textured surface are perceived as being the same size, the same shape, and at about the same spacing, making this image appear flat. In contrast, the image on the right shows that the dots near the top of the image are smaller, closer together, and more distorted than the other dots, giving the impression that they are farther away. Note that the left image and the right image in Fig. 151 show the exact same textured surface with the dots in the same places.

The texture gradient effect works not only on flat ground planes. It can also portray the three-dimensional shape of complicated objects and scenes. For instance, Fig. 152 is the same as Fig. 151, except that a canyon has been cut in the ground. The three-dimensional shape of the canyon in Fig. 152 is made apparent in the image on the right by the texture gradient depth cue. Note that there are no other depth cues present in this

image (except for a small amount of recess shading). The image on the left in Fig. 152 shows the same texture and the same canyon but now without the texture gradient depth cue present.

An additional example of the texture gradient depth cue is shown in Fig. 153. As Fig. 153 shows, a texture gradient does not have to consist solely of independent features or objects. Rather, it can consist of an interconnected pattern. The image on the right includes the texture gradient effect. As a result, the top of the image appears to be farther away from you than the bottom of the image. In contrast, the image on the left shows a texture but without the texture gradient effect, making it look flat.

Another example of the texture gradient depth cue is shown in Fig. 154. As Fig. 154 shows, a texture gradient does not have to consist of a pattern that has been painted on a flat surface. It can also consist of a large collection of three-dimensional objects that are situated so that they approximately form a flat surface (small rocks in this case).

12.11 Horizon Effect

For an object sitting on the ground, the physics dictates that the closer the object's center appears to be to the horizon, the farther away the object is from you. Your brain can therefore estimate how far away an object on the ground is by how close its center appears to be to the horizon line.

Fig. 155 shows the horizon effect depth cue. In the image on the left, all three objects are at the same vertical location in the image. In contrast, the image on the right shows the same three objects but at different vertical locations. Your brain sees the blue cone as visually closer to the horizon and therefore perceives that it is farther away from you than the other objects. At the same time, the red cylinder is visually the farthest from the horizon line, so it seems the closest.

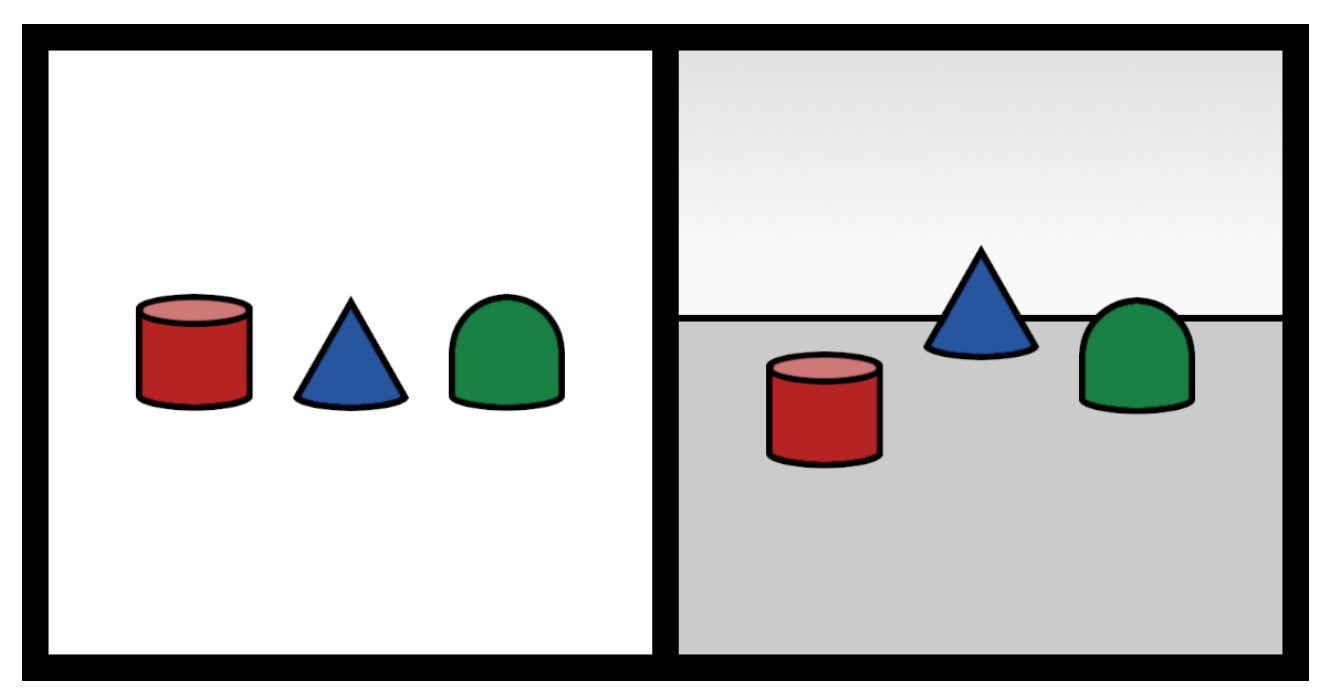


Figure 155. The horizon effect depth cue.

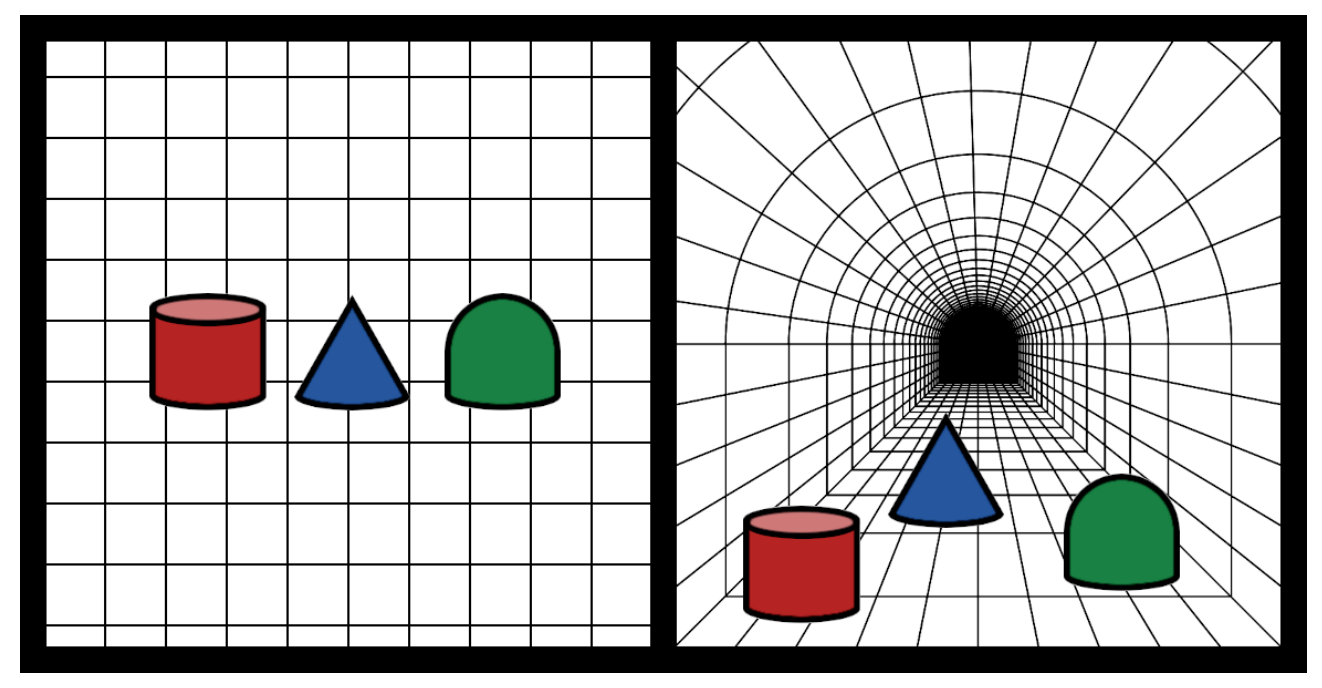


Figure 156. The horizon effect and parallel lines depth cues.

The horizon can also take the form of a vanishing point that is not necessarily the central horizon point. For instance, for objects sitting in a tunnel, the closer that an object appears to be to the tunnel's vanishing point, the farther away it

seems to be. Fig. 156 demonstrates the horizon effect depth cue associated with a vanishing point instead of a horizon line.

In the image on the right in Fig 156, the blue cone appears to be closer to the vanishing point

and therefore is perceived to be farther away from you. The image on the left shows the same scene, insofar as it is possible, without the horizon effect depth cue or the parallel lines depth cue.

12.12 Occlusion

When a near object is roughly in the same line of sight as a more distant object, the near object will partially or completely block the view of the distant object (assuming that it's not transparent). Therefore, the object that is being blocked from view must be farther away from you. This effect is called occlusion, interposition, eclipsing, or overlapping. Your brain understands this effect and can use it to determine the relative distances of objects. Fig. 157 demonstrates the occlusion depth cue.

In the image on the left in Fig. 157, the three objects are all clearly visible with no occlusion and therefore you cannot tell which object is closer. In contrast, the image on the right shows the same objects but includes occlusion. You are

therefore able to perceive that the red cylinder is closer to you and the blue cone is farther away. (A small amount of horizon effect had to be included to prevent the objects from unnaturally penetrating each other.) Note that the occlusion depth cue can only tell you which object is closer to you. It cannot tell you the absolute distance of an object.

The occlusion effect does not have to involve three-dimensional shapes. Even with flat pieces of paper, you can tell which piece of paper is farther away because it is the one being occluded. This is shown in Fig. 158.

The image on the right in Fig. 158 shows one paper occluding another paper, in two different configurations. In both configurations, the paper that is being partially blocked appears to be farther away.

The same two papers are shown in the image on the left in Fig. 158 but without the occlusion depth cue, making it impossible to tell which one is farther away.

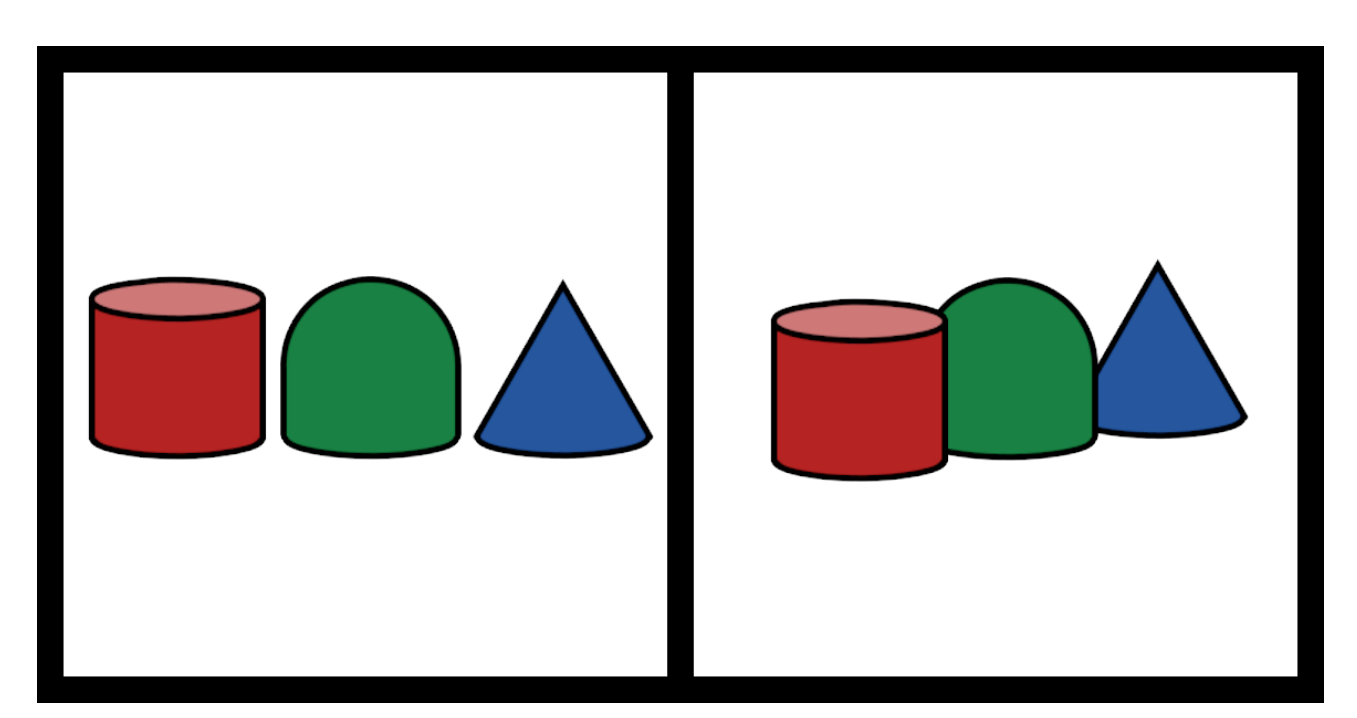


Figure 157. The occlusion effect depth cue.

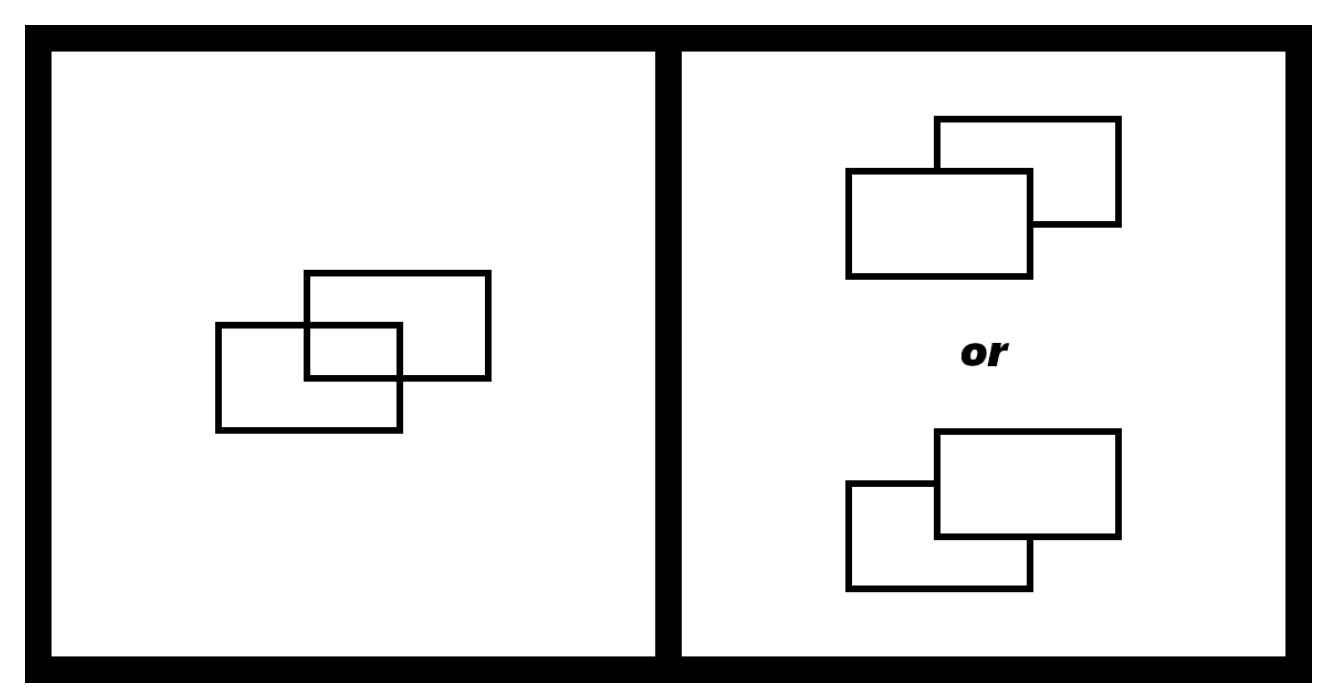


Figure 158. The occlusion effect depth cue.

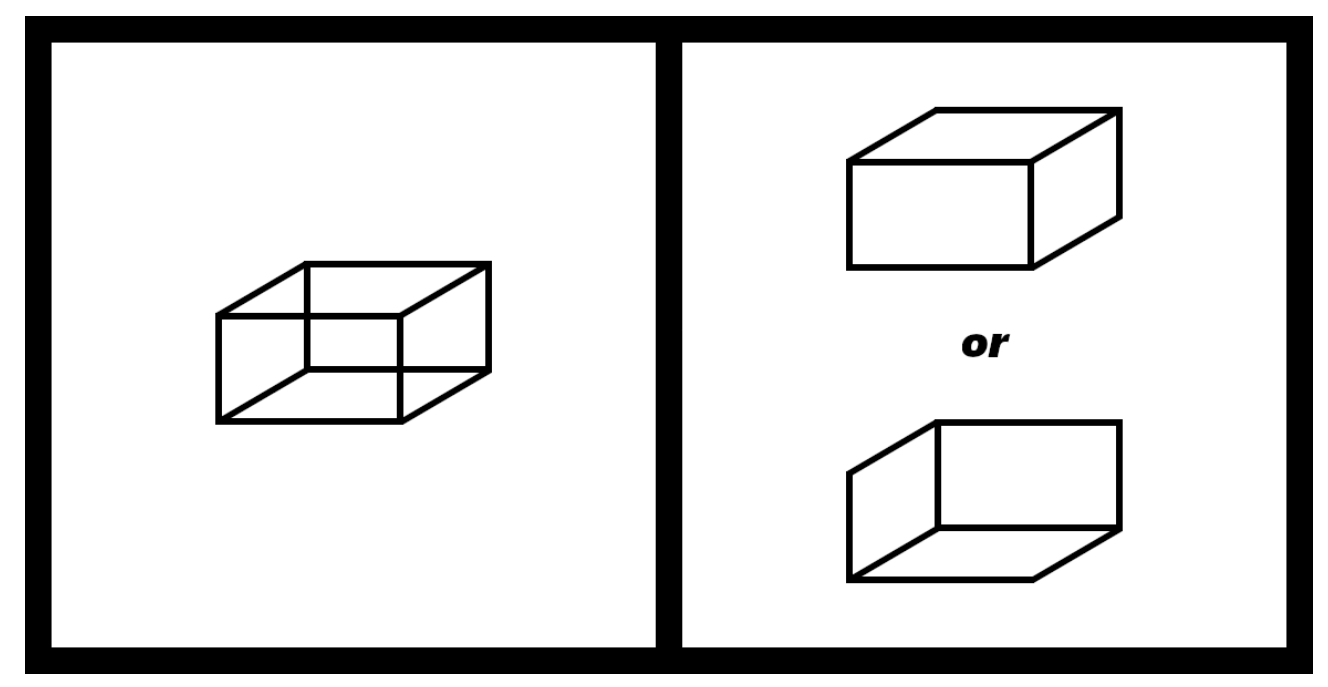


Figure 159. The occlusion effect depth cue.

Fig. 159 demonstrates how the front of an object occluding its back indicates that the front of the object is closer to you. The image on the right in Fig. 159 shows a box that is defined by its edges, presented in two different configurations. The occlusion effect gives you a sense of which face of the box is closest to you. In this way, occlusion can help give a sense of depth to an object. In contrast, the left image in Fig. 159 shows a box without occlusion information. As a result, you can't tell which configuration the box is in or which face is closest to you.

12.13 Surface Shading

The way that light falls on an object and scatters away depends on the three-dimensional shape of the object. Thus, your brain can extract depth information from the shading on an object. The parts of an object that are darker tend to be the parts that are titled away from the light source. Therefore, if the position of the light source can be estimated, the tilt in three-dimensional space

of each part of an object's surface can be deduced from its level of shading. The three-dimensional shape of the overall object can then be mentally reconstructed from the tilt of each part of its surface. Fig. 160 shows the surface shading depth cue for two simple objects.

Note that in this case, we are not focusing on the depth perception related to the position of each object but on the depth perception related to each object's three-dimensional shape. In the image on the right in Fig. 160, the surface shading enables you to see the circular object as a threedimensional sphere and the other object as a three-dimensional cylinder.

The fact that the observed shading changes smoothly along the object's surfaces enables you to perceive the sides of the cylinder and the entire sphere as smoothly round. In contrast, the image on the left in Fig. 160 shows the same objects but without surface shading. As a result, these two objects look like flat paper cutouts. Shading is an effective way for an artist to show depth.

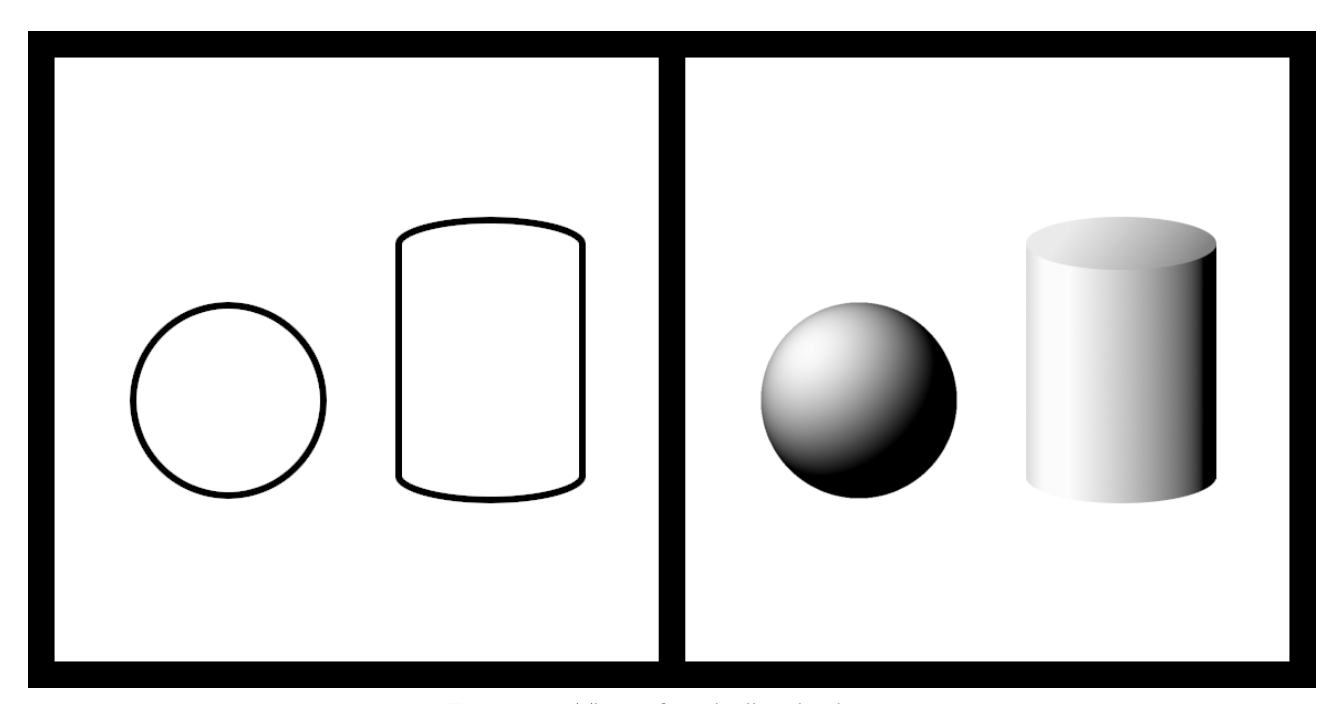


Figure 160. The surface shading depth cue.

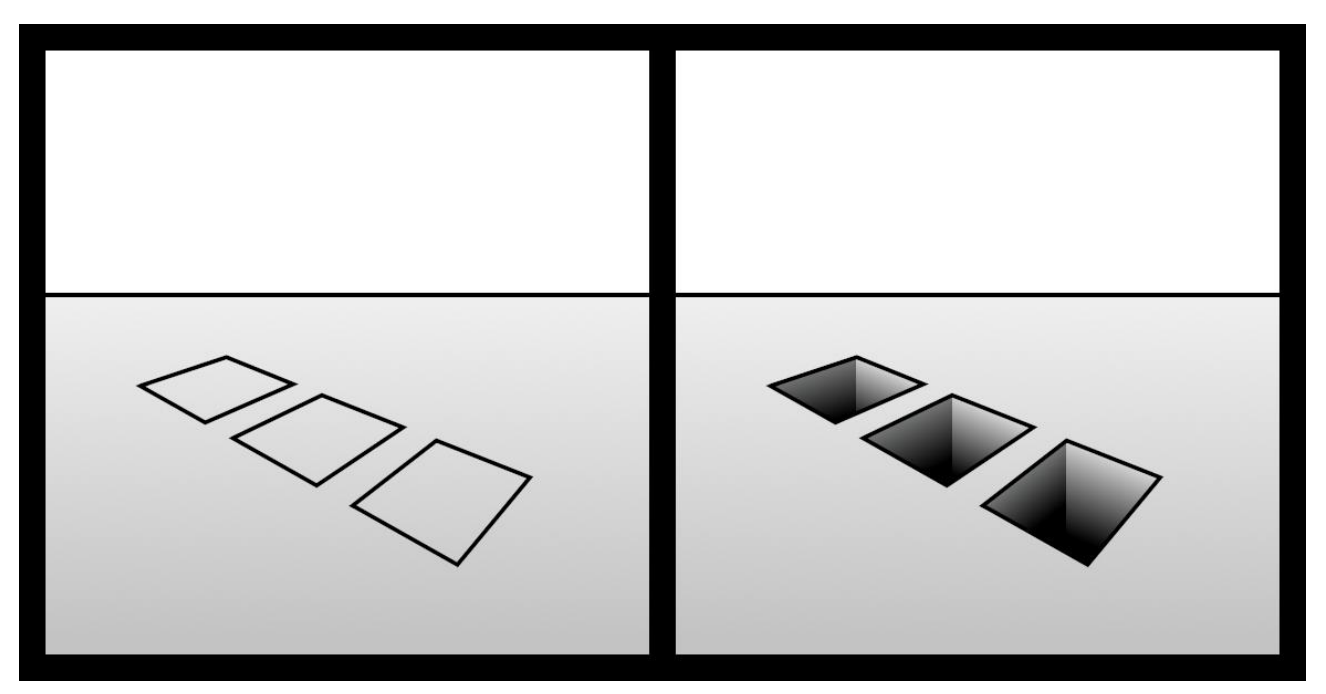


Figure 161. The recess shading depth cue.

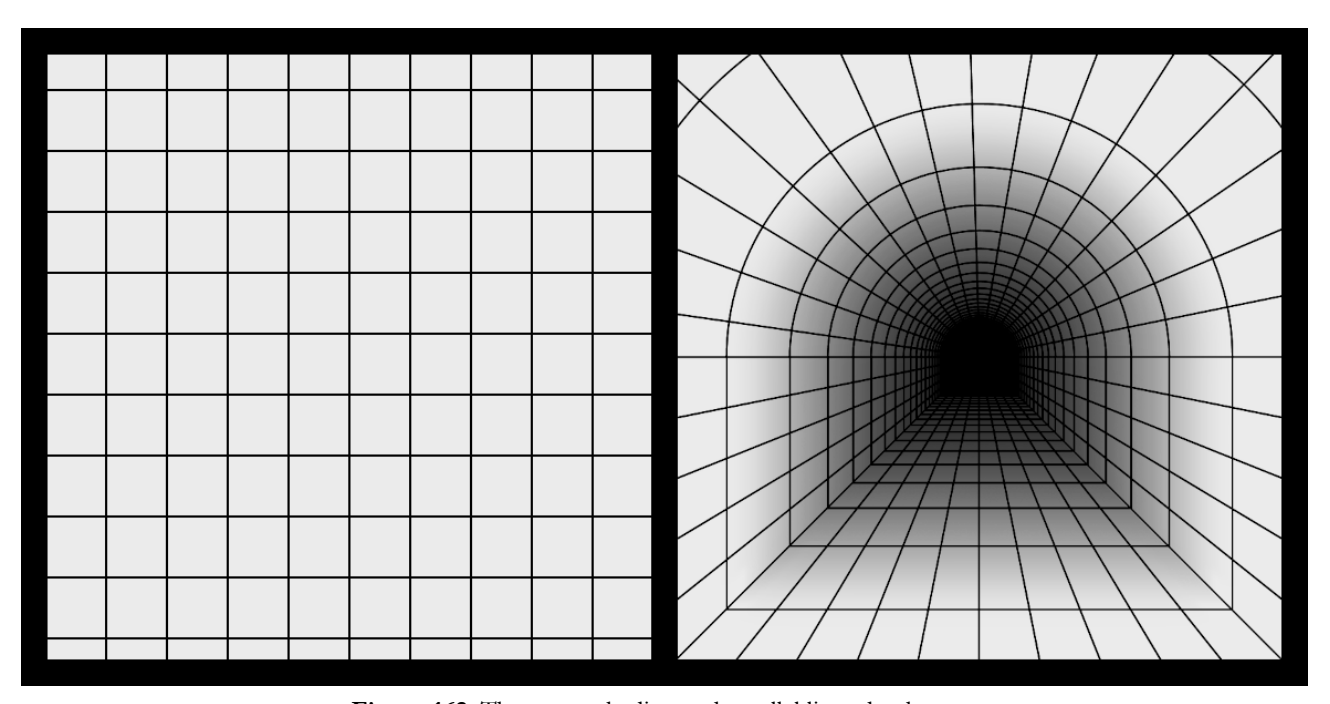


Figure 162. The recess shading and parallel lines depth cues.

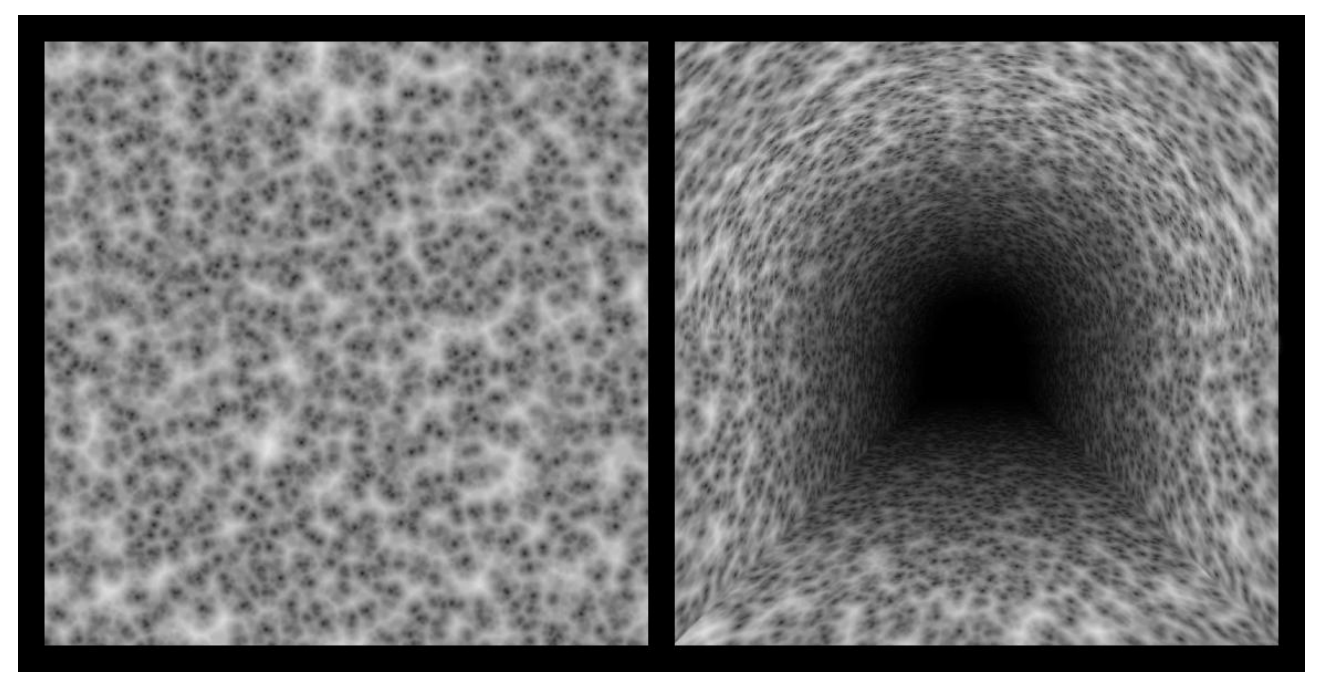


Figure 163. The recess shading and texture gradient depth cues.

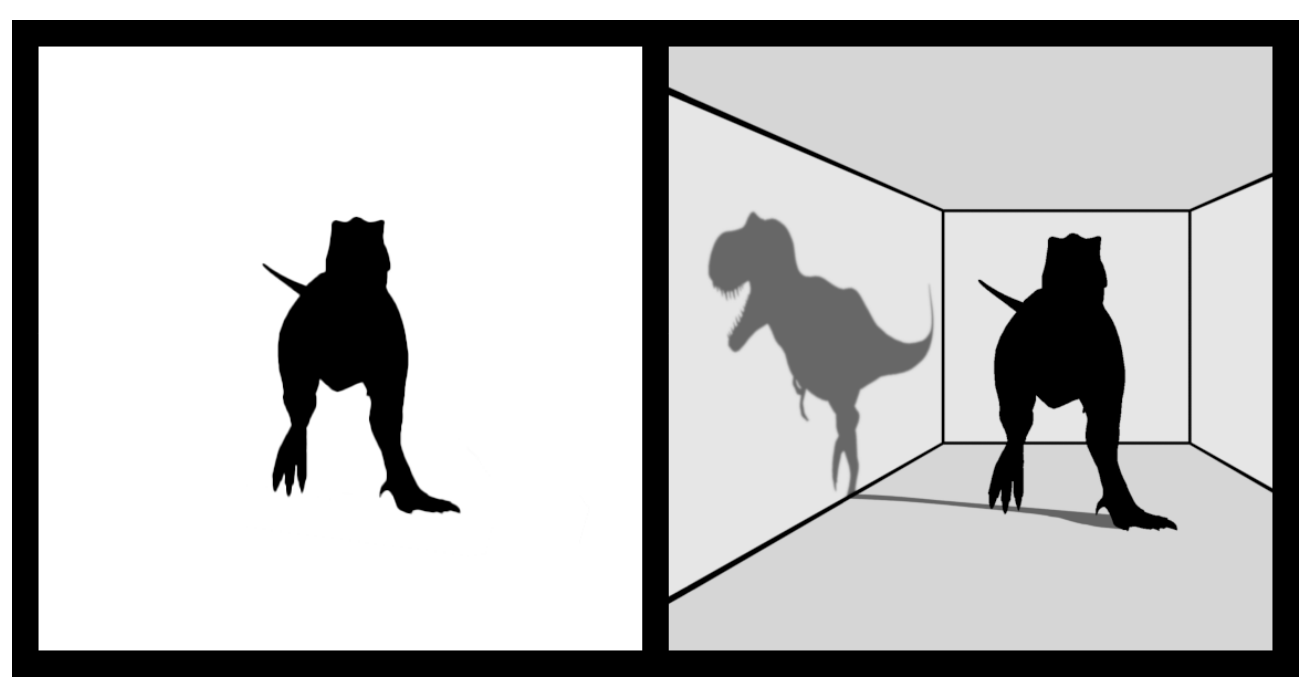


Figure 164. The shadow shape depth cue.

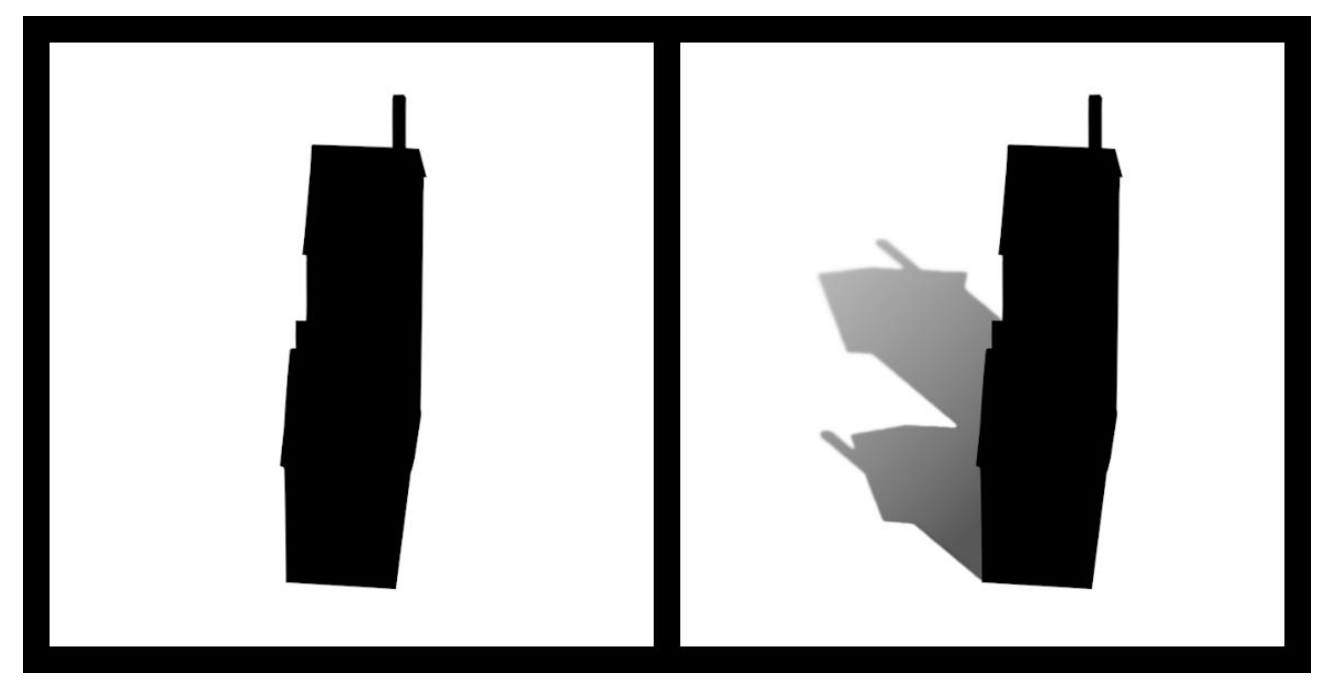


Figure 165. The shadow shape depth cue.

12.14 Recess Shading

The points on an object's or landscape's surface that are recessed will appear darker because light has a harder time reaching down into the recess. The observed recess shading therefore indicates the depth and shape of the recess.

Using this depth cue, your brain is able to perceive the presence, the shapes, and the depths of holes, recesses, cracks, corners, inlets, and narrow spaces. Fig. 161 demonstrates the recess shading depth cue.

The image on the left in Fig. 161 shows a land-scape containing three holes that have no recess shading. As a result, they do not even look like holes. In contrast, the image on the right in Fig. 161 shows the same holes but now with recess shading included. As you can see, the shading enables you to see the holes as holes and to see their three-dimensional shapes.

Fig. 162 also demonstrates the recess shading depth cue using a tunnel, this time combined with the parallel lines depth cue. As a result of the depth cues, the image on the right in Fig. 162

appears to show an arched tunnel that stretches away from you into the distance. As you can see, including two depth cues instead of one makes the image's sense of depth even more convincing. For comparison, the image on the left in Fig. 162 shows the same tunnel without any depth cues, insofar as that is possible.

Fig. 163 shows the same tunnel as in Fig. 162, but now the image includes the texture gradient and recess shading depth cues rather than the parallel lines and recess shading depth cues. For comparison, the image on the left in Fig. 163 shows the same tunnel without any depth cues, insofar as that is possible.

12.15 Shadow Shape

The shape of a shadow depends directly on the three-dimensional shape of the object that is casting the shadow and the angle of illumination. Therefore, your brain can partially deduce three-dimensional shape information from an object's shadow. Figs. 164 and 165 clearly demonstrate the shadow shape depth cue.

In the image on the left in Fig. 164, you can see the outline of some creature, but it is hard to discern its three-dimensional shape. In contrast, the image on the right in Fig. 164 shows the same creature but now its being illuminated from the side so that its shadow falls on the left wall. The shadow reveals the creature to be a T-Rex and partially reveals the three-dimensional shape of this T-Rex.

In general, this depth cue works even if the illumination is not aimed directly toward a wall, as demonstrated in Fig. 165. The image on the right in Fig. 165 involves a shadow that is cast obliquely on the ground. This shadow reveals that the structure is a set of townhouses. This shadow also enables your brain to more effectively see the townhouses as three-dimensional objects. In contrast, the image on the left in Fig. 165 shows the same structure without a shadow, which causes it to appear as a non-descript blob of black. If the angle of illumination changes, the shadow shape changes in a corresponding way.

12.16 Shadow Size, Location, and Blurriness

The size, location, and blurriness of an object's shadow all depend on how far away the object is from the shadowed surface. In general, the farther away an object is from the shadowed surface, the larger, the blurrier, and the more shifted its shadow will be. Your brain can therefore deduce distance information from the size, location, and blurriness of shadows. Fig. 166 demonstrates this depth cue.

The image on the right in Fig. 166 shows three balls and their shadows. The shadow of the rightmost ball is larger, blurrier, and more shifted downward, indicating that the rightmost ball is farther away from the ground and closer to you. In contrast, the image on the left in Fig. 166 contains the same three balls but without shadows so that there is no depth to the scene beyond the roundness of the balls. Fig. 167 also demonstrates these shadow effects.

The image on the right in Fig. 167 shows the shadow *location* depth cue at work but does not

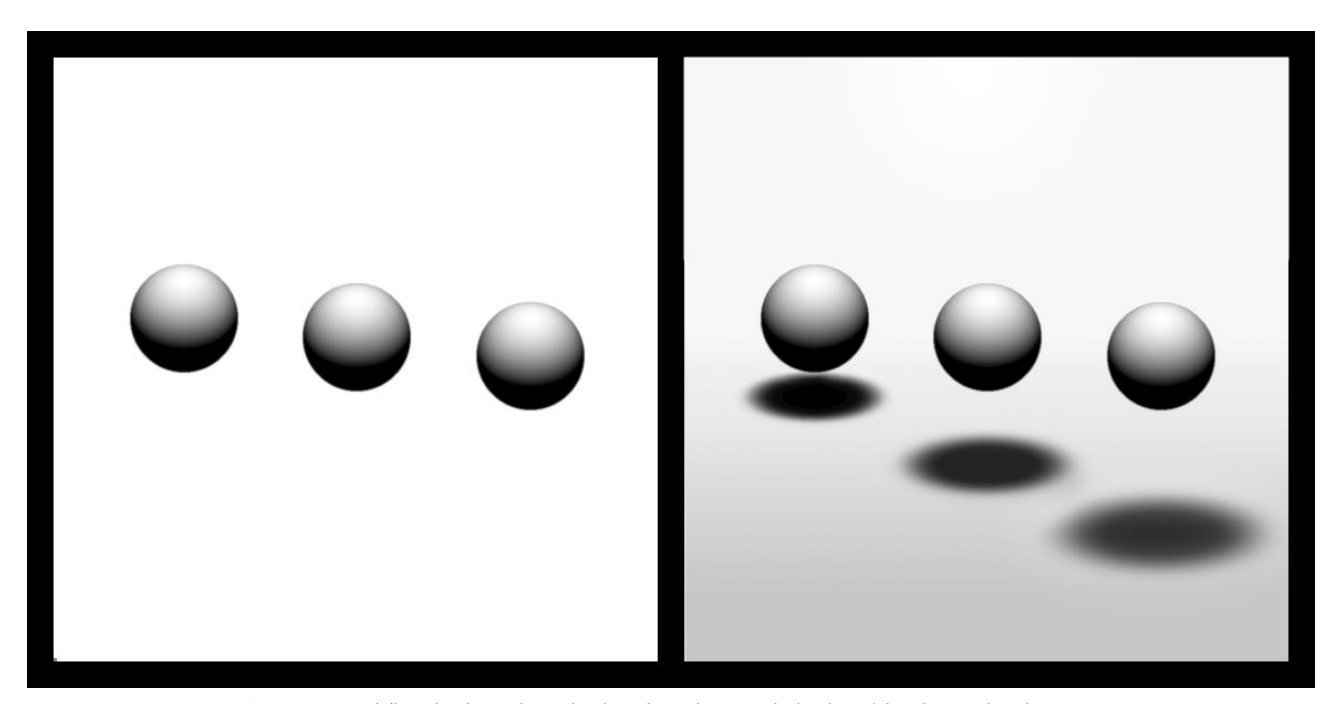


Figure 166. The shadow size, shadow location, and shadow blurriness depth cues.

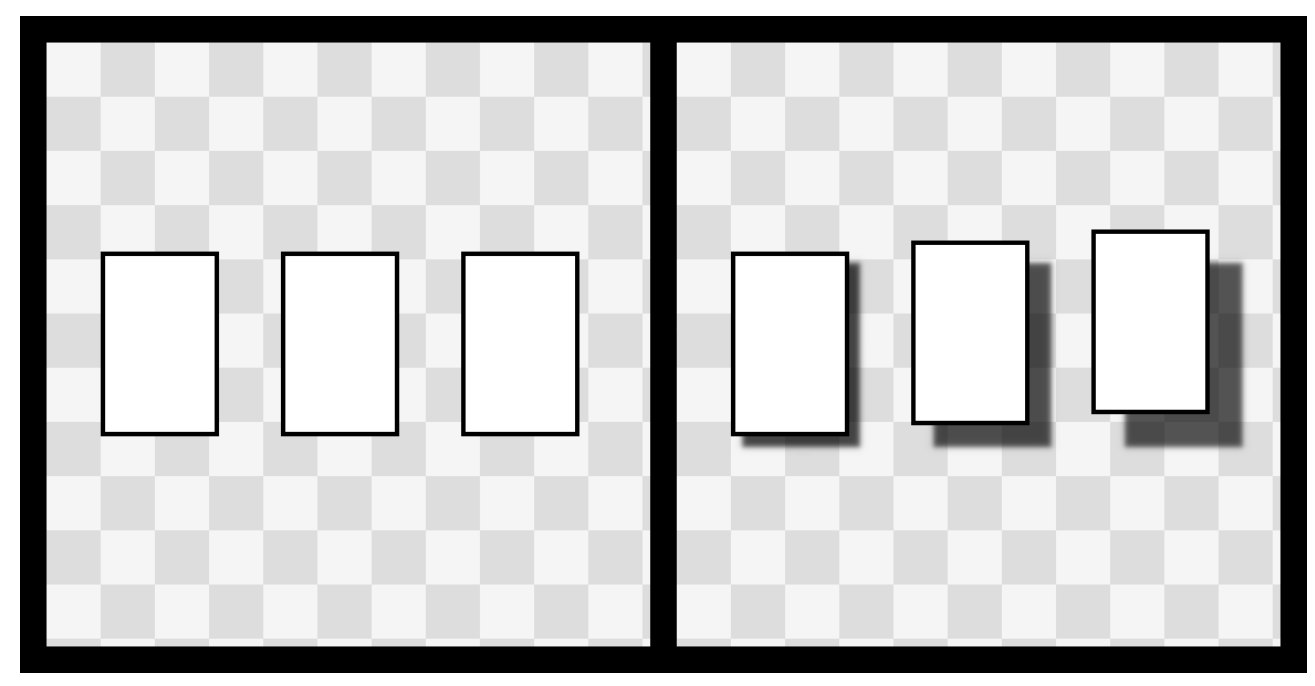


Figure 167. The shadow location depth cue.

include differences in shadow blurriness or shadow size. Even with just this one type of shadow depth cue (the shadow location depth cue), your brain can still perceive that the rightmost paper is farther away from the checkered surface and thus closer to you. In contrast, the image on the left in Fig. 167 does not have any shadow depth cues present and thus there is no sense of depth.

12.17 Atmospheric Effects

When an object is far away, the air between you and the object changes its appearance. Air is not perfectly transparent. Rather, the nitrogen and oxygen molecules that make up 99% of air give a distant object a slight whitish-blue tint under blue sky daytime lighting conditions. As an additional effect, the water droplets in the air can give the air a slight white or murky grey appearance. Both of these effects also cause the observed image to diminish in observed contrast, color saturation, and sharpness.

The farther away an object is, the more it will have a flat, muted blue-white color and a softer, blurrier appearance. Your brain can deduce the distance of an object based on how much its image is altered by atmospheric effects. Note that atmospheric effects will only become significant when the light from an observed object travels through large amounts of air. As a result, this cue only works for objects that are far away, such as mountains, bridges, and buildings (except if it's an extremely foggy day). Unless it's a very foggy day, you won't notice atmospheric effects for objects that are only a few feet away, or even a few dozen feet away.

During storms, atmospheric effects will give distant objects a gray tint rather than whitish-blue and sometimes even a green tint when tornadoes are present. At sunset and sunrise, atmospheric effects will give distant objects red, pink, orange, and yellow tints.

You probably use this visual cue more than you realize. Astronauts who have walked on the moon reported that because the moon lacked an atmosphere, the distant hills looked much closer than they actually were, which was disorienting.

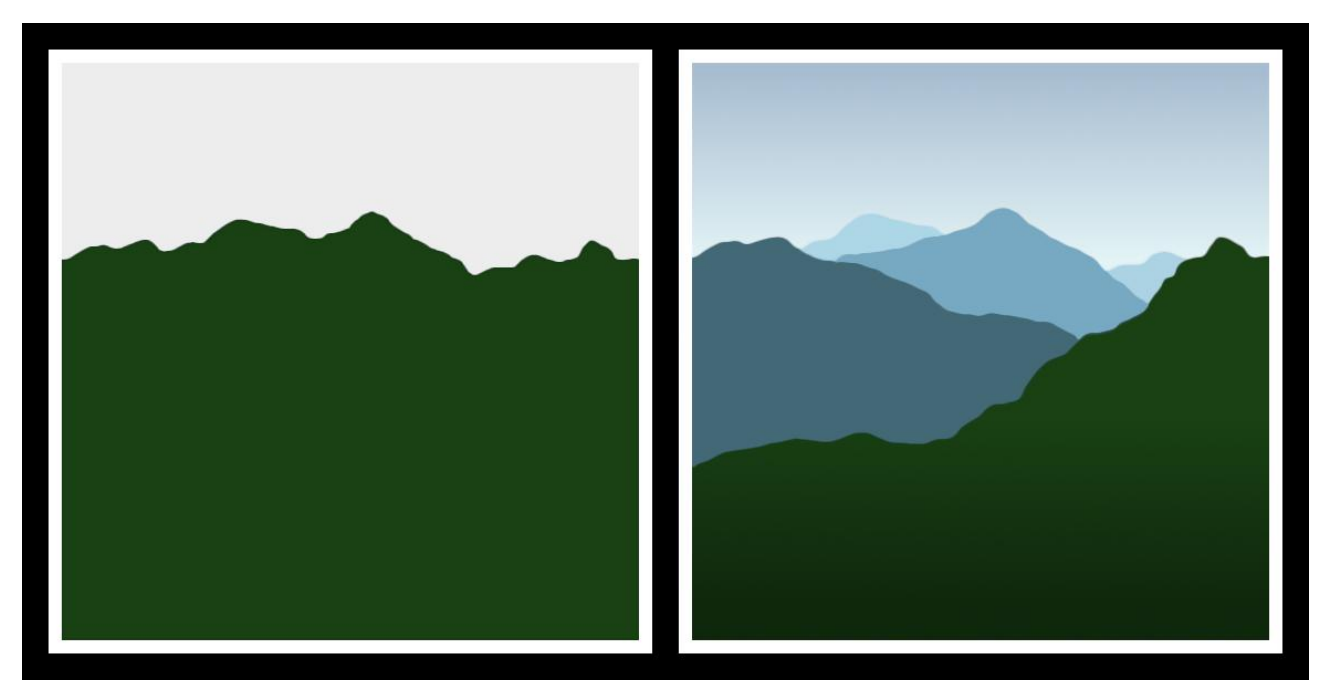


Figure 168. The atmospheric effects depth cue shown using a simple drawing.

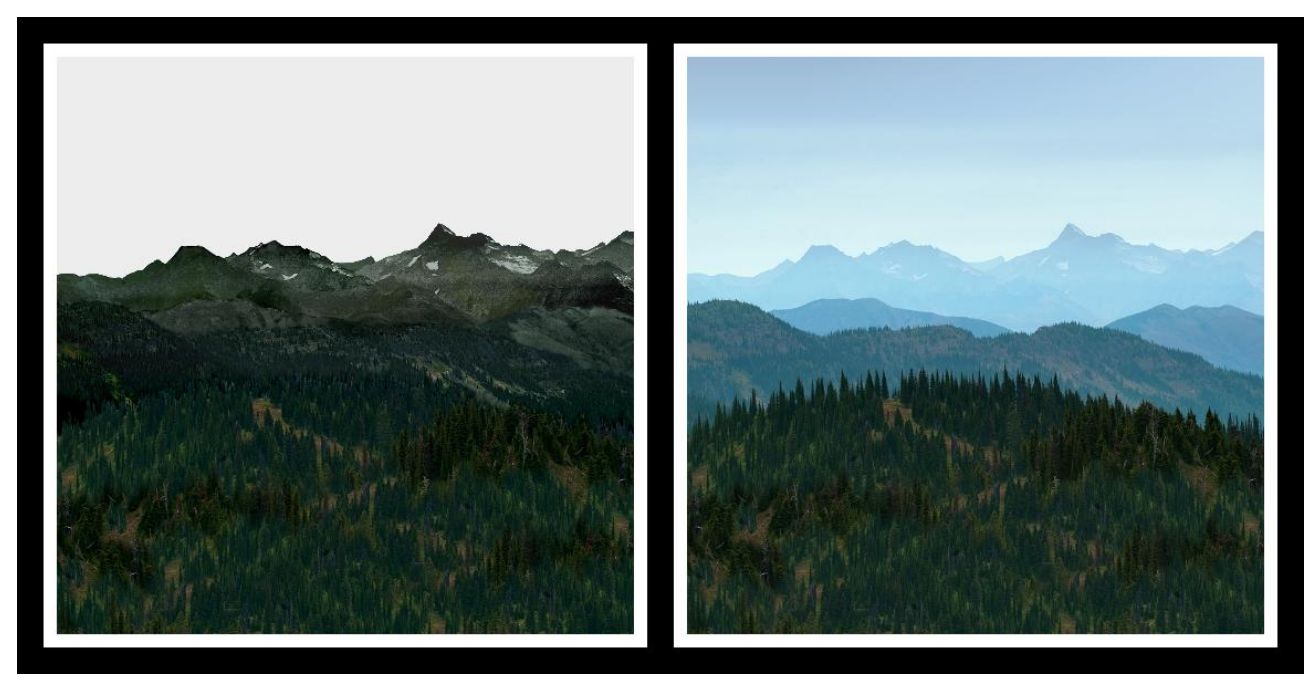


Figure 169. The atmospheric effects depth cue shown using a photo of the real world.

They reported that as they walked toward a hill, it seemed to recede at the same rate. Fig. 168 demonstrates the atmospheric effects depth cue. In the image on the right in Fig. 168, a series of mountains at different distances are observed to

have different shades and colors because of the intervening air, depending on how far away they are. In contrast, the image on the left in Fig. 168 shows the exact same mountains but without any atmospheric effects. As a result, all the mountains

visually merge together and look flat. Note that I intentionally drew Fig. 168 as simple as possible to clearly demonstrate atmospheric effects.

Fig. 169 also exhibits atmospheric effects but now using an actual photograph of the real world. The image on the right in Fig. 169 is a photograph of a mountain landscape with no photo editing or digital enhancements. The whitish-blue tints in this photo are completely natural and are what you would see with your naked eye if you were actually standing there looking out at this scene. This photograph shows that the farther away a mountain is, the more it appears whitish-blue, unsaturated, and contrast deficient. Note that the sky is whitish-blue for the same reason that the distant mountains are whitish-blue; because of the effect of the atmosphere on the light passing through it.

The image on the left in Fig. 169 shows the exact same photo but without any atmospheric effects. To create this image on the left, I took the raw photograph shown on the right and carefully removed the atmospheric effects using photo editing software and my understanding of the physics. This involved removing the whitish-blue tint and increasing the saturation and contrast, one layer of mountains at a time. Notice how all of the mountains in the left image in Fig. 169 seem to merge together into one indistinct mass without much depth. Interestingly, the image on the left looks like it came from a low-quality video game that failed to properly include atmospheric effects.

12.18 Accommodation and Pupil Response

In order for the human eye to properly focus on objects that are at different distances from it, the ciliary muscles in the eye must change the shape of the eye lens by changing the amount of muscle contraction. To bring a distant object into focus, the ciliary muscles relax, which allows the lens to

flatten. To bring a near object into focus, the ciliary muscles contract, which then pushes the lens into a rounder shape.

The human eye has a sensory apparatus to detect how much the ciliary muscles have been contracted. In this way, your brain can deduce the distance of an object by having the eyes focus on it and then sensing the contraction level of the ciliary muscles.

This depth cue depends on muscle contraction information rather than image information, so I cannot demonstrate how it works using images. Also, a regular computer screen or printed photo cannot enable the accommodation depth cue to be used.

Pupil response is also used for depth information during accommodation. The size of the pupil slightly affects how much an object appears to be in focus. The lens in each eye gives rise to optical aberrations. As a result, if more of the lens is used, then the image is blurrier. Thus, your pupils work along with the ciliary muscles to properly bring objects into focus. Your brain then utilizes pupil constriction information along with ciliary muscle contraction information to determine the object's distance.

12.19 Depth from Defocusing

When the human eye brings a certain real object into focus, objects that are at different distances will appear blurrier. The amount of observed blur depends on how far away in the forward direction the other objects are from the object that is in focus. Specifically, the farther away an object is in the gazing direction from the object that is in focus, the blurrier it will appear. Your brain can therefore deduce distance from the amount of defocusing blur. Fig. 170 demonstrates the depth from defocusing visual depth perception cue.

The image on the left in Fig. 170 shows three strawberries without defocusing blur. As a result,

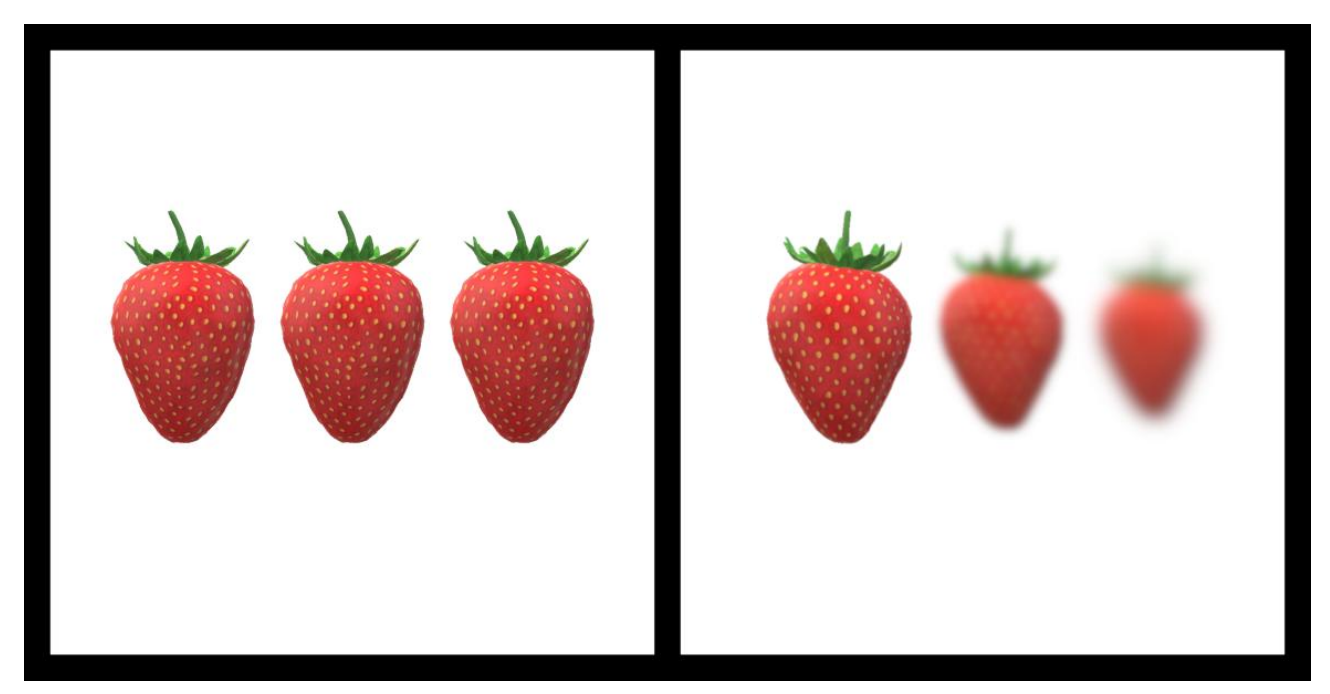


Figure 170. The depth from defocusing cue.

they all appear to be the same distance away. In contrast, the image on the right in Fig. 170 shows the same three strawberries with defocusing blur included. (I have also included a small amount of the relative size depth cue to prevent the image from looking unnatural.) As a result, the strawberry on the left appears to be closer to you.

12.20 Binocular Parallax

As demonstrated, the human visual system uses about nineteen different monocular depth cues. The exact number will depend on how you decide to group special cases into categories, such as the shadow depth cues.

In addition to all of these human monocular depth perception cues, there are two *binocular* visual cues used for depth perception, namely binocular parallax and vergence. This book was specifically about monocular depth cues and not binocular cues, so I include here the binocular depth cues for completeness, but only briefly.

One of the most important human depth cues is binocular (two-eye) parallax. Because each eye

is at a different location in the head, each eye sees a slightly different view of the world. The difference between what your left eye sees and what your right eye sees depends directly on the threedimensional shape of each object and its location in the three-dimensional world. The closer that an

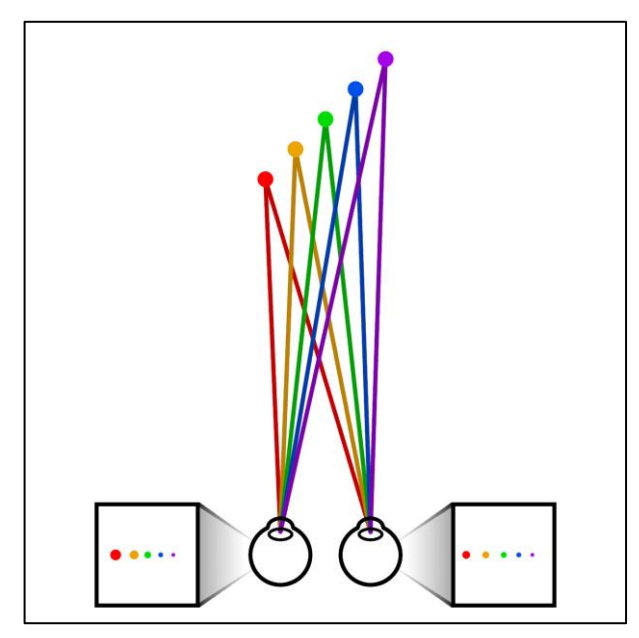


Figure 171. The binocular parallax depth cue.

object is to you, the greater will be the difference between what your left eye sees and what your right eye sees. The human brain is therefore able to extract depth information from the difference between what your two eyes see. If the image of a chair seen by your left eye and the image of the same chair seen by your right eye at the same time are nearly identical, then the chair must be far away. In contrast, if these two images of the chair are very different, then the object must be very close. This effect is represented in Fig. 171.

The overall geometric effect is called parallax. When a human is using two eyes in order to take advantage of parallax, it is called two-eye parallax or binocular parallax. The difference between the left-eye image and the right-eye is called binocular disparity. The ability of the brain to extract depth information from this binocular disparity is called stereopsis.

12.21 Vergence

The other binocular depth cue is vergence. When your eyes both look directly at the same object, they must both rotate slightly toward each other

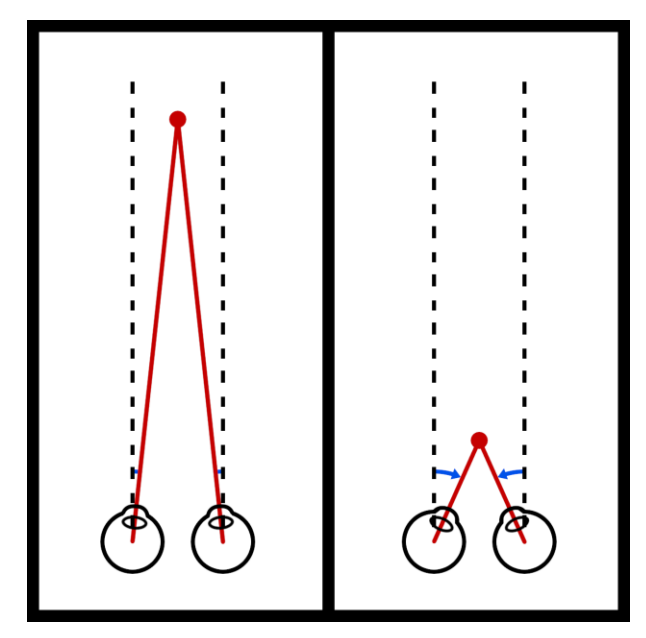


Figure 172. The binocular vergence depth cue.

to do this. How much your eyes rotate depends on how close the object is. When an object is far away from you, your two eyes only rotate toward each other a small amount in order to both be looking directly at the same object. In contrast, when an object is close to you, your two eyes must rotate toward each other a large amount in order to both be looking directly at the same object. This is demonstrated in Fig. 172.

The muscles that are involved in the eyeball rotations send signals to the brain indicating how much the eyes are rotated. The brain can then extract depth from this information. Note that this is an oculomotor depth cue and not purely a visual depth cue, so images on a flat screen can never enable this depth cue.

12.22 Summary

In summary, there are two binocular depth cues and about nineteen monocular depth cues. Socalled "3D" movie theaters that present binocular parallax depth cue information in addition to the traditional monocular depth cues require wearing special glasses to properly make your two eyes see slightly different images. These "3D" movies do not include all of the depth cues and are therefore not fully three-dimensional. Thus, these movies are more accurately called stereoscopic movies. Although "3D" movies do include the binocular parallax depth cue, this depth cue is not that useful for objects that are more than a few dozen feet away. This means that adding in the binocular parallax depth cue to a movie's presentation only gives noticeable improvements in 3D-realism for near objects in the filmed scene.

Also, regular movies that don't require wearing those special glasses already contain almost *all* of the monocular depth cues and are thus already very close to being 3D-realistic. As a result, so-called "3D" movies are not that much more 3D-realistic than regular movies. This is probably why

so-called "3D" movies have not become popular and have not displaced regular movies, despite having existed for over a hundred years.

Neither regular movies nor so-called "3D" movies enable the accommodation depth cue, the pupil response depth cue, the true depth from defocusing depth cue, the vergence depth cue, or the true motion parallax depth cue. Despite all of these missing depth cues, amazingly, movies still appear convincingly three-dimensional because they enable all of the other depth cues (except that regular movies do not include the binocular parallax cue, as already noted). True holograms enable all of the depth cues that regular movies and "3D" movies do not, in addition to almost all of the other depth cues and are therefore the closest to being 3D-realistic images. However, at the time of this writing, true holograms are only

still images and not moving pictures, and thus lack the kinetic depth effect. Additionally, true holograms are only a single color, which reduces the sense of realism. Perhaps in the future scientists will discover how to present true holograms in multiple colors and as moving pictures.

In conclusion, human vision is quite capable of seeing depth even if only one eye is functioning. Fortunately, this means that humans can see depth quite well when looking at regular movie screens, computer screens, television screens, and the screens of mobile devices (assuming that the displayed images are properly conveying monocular depth cues). It also means that artists who understand the monocular depth cues can create a convincing sense of depth when painting or drawing on paper, canvas, wood, or any other flat surface.

Citations

- 1. Howard, I. P., Rogers, B. J. (2012). *Perceiving in Depth.* United Kingdom: Oxford University Press, USA.
- 2. Ed. by Rogers, S. R., Epstein, W. (1995). *Perception of Space and Motion*. Netherlands: Elsevier Science.
- 3. Walsh, A. E., Bourges-Sévenier, M. (2001). Core Web3D. United Kingdom: Prentice Hall PTR.
- 4. Cole, R. V. (2012). Perspective for Artists. United States: Dover Publications.
- 5. McCoun, J., Reeves, L. (2010). *Binocular Vision: Development, Depth Perception, and Disorders*. United States: Nova Science Publishers.
- 6. Keating, M. P. (1988). Geometric, Physical, and Visual Optics. United States: Elsevier Health Sciences.
- 7. Looking Into Pictures: An Interdisciplinary Approach to Pictorial Space. (2003). United Kingdom: MIT Press.
- 8. Fatt, I., Weissman, B. A. (2013). *Physiology of the Eye: An Introduction to the Vegetative Functions.* United States: Elsevier Science.
- 9. Klein, S. B., Thorne, B. M. (2006). Biological Psychology. United Kingdom: Worth Publishers.
- 10. Livingstone, M. S. (2014). Vision and Art (Updated and Expanded Edition). United States: Harry N. Abrams.
- 11. Human and Machine Vision. (2014). United Kingdom: Elsevier Science.
- 12. Hecht, E. (1998). Optics. United Kingdom: Addison-Wesley.
- 13. Ibid.
- 14. Ibid.
- 15. Shi, S. (2022). Development and Application of Light-Field Cameras in Fluid Measurements. Switzerland: Springer International Publishing.
- 16. Lens, A., Nemeth, S. C., Ledford, J. K. (2008). Ocular Anatomy and Physiology. United States: SLACK.
- 17. Ibid.

Citations

- 18. Dale Purves, G. J. A. (2011). *Neuroscience*: United Kingdom: Oxford University Press, Incorporated.
- 19. Donner K. (2021). Temporal vision: measures, mechanisms and meaning. *The Journal of Experimental Biology*, 224(15), jeb222679. https://doi.org/10.1242/jeb.222679
- 20. Ibid.
- 21. Ibid.
- 22. Color Vision: From Genes to Perception. (2001). United Kingdom: Cambridge University Press.
- 23. Age-related Macular Degeneration: A Comprehensive Textbook. (2006). United Kingdom: Lippincott Williams & Wilkins.